

World Journal of *Gastroenterology*

World J Gastroenterol 2023 March 28; 29(12): 1765-1910



REVIEW

1765 Mitochondrial carnitine palmitoyltransferase-II dysfunction: A possible novel mechanism for nonalcoholic fatty liver disease in hepatocarcinogenesis
Yao M, Zhou P, Qin YY, Wang L, Yao DF

1779 Obesity and novel management of inflammatory bowel disease
Kim JH, Oh CM, Yoo JH

1795 Role of autoantibodies in the clinical management of primary biliary cholangitis
Rigopoulou EI, Bogdanos DP

MINIREVIEWS

1811 Artificial intelligence as a noninvasive tool for pancreatic cancer prediction and diagnosis
Faur AC, Lazar DC, Ghenciu LA

1824 New uses for an old remedy: Digoxin as a potential treatment for steatohepatitis and other disorders
Jamshed F, Dashi F, Ouyang X, Mehal WZ, Banini BA

1838 Autoimmune liver diseases and SARS-CoV-2
Sgamato C, Rocco A, Compare D, Minieri S, Marchitto SA, Maurea S, Nardone G

1852 Review of lymphoma in the duodenum: An update of diagnosis and management
Iwamuro M, Tanaka T, Okada H

1863 Comprehensive review on endoscopic ultrasound-guided tissue acquisition techniques for solid pancreatic tumor
Masuda S, Koizumi K, Shionoya K, Jinushi R, Makazu M, Nishino T, Kimura K, Sumida C, Kubota J, Ichita C, Sasaki A, Kobayashi M, Kako M, Haruki U

ORIGINAL ARTICLE

Basic Study

1875 Antihepatoma peptide, scolopentide, derived from the centipede scolopendra subspinipes mutilans
Hu YX, Liu Z, Zhang Z, Deng Z, Huang Z, Feng T, Zhou QH, Mei S, Yi C, Zhou Q, Zeng PH, Pei G, Tian S, Tian XF

1899 Linked color imaging *vs* Lugol chromoendoscopy for esophageal squamous cell cancer and precancerous lesion screening: A noninferiority study
Wang ZX, Li LS, Su S, Li JP, Zhang B, Wang NJ, Liu SZ, Wang SS, Zhang S, Bi YW, Gao F, Shao Q, Xu N, Shao BZ, Yao Y, Liu F, Linghu EQ, Chai NL

ABOUT COVER

Editorial Board of *World Journal of Gastroenterology*, Yirupaiyahgar KS Viswanath, Professor, Consultant Surgeon (Upper GI, Laparoscopic and Robotic Surgery), Honorary Professor Teesside University, President Elect BBUGSS United Kingdom, MCh Programme Director, South Tees Hospitals NHS Foundation Trust, James Cook, University Hospital, Marton Road, Middlesbrough TS43BW, Cleveland, United Kingdom. yksviswanath@nhs.net

AIMS AND SCOPE

The primary aim of *World Journal of Gastroenterology* (WJG, *World J Gastroenterol*) is to provide scholars and readers from various fields of gastroenterology and hepatology with a platform to publish high-quality basic and clinical research articles and communicate their research findings online. WJG mainly publishes articles reporting research results and findings obtained in the field of gastroenterology and hepatology and covering a wide range of topics including gastroenterology, hepatology, gastrointestinal endoscopy, gastrointestinal surgery, gastrointestinal oncology, and pediatric gastroenterology.

INDEXING/ABSTRACTING

The WJG is now abstracted and indexed in Science Citation Index Expanded (SCIE, also known as SciSearch®), Current Contents/Clinical Medicine, Journal Citation Reports, Index Medicus, MEDLINE, PubMed, PubMed Central, Scopus, Reference Citation Analysis, China National Knowledge Infrastructure, China Science and Technology Journal Database, and Superstar Journals Database. The 2022 edition of Journal Citation Reports® cites the 2021 impact factor (IF) for WJG as 5.374; IF without journal self cites: 5.187; 5-year IF: 5.715; Journal Citation Indicator: 0.84; Ranking: 31 among 93 journals in gastroenterology and hepatology; and Quartile category: Q2. The WJG's CiteScore for 2021 is 8.1 and Scopus CiteScore rank 2021: Gastroenterology is 18/149.

RESPONSIBLE EDITORS FOR THIS ISSUE

Production Editor: *Yu-Xi Chen*; Production Department Director: *Xu Guo*; Editorial Office Director: *Jia-Ru Fan*.

NAME OF JOURNAL

World Journal of Gastroenterology

ISSN

ISSN 1007-9327 (print) ISSN 2219-2840 (online)

LAUNCH DATE

October 1, 1995

FREQUENCY

Weekly

EDITORS-IN-CHIEF

Andrzej S Tarnawski

EDITORIAL BOARD MEMBERS

<http://www.wjgnet.com/1007-9327/editorialboard.htm>

PUBLICATION DATE

March 28, 2023

COPYRIGHT

© 2023 Baishideng Publishing Group Inc

INSTRUCTIONS TO AUTHORS

<https://www.wjgnet.com/bpg/gerinfo/204>

GUIDELINES FOR ETHICS DOCUMENTS

<https://www.wjgnet.com/bpg/GerInfo/287>

GUIDELINES FOR NON-NATIVE SPEAKERS OF ENGLISH

<https://www.wjgnet.com/bpg/gerinfo/240>

PUBLICATION ETHICS

<https://www.wjgnet.com/bpg/GerInfo/288>

PUBLICATION MISCONDUCT

<https://www.wjgnet.com/bpg/gerinfo/208>

ARTICLE PROCESSING CHARGE

<https://www.wjgnet.com/bpg/gerinfo/242>

STEPS FOR SUBMITTING MANUSCRIPTS

<https://www.wjgnet.com/bpg/GerInfo/239>

ONLINE SUBMISSION

<https://www.f6publishing.com>

Mitochondrial carnitine palmitoyltransferase-II dysfunction: A possible novel mechanism for nonalcoholic fatty liver disease in hepatocarcinogenesis

Min Yao, Ping Zhou, Yan-Yan Qin, Li Wang, Deng-Fu Yao

Specialty type: Oncology

Provenance and peer review:

Unsolicited article; Externally peer reviewed.

Peer-review model: Single blind

Peer-review report's scientific quality classification

Grade A (Excellent): 0

Grade B (Very good): 0

Grade C (Good): C, C

Grade D (Fair): 0

Grade E (Poor): 0

P-Reviewer: Ulasoglu C, Turkey;
Liu QJ, China

Received: June 20, 2022

Peer-review started: June 20, 2022

First decision: August 1, 2022

Revised: August 4, 2022

Accepted: March 9, 2023

Article in press: March 9, 2023

Published online: March 28, 2023



Min Yao, Department of Medical Immunology, Medical School of Nantong University & Research Center of Clinical Medicine, Affiliated Hospital of Nantong University, Nantong 226001, Jiangsu Province, China

Ping Zhou, Yan-Yan Qin, Department of Medical Immunology, Medical School of Nantong University, Nantong 226001, Jiangsu Province, China

Li Wang, Research Center for Intelligent Information Technology, Nantong University, Nantong 226019, Jiangsu Province, China

Deng-Fu Yao, Research Center of Clinical Medicine, Affiliated Hospital of Nantong University, Nantong 226001, Jiangsu Province, China

Corresponding author: Deng-Fu Yao, MD, PhD, Full Professor, Research Center of Clinical Medicine, Affiliated Hospital of Nantong University, No. 20 West Temple Road, Nantong 226001, Jiangsu Province, China. yaodf@ahnmc.com

Abstract

Nonalcoholic fatty liver disease (NAFLD) or metabolic-associated fatty liver disease has been characterized by the lipid accumulation with injury of hepatocytes and has become one of the most common chronic liver diseases in the world. The complex mechanisms of NAFLD formation are still under identification. Carnitine palmitoyltransferase-II (CPT-II) on inner mitochondrial membrane (IMM) regulates long chain fatty acid β -oxidation, and its abnormality has had more and more attention paid to it by basic and clinical research in NAFLD. The sequences of its peptide chain and DNA nucleotides have been identified, and the catalytic activity of CPT-II is affected on its gene mutations, deficiency, enzymatic thermal instability, circulating carnitine level and so on. Recently, the CPT-II dysfunction has been discovered in models of liver lipid accumulation. Meanwhile, the malignant transformation of hepatocyte-related CD44⁺ stem T cell activation, high levels of tumor-related biomarkers (AFP, GPC3) and abnormal activation of Wnt3a expression as a key signal molecule of the Wnt/ β -catenin pathway run parallel to the alterations of hepatocyte pathology. This review focuses on some of the progress of CPT-II inactivity on IMM with liver fatty accumulation as a possible novel pathogenesis for NAFLD in hepatocarcinogenesis.

Key Words: Carnitine palmitoyl transferase-II; Nonalcoholic fatty liver disease; Fatty acid β -oxidation; Carnitine; Hepatocyte malignant transformation; Mitochondrial membrane

©The Author(s) 2023. Published by Baishideng Publishing Group Inc. All rights reserved.

Core Tip: The complex mechanisms of nonalcoholic fatty liver disease formation are still under identification. Hepatic carnitine palmitoyl transferase-II (CPT-II) on inner mitochondrial membrane regulates long chain fatty acid β -oxidation and this abnormality has had more attention paid to it by basic and clinical research. The sequences of its peptide chain and DNA nucleotides have been identified and the catalytic activity of CPT-II is affected on its gene mutations, deficiency, enzymatic thermal instability, circulating carnitine level and so on. CPT-II dysfunction has been discovered in models of lipid accumulation. Meanwhile, the malignant transformation of hepatocyte-related CD44⁺ stem T cell activation, high levels of tumor-related biomarkers and abnormal Wnt3a expression as a key signal molecule of the Wnt/ β -catenin pathway run parallel to the alterations of hepatocyte pathology.

Citation: Yao M, Zhou P, Qin YY, Wang L, Yao DF. Mitochondrial carnitine palmitoyltransferase-II dysfunction: A possible novel mechanism for nonalcoholic fatty liver disease in hepatocarcinogenesis. *World J Gastroenterol* 2023; 29(12): 1765-1778

URL: <https://www.wjgnet.com/1007-9327/full/v29/i12/1765.htm>

DOI: <https://dx.doi.org/10.3748/wjg.v29.i12.1765>

INTRODUCTION

Non-alcoholic fatty liver disease (NAFLD) or metabolic-associated fatty liver disease (MAFLD) is a general term of liver diseases characterized by inflammation, fatty accumulation and hepatocyte dysfunction, except of alcohol or other clear liver injury factors[1-3]. Up until now, NAFLD has become a potentially serious liver disease that affects approximately 25% of the adult population in the world [4], and is divided into non-alcoholic fatty liver (NAFL) and non-alcoholic steatohepatitis (NASH) with or without liver fibrosis[4,5]. It has been shown that balloon like hepatocyte injury is based on NAFL. Most patients have no obvious symptoms and may not be diagnosed until they develop into liver cirrhosis or progress to hepatocellular carcinoma (HCC), and the effect of early clinical screening is poor [6]. Once NAFLD progresses to liver cirrhosis, it is difficult to reverse and there is a risk that HCC can't be ignored. Not only that, it also involves the occurrence of multiple systemic diseases in the body which are closely related to cardiovascular disease, chronic kidney disease and colorectal tumor which all threaten human health[7,8]. Therefore, finding the monitoring target in the malignant transformation of NAFLD has practical clinical significance for the prevention of NAFLD-related liver malignant diseases[9].

Lipid metabolism rearrangements in NAFLD contribute to disease progress that has emerged as one of the most risks for HCC, where metabolic reprogramming is a hallmark[10]. Hepatic carnitine palmitoyl transferases (CPTs) are critical for long-chain fatty acids (LCFAs) -oxidation, as they are capable of transport through the mitochondrial membrane[11]. CPT is made up of two separate proteins (CPT-I and CPT-II). CPT-I is located in the outer mitochondrial membrane (OMM) with three isoforms (liver CPT1a, muscle CPT1b and brain CPT1c) and CPT-II is in the inner mitochondrial membrane (IMM)[12,13]. The amino acid and cDNA nucleotide sequences of the ubiquitous CPT-II have been elucidated. The mutations or dysregulation of the CPTs, which are associated with many serious and even fatal diseases, are promising targets for developing drugs to treat type 2 diabetes (T2D) and obesity[14,15]. Dysregulated lipid metabolism is involved in human diseases, including chronic inflammatory diseases and inflammatory-related tumors[16]. CPTs play an important role in lipid metabolism and fatty acid oxidation (FAO) in mitochondria. CPT-II has been confirmed as a rate-limiting enzyme and in regulation of host immune responses[17,18]. However, the pathological role of CPT-II alteration with NAFLD remains to be identified[19]. This review summarizes the latest research findings of CPT-II, which are important for accurate or early monitoring of NAFLD malignant transformation.

CPT2 STRUCTURE

The most important function of the CPT family is to ensure that fatty acids enter the mitochondria for -oxidation. Transmembrane protein CPT-I is located in OMM and CPT-II is in IMM. Human CPT-II gene (CPT2) as an autosomal recessive trait encoded gene localizes on chromosomes 1 (1p32) and the gene

full length contains 3090 nucleotides and 5 exons, which can encode the enzyme protein peptide chain composed of 658 amino acids[20]. Summaries of *CPT2*, CPT-II and total numbers of its reported mutated sites are shown in Table 1. Human CPT-II (NM_000098) is a mitochondrial protein in IMM. CPT-II together with CPT-I oxidize LCFA in the mitochondria and play pivotal roles in the LCFA transport across the mitochondrial membrane for β -oxidation[21]. In molecular genetic aspects, *CPT2* is identified in about 70% of mutant alleles. There are variations in the *CPT2* genome, most of which are single-base substitutions, small insertions or discrete deletions[22,23]. Among the enzymatic system, CPT-II plays a rate-limiting role in the entry of fatty acids into mitochondrial FAO and is considered to be a key component of cellular metabolic homeostasis[24]. Anti-cancer drug oxaliplatin can activate CPT-II in gastrointestinal cancer cells and promote the catabolism of fatty acids[18]. Knocking down of *CPT2* by patient-derived xenograft models confirmed the regulating role of mitochondrial FAO in Src activation and metastasis of breast cancer[25]. However, a subset of substitutions, insertion or deletion, tend to cluster in all exons, especially in exon 4 and exon 5, suggesting that *CPT2* clustering is due to a combination of factors such as the rate of heterogeneous mutations in the genome, biophysical characteristics of exogenous carcinogens, endogenous dysregulation and large mutation events related to genome instability[26].

The enzymatic system that facilitates the transfer is known as CPT mainly in OMM or IMM and plays an important role in maintaining its structural and functional integrity. Liver cells must keep related metabolic homeostasis in a wide range of conditions and meet their ATP needs depending on FAO[27, 28]. CPT-II catalyzes transesterified acylcarnitine's transferred from cytosol into the intermembrane space (IMS) and the remaining acyl of acylcarnitine is changed back to CoA on IMM, which is next available for FAO. Meanwhile, the released carnitine is returned to the IMS of the mitochondrion *via* CACT and is available for fatty acid re-transport[29]. However, the deficiency or gene mutation of CPT-II can significantly affect mitochondrial FAO. Bezafibrate, as a well-known hypolipidemic drug, was tested to stimulate *CPT2* mutation, but it should be a challenge to restore normal LCFA oxidation from a series of other fatty acid mitochondrial diseases[30,31], indicated that CPT-II not only provides ATP for liver cells *via* FAO, but also its down-regulated expression affects the growth and malignant transformation of hepatocytes *via* cell damage, related signal molecules, stem cells, immunology and so on[32]. Therefore, the study of CPT-II will help to understand the pathogenesis and to develop a promising treatment of NAFLD.

Previous studies of *CPT2* mutations have identified the presence of single-base substitutions, and many other events such as double-base and multiple-base substitutions, insertions or deletions. The reported mutations among all five exons of *CPT2* and 89 mutated sites are shown in Table 2[33,34]. Most of *CPT2* or CPT-II mutations are located in exon 4 or exon 5. Biochemical consequences of these mutations are still controversial. The c.338 C>T (P.S113L) variant can be detected in most cases of Caucasians; in Japanese, c.1148 T>A (P.F383Y) is the most frequent variant allele and can obviously cause severe infant forms of symptoms. Among them, it may include deficiency of enzyme protein, enzyme inactivity or abnormality of enzymatic regulation. The protein encoded by this gene is a nuclear protein which is transported to the IMM. Due to the low activity, thermal instability, and short half-life of CPT-II, the CPT II variant exerts a dominant negative effect on homologous tetrameric proteins associated with mitochondrial LCFA oxidation impairment[35]. Recently, based on animal models or clinical studies, the crystal structures of CPT-II were determined in uninhibited forms and in complexes with inhibiting substrate analogs with anti-diabetic features. The crystal structures have a deep understanding of the enzymatic structure-function relationship which is conducive to the discovery of new inhibitors through structure-based drug design[36].

MITOCHONDRIAL CARNITINE SHUTTLE SYSTEM

Using fatty acids as ATP requires more than 20 enzymes and transporters, which are involved in the activation and transport of fatty acids into the mitochondria. The membrane transport system of fatty acid β -oxidation in mitochondria is shown in Figure 1. Mitochondrial FAO is one of the major pathways for fatty acid degradation and is critical for maintaining ATP balance in the human body[37,38]. When the glucose supply is limited, fatty acids are an important source of energy after absorption and during fasting. But even when glucose is sufficient, FAO still is the main source of energy for human tissues. A series of enzymes, transporters and other facilitating proteins with biochemistry and physiological functions are involved in FAO (Figure 1). The role of CPT in the LCFA oxidation, and this system includes CPT-I, carnitine-acylcarnitine translocase (CACT) and CPT-II. The acyl-CoA synthetase located in OMM catalyzes fatty acids to form acyl-CoA with ATP and CoA participation, and then, transports long-chain acyl-CoA by the delivery system into mitochondria, that is a carnitine shuttle system to enter the process for β -oxidation. Most genes encoding CPT-II are known to be recessive genetic defects and the clinical manifestations of the related diseases may include hypoglycemia, cardiomyopathy, arrhythmias and rhabdomyolysis; It also illustrates the importance of FAO during fasting and in liver and (heart) muscle function[39,40].

Table 1 Summary of *CPT2* gene and reported mutation sites

Exon	Size in bp	Nucleotides	Amino acids	Mut. no.	Mutation sites	
					Amino acids	Others
1	668	1-668	1-51	5	2	3
2	81	669-749	52-78	4	2	2
3	107	750-856	79-113	5	3	2
4	1305	857-2161	114-548	59	49	10
5	929	2162-3090	549-658	16	12	4

Mut no.: Total numbers of nucleotide mutation including insertion, delete or peptide variation from codon substitution; Others: Mutations from double or more nucleotide insertion, deletes and so on.

Table 2 List of known human carnitine palmitoyltransferase-II mutated sites[33,34]

Exon	Amino acid substitution	Others
1	Pro41Leu; Pro50His	36-38 insGC; 6_43dupGGGCC; 113_114dupGC
2	Pro55Arg; Ala67Gly	182_203del 22; 153-1G>A (Intron 2) ¹
3	Cys84Arg; Ala101Val; Ser113Leu	256_257delAG; 232+1G>A (Intron 3) ¹
4	Tyr120Cys; Leu121Gln; Arg124Gln; Arg124Ter; Asn146Thr; Arg151Gln; Arg151Trp; Arg161Trp; Lys164Ter; Arg167Gln; Pro173Ser; Glu174Lys; Tyr210Asp; Asp213Gly; Met214Thr; Gln216Arg; Pro227Leu; Arg231Trp; Arg247Trp; Lys274Met; Arg296Gln; Arg296Leu; Arg296Ter; Gly310Gly; Cys326Tyr; Asp328Gly; Met342Thr; Phe352Cys; Val368Ile; His369Gln; Arg382Lys; Phe383Tyr; Gln413Gln; Phe448Leu; Arg450Ter; Gly451Glu; Glu454Ter; Lys457Ter; Tyr479Phe; Tyr479Cys; Gly480Arg; Glu487Lys; Gly497Ser; Ile502Thr; Arg503Cys; Pro504Leu; Phe516Ser; Glu545Ala	1569_1570delCA; 1444_1447delACAG; 1634_1636delAAG; 1646_49del; 1273_1274delAC; 1238_1239delAG; 1543_1546delGCCT; 907_918ins11; 533insT; 534-558del25; 1645+5G>A (Intron 5) ¹
5	Arg560Gln; Leu575Pro; Asp576Gly; Ser588Cys; Ser590Asn; Gly600Arg; Pro604Ser; Val605Leu; Asp608His; Tyr628Ser; Arg631Cys; Leu644Ser	1816_1817delGT; 1923_1935del; 340+1G>A (Intron 4) ¹ ; 340+5G>A (Intron 4) ¹

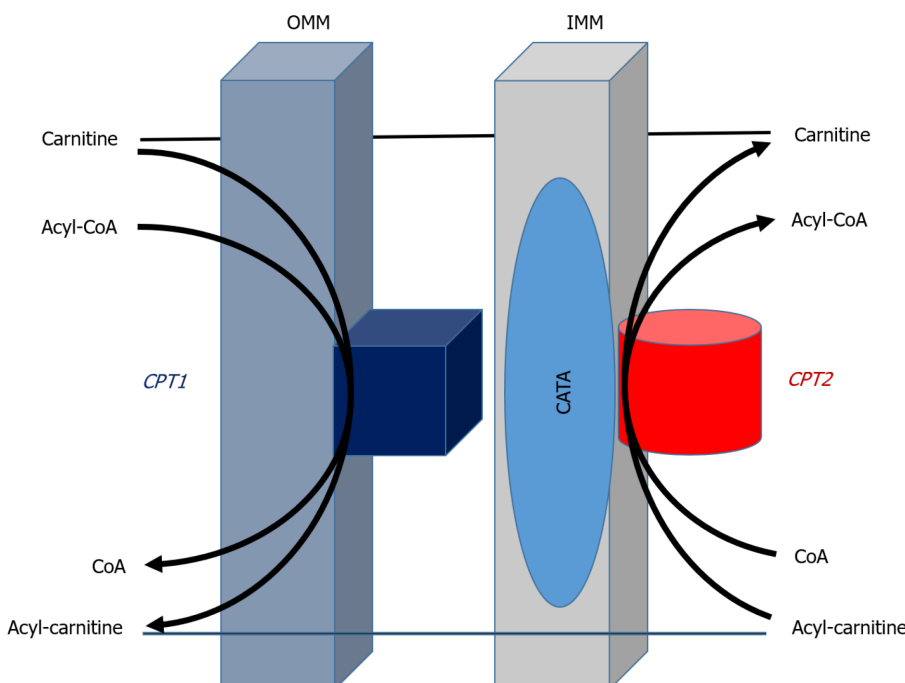
¹Intron.

Mutations are listed on Human Gene Mutation Database from Stenson *et al*[33] and Yao *et al*[30].

The carnitine shuttle system controls fatty acid translocation across the mitochondrial membrane. Key enzymes determine the competition of glycolysis *vs* mitochondrial FAO defined by the Randle cycle. This transport system with CACT is an important part of fatty acid esterification through OMM and IMM of mitochondria (Figure 1). First, CPT-I at OMM catalyzes long-chain acyl-CoA along with carnitine conversion to long-chain acylcarnitine and CoA is transported to the mitochondrial interior with help of translocase on the mitochondrial intima[41,42]. After that, the transesterified acylcarnitine's are transported from the cytosol into the IMM space as CACT acylcarnitine releases carnitine by CPT-II catalysis, and converts it to an acyl group from carnitine to acyl-CoA, available for β -oxidation. Released carnitine returns to the IMM space of the mitochondria for fatty acid re-transport[43]. CPT-II plays an important regulatory role in FAO and its function affects fatty acid metabolism. More importantly, CPTs in the carnitine shuttle system can be used as a drug target to reduce gluconeogenesis or restore liposome balance. Therefore, it has the potential value of gene therapy or immunotherapy, and the further study of the mechanism of CPTs could provide useful ideas for clinical treatment of related diseases[44,45].

EFFECT FACTORS OF CPT-II ACTIVITY

Lipid metabolism involves a variety of biological processes, including the most important lipid metabolic pathway (FAO with carnitine shuttle system). The mutations or dysregulation of hepatic CPT-II have been linked to many serious or even fatal human diseases, and it should be a promising target for developing drugs to treat T2D or obesity[46]. However, the deficiency, over-expression or inactivation of liver CPT-II might ultimately lead to disruption of immune homeostasis, thereby increasing the risk of various inflammatory diseases and even tumors. There is some evidence that CPT-II or the associated mitochondrial LCFA are involved in the development and progression of these related diseases. Thus, the agonists or inhibitors targeting the CPTs or carnitine shuttle system have



DOI: 10.3748/wjg.v29.i12.1765 Copyright ©The Author(s) 2023.

Figure 1 Transport system of fatty acid oxidation in outer mitochondrial membrane and inner mitochondrial membrane[11,65]. Fatty acid β -oxidation is catalyzed by enzymes located in outer and inner mitochondrial membrane to form acyl-coenzyme A (CoA) in the participation with ATP and CoA. Carnitine palmitoyltransferase (CPT)-I promotes the conversion of acyl-CoA to acyl-carnitine that is transported to mitochondrial interior with the help of translocase on the intima of mitochondria. Under the catalysis of CPT-II, acylcarnitine releases carnitine, and then converted to acyl-CoA to enter β -oxidation. The CPT system with carnitine acyl-carnitine translocase play a vital part in the transport system for esterification of fatty acids through the mitochondrial membrane and CPT-II as a key rate-limiting enzyme for fatty acid β -oxidation. OMM: Outer mitochondrial membrane; IMM: Inner mitochondrial membrane; CACT: Carnitine acyl-carnitine translocase; CPT: Carnitine palmitoyltransferase; CoA: Coenzyme A.

emerged as novel therapies for these diseases[47]. Normal function of FAO in IMM is closely dependent on the catalytic activity of CPT-II that could be affected by *CPT2* variation, the amino acid substitution of enzyme, inhibition of enzyme activity, circulating carnitine level and so on.

CPT-II deficiency

Hepatic CPT-II deficiency is one of the most common forms of mitochondrial FAO disorders (FAODs) and have several clinical presentations that have been known for a long time. However, its phenotypic variability remains fascinating[48]. The clinical phenotypes of CPT-II deficiency are classified into muscular, severe infantile and fatal neonatal types. In addition, neonatal-onset CPT-II deficiency is often accompanied by brain and kidney organ dysfunction features, such as in the 1st mo of life, and is almost always fatal. Three different phenotypes (neonatal, infant and adult onset) have been identified, all with autosomal recessive inheritance patterns[49]. The clinical phenotype of adult CPT-II deficiency is mostly benign, and only with additional external stimuli, such as high-intensity exercise, can lead to major myopathy symptoms. However, the perinatal and infantile CPT-II deficiency usually involves multiple organ systems, especially when occurring in the perinatal period as it is the most serious form and is often fatal[50]. The application of mass spectrometry technology to analyze acylcarnitine profiles in blood has revolutionized the FAOD diagnosis, including CPT-II deficiency. In most cases, the number of *CPT2* mutations is increasing and there is a clear genotype-phenotype correlation. However, the clinical variants in some patients might contain other genetic or environmental factors[51].

In the clinical setting, the manifestations of patients with CPT-II deficiency include severe infant liver disorders, myocardial infarction, fatality in neonates and myopathy (usually mild, from infancy to adulthood). Some patients have serious multi-system disease that includes liver function failure, cardiomyopathy, epilepsy, hypoglycemia and premature death, while others are characterized by muscle pain and weakness which is sometimes accompanied by myoglobinuria[52]. The proband was diagnosed for CPT-II deficiency by finding a decrease in muscle CPT activity or by identifying a biallelic variant of *CPT2* in a molecular genetics test. A total of six mutations have been identified, including four new ones. Among those mutations, the S113 L mutation is common in about 50% of the mutant alleles. Three of the six mutations (3/6) have been found in a few unrelated patients, while others have been found in only one family with genetic heterogeneity. To date, about 100 *CPT2* mutations have been discovered. Prenatal diagnosis is provided when the risk of infant/severe CPT-II deficiency is 1/4. Infantile CPT-II presents as a severe hypoglycemic episode of ketoacidosis, occasionally associated with

heart damage and usually resulting in sudden death before age 1[50]. Treatment for CPT2 deficiency includes a low-fat diet in rich triglyceride or carnitine and avoiding fasting or hyperkinesis[53].

Thermal instability of CPT-II

CPT-II activation is associated with disorders of mitochondrial β -oxidation of LCFA in IMM. Based on the crystal structure of mouse CAT, the active site of CPT-II is located at the interface between two domains, extending in tunnels through the enzyme protein centers, alone or in complex with its substrate carnitine or CoA[54]. In this tunnel, carnitine combines with CoA and its opposite is catalytic His³⁴³ residue. The information of CPT-II structure provides a molecular basis to understand the catalytic activity of CAT or to design their inhibitors. In addition, the carnitine might contribute to the catalytic stabilization of oxygen ions in the reaction intermediates. Hepatic CPT-II is sensitive to inhibition by metabolites of fatty acids, Triton X-100, or malonyl-CoA[55].

Artificially recombinant His6-N-hCPT2 and His6-N-hCPT2/S113L showed the same enzymatic activity for wild-type or S113L variants of CPT-II[56]. However, the mutant CPT-II exhibited abnormal destabilization at 40 °C or 45 °C and was more sensitive to be inhibited by malonyl-CoA. The thermal solubility of mutant CPT-II, which may explain the symptoms of CPT-II deficiency may mainly occur during prolonged exercise, infection, and exposure to cold. In addition, CPT II abnormalities are likely to be largely suppressed when fatty acid metabolism is stressed[54]. The unstable CPT II variants with enzymatic inactivity might lower mitochondrial fuel utilization under the phenotypic threshold during patients with hyperthermia, thus suggesting that hepatic CPT-II should play a pathological role in NAFLD progression.

High-risk patients have thermolabile genetic backgrounds of CPT-II in LCFA metabolism. However, until now, no related mutation of CPT-II was reported in NAFLD patients[57,58]. Almost fatal or handicapped virus-associated encephalopathy cases exhibited transiently higher serum LCAC levels during fever more than 40 °C. The specific activity of patients' CPT-II (0.4 ± 0.06 nMol/min/mg) was 36% of normal control (1.1 ± 0.3 nMol/min/mg protein) at 37 °C. The CPT-II specific activity in the patient group was down to 50% for 2 h at 41 °C, and CPT-II in the normal control group still was 91.4%, and the sequencing analysis of patients' CPT2 gene revealed compound (1055T>G/F352C) + (1102G>A/V368I) heterozygous variations[46,59]. F352C substitution was only reported in the Japanese study, and V368I polymorphic variation has relatively mild effects related to CPT-II deficiency[47,60]. The CPT-II mutation or dysregulation has been linked to more serious, even fatal diseases, and these data should be promising molecule targets to develop therapeutic agents for NAFLD in future.

Carnitine level

Carnitine as a substance has a wide range of biological functions, including transport of LCAD from the cytoplasm to the mitochondrial matrix, regulation of acetyl-CoA/CoA, control of acyl transport between organelles and prevention of oxidative stress[58]. Maintaining normal fat metabolism depends on carnitine concentration that is synthesized in most eucaryotic organisms[61]. The methylation of lysine initiates the biosynthesis of carnitine. The formed trimethyllysine is then converted to butylbetaine in all tissues and finally hydroxylated to carnitine in the liver and released from the tissues, which are then actively absorbed by all other tissues[62,63]. This transfer requires the enzyme and transporter that accumulates carnitine within the cell (OCTN2 carnitine transporter), which is conjugated to LCFA (CPT-I), to transfer acylcarnitine's through IMM (CACT), and to transfer carnitines through the IMM (CACT), fatty acids were conjugated back to CoA for subsequent -oxidation (CPT-II). The regulation of carnitine synthesis is still incompletely understood because the turnover of carnitine in the human body is slow[64].

Carnitine is essential for proper fat metabolism, producing ATP, and the transport of LFAC or medium fatty acid chains (MFAC). It attracts LFAC and MFAC, after it breaks them down, and then takes them to the cell's mitochondria for FAO. And as it turns out, the body burns more fat, providing the body with more natural energy in the process[65,66]. According to the previous study, using a carnitine antagonist 3-(2,2,2-trimethylpropionate hydrazine dihydrate, THP) resulted in lipid accumulation with increased liver weight in wild-type mice. The competition between THP and carnitine inhibited CPT-II activity, resulting in carnitine deficiency, acyl CoA and fat accumulation[67]. Clinical data showed that the blood carnitine concentration in NAFLD patients was lower than those in healthy people, and the level in NAFLD cases with liver cirrhosis accounted for only 22% of normal people[68,69]. The concentration of carnitine in patients with liver disease is low, the fat accumulation in rat liver tissue, the content of total fatty acids, free fatty acids, short chain fatty acids (SCFC) and LCFA in liver, and the content of chain, long chain, short chain and total fatty acids in circulating blood also change. During patients with hepatitis B or hepatitis C virus infection, or with mitochondrial FAODs present with NAFLD or severe liver diseases, enough carnitine should play an important role in the mitochondrial carnitine shuttle system, suggesting that circulating carnitine level affects FAO, ameliorates mitochondrial dysfunction, reduces insulin resistance and improves NAFLD progression [70,71].

CPT-II INACTIVITY IN NAFLD

NAFLD pathogenesis is much more complicated with multi-factorial events. Recently, the low activity of CPT-II on IMM during NAFLD progression has attracted much attention both in basic and clinical aspects[72,73]. Although many theories of NAFLD with abnormal lipid metabolism[8,74,75] such as insulin resistance (IR), lipid peroxidation, cytokine expression, iron overload, genetics, environment, immunity, drugs, living habits and so on. However, there are still many problems in the study of NAFLD pathogenesis. According to these theories, the IR stimulates liver fat accumulation and triglycerides, resulting in the first strike to NAFLD formation; then oxidative stress and lipid peroxidation aggravate hepatocyte injury to develop into the second strike that starts with asymptomatic steatosis, and continues to cell inflammation, steatohepatitis, fibrosis or hepatocyte malignant transformation[76, 77]; hence a "multiple hit" hypothesis seems a more accurate proposal[78,79]. Up to now, the new discovery of loss of CPT-II activity has been confirmed in lipid accumulating models that should be one of the NAFLD mechanisms.

Ideal NAFLD models should correctly reflect both histopathology and pathophysiology, and imitate certain aspects of NAFLD which are divided into genetic, dietary and combination models referring to advantages and disadvantages[80,81]. Also, the models based on biological knowledge are reliable and reproducible, having low mortality, and being compatible with simple and feasible methods, not only in elucidating pathogenesis for understanding NAFLD but also in examining therapeutic effects of various agents to develop tools and giving crucial information. Inhibiting CPT-II activity is related to a disorder of lipid metabolism, which may be related to NAFLD pathogenesis and down-regulating CPT-II in liver tissues. Gene defects are associated with mitochondrial LCFA oxidation disorders[82,83].

In order to determine the independent and interdependent roles of triglyceride (TG) hydrolysis and FAO, liver-specific defects in mice were generated in TG hydrolysis (*AtgL*^{-/-}), FAO (*CPT2L*^{-/-}), or both (double knockout)[73,84]. Loss of a single component of FAO [*CPT2*, adipose TG lipase (*Atgl*), and peroxisome proliferators-activated receptor- α (PPAR- α)] resulting in a major independent effect on the morphology of liver cells, gene expression, and intermediate metabolism in response to fasting[84]. However, the mice in the high-fat diet (HFD) model revealed an interdependent role for *Atgl* and *CPT2*, as deletion of only one gene lead to NAFLD; But loss of both components leads to significant hepatocyte inflammation and liver fibrosis[85].

CPT-II IN HEPATOCARCINOGENESIS

During NAFLD progression, the transcription factors E2f1 and E2f2 contributed to NAFLD-associated mice HCC and their involvement in metabolic recombination[72,85]. The expressions of E2f1 and E2f2 were significantly increased in the NAFLD-associated HCC in mice induced with HFD plus diethyl-nitrosamine (Den). However, the *E2f1*^{-/-} and *E2f2*^{-/-} mice were resistant to DEN-HFD-induced hepatocarcinogenesis and were associated with lipid accumulation. The administration of DEN-HFD in the *E2f1*^{-/-} and *E2f2*^{-/-} mice enhanced FAO and increased expression of *CPT2* because of CPT2 as an essential enzyme for FAO, whose down-regulation was linked to the NAFLD-related hepatocarcinogenesis[86]. The mouse models of obesity-driven and NASH-driven HCC typically exhibit robust steatosis in HCC cells, as seem to be seen in the human NASH-HCC. The livers and HCC tissues from diethyl-nitrosamine-injected mice fed either control or HFD were subjected to comprehensive metabolome analysis[80,87]. Extensive acylcarnitine's accumulation was seen in liver cancer tissue and in the sera of HFD-fed mice. A similar increasing level was seen in sera from patients with NASH-associated liver cancer. The increase of acylcarnitine might be related to the CPT-II down-regulation, suggesting that acylcarnitine is a surrogate marker of the down-regulation of CPT-II and directly participates in the development of hepatocarcinogenesis.

The down-regulation of CPT-II caused FAO inhibition which might be the cause of steatosis in HCC. The knockdown of the *CPT2* gene in HCC cells could inhibit the Src-mediated activation of JNK and produce anti-lipotoxicity. Furthermore, oleylcarnitine promotes spheroid formation in HCC cells through STAT3 activation[88,89]. HFD feeding and carnitine supplementation synergistically enhance hepatocarcinogenesis with acylcarnitine accumulation *in vivo*. The CPT-II level in HCC mice was significantly lower than those in control or NAFLD mice, and was negatively correlated with the degree of hepatocyte malignant transformation[90,91]. A series of experiments confirmed that CPT-II was inactivated, suggesting that low CPT-II expression in IMM might lead to liver lipid accumulation and participate in promoting NAFLD malignant transformation[92].

CPT-II INVERSE-CORRELATED WITH HCC MARKERS

Based on clinical and basic evidences, abnormal lipid accumulation was associated with NAFLD malignant transformation. However, only a few studies have been reported on the relationship between CPT-II activation and HCC progression. The alteration of CPT-II expression might be an important link

in the obstruction of FAO and abnormal lipid accumulation[93]. Based on above findings, some scholars sequenced the whole gene of the mitochondrial CPT-II in NAFLD patients, and found that *CPT2* variation was significantly associated with CPT-II activity that might be the key factor of NAFLD or related cirrhosis/HCC because its inactivation is closely related to an energy production disorder in models of NAFLD[94,95]. The dynamic alterations of CPT-II expression located on IMM during malignant transformation of hepatocytes in SD rats induced by chemical carcinogens (2-fluorenlyacetamide, 2-FAA) were investigated under lipid accumulation[19]. For the first time, the progressively decreasing expression of CPT-II at mRNA or protein level were reported, and the significantly increasing HCC related to molecular markers were confirmed during the rat hepatocarcinogenesis.

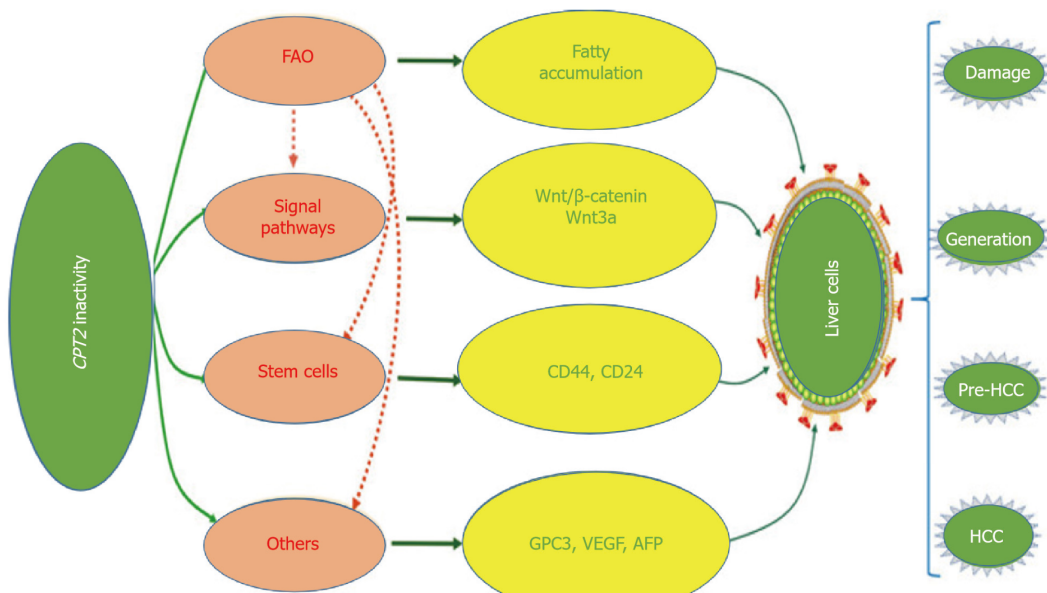
There has been a rise in the prevalence of NAFLD, paralleling a worldwide increase in MAFLD and HCC[96]. According to the dynamic pathological alterations of the model, a continuum of morphological abnormalities on liver sections has a variable course, from normal hepatocytes, lipid accumulation, cell denaturation, precancerous lesion and HCC formation. Compared with the control liver sections, there was a large amount of fat in the hepatocytes of the model rats by the oil red O staining; In the meantime, transmembrane glycoprotein CD44 activation promotes inflammatory cell recruitment and plays a key role of being linked to NAFLD progression to HCC[97-99]. CPT-II has been demonstrated to interact in forming supramolecular complexes that facilitate the passage of acylcarnitine and its expression was gradually decreased in malignant transformation of hepatocytes in NAFLD. However, the reported HCC biomarkers such as AFP, GPC3[100] and Wnt3a[101] were significantly increasing expressions in hepatocarcinogenesis except for CD44 as one of the most frequently reported cancer stem-like cell markers[102]. These data suggested that the alteration of CPT-II expression should be associated with the malignant progression of NAFLD.

Metabolically related NAFLD is emerging as a major cause of HCC in Western countries[103-105]. This presents an additional challenge, as NAFLD-related HCC tend to be advanced in elderly patients with comorbidities and their prognosis is very poor[106]. The pathogenesis of NAFLD-associated HCC is multifactorial and remains to be identified, although the risk of hepatocarcinogenesis is undoubtedly increased as NAFLD progresses to NASH and cirrhosis[107]. The new findings of CPT-II are useful for understanding NAFLD and HCC and should hopefully lead to the development of clinically relevant biomarkers and strategies to help identify high-risk patients, early use of preventive measures or better treatment[108]. Energy metabolism is a prerequisite for maintaining normal life activities. NAFLD is caused by excessive lipid accumulation in hepatocytes and is regarded as one of the most common liver diseases[109,110]. The down-regulation of *CPT2* in IMM was one of the main causes of acyl carnitine accumulation, which was also seen in malignant transformation of hepatocytes, suggesting that CPT-II inactivity or dysfunction might become a new mechanism of blocked lipid oxidation for HCC.

CONCLUSION

Owing to its high prevalence and potential risk, NAFLD has become a major health concern worldwide. Hepatocyte CPT-II variation or activity alteration undoubtedly has a significant impact on aggravating liver fatty accumulation, inducing activation of cancer-related stem cells, and malignant transformation of hepatocytes (Figure 2), especially in patients with HBV chronic infection. The phenomenon of CPT-II inactivation as warning signs of NAFLD malignant transformation needs attention. However, its specific regulatory mechanism is unknown, so this is a good research prospect. At present, the exact relationship between CPT-II and NAFLD remains to be explored. It is believed that with the vigorous development of molecular biological theory and technology, understanding the function of CPT-II physiology will continue to deepen, which has guided significant knowledge for CPT-II alteration during NAFLD progression. At the same time, it also brings hope and provides a theoretical basis for the assumption of early intervention of NAFLD or human related diseases and CPT-II can be used as a molecular target for monitoring or therapy.

Hepatocyte CPT-II variation or activity alteration undoubtedly has a significant impact on aggravating liver fatty accumulation, inducing activation of cancer-related stem cells, and malignant transformation of hepatocytes.



DOI: 10.3748/wjg.v29.i12.1765 Copyright ©The Author(s) 2023.

Figure 2 Carnitine palmitoyltransferase-II inactivity in hepatocarcinogenesis. Disorder of lipid metabolism may be related to the pathogenesis of nonalcoholic fatty liver disease with malignant transformation of hepatocytes. AFP: Alpha-fetoprotein; CoA: Coenzyme A; CPT2: Carnitine palmitoyl transferase 2; FAO: Fatty acid oxidation; HCC: Hepatocellular carcinoma; VEGF: Vascular endothelial-derived growth factor.

FOOTNOTES

Author contributions: Yao M, Zhou P and Qin YY contributed equally to this work, designed, collected and analyzed the data, prepared the first draft and performed subsequent revisions; Yao DF and Wang L provided critical review; All authors have read and agreed to the published version of the manuscript.

Supported by the National Natural Science Foundation of China, No. 81873915 and No. 31872738; the Key Plan of Nantong S&T Development, No. MS12020021; and the S&T Program of Medical School of Nantong University, No. TDYX2021010.

Conflict-of-interest statement: All the authors report no relevant conflicts of interest for this article.

Open-Access: This article is an open-access article that was selected by an in-house editor and fully peer-reviewed by external reviewers. It is distributed in accordance with the Creative Commons Attribution NonCommercial (CC BY-NC 4.0) license, which permits others to distribute, remix, adapt, build upon this work non-commercially, and license their derivative works on different terms, provided the original work is properly cited and the use is non-commercial. See: <https://creativecommons.org/Licenses/by-nc/4.0/>

Country/Territory of origin: China

ORCID number: Min Yao 0000-0002-5473-0186; Ping Zhou 0000-0002-9957-8704; Yan-Yan Qin 0000-0001-9181-4074; Li Wang 0000-0003-2838-9807; Deng-Fu Yao 0000-0002-3448-7756.

S-Editor: Gong ZM

L-Editor: Filipodia

P-Editor: Gong ZM

REFERENCES

- 1 Stefan N, Cusi K. A global view of the interplay between non-alcoholic fatty liver disease and diabetes. *Lancet Diabetes Endocrinol* 2022; **10**: 284-296 [PMID: 35183303 DOI: 10.1016/S2213-8587(22)00003-1]
- 2 Segura-Azuara NLÁ, Varela-Chinchilla CD, Trinidad-Calderón PA. MAFLD/NAFLD Biopsy-Free Scoring Systems for Hepatic Steatosis, NASH, and Fibrosis Diagnosis. *Front Med (Lausanne)* 2021; **8**: 774079 [PMID: 35096868 DOI: 10.3389/fmed.2021.774079]
- 3 Rohm TV, Meier DT, Olefsky JM, Donath MY. Inflammation in obesity, diabetes, and related disorders. *Immunity* 2022; **55**: 31-55 [PMID: 35021057 DOI: 10.1016/j.jimmuni.]
- 4 Lazarus JV, Mark HE, Anstee QM, Arab JP, Batterham RL, Castera L, Cortez-Pinto H, Crespo J, Cusi K, Dirac MA,

Francque S, George J, Hagström H, Huang TT, Ismail MH, Kautz A, Sarin SK, Loomba R, Miller V, Newsome PN, Ninburg M, Ocamo P, Ratziu V, Rinella M, Romero D, Romero-Gómez M, Schattenberg JM, Tsochatzis EA, Valenti L, Wong VW, Yilmaz Y, Younossi ZM, Zelber-Sagi S; NAFLD Consensus Consortium. Advancing the global public health agenda for NAFLD: a consensus statement. *Nat Rev Gastroenterol Hepatol* 2022; **19**: 60-78 [PMID: 34707258 DOI: 10.1038/s41575-021-00523-4]

5 **Tacke F**, Weiskirchen R. Non-alcoholic fatty liver disease (NAFLD)/non-alcoholic steatohepatitis (NASH)-related liver fibrosis: mechanisms, treatment and prevention. *Ann Transl Med* 2021; **9**: 729 [PMID: 33987427 DOI: 10.21037/atm-20-4354]

6 **Tamaki N**, Ajmera V, Loomba R. Non-invasive methods for imaging hepatic steatosis and their clinical importance in NAFLD. *Nat Rev Endocrinol* 2022; **18**: 55-66 [PMID: 34815553 DOI: 10.1038/s41574-021-00584-0]

7 **Scorletti E**, Carr RM. A new perspective on NAFLD: Focusing on lipid droplets. *J Hepatol* 2022; **76**: 934-945 [PMID: 34793866 DOI: 10.1016/j.jhep.2021.11.009]

8 **Foerster F**, Gairing SJ, Müller L, Galle PR. NAFLD-driven HCC: Safety and efficacy of current and emerging treatment options. *J Hepatol* 2022; **76**: 446-457 [PMID: 34555422 DOI: 10.1016/j.jhep.2021.09.007]

9 **Du D**, Liu C, Qin M, Zhang X, Xi T, Yuan S, Hao H, Xiong J. Metabolic dysregulation and emerging therapeutical targets for hepatocellular carcinoma. *Acta Pharm Sin B* 2022; **12**: 558-580 [PMID: 35256934 DOI: 10.1016/j.apsb.2021.09.019]

10 **Metwally M**, Berg T, Tsochatzis EA, Eslam M. Translation Reprogramming as a Novel Therapeutic Target in MAFLD. *Adv Biol (Weinh)* 2022; **6**: e2101298 [PMID: 35240009 DOI: 10.1002/adbi.202101298]

11 **Bonnefont JP**, Djouadi F, Prip-Buus C, Gobin S, Munnich A, Bastin J. Carnitine palmitoyltransferases 1 and 2: biochemical, molecular and medical aspects. *Mol Aspects Med* 2004; **25**: 495-520 [PMID: 15363638 DOI: 10.1016/j.mam.2004.06.004]

12 **Weber M**, Mera P, Casas J, Salvador J, Rodríguez A, Alonso S, Sebastián D, Soler-Vázquez MC, Montironi C, Recalde S, Fuchó R, Calderón-Domínguez M, Mir JF, Bartrons R, Escola-Gil JC, Sánchez-Infantes D, Zorzano A, Llorente-Cortes V, Casals N, Valenti V, Frühbeck G, Herrero L, Serra D. Liver CPT1A gene therapy reduces diet-induced hepatic steatosis in mice and highlights potential lipid biomarkers for human NAFLD. *FASEB J* 2020; **34**: 11816-11837 [PMID: 32666604 DOI: 10.1096/fj.202000678R]

13 **Sangineto M**, Bukke VN, Bellanti F, Tamborra R, Moola A, Duda L, Villani R, Romano AD, Serviddio G. A Novel Nutraceuticals Mixture Improves Liver Steatosis by Preventing Oxidative Stress and Mitochondrial Dysfunction in a NAFLD Model. *Nutrients* 2021; **13** [PMID: 33671262 DOI: 10.3390/nu13020652]

14 **Li L**, Yang X. The Essential Element Manganese, Oxidative Stress, and Metabolic Diseases: Links and Interactions. *Oxid Med Cell Longev* 2018; **2018**: 7580707 [PMID: 29849912 DOI: 10.1155/2018/7580707]

15 **Zhou R**, Lin C, Cheng Y, Zhuo X, Li Q, Xu W, Zhao L, Yang L. Liraglutide Alleviates Hepatic Steatosis and Liver Injury in T2MD Rats via a GLP-1R Dependent AMPK Pathway. *Front Pharmacol* 2020; **11**: 600175 [PMID: 33746742 DOI: 10.3389/fphar.]

16 **Dall M**, Hassing AS, Treebak JT. NAD⁺ and NAFLD - caution, causality and careful optimism. *J Physiol* 2022; **600**: 1135-1154 [PMID: 33932956 DOI: 10.1113/JP280908]

17 **Petrick HL**, Holloway GP. Cytosolic reverse CrAT activity in cardiac tissue: potential importance for fuel selection. *Biochem J* 2018; **475**: 1267-1269 [PMID: 29632149 DOI: 10.1042/BCJ20180121]

18 **Wang Y**, Lu JH, Wang F, Wang YN, He MM, Wu QN, Lu YX, Yu HE, Chen ZH, Zhao Q, Liu J, Chen YX, Wang DS, Sheng H, Liu ZX, Zeng ZL, Xu RH, Ju HQ. Inhibition of fatty acid catabolism augments the efficacy of oxaliplatin-based chemotherapy in gastrointestinal cancers. *Cancer Lett* 2020; **473**: 74-89 [PMID: 31904482 DOI: 10.1016/j.canlet.2019.12.036]

19 **Gu JJ**, Yao M, Yang J, Cai Y, Zheng WJ, Wang L, Yao DB, Yao DF. Mitochondrial carnitine palmitoyl transferase-II inactivity aggravates lipid accumulation in rat hepatocarcinogenesis. *World J Gastroenterol* 2017; **23**: 256-264 [PMID: 28127199 DOI: 10.3748/wjg.v23.i2.256]

20 **Rufer AC**, Thoma R, Hennig M. Structural insight into function and regulation of carnitine palmitoyltransferase. *Cell Mol Life Sci* 2009; **66**: 2489-2501 [PMID: 19430727 DOI: 10.1007/s00018-009-0035-1]

21 **Rufer AC**, Thoma R, Benz J, Stihle M, Gsell B, De Roo E, Banner DW, Mueller F, Chomienne O, Hennig M. The crystal structure of carnitine palmitoyltransferase 2 and implications for diabetes treatment. *Structure* 2006; **14**: 713-723 [PMID: 16615913 DOI: 10.1016/j.str.2006.01.008]

22 **Trauner M**, Fuchs CD. Novel therapeutic targets for cholestatic and fatty liver disease. *Gut* 2022; **71**: 194-209 [PMID: 34615727 DOI: 10.1136/gutjnl-2021-324305]

23 **Filali-Moucef Y**, Hunter C, Roccio F, Zagkou S, Dupont N, Primard C, Proikas-Cezanne T, Reggiori F. The ménage à trois of autophagy, lipid droplets and liver disease. *Autophagy* 2022; **18**: 50-72 [PMID: 33794741 DOI: 10.1080/15548627.2021.1895658]

24 **Han S**, Wei R, Zhang X, Jiang N, Fan M, Huang JH, Xie B, Zhang L, Miao W, Butler AC, Coleman MA, Vaughan AT, Wang Y, Chen HW, Liu J, Li JJ. CPT1A/2-Mediated FAO Enhancement-A Metabolic Target in Radioresistant Breast Cancer. *Front Oncol* 2019; **9**: 1201 [PMID: 31803610 DOI: 10.3389/fonc.2019.01201]

25 **Park JH**, Vithayathil S, Kumar S, Sung PL, Dobrolecki LE, Putluri V, Bhat VB, Bhowmik SK, Gupta V, Arora K, Wu D, Tsouko E, Zhang Y, Maity S, Donti TR, Graham BH, Frigo DE, Coarfa C, Yotnda P, Putluri N, Sreekumar A, Lewis MT, Creighton CJ, Wong LC, Kaipparettu BA. Fatty Acid Oxidation-Driven Src Links Mitochondrial Energy Reprogramming and Oncogenic Properties in Triple-Negative Breast Cancer. *Cell Rep* 2016; **14**: 2154-2165 [PMID: 26923594 DOI: 10.1016/j.celrep.2016.02.004]

26 **de Carvalho Ribeiro M**, Szabo G. Role of the Inflammasome in Liver Disease. *Annu Rev Pathol* 2022; **17**: 345-365 [PMID: 34752711 DOI: 10.1146/annurev-pathmechdis-032521-102529]

27 **Rufer AC**, Lomize A, Benz J, Chomienne O, Thoma R, Hennig M. Carnitine palmitoyltransferase 2: analysis of membrane association and complex structure with a substrate analog. *FEBS Lett* 2007; **581**: 3247-3252 [PMID: 17585909 DOI: 10.1016/j.febslet.]

28 **Song A**, Park Y, Kim B, Lee SG. Modulation of Lipid Metabolism by Trans-Anethole in Hepatocytes. *Molecules* 2020;

25: 4946 [PMID: 33114589 DOI: 10.3390/molecules]

29 **Wang J**, Xiang H, Lu Y, Wu T, Ji G. The role and therapeutic implication of CPTs in fatty acid oxidation and cancers progression. *Am J Cancer Res* 2021; **11**: 2477-2494 [PMID: 34249411]

30 **Yao M**, Cai M, Yao D, Xu X, Yang R, Li Y, Zhang Y, Kido H. Abbreviated half-lives and impaired fuel utilization in carnitine palmitoyltransferase II variant fibroblasts. *PLoS One* 2015; **10**: e0119936 [PMID: 25781464 DOI: 10.1371/journal.]

31 **Yao M**, Yao D, Yamaguchi M, Chida J, Kido H. Bezafibrate upregulates carnitine palmitoyltransferase II expression and promotes mitochondrial energy crisis dissipation in fibroblasts of patients with influenza-associated encephalopathy. *Mol Genet Metab* 2011; **104**: 265-272 [PMID: 21816645 DOI: 10.1016/j.ymgme.2011.07.009]

32 **Gu JJ**, Yao M, Cai Y, Fang M, Wang L, Zheng WJ, Yao DB, Dong ZZ, Yao DF. [Dynamic expression of carnitine palmitoyltransferase II in the mitochondrial inner membrane during hepatocyte malignant transformation induced by lipid accumulation]. *Zhonghua Gan Zang Bing Za Zhi* 2017; **25**: 279-284 [PMID: 28494547 DOI: 10.3760/cma.j.issn.1007-3418.2017.04.009]

33 **Stenson PD**, Ball EV, Mort M, Phillips AD, Shaw K, Cooper DN. The Human Gene Mutation Database (HGMD) and its exploitation in the fields of personalized genomics and molecular evolution. *Curr Protoc Bioinformatics* 2012; **Chapter 1**: Unit1.13 [PMID: 22948725 DOI: 10.1002/0471250953.bi0113s39]

34 **Xue Y**, Chen Y, Ayub Q, Huang N, Ball EV, Mort M, Phillips AD, Shaw K, Stenson PD, Cooper DN, Tyler-Smith C; 1000 Genomes Project Consortium. Deleterious- and disease-allele prevalence in healthy individuals: insights from current predictions, mutation databases, and population-scale resequencing. *Am J Hum Genet* 2012; **91**: 1022-1032 [PMID: 23217326 DOI: 10.1016/j.ajhg.2012.10.015]

35 **Lehmann D**, Zierz S. Normal protein content but abnormally inhibited enzyme activity in muscle carnitine palmitoyltransferase II deficiency. *J Neurol Sci* 2014; **339**: 183-188 [PMID: 24602495 DOI: 10.1016/j.jns.2014.02.011]

36 **Yao D**, Mizuguchi H, Yamaguchi M, Yamada H, Chida J, Shikata K, Kido H. Thermal instability of compound variants of carnitine palmitoyltransferase II and impaired mitochondrial fuel utilization in influenza-associated encephalopathy. *Hum Mutat* 2008; **29**: 718-727 [PMID: 18306170 DOI: 10.1002/humu.20717]

37 **Houten SM**, Violante S, Ventura FV, Wanders RJ. The Biochemistry and Physiology of Mitochondrial Fatty Acid β -Oxidation and Its Genetic Disorders. *Annu Rev Physiol* 2016; **78**: 23-44 [PMID: 26474213 DOI: 10.1146/annurev-physiol-021115-105045]

38 **Fucho R**, Casals N, Serra D, Herrero L. Ceramides and mitochondrial fatty acid oxidation in obesity. *FASEB J* 2017; **31**: 1263-1272 [PMID: 28003342 DOI: 10.1096/fj.]

39 **Angajala A**, Lim S, Phillips JB, Kim JH, Yates C, You Z, Tan M. Diverse Roles of Mitochondria in Immune Responses: Novel Insights Into Immuno-Metabolism. *Front Immunol* 2018; **9**: 1605 [PMID: 30050539 DOI: 10.3389/fimmu.2018.01605]

40 **Serra D**, Mera P, Malandrino MI, Mir JF, Herrero L. Mitochondrial fatty acid oxidation in obesity. *Antioxid Redox Signal* 2013; **19**: 269-284 [PMID: 22900819 DOI: 10.1089/ars.2012.4875]

41 **Schlaepfer IR**, Joshi M. CPT1A-mediated Fat Oxidation, Mechanisms, and Therapeutic Potential. *Endocrinology* 2020; **161**: bqz046 [PMID: 31900483 DOI: 10.1210/endocr/bqz046]

42 **Casals N**, Zammit V, Herrero L, Fadó R, Rodríguez-Rodríguez R, Serra D. Carnitine palmitoyltransferase 1C: From cognition to cancer. *Prog Lipid Res* 2016; **61**: 134-148 [PMID: 26708865 DOI: 10.1016/j.plipres.2015.11.004]

43 **Isackson PJ**, Bennett MJ, Vladutiu GD. Identification of 16 new disease-causing mutations in the CPT2 gene resulting in carnitine palmitoyltransferase II deficiency. *Mol Genet Metab* 2006; **89**: 323-331 [PMID: 16996287 DOI: 10.1016/j.ymgme.2006.08.004]

44 **Qu Q**, Zeng F, Liu X, Wang QJ, Deng F. Fatty acid oxidation and carnitine palmitoyltransferase I: emerging therapeutic targets in cancer. *Cell Death Dis* 2016; **7**: e2226 [PMID: 27195673 DOI: 10.1038/cddis.2016.132]

45 **Eng JM**, Estall JL. Diet-Induced Models of Non-Alcoholic Fatty Liver Disease: Food for Thought on Sugar, Fat, and Cholesterol. *Cells* 2021; **10** [PMID: 34359974 DOI: 10.3390/cells10071805]

46 **Cacciola NA**, Sgadari M, Sepe F, Petillo O, Margarucci S, Martano M, Maiolino P, Restucci B. Metabolic Flexibility in Canine Mammary Tumors: Implications of the Carnitine System. *Animals (Basel)* 2021; **11** [PMID: 34679988 DOI: 10.3390/ani11102969]

47 **Wang M**, Wang K, Liao X, Hu H, Chen L, Meng L, Gao W, Li Q. Carnitine Palmitoyltransferase System: A New Target for Anti-Inflammatory and Anticancer Therapy? *Front Pharmacol* 2021; **12**: 760581 [PMID: 34764874 DOI: 10.3389/fphar.2021.]

48 **Mccormick BJ**, Chirila RM. Carnitine palmitoyltransferase-II deficiency: case presentation and review of the literature. *Rom J Intern Med* 2021; **59**: 420-424 [PMID: 34118800 DOI: 10.2478/rjim-2021-0021]

49 **Sigauke E**, Rakheja D, Kitson K, Bennett MJ. Carnitine palmitoyltransferase II deficiency: a clinical, biochemical, and molecular review. *Lab Invest* 2003; **83**: 1543-1554 [PMID: 14615409 DOI: 10.1097/01.lab.0000098428.51765.83]

50 **Tajima G**, Hara K, Yuasa M. Carnitine palmitoyltransferase II deficiency with a focus on newborn screening. *J Hum Genet* 2019; **64**: 87-98 [PMID: 30514913 DOI: 10.1038/s10038-018-0530-z]

51 **Lehmann D**, Motlagh L, Robaa D, Zierz S. Muscle Carnitine Palmitoyltransferase II Deficiency: A Review of Enzymatic Controversy and Clinical Features. *Int J Mol Sci* 2017; **18** [PMID: 28054946 DOI: 10.3390/ijms]

52 **Kilfoyle D**, Hutchinson D, Potter H, George P. Recurrent myoglobinuria due to carnitine palmitoyltransferase II deficiency: clinical, biochemical, and genetic features of adult-onset cases. *N Z Med J* 2005; **118**: U1320 [PMID: 15776096]

53 **Taggart RT**, Smail D, Apolito C, Vladutiu GD. Novel mutations associated with carnitine palmitoyltransferase II deficiency. *Hum Mutat* 1999; **13**: 210-220 [PMID: 10090476 DOI: 10.1002/(SICI)1098-1004(1999)13:3<210::AID-HUMU5>3.0.CO;2-0]

54 **Joshi PR**, Deschauer M, Zierz S. Carnitine palmitoyltransferase II (CPT II) deficiency: genotype-phenotype analysis of 50 patients. *J Neurol Sci* 2014; **338**: 107-111 [PMID: 24398345 DOI: 10.1016/j.jns.2013.12.026]

55 **Jogl G**, Hsiao YS, Tong L. Structure and function of carnitine acyltransferases. *Ann N Y Acad Sci* 2004; **1033**: 17-29

[PMID: 15591000 DOI: 10.1196/annals.1320.002]

56 **Motlagh L**, Golbik R, Sippl W, Zierz S. Stabilization of the thermolabile variant S113L of carnitine palmitoyltransferase II. *Neurol Genet* 2016; **2**: e53 [PMID: 27123472 DOI: 10.1212/NXG.0000000000000053]

57 **Dang Y**, Xu J, Zhu M, Zhou W, Zhang L, Ji G. Gan-Jiang-Ling-Zhu decoction alleviates hepatic steatosis in rats by the miR-138-5p/CPT1B axis. *Biomed Pharmacother* 2020; **127**: 110127 [PMID: 32325349 DOI: 10.1016/j.bioph.2020.110127]

58 **Xu A**, Wang B, Fu J, Qin W, Yu T, Yang Z, Lu Q, Chen J, Chen Y, Wang H. Diet-induced hepatic steatosis activates Ras to promote hepatocarcinogenesis via CPT1a. *Cancer Lett* 2019; **442**: 40-52 [PMID: 30401637 DOI: 10.1016/j.canlet.2018.10.024]

59 **Yao D**, Yao M, Yamaguchi M, Chida J, Kido H. Characterization of compound missense mutation and deletion of carnitine palmitoyltransferase II in a patient with adenovirus-associated encephalopathy. *J Med Invest* 2011; **58**: 210-218 [PMID: 21921422 DOI: 10.2152/jmi.58.210]

60 **Jogl G**, Tong L. Crystal structure of carnitine acetyltransferase and implications for the catalytic mechanism and fatty acid transport. *Cell* 2003; **112**: 113-122 [PMID: 12526798 DOI: 10.1016/S0092-8674(02)01228-X]

61 **Abolfathi M**, Mohd-Yusof BN, Hanipah ZN, Mohd Redzwan S, Yusof LM, Khosroshahi MZ. The effects of carnitine supplementation on clinical characteristics of patients with non-alcoholic fatty liver disease: A systematic review and meta-analysis of randomized controlled trials. *Complement Ther Med* 2020; **48**: 102273 [PMID: 31987257 DOI: 10.1016/j.ctim.2019.102273]

62 **Li N**, Zhao H. Role of Carnitine in Non-alcoholic Fatty Liver Disease and Other Related Diseases: An Update. *Front Med (Lausanne)* 2021; **8**: 689042 [PMID: 34434943 DOI: 10.3389/fmed.2021.689042]

63 **Savic D**, Hodson L, Neubauer S, Pavlides M. The Importance of the Fatty Acid Transporter L-Carnitine in Non-Alcoholic Fatty Liver Disease (NAFLD). *Nutrients* 2020; **12** [PMID: 32708036 DOI: 10.3390/nu12082178]

64 **Baker PR 2nd**, Friedman JE. Mitochondrial role in the neonatal predisposition to developing nonalcoholic fatty liver disease. *J Clin Invest* 2018; **128**: 3692-3703 [PMID: 30168806 DOI: 10.1172/JCI120846]

65 **Poulos JE**, Kalogerinis PT, Milanov V, Kalogerinis CT, Poulos EJ. The Effects of Vitamin E, Silymarin and Carnitine on the Metabolic Abnormalities Associated with Nonalcoholic Liver Disease. *J Diet Suppl* 2022; **19**: 287-302 [PMID: 33491528 DOI: 10.1080/19390211.2021.1874587]

66 **Sogabe M**, Okahisa T, Kurihara T, Takehara M, Kagemoto K, Okazaki J, Kida Y, Hirao A, Tanaka H, Tomonari T, Taniguchi T, Okamoto K, Nakasono M, Takayama T. Differences among patients with and without nonalcoholic fatty liver disease having elevated alanine aminotransferase levels at various stages of metabolic syndrome. *PLoS One* 2020; **15**: e0238388 [PMID: 32866186 DOI: 10.1371/journal.pone.0238388]

67 **Gu J**, Yao M, Yao D, Wang L, Yang X. Nonalcoholic Lipid Accumulation and Hepatocyte Malignant Transformation. *J Clin Transl Hepatol* 2016; **4**: 123-130 [PMID: 27350942 DOI: 10.14218/JCTH.2016.00010]

68 **Enooku K**, Nakagawa H, Fujiwara N, Kondo M, Minami T, Hoshida Y, Shibahara J, Tateishi R, Koike K. Altered serum acylcarnitine profile is associated with the status of nonalcoholic fatty liver disease (NAFLD) and NAFLD-related hepatocellular carcinoma. *Sci Rep* 2019; **9**: 10663 [PMID: 31337855 DOI: 10.1038/s41598-019-47216-2]

69 **da Silva RP**, Kelly KB, Al Rajabi A, Jacobs RL. Novel insights on interactions between folate and lipid metabolism. *Biofactors* 2014; **40**: 277-283 [PMID: 24353111 DOI: 10.1002/biof.1154]

70 **Giannakouli VG**, Dubovan P, Papoutsi E, Kataki A, Koskinas J. Senescence in HBV-, HCV- and NAFLD- Mediated Hepatocellular Carcinoma and Senotherapy: Current Evidence and Future Perspective. *Cancers (Basel)* 2021; **13** [PMID: 34572959 DOI: 10.3390/cancers13184732]

71 **Das UN**. Beneficial role of bioactive lipids in the pathobiology, prevention, and management of HBV, HCV and alcoholic hepatitis, NAFLD, and liver cirrhosis: A review. *J Adv Res* 2019; **17**: 17-29 [PMID: 31193303 DOI: 10.1016/j.jare.2018.12.006]

72 **González-Romero F**, Mestre D, Aurrekoetxea I, O'Rourke CJ, Andersen JB, Woodhoo A, Tamayo-Caro M, Varela-Rey M, Palomo-Irigoyen M, Gómez-Santos B, de Urturi DS, Núñez-García M, García-Rodríguez JL, Fernández-Ares L, Buqué X, Iglesias-Ara A, Bernales I, De Juan VG, Delgado TC, Goikoetxea-Usandizaga N, Lee R, Bhanot S, Delgado I, Perugorria MJ, Errazti G, Mosteiro L, Gatzambide S, Martinez de la Piscina I, Irizubia P, Crespo J, Banales JM, Martínez-Chantar ML, Castaño L, Zubiaga AM, Aspichuela P. E2F1 and E2F2-Mediated Repression of CPT2 Establishes a Lipid-Rich Tumor-Promoting Environment. *Cancer Res* 2021; **81**: 2874-2887 [PMID: 33771899 DOI: 10.1158/0008-5472.CAN-20-2052]

73 **Fujiwara N**, Nakagawa H, Enooku K, Kudo Y, Hayata Y, Nakatsuka T, Tanaka Y, Tateishi R, Hikiba Y, Misumi K, Tanaka M, Hayashi A, Shibahara J, Fukayama M, Arita J, Hasegawa K, Hirschfield H, Hoshida Y, Hirata Y, Otsuka M, Tateishi K, Koike K. CPT2 downregulation adapts HCC to lipid-rich environment and promotes carcinogenesis via acylcarnitine accumulation in obesity. *Gut* 2018; **67**: 1493-1504 [PMID: 29437870 DOI: 10.1136/gutnl-2017-315193]

74 **Cheung KP**, Taylor KR, Jameson JM. Immunomodulation at epithelial sites by obesity and metabolic disease. *Immunol Res* 2012; **52**: 182-199 [PMID: 22160809 DOI: 10.1007/s12026-011-8261-7]

75 **Dhamija E**, Paul SB, Kedia S. Non-alcoholic fatty liver disease associated with hepatocellular carcinoma: An increasing concern. *Indian J Med Res* 2019; **149**: 9-17 [PMID: 31115369 DOI: 10.4103/ijmr.IJMR_1456_17]

76 **Oseini AM**, Sanyal AJ. Therapies in non-alcoholic steatohepatitis (NASH). *Liver Int* 2017; **37** Suppl 1: 97-103 [PMID: 28052626 DOI: 10.1111/liv.13302]

77 **Stefan N**, Häring HU, Cusi K. Non-alcoholic fatty liver disease: causes, diagnosis, cardiometabolic consequences, and treatment strategies. *Lancet Diabetes Endocrinol* 2019; **7**: 313-324 [PMID: 30174213 DOI: 10.1016/S2213-8587(18)30154-2]

78 **Pinweha P**, Rattanapornsompong K, Charoensawan V, Jitrapakdee S. MicroRNAs and oncogenic transcriptional regulatory networks controlling metabolic reprogramming in cancers. *Comput Struct Biotechnol J* 2016; **14**: 223-233 [PMID: 27358718 DOI: 10.1016/j.csbj.2016.05.005]

79 **Yi YS**. Regulatory Roles of Caspase-11 Non-Canonical Inflammasome in Inflammatory Liver Diseases. *Int J Mol Sci* 2022; **23** [PMID: 35563377 DOI: 10.3390/ijms23094986]

80 **Lee J**, Choi J, Selen Alpergin ES, Zhao L, Hartung T, Scafidi S, Riddle RC, Wolfgang MJ. Loss of Hepatic Mitochondrial Long-Chain Fatty Acid Oxidation Confers Resistance to Diet-Induced Obesity and Glucose Intolerance. *Cell Rep* 2017; **20**: 655-667 [PMID: 28723568 DOI: 10.1016/j.celrep.2017.06.080]

81 **Selen ES**, Choi J, Wolfgang MJ. Discordant hepatic fatty acid oxidation and triglyceride hydrolysis leads to liver disease. *JCI Insight* 2021; **6** [PMID: 33491665 DOI: 10.1172/jci.insight.135626]

82 **Liu X**, Zhang J, Ming Y, Chen X, Zeng M, Mao Y. The aggravation of mitochondrial dysfunction in nonalcoholic fatty liver disease accompanied with type 2 diabetes mellitus. *Scand J Gastroenterol* 2015; **50**: 1152-1159 [PMID: 25877002 DOI: 10.3109/00365521.2015.1030687]

83 **Jun DW**, Cho WK, Jun JH, Kwon HJ, Jang KS, Kim HJ, Jeon HJ, Lee KN, Lee HL, Lee OY, Yoon BC, Choi HS, Hahn JS, Lee MH. Prevention of free fatty acid-induced hepatic lipotoxicity by carnitine via reversal of mitochondrial dysfunction. *Liver Int* 2011; **31**: 1315-1324 [PMID: 22093454 DOI: 10.1111/j.1478-3231.2011.02602.x]

84 **Amato A**, Caldara GF, Nuzzo D, Baldassano S, Picone P, Rizzo M, Mulè F, Di Carlo M. NAFLD and Atherosclerosis Are Prevented by a Natural Dietary Supplement Containing Curcumin, Silymarin, Guggul, Chlorogenic Acid and Inulin in Mice Fed a High-Fat Diet. *Nutrients* 2017; **9** [PMID: 28505074 DOI: 10.3390/nu9050492]

85 **Lee Y**, Kim BR, Kang GH, Lee GJ, Park YJ, Kim H, Jang HC, Choi SH. The Effects of PPAR Agonists on Atherosclerosis and Nonalcoholic Fatty Liver Disease in ApoE-/-FXR-/- Mice. *Endocrinol Metab (Seoul)* 2021; **36**: 1243-1253 [PMID: 34986301 DOI: 10.3803/EnM.2021.1100]

86 **Kim JH**, Lee BR, Choi ES, Lee KM, Choi SK, Cho JH, Jeon HB, Kim E. Reverse Expression of Aging-Associated Molecules through Transfection of miRNAs to Aged Mice. *Mol Ther Nucleic Acids* 2017; **6**: 106-115 [PMID: 28325277 DOI: 10.1016/j.omtn.]

87 **Schulien I**, Hasselblatt P. Diethylnitrosamine-induced liver tumorigenesis in mice. *Methods Cell Biol* 2021; **163**: 137-152 [PMID: 33785162 DOI: 10.1016/bs.mcb.2020.08.006]

88 **Attia YM**, Tawfiq RA, Gibrel AA, Ali AA, Kassem DH, Hammam OA, Elmazar MM. Activation of FXR modulates SOCS3/Jak2/STAT3 signaling axis in a NASH-dependent hepatocellular carcinoma animal model. *Biochem Pharmacol* 2021; **186**: 114497 [PMID: 33675775 DOI: 10.1016/j.bcp.2021.114497]

89 **Zhou M**, Mok MT, Sun H, Chan AW, Huang Y, Cheng AS, Xu G. The anti-diabetic drug exenatide, a glucagon-like peptide-1 receptor agonist, counteracts hepatocarcino-genesis through cAMP-PKA-EGFR-STAT3 axis. *Oncogene* 2017; **36**: 4135-4149 [PMID: 28319060 DOI: 10.1038/onc.2017.38]

90 **Khan H**, Ullah H, Nabavi SM. Mechanistic insights of hepatoprotective effects of curcumin: Therapeutic updates and future prospects. *Food Chem Toxicol* 2019; **124**: 182-191 [PMID: 30529260 DOI: 10.1016/j.fct.2018.12.002]

91 **Holczbauer Á**, Wangensteen KJ, Shin S. Cellular origins of regenerating liver and hepatocellular carcinoma. *JHEP Rep* 2022; **4**: 100416 [PMID: 35243280 DOI: 10.1016/]

92 **Brown ZJ**, Fu Q, Ma C, Kruhlak M, Zhang H, Luo J, Heinrich B, Yu SJ, Zhang Q, Wilson A, Shi ZD, Swenson R, Greten TF. Carnitine palmitoyltransferase gene upregulation by linoleic acid induces CD4⁺ T cell apoptosis promoting HCC development. *Cell Death Dis* 2018; **9**: 620 [PMID: 29795111 DOI: 10.1038/s41419-018-0687-6]

93 **Paul B**, Lewinska M, Andersen JB. Lipid alterations in chronic liver disease and liver cancer. *JHEP Rep* 2022; **4**: 100479 [PMID: 35469167 DOI: 10.1016/j.jhep.2022.100479]

94 **Ham JR**, Lee HI, Choi RY, Sim MO, Seo KI, Lee MK. Anti-steatotic and anti-inflammatory roles of syringic acid in high-fat diet-induced obese mice. *Food Funct* 2016; **7**: 689-697 [PMID: 26838182 DOI: 10.1039/c5fo01329a]

95 **Liu Q**, Pan R, Ding L, Zhang F, Hu L, Ding B, Zhu L, Xia Y, Dou X. Rutin exhibits hepatoprotective effects in a mouse model of non-alcoholic fatty liver disease by reducing hepatic lipid levels and mitigating lipid-induced oxidative injuries. *Int Immunopharmacol* 2017; **49**: 132-141 [PMID: 28577437 DOI: 10.1016/j.intimp.2017.05.026]

96 **Friedman SL**, Neuschwander-Tetri BA, Rinella M, Sanyal AJ. Mechanisms of NAFLD development and therapeutic strategies. *Nat Med* 2018; **24**: 908-922 [PMID: 29967350 DOI: 10.1038/s41591-018-0104-9]

97 **Patouraux S**, Rousseau D, Bonnafous S, Lebeaupin C, Luci C, Canivet CM, Schneck AS, Bertola A, Saint-Paul MC, Iannelli A, Gugenheim J, Anty R, Tran A, Bailly-Maitre B, Gual P. CD44 is a key player in non-alcoholic steatohepatitis. *J Hepatol* 2017; **67**: 328-338 [PMID: 28323124 DOI: 10.1016/j.jhep.2017.03.003]

98 **Egan CE**, Daugherty EK, Rogers AB, Abi Abdallah DS, Denkers EY, Maurer KJ. CCR2 and CD44 promote inflammatory cell recruitment during fatty liver formation in a lithogenic diet fed mouse model. *PLoS One* 2013; **8**: e65247 [PMID: 23762326 DOI: 10.1371/journal.pone.0065247]

99 **Fang M**, Yao M, Yang J, Zheng WJ, Wang L, Yao DF. Abnormal CD44 activation of hepatocytes with nonalcoholic fatty accumulation in rat hepatocarcinogenesis. *World J Gastrointest Oncol* 2020; **12**: 66-76 [PMID: 31966914 DOI: 10.4251/wjgo.v12.i1.66]

100 **Yao M**, Yao DF, Bian YZ, Zhang CG, Qiu LW, Wu W, Sai WL, Yang JL, Zhang HJ. Oncofetal antigen glycan-3 as a promising early diagnostic marker for hepatocellular carcinoma. *Hepatobiliary Pancreat Dis Int* 2011; **10**: 289-294 [PMID: 21669573 DOI: 10.1016/S1499-3872(11)60048-9]

101 **Yao M**, Yang JL, Wang DF, Wang L, Chen Y, Yao DF. Encouraging specific biomarkers-based therapeutic strategies for hepatocellular carcinoma. *World J Clin Cases* 2022; **10**: 3321-3333 [PMID: 35611205 DOI: 10.12998/wjcc.v10.i11.3321]

102 **Wu XF**, Sha CX, Yang JL, Liu Y, Zhou P, Yao DF, Yao M. [Abnormal expression of CD44 aggravates liver disease progression in patients with non-alcoholic fatty liver disease accompanied with hepatitis B virus replication]. *Zhonghua Gan Zang Bing Za Zhi* 2021; **29**: 1083-1088 [PMID: 34933427 DOI: 10.3760/cma.j.cn501113-20210713-00338]

103 **Anstee QM**, Reeves HL, Kotsilitsi E, Govaere O, Heikenwalder M. From NASH to HCC: current concepts and future challenges. *Nat Rev Gastroenterol Hepatol* 2019; **16**: 411-428 [PMID: 31028350 DOI: 10.1038/s41575-019-0145-7]

104 **Meroni M**, Longo M, Rustichelli A, Dongiovanni P. Nutrition and Genetics in NAFLD: The Perfect Binomium. *Int J Mol Sci* 2020; **21** [PMID: 32340286 DOI: 10.3390/ijms21082986]

105 **Singal AG**, Lampertico P, Nahon P. Epidemiology and surveillance for hepatocellular carcinoma: New trends. *J Hepatol* 2020; **72**: 250-261 [PMID: 31954490 DOI: 10.1016/j.jhep.2019.08.025]

106 **Geh D**, Anstee QM, Reeves HL. NAFLD-Associated HCC: Progress and Opportunities. *J Hepatocell Carcinoma* 2021; **8**:

223-239 [PMID: 33854987 DOI: 10.2147/]

107 **Harris PS**, Hansen RM, Gray ME, Massoud OI, McGuire BM, Shoreibah MG. Hepatocellular carcinoma surveillance: An evidence-based approach. *World J Gastroenterol* 2019; **25**: 1550-1559 [PMID: 30983815 DOI: 10.3748/wjg.v25.i13.1550]

108 **Fujiwara N**, Friedman SL, Goossens N, Hoshida Y. Risk factors and prevention of hepatocellular carcinoma in the era of precision medicine. *J Hepatol* 2018; **68**: 526-549 [PMID: 28989095 DOI: 10.1016/j.jhep.2017.09.016]

109 **Márquez-Quiroga LV**, Arellanes-Robledo J, Vásquez-Garzón VR, Villa-Treviño S, Muriel P. Models of nonalcoholic steatohepatitis potentiated by chemical inducers leading to hepatocellular carcinoma. *Biochem Pharmacol* 2022; **195**: 114845 [PMID: 34801522 DOI: 10.1016/j.bcp.2021.114845]

110 **Clutton-Brock TH**, Iason GR. Sex ratio variation in mammals. *Q Rev Biol* 1986; **61**: 339-374 [PMID: 3532167 DOI: 10.1186/s12885-022-09433-3]

Submit a Manuscript: <https://www.f6publishing.com>

World J Gastroenterol 2023 March 28; 29(12): 1779-1794

DOI: [10.3748/wjg.v29.i12.1779](https://doi.org/10.3748/wjg.v29.i12.1779)

ISSN 1007-9327 (print) ISSN 2219-2840 (online)

REVIEW

Obesity and novel management of inflammatory bowel disease

Jee Hyun Kim, Chang-Myung Oh, Jun Hwan Yoo

Specialty type: Gastroenterology and hepatology

Jee Hyun Kim, Jun Hwan Yoo, Department of Gastroenterology, CHA Bundang Medical Center, CHA University School of Medicine, Seongnam 13496, South Korea

Provenance and peer review:
Invited article; Externally peer reviewed.

Chang-Myung Oh, Department of Biomedical Science and Engineering, Gwangju Institute of Science and Technology, Gwangju 62465, South Korea

Peer-review model: Single blind

Jun Hwan Yoo, Institute of Basic Medical Sciences, CHA University School of Medicine, Seongnam 13496, South Korea

Peer-review report's scientific quality classification
Grade A (Excellent): A
Grade B (Very good): B
Grade C (Good): 0
Grade D (Fair): 0
Grade E (Poor): 0

Corresponding author: Jun Hwan Yoo, MD, PhD, Associate Professor, Department of Gastroenterology, CHA Bundang Medical Center, CHA University School of Medicine, 59 Yatap-ro, Bundang-gu, Seongnam 13496, South Korea. jhyoo@cha.ac.kr

P-Reviewer: Liu D, China; Nambi G, Saudi Arabia

Received: October 29, 2022

Peer-review started: October 29, 2022

First decision: January 3, 2023

Revised: January 13, 2023

Accepted: March 14, 2023

Article in press: March 14, 2023

Published online: March 28, 2023



Abstract

Obesity is prevalent within the inflammatory bowel disease (IBD) population, particularly in newly developed countries. Several epidemiological studies have suggested that 15%-40% of IBD patients are obese, and there is a potential role of obesity in the pathogenesis of IBD. The dysfunction of mesenteric fat worsens the inflammatory course of Crohn's disease and may induce formation of strictures or fistulas. Furthermore, obesity may affect the disease course or treatment response of IBD. Given the increasing data supporting the pathophysiologic and epidemiologic relationship between obesity and IBD, obesity control is being suggested as a novel management for IBD. Therefore, this review aimed to describe the influence of obesity on the outcomes of IBD treatment and to present the current status of pharmacologic or surgical anti-obesity treatments in IBD patients.

Key Words: Obesity; Inflammatory bowel disease; Crohn's disease; Ulcerative colitis

©The Author(s) 2023. Published by Baishideng Publishing Group Inc. All rights reserved.

Core Tip: Obesity is prevalent within the inflammatory bowel disease (IBD) population, particularly in newly developed countries. The dysfunction of mesenteric fat worsens the inflammatory course of Crohn's disease and may induce formation of strictures or fistulas. Furthermore, obesity may affect the disease course or treatment response of IBD. Along with the increasing data that support pathophysiologic and epidemiologic relationship between obesity and IBD, attention is being focused on obesity control as a novel management of IBD. The main purpose of this review is to describe the influence of obesity on the outcomes of IBD treatment and to present the current status of pharmacologic or surgical anti-obesity treatments in IBD patients.

Citation: Kim JH, Oh CM, Yoo JH. Obesity and novel management of inflammatory bowel disease. *World J Gastroenterol* 2023; 29(12): 1779-1794

URL: <https://www.wjgnet.com/1007-9327/full/v29/i12/1779.htm>

DOI: <https://dx.doi.org/10.3748/wjg.v29.i12.1779>

INTRODUCTION

Inflammatory bowel disease (IBD), including Crohn's disease (CD) and ulcerative colitis (UC), is a chronic inflammatory condition with an unclear etiology and pathophysiology that remain to be fully elucidated[1,2]. Obesity is a pathological condition in which there is an abnormal or excessive accumulation of body fat resulting from an imbalance between energy intake and consumption. In Western populations, a body mass index (BMI) exceeding 25 kg/m² is commonly classified as an overweight condition, and a BMI over 30 kg/m² is regarded as an obese condition. In Asian populations, the diagnostic thresholds for obesity and overweight have been established as BMIs of 25 kg/m² and 23 kg/m², respectively[3]. Obesity is a clear risk factor for a spectrum of chronic diseases, including type 2 diabetes, cardiovascular disease, respiratory problems, and cancer. Moreover, obesity is also associated with the occurrence of autoimmune diseases such as rheumatoid arthritis, psoriasis, and systemic lupus erythematosus[4].

The worldwide prevalence of obesity has nearly tripled since 1975[5], and IBD has also shown a similar trend[6]. This analogous increase is perhaps related to lifestyle changes caused by westernization and urbanization, including the lack of exercise and a westernized diet, which are common risk factors for obesity and IBD. Historically, it has been common for clinicians to associate IBD patients with a low or normal BMI due to the complications of IBD such as decreased food intake, malabsorption, weight loss, and nutritional deficiencies. However, obesity is increasingly being associated with IBD due to its overall pro-inflammatory effect. Several epidemiological studies have suggested that 15%-40% of IBD patients are obese[7-11], and hypothesize that obesity contributes to the development of IBD. Furthermore, obesity may affect the disease course or treatment response of IBD. With the increasing data supporting pathophysiologic and epidemiologic relationship between obesity and IBD, research interest on interventions for obesity as a novel management of IBD is also increasing.

The present review aims to provide a comprehensive summary of the pathophysiology of obesity in IBD, the influence of obesity on IBD outcomes, the effect of obesity on IBD management, and the potential impact of obesity treatment on IBD outcomes. Further, this review aimed to present the current status of anti-obesity treatments in IBD patients.

PREVALENCE OF OBESITY IN IBD PATIENTS

Previous studies have reported that 15%-40% of IBD patients are obese and 20%-40% are overweight[7-11]. Additionally, severe obesity (BMI ≥ 40 kg/m²) is also reported in 2%-3.2% of IBD patients[7]. The prevalence of obesity among IBD patients has been observed to increase over time, which appears to correspond with the global trend of rising obesity rates. A single-center study in France confirmed that the proportion of obesity among CD patients from 1974 to 2000 increased from 1.7% before 1981 to 4% after 1990[12]. A single-center study in Korea, utilizing data from the Asan IBD Registry from 1989 to 2016, reported that out of 6803 patients diagnosed with IBD, 16 with CD and 27 with UC were classified as obese (BMI ≥ 30 kg/m²). The study did not reveal any clinically meaningful differences between the obese and non-obese patient groups[13]. An analysis of 10282 CD patients enrolled in a randomized controlled clinical trial revealed a significant increase in mean BMI at enrollment, which rose from 20.8 kg/m² in 1991 to 27.0 kg/m² in 2008[14].

RELATIONSHIP BETWEEN OBESITY AND IBD

Obesity as a precursor to the onset of IBD

Obesity may be a potential risk factor for developing IBD, particularly CD (Table 1). In the United States Nurses' Health Study, which followed around 110000 women, found that obesity at age 18 was a significant predictor for the development of CD but not UC, when compared to individuals with a normal BMI [adjusted hazard ratio (aHR) = 2.33; 95% confidence interval (CI): 1.15-4.69][15]. This study exhibited that a higher degree of weight gain (between the ages of 18 and enrolment) was linked with elevated risk of developing CD (weight gain > 13.6 kg vs < 2.3 kg; HR = 1.52; 95%CI: 0.87-2.65). The Copenhagen School Health Records Register cohort study investigated the potential association between BMI during the ages of 7 to 13 years and the onset of adult-onset IBD[16]. Obesity in early adolescence has been shown to increase the risk of CD before the age of 30 years (HR = 1.2; 95%CI: 1.1-1.3) while decreasing the risk of UC (HR = 0.9; 95%CI: 0.9-1.0). In a recent meta-analysis of five prospective cohort studies, obesity was found to be associated with an elevated risk of developing older-onset CD, while no significant association was found with UC[17]. The analysis showed that obese patients had an increased risk of developing CD compared to those with a normal BMI (aHR = 1.34; 95%CI: 1.05-1.71; $I^2 = 0\%$). Moreover, every 5 kg/m² increase in baseline BMI was found to correspond to a 16% increase in the risk of CD (aHR = 1.16; 95%CI: 1.05-1.22; $I^2 = 0\%$). However, the European Prospective Investigation into Cancer and Nutrition-IBD study, which involved a large sample size, concluded no significant correlation between BMI and the incidence of IBD, showing contrasting results to previous studies[18].

Obesity caused by IBD

Weight gain may occur during the treatment of IBD. Several preclinical data suggest that, in IBD patients, imbalance of gut microbiota and altered metabolic intestinal signaling mediated by hormones, bile acids, and satiety-related peptides have been implicated in the development of obesity and dysmetabolism[19,20]. Smoking cessation as a lifestyle modification and utilization of corticosteroids could affect the weight gain in IBD patients[21,22]. Additionally, there are a few studies investigating weight gain among IBD patients treated with biologic therapies, especially anti-tumor necrosis factor alpha (TNF)- α therapy. In 21 CD patients, total abdominal fat increased by 18% after 8 wk of infliximab induction therapy ($P = 0.027$)[23]. A recent retrospective study examined the longitudinal changes in weight among patients with IBD receiving different biologic drugs including infliximab, adalimumab, vedolizumab and ustekinumab[24]. The study revealed a statistically significant increase in body weight over time among patients receiving infliximab and vedolizumab, with the infliximab/vedolizumab group experiencing a greater degree of weight gain as compared to the adalimumab group. Moreover, observed weight gain among IBD patients undergoing biologic therapy was found to be linked with other clinical factors, such as male gender, high levels of C-reactive protein (CRP), and low serum albumin.

OBESITY AND IBD PATHOGENESIS

Obesity induces a chronic, low-grade inflammatory state, characterized by the release of multiple pro-inflammatory signaling molecules from hypertrophic adipocytes in mesenteric visceral adipose tissue (VAT)[25-27]. Mesenteric VAT is characterized by the presence of M1 macrophages that secrete a variety of inflammatory cytokines and it has the potential to affect intestinal barrier function[28,29]. Several studies have established a relationship between adipocyte mass and the degree of cytokine expression [30]. Obesity has been shown to be positively associated with visceral adiposity, as determined by volumetric cross-sectional imaging analysis. Furthermore, in obese individuals, there is a direct correlation between visceral adiposity and circulating levels of interleukin-6 (IL-6). Additionally, BMI has been found to be linked with increased levels of CRP in this population[31].

Other mechanisms of obesity in IBD include intestinal barrier dysfunction and alterations in the intestinal microbiota (Figure 1). Obesity and IBD are associated with dysbiosis along with a reduction in bacterial diversity[32]. High fat diet during obesity decreases the diversity of the gut microbiota (dysbiosis), which, in turn, leads to the reduction of anti-inflammatory bacterial species or metabolites. These changes can trigger innate immune system by activation of pattern recognition receptors, including Nod-like receptors or Toll-like receptors, which are present on intestinal epithelial cells or dendritic cells. Pro-inflammatory cytokines secreted from innate immune system can also contribute to increased intestinal permeability, which may increase the risk of bacterial translocation[17,25]. Numerous studies have demonstrated that impaired gut barrier function is a characteristic feature of obesity. This dysfunction permit increased bacterial translocation, leading to the subsequent initiation of systemic inflammation[33,34].

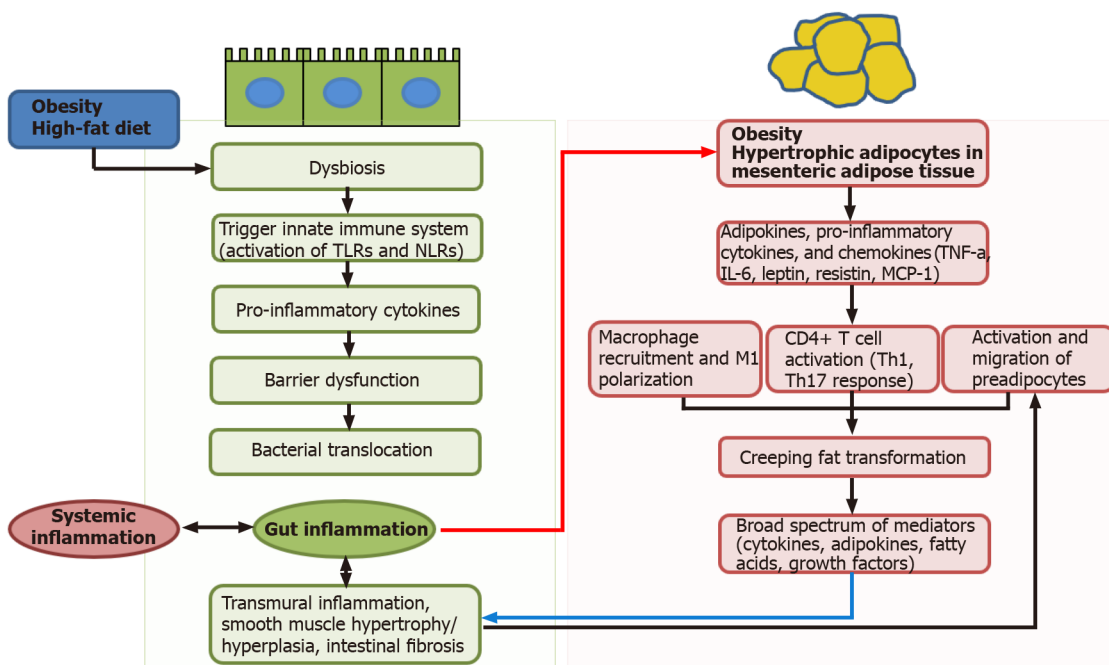
Accumulating evidence suggests a connection between changes in the mesenteric fat and IBD, in particular CD[27]. Intestinal barrier dysfunction and transmural inflammation may induce bacterial translocation to the surrounding mesenteric adipose tissue, which subsequently leads to the adipocyte

Table 1 Relationship between obesity and inflammatory bowel disease (obesity as a precursor to the onset of inflammatory bowel disease)

Ref.	Study design and study population	Key findings
Khalili et al[15], 2015	United States Nurses' Health Study cohort study: Prospective cohort study of United States women ($n = 111498$ women); BMI at age 18, baseline, and every 2 yr since baseline was obtained; 2028769 person-years of follow up. CD ($n = 153$); UC ($n = 229$)	Obesity at age 18 was an independent risk factor for the development of CD compared to normal BMI (aHR = 2.33, 95%CI: 1.15-4.69). No association between BMI at age 18, baseline BMI, and updated BMI and risk of UC. Higher weight gain was associated with increased risk of CD ($P_{trend} = 0.04$). A greater magnitude of weight gain (from age 18 to age at enrolment) associated with increased risk of developing CD (weight gain > 13.6 kg vs < 2.3 kg, HR = 1.52, 95%CI: 0.87-2.65). No association between weight change (from age 18 to baseline) and risk of UC ($P_{trend} = 0.17$) (weight gain > 13.6 kg vs < 2.3 kg, HR = 0.92, 95%CI: 0.60-1.40)
Harpsøe et al[101], 2014	Danish National Birth Cohort study: A large population-based cohort study ($n = 75008$ women); BMI: Obtained at study baseline (based on prepregnancy body weight); median 11.4 yr of follow-up. CD ($n = 138$); UC ($n = 394$)	An increased risk of developing fetal CD in both underweight (HR = 2.57, 95%CI: 1.30-5.06) and obese women (HR = 1.88, 95%CI: 1.02-3.47) compared with normal-weight women, pointing to a U-shaped association. No association between pregnancy obesity and risk of developing UC (HR = 0.77, 95%CI: 0.48-1.25)
Jensen et al[16], 2018	Copenhagen School Health Records Register cohort study: Cohort from the Copenhagen School Health Records Register ($n = 316799$); relationship between BMI in the ages of 7 to 13 yr and adult-onset IBD; BMI: Obtained at ages 7 through 13 yr; approximately 10 million person-years of follow-up. CD ($n = 1500$); UC ($n = 2732$)	Obesity in early adolescence (at each age from 7 to 13 yr) increased the risk of CD diagnosed before age 30 yr (HR = 1.2, 95%CI: 1.1-1.3) while decreasing the risk of UC (HR = 0.9, 95%CI: 0.9-1.0). No associations between changes in BMI between 7 and 13 yr and later risk of CD or UC
Chan et al [17], 2022	Pooled analysis of 5 prospective cohort studies from the Dietary and Environmental Factors IN-IBD study ($n = 601009$): BMI: Obtained at study baseline and during follow-up period; 10110018 person-years of follow-up. CD ($n = 563$); UC ($n = 1047$)	Obesity was associated with an increased risk of older-onset CD but not UC. The risk of developing CD increased in obese patients compared against those with a normal BMI (aHR = 1.34, 95%CI: 1.05-1.7, $I^2 = 0\%$). Each 5 kg/m ² increment in baseline BMI was associated with a 16% increase in risk of CD (aHR = 1.16, 95%CI: 1.05-1.22; $I^2 = 0\%$). With each 5 kg/m ² increment in early adulthood BMI (age 18-20 years), there was a 22% increase in risk of CD (pooled aHR = 1.22, 95%CI: 1.05-1.40, $I^2 = 13.6\%$). An increase in waist-hip ratio was associated with an increased risk of CD that did not reach statistical significance (pooled aHR across quartiles = 1.08, 95%CI: 0.97-1.19, $I^2 = 0\%$). No associations were observed between measures of obesity and risk of UC. For every 5 kg/m ² increase in BMI, the multivariable-adjusted HR was 1.00 (95%CI: 0.90-1.05). For every 5 kg/m ² increase in early adulthood BMI, the multivariable-aHR for UC was 1.05 (95%CI: 0.90-1.22, $I^2 = 0\%$)
Chan et al [18], 2013	European Prospective Investigation into Cancer and Nutrition-IBD study ($n = 300724$): BMI: Obtained at study baseline and during follow-up period. CD ($n = 75$); UC ($n = 177$)	No associations with the four higher categories of BMI compared with a normal BMI for UC ($P_{trend} = 0.36$) or CD ($P_{trend} = 0.83$). The lack of associations was consistent when BMI was analyzed as a continuous or binary variable (BMI $18.5 < 25.0$ vs ≥ 25 kg/m ²). Physical activity and total energy intake, factors that influence BMI, did not show any association with UC (physical activity, $P_{trend} = 0.79$; total energy intake, $P_{trend} = 0.18$) or CD (physical activity, $P_{trend} = 0.42$; total energy, $P_{trend} = 0.11$)

BMI: Body mass index; IBD: Inflammatory bowel disease; aHR: Adjusted hazard ratio; CI: Confidence interval; CD: Crohn's disease; US: Ulcerative colitis.

hypertrophy (red arrow, Figure 1). The hypertrophic adipocytes releases pro-inflammatory cytokines, adipokines, and chemokines such as TNF- α , IL-6, leptin, resistin, and monocyte chemoattractant protein-1). These pro-inflammatory mediators can induce the infiltration of M1 macrophages and CD4+ T cell activation into T helper (Th) 1 and Th17 cells[35]. This process may contribute to the development of hypertrophic mesenteric fat wrapping around the inflamed intestine, known as "creeping fat" that is pathognomonic of CD[27]. Creeping fat itself is thought to be an intrinsic component of inflammatory dysregulation in the pathogenesis of CD. Compared to other VAT, creeping fat demonstrates greater immunological activity. Additionally, there is a significant correlation between the extent of creeping fat and the degree of histological inflammation, as well as the level of infiltration by lymphocytes or macrophages[36]. In addition, the creeping fat formation may be induced by migration of preadipocytes from mesenteric VAT in response to the increased fibronectin signal released from activated muscularis propria smooth muscle cells in inflamed gut[37]. The presence of creeping fat in CD patients has been associated with various pathological changes, including muscularis propria hyperplasia, transmural inflammation, and intestinal fibrosis. These alterations may contribute to the stricturing form of the disease[37,38]. Notably, creeping fat has been found to contain higher levels of fibrotic tissue and T cells in the ileum, as compared to colonic fat from patients with either CD or UC[39]. Creeping fat secretes a broad spectrum of pro-inflammatory and pro-fibrotic mediators such as adipokines, cytokines, fatty acids, and growth factors[40]. Moreover, expression of leptin and adiponectin is elevated in the creeping fat of CD patients. The severity and activity of CD have been correlate with the levels of other adipokines, including resistin[41]. A case-control study showed that the gene expression profile of creeping fat in CD patients was similar to that of VAT from obese patients, indicating a greater inflammatory state as compared to VAT obtained from non-obese individuals[42].



DOI: 10.3748/wjg.v29.i12.1779 Copyright ©The Author(s) 2023.

Figure 1 High fat or Western diets decreases the diversity of the gut microbiota (dysbiosis), leading to the reduction of anti-inflammatory bacterial species or metabolites. These changes can trigger innate immune system by activation of pattern recognition receptors such as Toll-like receptors or Nod-like receptors on intestinal epithelial cells or innate immune cells. Pro-inflammatory cytokines secreted from innate immune system induces barrier dysfunction and subsequent bacterial translocation. Low grade chronic inflammation in gut and bacterial translocation to mesenteric adipose tissue leads to the adipocyte hypertrophy (red arrow). The hypertrophic adipocytes release adipokines, pro-inflammatory cytokines, and chemokines such as tumor necrosis factor alpha, interleukin-6, leptin, resistin, and monocyte chemoattractant protein-1. These pro-inflammatory mediators can induce macrophage recruitment and polarization and CD4+ T cell activation into T helper 1 (Th1) and Th17 cells. Finally, this process can drive the hypertrophic mesenteric fat wrapping around the inflamed bowel, creeping fat. Creeping fat secretes a broad spectrum of mediators, and induce smooth muscle hypertrophy/hyperplasia, transmural inflammation, intestinal fibrosis. TLR: Toll-like receptor; NLR: Nod-like receptor; TNF- α : Tumor necrosis factor alpha; IL-6: Interleukin; MCP-1: Monocyte chemoattractant protein 1; Th: T helper.

IMPACT OF OBESITY ON THE NATURAL HISTORY AND OUTCOMES OF IBD

The effect of obesity on the disease phenotype of IBD remains uncertain. While a retrospective review has indicated that obesity may be a risk factor for perineal disease in IBD[12], other studies have not found any differences in disease distribution or behavior between patients with UC or CD who are obese compared to those who are not[8,43]. Obesity has been linked to increased disease activity and unfavorable clinical outcomes in several chronic inflammatory diseases, such as psoriasis and rheumatoid arthritis[44,45]. However, evidence regarding the effect of obesity on outcomes in IBD is limited and inconclusive. A study of 581 IBD patients showed that obese individuals had significantly lower frequencies of hospitalization (42.1% vs 66.0%, $P < 0.001$) and a reduced likelihood of requiring surgical intervention (41.1% vs 61.1%, $P = 0.02$), when compared to those patients with normal BMI[8]. However, in other population-based study for 143190 IBD patients, it was demonstrated that obesity was an independent predictor of higher rates of all-cause re-admission at both 30 d [18% vs 13%; adjusted odds ratio (aOR) = 1.16; $P = 0.005$] and 90 d (29% vs 21%; aOR = 1.27; $P < 0.0001$), in comparison with non-obese patients[46]. A systematic review reported that there is no significant difference in the rates of corticosteroid usage, hospitalization, surgical intervention, or emergency room visits between obese and normal-weight individuals with IBD[7]. This finding has been supported by a recent retrospective study conducted in South Korea, which found no significant differences in clinical features or treatment outcomes between obese and non-obese patients with IBD, as measured by the cumulative probabilities of receiving various treatments[13].

In CD, many studies show that obesity may indeed have a beneficial effect. A previous report supports this hypothesis by showing that the small VAT adipocytes in CD patients exhibit higher anti-inflammatory genes, which implies a potential protective role of VAT in CD[42]. A retrospective analysis of 221 patients with CD found that an increase of 1 kg/m² in BMI at diagnosis led to a 5% reduction in the risk of requiring surgical intervention in the future (HR = 0.95; 95%CI: 0.91-0.99). Whereas, the risk of corticosteroid use or future hospitalization did not differ[47]. The results of a retrospective study showed that obese patients with CD had lower frequencies of corticosteroid usage, anti-TNF treatment, hospitalization, and surgery in contrast to those with normal weight[8]. However, there were also contrasting results. For instance, one study reported that obese patients with CD were more at risk of active disease (OR = 1.50; 95%CI: 1.07-2.11) or hospitalization (OR = 2.35; 95%CI: 1.56-

3.52)[12]. Alternatively, a prospective case-control study revealed no correlation between BMI and the risk of undergoing surgery or using corticosteroids in the future[9].

In UC, several studies suggest that obesity may have a worse prognosis. In one population-based cohort study that included 267 patients with UC, each incremental increase in BMI by 1 kg/m² was associated with a 3.4% increase in the risk of hospitalization ($P = 0.052$) and a 6% increase in the risk of surgery ($P = 0.01$)[47]. A recent population-based cohort of 417 UC patients, of whom 20.6% were obese, confirmed that obesity among individuals with UC may have unfavorable prognostic implication, particularly with regards to the subsequent hospitalization (HR = 1.72; 95%CI: 1.10-2.71; $P = 0.018$) and corticosteroid usage (HR = 1.026; 95%CI: 1.00-1.05; $P = 0.05$) in comparison to patients with normal weight[48]. Moreover, an increase of 1 kg/m² in BMI was associated with a 5% escalation in the probability of subsequent hospitalization (HR = 1.05; 95%CI: 1.01-1.08; $P = 0.008$) and a 2.6% increase in the chance of requiring corticosteroid usage (HR = 1.026; 95%CI: 1.00-1.05; $P = 0.05$). However, the retrospective analysis of 284 UC patients showed that obese people displayed a reduced risk of developing complications[8].

IMPACT OF OBESITY ON THE MANAGEMENT OF IBD

Medical management

There is evidence to suggest that obesity may be an adverse prognostic factor in a patient's response to drug therapy. The reason being obesity is considered a chronic inflammatory state and obesity can affect the pharmacokinetics of drugs. Obesity may decrease drug half-life and trough levels due to an increase in drug clearance and volume of distribution.

Immunomodulators: Despite extensive clinical experience with thiopurine, few studies have evaluated clinical predictors of response to thiopurine in IBD. A retrospective study of 1176 IBD patients evaluating azathioprine responsiveness based on BMI found that a reciprocal association between BMI and outcomes in patients with UC and CD. More specifically, favorable outcomes were observed in UC patients with a BMI below 25 kg/m² and in CD patients with a BMI exceeding 25 kg/m²[49]. In a cohort of 132 patients with IBD treated with thiopurines dosed according to BMI, a study found that patients with obesity were less likely to reaching optimal therapeutic concentrations of the thiopurine metabolite, 6-thioguanine, which has been shown to correlate with remission of IBD[50].

Anti TNF- α therapy: Several data have suggested that obesity may induce a reduced response to anti-TNF- α agents[51]. The augmented clearance and expanded volumes of distribution associated with obesity can lead to lower trough levels, resulting in either a diminished response or a heightened risk of response loss to anti-TNF- α agents. For adalimumab, body weight has been shown to be the most significant predictor of drug clearance and volume of distribution in psoriasis patients[52]. In contrast to other rheumatoid conditions, studies examining the impact of obesity on anti-TNF therapy in IBD have produced inconsistent findings.

Obesity has been linked to an increased risk of failure of anti-TNF therapy, irrespective of the method of administration (subcutaneous *vs* intravenous) and dosing regimens (weight-based *vs* fixed-dose regimens). These results could imply that there is an intrinsic factor to obesity that reduces treatment response, regardless of drug level and mode of exposure. A recent meta-analysis found that obese patients with UC were at a greater risk of anti-TNF- α treatment failure (OR = 1.41; 95%CI: 1.01-1.98; $P = 0.045$) than non-obese patients, irrespective of whether they received fixed-dose or weight-based treatment regimens[53]. Furthermore, in another study that evaluated 160 UC patients treated with various biologic agents, both weight-based (infliximab) and fixed-dose regimens (adalimumab, certolizumab, vedolizumab, and golimumab), regardless of the type of biologic used, an increase in BMI of 1 was associated with a 4% greater risk of treatment failure (aHR = 1.04; 95%CI: 1.00-1.08) for all patients [54]. However, a pooled data analysis of over 1200 infliximab-treated IBD patients reported that BMI did not have a significant effect on clinical remission rate[55]. A metaanalysis for multiple immune-mediated diseases showed that obesity was associated with anti-TNF therapy failure in several rheumatic diseases, but no such association was observed in IBD[56]. However, in a recent meta-analysis including the newer 6 articles into the meta-analysis, obesity was associated with higher risk of failing anti-TNF therapy in UC patients, but not in CD patients[53]. Although there are insufficient studies on the impact of obesity on safety of biologic agents, a cohort study of over 6000 biologic-treated IBD patients reported no association between obesity and an increased risk of serious infections[57].

Vedolizumab: There is insufficient data regarding the potential impact of obesity on the therapeutic efficacy of vedolizumab in the management of IBD. Vedolizumab trough drug levels are known to be inversely proportional to body weight[58]. A recent retrospective study showed that obesity was not significantly related to increased rates of dose escalation for vedolizumab therapy[59]. However, a higher BMI was linked to reduced rates of vedolizumab discontinuation and CRP normalization, although not with endoscopic remission.

Ustekinumab: In chronic inflammatory conditions other than IBD, such as psoriasis and rheumatoid arthritis, obesity may negatively affect the clinical response to biological drugs. Of note, anti-interleukin drugs appear to be more strongly affected by BMI than anti-TNF- α drugs. However, in IBD, there is very little research on the impact of obesity on treatment response with this drug. A *post hoc* analysis of IM-UNITI study, which evaluated the efficacy of ustekinumab for maintenance of CD, revealed a statistically significant decrease in ustekinumab trough levels among obese patients (median 2.98 mcg/mL) compared to patients with overweight (4.84 mcg/mL; $P = 0.021$) and underweight or normal weight (4.43 mcg/mL; $P = 0.014$)^[60]. While BMI appeared to have an impact on ustekinumab drug levels, it was not found to be a significant predictor of clinical remission.

Tofacitinib: A pharmacokinetic profile of tofacitinib revealed that increased body weight had some effect on the drug's plasma concentrations, with higher body weight associated with lower peak and higher trough concentrations. However, these differences were considered to be not clinically significant^[61]. The evidence suggests that psoriatic arthritis patients with a baseline BMI over 35 kg/m² have lower rates of response to tofacitinib than those with lower baseline BMI^[62]. However, in a *post hoc* analysis of the OCTAVE studies, effectiveness and safety profile of tofacitinib in UC patients is not impacted by obesity^[63]. In the UC population, BMI was not identified as a significant predictor of outcomes, and no clear relationship between BMI and adverse events was observed.

Surgical management

It has been well established that obesity increase operative time and the risk for conversion to laparotomy^[64]. Obesity also may heighten the risk of short-term perioperative complications, such as surgical site infections and wound complications after abdominal surgery^[65]. Obesity also makes surgery for IBD more challenging, particularly those requiring pelvic exposure. A study involving 382637 inpatient hospitalizations for surgery in IBD patients revealed that obese patients had significantly higher rates of postoperative complications. Specifically, the study found that obese patients had increased odds of postoperative wound complications (OR = 1.35, $P = 0.01$), pulmonary complications (OR = 1.21, $P = 0.02$), infections (OR = 1.16, $P = 0.02$), and shock (OR = 1.30, $P = 0.02$)^[66]. A recent meta-analysis strongly supported the association between obesity and postoperative complications in IBD^[67].

Stoma creation and ileal pouch-anal anastomosis (IPAA) in obese patients are more difficult to perform and also appear to increase the risk of complications in IBD patients. Obesity has been identified as a risk factor for stoma-related complications^[68]. Additionally, it may increase the likelihood of postoperative complications, including pelvic sepsis, which has been shown to have a negative impact on long-term pouch function^[69]. However, several studies have indicated that overweight and obese patients who undergo a three-stage IPAA procedure with the utilization of a diverting stoma may achieve comparable long-term outcomes to non-obese patients^[64].

IMPACT OF OBESITY TREATMENT ON IBD OUTCOMES

Given the rising prevalence of obesity within the IBD population, there is a growing need to explore the effects of weight loss interventions on outcomes of IBD. It is widely recognized that weight loss can have a favorable influences on the outcome of numerous chronic diseases^[70]. Despite considerable evidence that obesity has a negative influence on the response to therapies for IBD, there is currently a lack of data regarding whether interventions aimed at treating obesity can improve outcomes in individuals with IBD. To date, no interventional studies have been conducted specifically to investigate the impact of intentional weight loss on IBD.

Current therapeutic strategies to obesity includes lifestyle modifications, pharmacologic treatment, bariatric surgery, and bariatric endoscopic applications, of which the intragastric balloon is the most widely used. The European Society for Clinical Nutrition and Metabolism (ESPEN)/United European Gastroenterology (UEG) guidelines suggest that the management of obesity in patients with IBD should involve a stepwise approach, starting with dietary and lifestyle interventions. If necessary, anti-obesity drugs or bariatric surgery can be considered as options (Table 2). However, the guidelines do not provide a one-size-fits-all approach and individualized care is recommended^[71].

Lifestyle and dietary interventions

A combination of dietary adjustments, physical exercise, and behavioral modifications as part of a lifestyle intervention is generally considered the preferred approach for achieving weight loss in the general population. Of course, IBD patients should also consider this approach, but there are special considerations in this cohort that require the advice of a certified dietitian. Specifically, individuals with active IBD may find it challenging to tolerate certain "healthy" foods, such as fruits and vegetables, which are commonly recommended as part of a healthy diet. Additionally, IBD patients, despite being overweight, may be vulnerable to the deficiency of various vitamins and micronutrients, and thus

Table 2 Impact of obesity treatment on inflammatory bowel disease outcomes

Interventions	Study design	Key finding	Ref.
Lifestyle and dietary interventions			
Diet: No data on the effects of overall calorie intake or supervised dietary weight loss on outcomes in IBD patients	Retrospective study: (1) Impact of mediterranean diet on the liver steatosis, clinical disease activity, and QoL in IBD patients ($n = 142$); (2) 84 UC, 58 CD; and (3) BMI: Collected at study baseline and after 6 mo	Diet-adherent CD and UC improved BMI (UC: -0.42 , $P = 0.002$; CD: -0.48 , $P = 0.032$) and waist circumference (UC: -1.25 cm, $P = 0.037$; CD: -1.37 cm, $P = 0.041$). The number of patients affected by liver steatosis of any grade was significantly reduced in both groups after mediterranean diet intervention (UC: 36.9% vs 21.4%, $P = 0.0016$; CD: 46.6% vs 31.0%, $P < 0.001$). Mediterranean diet improved QoL in both UC and CD	Chicco et al[72], 2021
Exercise: (1) Anti-inflammatory effects through a variety of mechanisms, including reducing visceral fat, reducing the secretion of inflammatory adipokines, and reducing stress-induced intestinal barrier dysfunction; and (2) Experts have recommended a prescription of exercise for IBD patients that consists of walking 20-30 min at 60% of maximal heart rate 3 d per week along with resistance training 2-3 times per week for its impact on bone mineral density[102], however this has not been tested prospectively	Prospective study: IBD patients with mild active disease or in remission ($n = 32$)	IBD patients performed low-intensity walking at an interval of 3 times per week for a duration of 3 mo. IBD patients who exercise have improved sense of well-being and QoL	Ng et al [103], 2007
	30 patients with moderate-to-mild CD. Randomized to moderate-intensity running 3 x weekly for 10 wk vs usual care	No significant difference in total IBDQ scores, IBDQ social subscores did improve in intervention group ($P = 0.023$). No disease exacerbation	Klare et al [104], 2015
	Prospective study: Using the Crohn's and Colitis Foundation of America Partners Internet-based cohort of IBD patients ($n = 1857$); 549 UC, 1308 CD	Reduced risk of CD exacerbation (RR = 0.72, 95%CI: 0.55-0.94), reduced risk of UC exacerbation (RR = 0.78, 95%CI: 0.54-1.13), with higher levels of exercise	Jones et al [74], 2015
Pharmacologic treatment: BMI of 30 kg/m ² or a BMI of 27 kg/m ² with obesity-related diseases (e.g., hypertension, type 2 diabetes mellitus, and sleep apnea)	Orlistat: (1) By inhibiting gastric and pancreatic lipases, reducing absorption of monoacglycerides and free fatty acids; and (2) Should be avoided in IBD patients because of the mechanism of action and common side effect	No data on the effect of Orlistat on outcomes in IBD patients	
	Liraglutide: Glucagon-like peptide-1 receptor agonist also known as incretin mimetics	Case report: CD patient with type 2 diabetes and active CD	Kuwata et al[76], 2014
	A nationwide cohort study using Danish registries: Patients with IBD and type 2 diabetes ($n = 3751$)	Switching from insulin to liraglutide improved glycemic control and the QoL scores	Villumsen et al[77], 2021
	Naltrexone/bupropion: Naltrexone and bupropion alone may have anti-inflammatory properties	Case report: CD patient with type 2 diabetes and active CD	Lie et al [78], 2018
	Uncontrolled studies of IBD patients not in remission ($n = 47$): Low-dose naltrexone for 12 wk	Low dose naltrexone induced clinical improvement in 74.5%, and remission in 25.5% of patients	
	Retrospective study of IBD patients who had received low-dose naltrexone ($n = 582$)	Initiation of low-dose naltrexone in IBD was followed by reduced dispensing of several drugs considered essential in the treatment of IBD	Raknes et al[79], 2018
	Large retrospective cohort study using United States administrative claims data ($n = 1731$): Compared new users of topiramate with users of other anticonvulsant/anti-migraine medications	Topiramate use was not associated with markers of IBD flares including steroid prescriptions (HR = 1.14, 95%CI: 0.74-1.73), initiation of biologic agents (HR = 0.93, 95%CI: 0.39-2.19), abdominal surgery (HR = 1.04, 95%CI: 0.17-6.41), or hospitalization (HR = 0.86, 95%CI: 0.62-1.19)	Crocket et al[83], 2014
Bariatric endoscopic applications	Intragastric balloon: Weight loss achieved through endoscopic bariatric interventions might achieve the same effect on outcomes in IBD as in other autoimmune diseases, but has not been studied	Case report of UC patient	Manguso et al[88], 2008

Bariatric surgery: BMI $\geq 40 \text{ kg/m}^2$ or 35-39.9 kg/m ² with obesity-related comorbidities and previously failed to achieve adequate weight reduction with non-surgical interventions	Bariatric surgery: (1) Several studies have demonstrated that bariatric surgery is likely feasible, safe, and effective weight loss strategy, that may lead to improved outcomes of IBD patients; and (2) No RCTs or prospective studies were found that compared the different bariatric procedures in patients with IBD	Case-control study of 85 IBD patients, matched to non-IBD patients with BS ($n = 85$): (1) 20 UC, 64 CD, 1 unclassified IBD; (2) BMI $41.6 \pm 5.9 \text{ kg/m}^2$; and (3) 3 RYGB/73 SG/12 LAGB	Bariatric surgery is a safe and effective procedure in obese IBD patients: (1) At a mean follow-up of 34 mo, mean weight was $88.6 \pm 22.4 \text{ kg}$; (2) Complications: 8 (9%); and (3) No difference was observed between cases and controls for postoperative complications ($P = 0.31$), proportion of weight loss ($P = 0.27$), or postoperative deficiencies ($P = 0.99$)	Reenaers et al [93], 2022
		Case-control study of 25 IBD patients who underwent BS, matched to IBD patients who did not undergo BS ($n = 47$)	IBD patients with weight loss after BS had fewer IBD-related complications compared with matched controls: (1) Median decrease in body mass index after bariatric surgery was 12.2; and (2) Rescue corticosteroid usage and IBD-related surgeries were numerically less common in cases than controls (24% vs 52%, OR = 0.36, 95%CI: 0.08-1.23; 12% vs 28%, OR = 0.2, 95%CI: 0.004-1.79)	Braga Neto et al [95], 2020
		Retrospective review ($n = 20$): (1) 13 UC, 7 CD; (2) BMI $50.1 \pm 9 \text{ kg/m}^2$; and (3) 9 SG/7 RYGB/3 AGB/ 1 AGB to RYGB	BS is safe and mitigate IBD: (1) Weight loss: $14.3 \pm 5.7 \text{ kg/m}^2$ or 58.9% $\pm 21.1\%$; (2) Complications: Early 7 (5 Dr, 1 PE, 1 WI), late 5 (2 Pnt, 2 VH, 1 MU), mortality 1 (unrelated); and (3) IBD status after BS: Remit 9, exacerbate 2, no change 9	Aminian et al [91], 2016
		Prospective case-control study ($n = 6/101$): (1) 1 UC, 5 CD; (2) BMI $40.6 \pm 3.74 \text{ kg/m}^2$; and (3) 1 Maclean gastroplasty/1 SG + end colostomy/2 SG/2 SG + ileocecal resection	BS is safe and effective and IBD Rx decreasing: (1) Weight loss: $11.45 \pm 2.8 \text{ kg/m}^2$ or 28.14% $\pm 6.6\%$; (2) Complications: Late 1 (1 vomiting/dysphagia); and (3) IBD status after BS: Remit 5, exacerbate 1	Colombo et al [105], 2015
		Prospective study ($n = 10$): (1) 2 UC, 8 CD; (2) BMI $42.6 \pm 5.6 \text{ kg/m}^2$; and (3) 9 LSG/1 LAGB	BS is effective and safe: (1) Weight loss: $71.4 \pm 5.9 \text{ EWL\%}$; (2) Complications: Early 1 (1 SLL) late 4 (4 VitD); and (3) IBD status after BS: Remit 2, exacerbate 3, no change 3, improved 1	Keidar et al [106], 2015
		Retrospective case-control ($n = 4$): (1) 4 CD; (2) BMI $45 \pm 5.3 (40-51) \text{ kg/m}^2$; and (3) 4 LSG	SG is safe in CD: (1) Weight loss: $32.8 \pm 4.3 \text{ kg/m}^2$ or 60.2% $\pm 13.7\%$ EWL; (2) Complications: Early 1 (1 SLB); and (3) IBD status after BS: Remit 4	Ungar et al [107], 2013
		Retrospective inpatient study ($n = 493/15319$): (1) 245 UC, 248 CD; (2) BMI $40.6 \pm 3.74 \text{ kg/m}^2$; and (3) 48% SG, 35% RYGB, 17% LAGB	Complications: 0.4% malnutrition, 0.2% thromboembolism, 12% strictures, 0.6% renal failure; prior-bariatric surgery was associated with decreased IRR for renal failure, under-nutrition, and fistulæ formation in morbidly obese IBD patients [(IRR = 0.1, 95%CI: 0.02-0.3; $P < 0.001$), (IRR = 0.2, 95%CI: 0.05-0.8; $P = 0.03$), and (IRR = 0.1, 95%CI: 0.2-0.8; $P = 0.03$), respectively]	Sharma et al [108], 2018

IBD: Inflammatory bowel disease; QoL: Quality of life; CD: Crohn's disease; UC: Ulcerative colitis; RR: Risk ratios; IBDQ: Inflammatory bowel disease questionnaire; IRR: Incidence rate ratio; BS: Bariatric surgery; OR: Odds ratio; Dr: Dehydration; EWL: Excess weight loss; LAGB: Laparoscopic adjustable gastric banding; MU: Marginal ulcer; PE: Pulmonary embolism; Pnt: Pancreatitis; Rx: Treatment; SG: Sleeve gastrectomy; SLB: Staple line bleeding; SLL: Staple line leak; VH: Ventral hernia; VitD: Vitamin deficiency; WI: Wound infection; CI: Confidence interval; RCT: Randomized control trial; RYGB: Roux-en-Y gastric bypass.

careful consideration of a balanced diet is essential. One study involving IBD patients showed improvements in body weight, waist circumference, and steatosis when a mediterranean diet was prescribed[72]. There is no available data to provide evidence on the impact of overall calorie intake or supervised dietary weight loss on outcomes in patients with IBD.

Moreover, exercise may have a positive effect on regulating IBD activity. Moderate-intensity exercise has been shown to have anti-inflammatory effects through a variety of mechanisms, such as reducing visceral fat, decreasing the secretion of inflammatory adipokines, and reducing stress-induced dysfunction of the intestinal barrier[73]. A prospective study suggested that high levels of physical exercise may be associated with a lower risk of active disease in IBD patients[74]. However, it should be noted that these studies have primarily relied on subjective measures of well-being and have not utilized specific objective indicators of disease activity.

Pharmacologic treatment

Currently, anti-obesity treatment is often recommended for patients with a BMI of 30 kg/m² or above, or a BMI of 27 kg/m² or higher in the presence of obesity-related comorbidities[75]. There are several prescription drugs (orlistat, liraglutide, phentermine-topiramate and naltrexone-bupropion) available for weight loss, but there are no randomized controlled trials of these anti-obesity drugs in patients with IBD. The ESPEN/UEG guideline recommends that anti-obesity drugs may be utilized in patients with IBD, provided they are indicated for such use, with the exception of orlistat. Orlistat should be avoided due to its mechanism of action and associated adverse effects. Notably, a case report demonstrated the use of liraglutide, a glucagon-like peptide 1 (GLP-1) receptor agonist, in a patient with active CD and type 2 diabetes resulted in improved glycemic control and quality of life scores following a switch from insulin therapy[76]. A recent cohort study of patients with both IBD and type 2 diabetes showed that treatment with GLP-1-based therapies was linked with a lower risk of adverse clinical events, defined as a composite of the need for oral corticosteroid treatment, TNF- α -inhibitor treatment, IBD-related hospitalization, or IBD-related major surgery, as compared to treatment with other antidiabetic therapies [adjusted incidence rate ratio (IRR) = 0.52, 95%CI: 0.42-0.65][77]. These observations suggest that GLP-1 based therapies may be a novel treatment option for IBD. Naltrexone and bupropion individually may have anti-inflammatory properties. Two small uncontrolled studies of IBD patients showed that naltrexone alone reduced disease activity and induced endoscopic response[78]. The initiation of low-dose naltrexone in IBD patients has been found to result in a decrease in the prescription of several medications that are typically deemed crucial for the treatment of IBD[79]. Bupropion has been associated with clinical improvement in case reports and case series in IBD patients[80,81]. Phentermine-topiramate is a weight-loss drug that has demonstrated highly efficacy in promoting weight loss in obese individuals. While the precise mechanisms are still being investigated, preclinical studies have provided evidence supporting the anti-inflammatory properties of both topiramate and phentermine. Early experimental evidence indicated that topiramate could significantly reduce colonic tissue injury in animal models of IBD. However, these findings were not corroborated in a subsequent retrospective cohort study conducted in human subjects[82,83]. A phase 2 clinical trial is currently in progress to investigate the effectiveness and safety of phentermine-topiramate in obese biologic-treated patients with UC (NCT04721873). Sodium-glucose linked transporter 2 inhibitor is the new glucose lowering drug, which has shown beneficial effects on the obesity and heart failure as well as type 2 diabetes[84]. This drug significantly improved acetic acid-induced IBD in animal models by activating autophagy signaling, inhibiting apoptosis and pro-inflammatory cytokines, lowering oxidative stress, and increasing wound healing[85-87].

Bariatric endoscopic applications

Intragastric balloon therapies are a minimally invasive and temporary treatment for inducing weight loss in obese patients. While this approach has been used successfully in the management of obesity, there is limited research on the effectiveness and safety of intragastric balloon therapy in patients with IBD. Although a small series has examined the application of intragastric ballooning in patients with IBD, reports that detail the long-term outcomes associated with weight loss and complications are lacking. The use of intragastric balloon is currently contraindicated for IBD patients due to concerns about the potential for exacerbation of symptoms and complications. A case report demonstrated that the placement of an intragastric balloon for weight loss may exacerbate symptoms of UC[88]. Further, there is currently a scarcity of high-quality evidence regarding the efficacy of other endoscopic procedures for weight loss in patients with IBD.

Bariatric surgery

For the general population, in obese patients with BMI \geq 40 kg/m² or 35-39.9 kg/m² with obesity-related comorbidities and previously failed to achieve adequate weight reduction with non-surgical interventions, bariatric surgery is superior to lifestyle and diet interventions and reduces mortality[89]. There are several different techniques for bariatric surgery, the most common being a Roux-en-Y gastric bypass (RYGB) and a sleeve gastrectomy (SG). These are now mainly performed laparoscopically.

Although data are sparse, bariatric surgery may be a viable, effective, and safe weight loss approach that could potentially result in improved outcomes for patients with IBD[90-93]. In most cases revised from two systematic reviews, weight loss resulting from bariatric surgery can be beneficial in achieving remission, reducing disease activity, and decreasing medication dependence in patients with IBD[92, 94]. Bariatric surgery resulted in similar weight loss and risk of complications in IBD patients as in non-IBD patients. A case-control study that included 88 bariatric procedures performed on 85 IBD patients, matched 1:2 for age, sex, BMI, hospital of surgery, and type of bariatric surgery with non-IBD patients who underwent bariatric surgery, found that bariatric surgery was a safe and effective intervention for weight loss, producing similar results to those observed in the control group over a 2-year period[93]. A case-control study involving 25 patients with IBD who received bariatric surgery, and matched with IBD patients who did not undergo bariatric surgery, found that the usage of rescue corticosteroids and the requirement for IBD-related surgery were less prevalent in the former group than in the controls [95]. However, long-term effects of bariatric surgery in IBD patients are poorly understood.

Although conclusive findings have yet to be derived from randomized trials, current evidence suggests that SG may confer an advantage over RYGB in patients with IBD, as SG solely involves the stomach and thus may minimize the risk of small intestinal bacterial overgrowth[90,96]. By avoiding anatomical alterations in the small intestine, the risk of complications such as strictures, abscesses, and fistulas may be reduced and future IBD-related surgeries may be simplified.

De-novo IBD after bariatric surgery

The development of *de-novo* IBD subsequent to bariatric surgery has been reported in several studies. The potential mechanisms underlying this association include exposure to viable toxins as a result of anatomical alterations, increased release of cytokines due to changes in adipose tissue, and alterations in the gut microbiome[95,97]. A Danish nationwide population-based cohort study has reported that bariatric surgery is related to an increased risk of developing new-onset CD, but not UC[98]. After bariatric surgery, the onset of IBD symptoms varied from 1 mo to 16 years[97]. In a case series, it was found that 44 patients who had previously received bariatric surgery, with RYGB being the most common procedure, developed *de-novo* IBD after a median latency period of 7 years[99]. Recent meta-analysis including 149385 patients reported that the pooled odds ratio for the *de-novo* IBD following bariatric surgery is 1.17[100]. Thus, the possibility of *de-novo* IBD should be taken into account as a potential cause of symptoms such as abdominal pain and diarrhea in patients who have undergone bariatric surgery.

CONCLUSION

Both obesity and IBD are rapidly increasing in modern society, and the proportion of obesity among IBD patients is also reported to be higher now than that in the past. There are claims that obesity contributes to the pathogenesis of IBD or that there are common factors contributing to both diseases, such as dysbiosis, but it is still insufficient to know the causal relationship or direction between them. Although data to assess the effect of obesity on outcomes in IBD are sparse and inconclusive, obesity may have a protective effect in CD and a poorer prognosis in UC. Obesity can clearly affect the treatment of IBD or surgery. Therefore, clinicians need to be aware that obesity can affect the treatment response to drugs and increase surgical complications. Although there are few studies, obesity treatment appears to have the potential to have a relatively favorable effect on IBD outcomes. Bariatric surgery appears to be relatively safe and effective in obese IBD patients. Therefore, it is necessary to compare the benefits and side effects of bariatric surgery for IBD patients. Some patients develop new onset IBD, especially CD, after bariatric surgery, so clinicians are advised to keep this in mind.

FOOTNOTES

Author contributions: Kim JH, Oh CM and Yoo JH have substantial contributions to conception and design of the review, and literature review; Kim JH drafted and edited the article; Oh CM and Yoo JH revised the manuscript critically for important intellectual content; Kim JH and Yoo JH worked together for the final approval of the version to be published.

Supported by National Research Foundation of Korea grant from the Korean government, the Ministry of Science and ICT, NRF-2020R1F1A1066323 and NRF-2021R1F1A1061550.

Conflict-of-interest statement: All the authors report no relevant conflicts of interest for this article.

Open-Access: This article is an open-access article that was selected by an in-house editor and fully peer-reviewed by external reviewers. It is distributed in accordance with the Creative Commons Attribution NonCommercial (CC BY-NC 4.0) license, which permits others to distribute, remix, adapt, build upon this work non-commercially, and license their derivative works on different terms, provided the original work is properly cited and the use is non-commercial. See: <https://creativecommons.org/Licenses/by-nc/4.0/>

Country/Territory of origin: South Korea

ORCID number: Jun Hwan Yoo 0000-0002-5810-4019.

S-Editor: Wang JJ

L-Editor: A

P-Editor: Wang JJ

REFERENCES

- 1 **Kaibullayeva J**, Ualiyeva A, Oshibayeva A, Dushpanova A, Marshall JK. Prevalence and patient awareness of inflammatory bowel disease in Kazakhstan: a cross-sectional study. *Intest Res* 2020; **18**: 430-437 [PMID: 32988164 DOI: 10.5217/ir.2019.00099]
- 2 **Keller R**, Mazurak N, Fantasia L, Fusco S, Malek NP, Wehkamp J, Enck P, Klag T. Quality of life in inflammatory bowel diseases: it is not all about the bowel. *Intest Res* 2021; **19**: 45-52 [PMID: 32093437 DOI: 10.5217/ir.2019.00135]
- 3 **Nam GE**, Park HS. Perspective on Diagnostic Criteria for Obesity and Abdominal Obesity in Korean Adults. *J Obes Metab Syndr* 2018; **27**: 134-142 [PMID: 31089555 DOI: 10.7570/jomes.2018.27.3.134]
- 4 **Kinlen D**, Cody D, O'Shea D. Complications of obesity. *QJM* 2018; **111**: 437-443 [PMID: 29025162 DOI: 10.1093/qjmed/hcx152]
- 5 **World Health Organization**. Fact sheet: obesity and overweight. [cited 14 September 2022]. Available from: <https://www.who.int/news-room/fact-sheets/detail/obesity-and-overweight>
- 6 **Kaplan GG**. The global burden of IBD: from 2015 to 2025. *Nat Rev Gastroenterol Hepatol* 2015; **12**: 720-727 [PMID: 26323879 DOI: 10.1038/nrgastro.2015.150]
- 7 **Seminario JL**, Koutroubakis IE, Ramos-Rivers C, Hashash JG, Dudekula A, Regueiro M, Baiddo L, Barrie A, Swoger J, Schwartz M, Weyant K, Dunn MA, Binion DG. Impact of Obesity on the Management and Clinical Course of Patients with Inflammatory Bowel Disease. *Inflamm Bowel Dis* 2015; **21**: 2857-2863 [PMID: 26241001 DOI: 10.1097/MIB.0000000000000560]
- 8 **Flores A**, Burstein E, Cipher DJ, Feagins LA. Obesity in Inflammatory Bowel Disease: A Marker of Less Severe Disease. *Dig Dis Sci* 2015; **60**: 2436-2445 [PMID: 25799938 DOI: 10.1007/s10620-015-3629-5]
- 9 **Pringle PL**, Stewart KO, Peloquin JM, Sturgeon HC, Nguyen D, Sauk J, Garber JJ, Yajnik V, Ananthakrishnan AN, Chan AT, Xavier RJ, Khalili H. Body Mass Index, Genetic Susceptibility, and Risk of Complications Among Individuals with Crohn's Disease. *Inflamm Bowel Dis* 2015; **21**: 2304-2310 [PMID: 26181430 DOI: 10.1097/MIB.0000000000000498]
- 10 **Lynn AM**, Harmsen WS, Tremaine WJ, Loftus EV. Su1872-Trends in the Prevalence of Overweight and Obesity at the Time of Inflammatory Bowel Disease Diagnosis: A Population-Based Study. *Gastroenterology* 2018; **154**: S-614 [DOI: 10.1016/S0016-5085(18)32218-2]
- 11 **Nic Suibhne T**, Raftery TC, McMahon O, Walsh C, O'Morain C, O'Sullivan M. High prevalence of overweight and obesity in adults with Crohn's disease: associations with disease and lifestyle factors. *J Crohns Colitis* 2013; **7**: e241-e248 [PMID: 23040290 DOI: 10.1016/j.crohns.2012.09.009]
- 12 **Blain A**, Cattan S, Beaugerie L, Carbonnel F, Gendre JP, Cosnes J. Crohn's disease clinical course and severity in obese patients. *Clin Nutr* 2002; **21**: 51-57 [PMID: 11884013 DOI: 10.1054/clnu.2001.0503]
- 13 **Kim SK**, Lee HS, Kim BJ, Park JH, Hwang SW, Yang DH, Ye BD, Byeon JS, Myung SJ, Yang SK, Park SH. The Clinical Features of Inflammatory Bowel Disease in Patients with Obesity. *Can J Gastroenterol Hepatol* 2021; **2021**: 9981482 [PMID: 34381741 DOI: 10.1155/2021/9981482]
- 14 **Moran GW**, Dubeau MF, Kaplan GG, Panaccione R, Ghosh S. The increasing weight of Crohn's disease subjects in clinical trials: a hypothesis-generating time-trend analysis. *Inflamm Bowel Dis* 2013; **19**: 2949-2956 [PMID: 23945182 DOI: 10.1097/MIB.0b013e31829936a4]
- 15 **Khalili H**, Ananthakrishnan AN, Komijeti GG, Higuchi LM, Fuchs CS, Richter JM, Chan AT. Measures of obesity and risk of Crohn's disease and ulcerative colitis. *Inflamm Bowel Dis* 2015; **21**: 361-368 [PMID: 25563694 DOI: 10.1097/MIB.0000000000000283]
- 16 **Jensen CB**, Ängquist LH, Mendall MA, Sørensen TIA, Baker JL, Jess T. Childhood body mass index and risk of inflammatory bowel disease in adulthood: a population-based cohort study. *Am J Gastroenterol* 2018; **113**: 694-701 [PMID: 29535417 DOI: 10.1038/s41395-018-0031-x]
- 17 **Chan SSM**, Chen Y, Casey K, Olen O, Ludvigsson JF, Carbonnel F, Oldenburg B, Gunter MJ, Tjønneland A, Grip O; DEFINE-IBD Investigators, Lochhead P, Chan AT, Wolk A, Khalili H. Obesity is Associated With Increased Risk of Crohn's disease, but not Ulcerative Colitis: A Pooled Analysis of Five Prospective Cohort Studies. *Clin Gastroenterol Hepatol* 2022; **20**: 1048-1058 [PMID: 34242756 DOI: 10.1016/j.cgh.2021.06.049]
- 18 **Chan SS**, Luben R, Olsen A, Tjønneland A, Kaaks R, Teucher B, Lindgren S, Grip O, Key T, Crowe FL, Bergmann MM, Boeing H, Hallmans G, Karling P, Overvad K, Palli D, Masala G, Kennedy H, vanSchaik F, Bueno-de-Mesquita B, Oldenburg B, Khaw KT, Riboli E, Hart AR. Body mass index and the risk for Crohn's disease and ulcerative colitis: data from a European Prospective Cohort Study (The IBD in EPIC Study). *Am J Gastroenterol* 2013; **108**: 575-582 [PMID: 23318483 DOI: 10.1038/ajg.2012.453]
- 19 **Zietek T**, Rath E. Inflammation Meets Metabolic Disease: Gut Feeling Mediated by GLP-1. *Front Immunol* 2016; **7**: 154 [PMID: 27148273 DOI: 10.3389/fimmu.2016.00154]
- 20 **Karmiris K**, Koutroubakis IE, Xidakis C, Polychronaki M, Voudouri T, Kouroumalis EA. Circulating levels of leptin, adiponectin, resistin, and ghrelin in inflammatory bowel disease. *Inflamm Bowel Dis* 2006; **12**: 100-105 [PMID: 16432373 DOI: 10.1097/01.MIB.0000200345.38837.46]
- 21 **Tian J**, Venn A, Otahal P, Gall S. The association between quitting smoking and weight gain: a systemic review and meta-analysis of prospective cohort studies. *Obes Rev* 2016; **17**: 1014 [PMID: 27612637 DOI: 10.1111/obr.12448]
- 22 **Berthon BS**, MacDonald-Wicks LK, Wood LG. A systematic review of the effect of oral glucocorticoids on energy intake, appetite, and body weight in humans. *Nutr Rev* 2014; **34**: 179-190 [PMID: 24655484 DOI: 10.1016/j.nutres.2013.12.006]
- 23 **Parmentier-Decrucq E**, Duhamel A, Ernst O, Fermont C, Louvet A, Vernier-Massouille G, Cortot A, Colombel JF, Desreumaux P, Peyrin-Biroulet L. Effects of infliximab therapy on abdominal fat and metabolic profile in patients with Crohn's disease. *Inflamm Bowel Dis* 2009; **15**: 1476-1484 [PMID: 19291781 DOI: 10.1002/ibd.20931]
- 24 **Kaazan P**, Tan Z, Maiyani P, Mickenbecker M, Edwards S, McIvor C, Andrews JM. Weight and BMI Patterns in a Biologics-Treated IBD Cohort. *Dig Dis Sci* 2022; **67**: 5628-5636 [PMID: 35366751 DOI: 10.1007/s10620-022-07488-7]
- 25 **Winer DA**, Luck H, Tsai S, Winer S. The Intestinal Immune System in Obesity and Insulin Resistance. *Cell Metab* 2016;

23: 413-426 [PMID: 26853748 DOI: 10.1016/j.cmet.2016.01.003]

26 **Balistreri CR**, Caruso C, Candore G. The role of adipose tissue and adipokines in obesity-related inflammatory diseases. *Mediators Inflamm* 2010; **2010**: 802078 [PMID: 20671929 DOI: 10.1155/2010/802078]

27 **Bilski J**, Mazur-Bialy A, Wojcik D, Surmiak M, Magierowski M, Sliwowski Z, Pajdo R, Kwiecien S, Danielak A, Ptak-Belowska A, Brzozowski T. Role of Obesity, Mesenteric Adipose Tissue, and Adipokines in Inflammatory Bowel Diseases. *Biomolecules* 2019; **9** [PMID: 31779136 DOI: 10.3390/biom9120780]

28 **Drouet M**, Dubuquoy L, Desreumaux P, Bertin B. Visceral fat and gut inflammation. *Nutrition* 2012; **28**: 113-117 [PMID: 22208553 DOI: 10.1016/j.nut.2011.09.009]

29 **Peyrin-Biroulet L**, Chamaillard M, Gonzalez F, Beclin E, Decourcelle C, Antunes L, Gay J, Neut C, Colombel JF, Desreumaux P. Mesenteric fat in Crohn's disease: a pathogenetic hallmark or an innocent bystander? *Gut* 2007; **56**: 577-583 [PMID: 16956921 DOI: 10.1136/gut.2005.082925]

30 **Das UN**. Is obesity an inflammatory condition? *Nutrition* 2001; **17**: 953-966 [PMID: 11744348 DOI: 10.1016/s0899-9007(01)00672-4]

31 **Colombel JF**, Solem CA, Sandborn WJ, Booya F, Loftus EV Jr, Harmsen WS, Zinsmeister AR, Bodily KD, Fletcher JG. Quantitative measurement and visual assessment of ileal Crohn's disease activity by computed tomography enterography: correlation with endoscopic severity and C reactive protein. *Gut* 2006; **55**: 1561-1567 [PMID: 16648154 DOI: 10.1136/gut.2005.084301]

32 **Kim A**. Dysbiosis: A Review Highlighting Obesity and Inflammatory Bowel Disease. *J Clin Gastroenterol* 2015; **49** Suppl 1: S20-S24 [PMID: 26447959 DOI: 10.1097/MCG.0000000000000356]

33 **Cani PD**, Amar J, Iglesias MA, Poggi M, Knauf C, Bastelica D, Neyrinck AM, Fava F, Tuohy KM, Chabo C, Waget A, Delmée E, Cousin B, Sulpice T, Chamontin B, Ferrières J, Tanti JF, Gibson GR, Casteilla L, Delzenne NM, Alessi MC, Burcelin R. Metabolic endotoxemia initiates obesity and insulin resistance. *Diabetes* 2007; **56**: 1761-1772 [PMID: 17456850 DOI: 10.2337/db06-1491]

34 **Boutagy NE**, McMillan RP, Frisard MI, Hulver MW. Metabolic endotoxemia with obesity: Is it real and is it relevant? *Biochimie* 2016; **124**: 11-20 [PMID: 26133659 DOI: 10.1016/j.biochi.2015.06.020]

35 **Suau R**, Pardina E, Domènech E, Lorén V, Manyé J. The Complex Relationship Between Microbiota, Immune Response and Creeping Fat in Crohn's Disease. *J Crohns Colitis* 2022; **16**: 472-489 [PMID: 34528668 DOI: 10.1093/ecco-jcc/jjab159]

36 **Kredel LI**, Siegmund B. Adipose-tissue and intestinal inflammation - visceral obesity and creeping fat. *Front Immunol* 2014; **5**: 462 [PMID: 25309544 DOI: 10.3389/fimmu.2014.00462]

37 **Mao R**, Doyon G, Gordon IO, Li J, Lin S, Wang J, Le THN, Elias M, Kurada S, Southern B, Olman M, Chen M, Zhao S, Dejanovic D, Chandra J, Mukherjee PK, West G, Van Wagoner DR, Fiocchi C, Rieder F. Activated intestinal muscle cells promote preadipocyte migration: a novel mechanism for creeping fat formation in Crohn's disease. *Gut* 2022; **71**: 55-67 [PMID: 33468536 DOI: 10.1136/gutjnl-2020-323719]

38 **Mao R**, Kurada S, Gordon IO, Baker ME, Gandhi N, McDonald C, Coffey JC, Rieder F. The Mesenteric Fat and Intestinal Muscle Interface: Creeping Fat Influencing Stricture Formation in Crohn's Disease. *Inflamm Bowel Dis* 2019; **25**: 421-426 [PMID: 30346528 DOI: 10.1093/ibd/izy331]

39 **Kredel LI**, Jödicke LJ, Scheffold A, Gröne J, Glauben R, Erben U, Kühl AA, Siegmund B. T-cell Composition in Ileal and Colonic Creeping Fat - Separating Ileal from Colonic Crohn's Disease. *J Crohns Colitis* 2019; **13**: 79-91 [PMID: 30272118 DOI: 10.1093/ecco-jcc/jjy146]

40 **Karaskova E**, Velganova-Veghova M, Geryk M, Foltenova H, Kucerova V, Karasek D. Role of Adipose Tissue in Inflammatory Bowel Disease. *Int J Mol Sci* 2021; **22** [PMID: 33921758 DOI: 10.3390/ijms22084226]

41 **Batra A**, Zeitz M, Siegmund B. Adipokine signaling in inflammatory bowel disease. *Inflamm Bowel Dis* 2009; **15**: 1897-1905 [PMID: 19408337 DOI: 10.1002/ibd.20937]

42 **Zulian A**, Cancello R, Micheletto G, Gentilini D, Gilardini L, Danelli P, Invitti C. Visceral adipocytes: old actors in obesity and new protagonists in Crohn's disease? *Gut* 2012; **61**: 86-94 [PMID: 21930728 DOI: 10.1136/gutjnl-2011-300391]

43 **Barroso T**, Conway F, Emel S, McMillan D, Young D, Karteszi H, Gaya DR, Gerasimidis K. Patients with inflammatory bowel disease have higher abdominal adiposity and less skeletal mass than healthy controls. *Ann Gastroenterol* 2018; **31**: 566-571 [PMID: 30174393 DOI: 10.20524/aog.2018.0280]

44 **Iannone F**, Lopalco G, Rigante D, Orlando I, Cantarini L, Lapadula G. Impact of obesity on the clinical outcome of rheumatologic patients in biotherapy. *Autoimmun Rev* 2016; **15**: 447-450 [PMID: 26808074 DOI: 10.1016/j.autrev.2016.01.010]

45 **Versini M**, Jeandel PY, Rosenthal E, Shoenfeld Y. Obesity in autoimmune diseases: not a passive bystander. *Autoimmun Rev* 2014; **13**: 981-1000 [PMID: 25092612 DOI: 10.1016/j.autrev.2014.07.001]

46 **Weissman S**, Patel K, Kolli S, Lipcsey M, Qureshi N, Elias S, Walfish A, Swaminath A, Feuerstein JD. Obesity in Inflammatory Bowel Disease Is Associated with Early Readmissions Characterised by an Increased Systems and Patient-level Burden. *J Crohns Colitis* 2021; **15**: 1807-1815 [PMID: 33999137 DOI: 10.1093/ecco-jcc/jjab088]

47 **Lynn AM**, Harmsen WS, Tremaine WJ, Bazerbachi F, Dayyeh BKA, Loftus EVJG. Su1887-Impact of Obesity on Future IBD-Related Complications in a Population-Based Cohort of Crohn's Disease (CD) and Ulcerative Colitis (UC) Patients. *Gastroenterology* 2018; **154**: S-620 [DOI: 10.1016/S0016-5085(18)32233-9]

48 **Johnson AM**, Harmsen WS, Aniwan S, Tremaine WJ, Abu Dayyeh BK, Loftus EV. Prevalence and Impact of Obesity on Disease-specific Outcomes in a Population-based Cohort of Patients with Ulcerative Colitis. *J Crohns Colitis* 2021; **15**: 1816-1823 [PMID: 34117877 DOI: 10.1093/ecco-jcc/jjab097]

49 **Holtmann MH**, Krummenauer F, Claas C, Kremeyer K, Lorenz D, Rainer O, Vogel I, Böcker U, Böhm S, Büning C, Duchmann R, Gerken G, Herfarth H, Lügering N, Kruis W, Reinshagen M, Schmidt J, Stallmach A, Stein J, Sturm A, Galle PR, Hommes DW, D'Haens G, Rutgeerts P, Neurath MF. Significant differences between Crohn's disease and ulcerative colitis regarding the impact of body mass index and initial disease activity on responsiveness to azathioprine: results from a European multicenter study in 1,176 patients. *Dig Dis Sci* 2010; **55**: 1066-1078 [PMID: 19513841 DOI: 10.1007/s10620-010-1584-1]

10.1007/s10620-009-0846-9]

50 **Poon SS**, Asher R, Jackson R, Kneebone A, Collins P, Probert C, Dibb M, Subramanian S. Body Mass Index and Smoking Affect Thioguanine Nucleotide Levels in Inflammatory Bowel Disease. *J Crohns Colitis* 2015; **9**: 640-646 [PMID: 25968584 DOI: 10.1093/ecco-jcc/jjv084]

51 **Harper JW**, Sinanan MN, Zisman TL. Increased body mass index is associated with earlier time to loss of response to infliximab in patients with inflammatory bowel disease. *Inflamm Bowel Dis* 2013; **19**: 2118-2124 [PMID: 23863401 DOI: 10.1097/MIB.0b013e31829cf401]

52 **Mostafa NM**, Nader AM, Noertersheuser P, Okun M, Awini WM. Impact of immunogenicity on pharmacokinetics, efficacy and safety of adalimumab in adult patients with moderate to severe chronic plaque psoriasis. *J Eur Acad Dermatol Venereol* 2017; **31**: 490-497 [PMID: 27545848 DOI: 10.1111/jdv.13884]

53 **Dai ZH**, Xu XT, Ran ZH. Associations Between Obesity and the Effectiveness of Anti-Tumor Necrosis Factor- α Agents in Inflammatory Bowel Disease Patients: A Literature Review and Meta-analysis. *Ann Pharmacother* 2020; **54**: 729-741 [PMID: 31955605 DOI: 10.1177/1060028019900660]

54 **Kurnool S**, Nguyen NH, Proudfoot J, Dulai PS, Boland BS, Vande Castele N, Evans E, Grunvald EL, Zarrinpar A, Sandborn WJ, Singh S. High body mass index is associated with increased risk of treatment failure and surgery in biologic-treated patients with ulcerative colitis. *Aliment Pharmacol Ther* 2018; **47**: 1472-1479 [PMID: 29665045 DOI: 10.1111/apt.14665]

55 **Singh S**, Proudfoot J, Xu R, Sandborn WJ. Obesity and Response to Infliximab in Patients with Inflammatory Bowel Diseases: Pooled Analysis of Individual Participant Data from Clinical Trials. *Am J Gastroenterol* 2018; **113**: 883-889 [PMID: 29867171 DOI: 10.1038/s41395-018-0104-x]

56 **Singh S**, Facciorusso A, Singh AG, Vande Castele N, Zarrinpar A, Prokop LJ, Grunvald EL, Curtis JR, Sandborn WJ. Obesity and response to anti-tumor necrosis factor- α agents in patients with select immune-mediated inflammatory diseases: A systematic review and meta-analysis. *PLoS One* 2018; **13**: e0195123 [PMID: 29771924 DOI: 10.1371/journal.pone.0195123]

57 **Singh S**, Heien HC, Sangaralingham L, Shah ND, Sandborn WJ. Obesity Is Not Associated With an Increased Risk of Serious Infections in Biologic-Treated Patients With Inflammatory Bowel Diseases. *Clin Transl Gastroenterol* 2021; **12**: e00380 [PMID: 34228004 DOI: 10.14309/ctg.00000000000000380]

58 **Al-Bawardy B**, Ramos GP, Willrich MAV, Jenkins SM, Park SH, Aniwan S, Schoenoff SA, Bruining DH, Papadakis KA, Raffals L, Tremaine WJ, Loftus EV. Vedolizumab Drug Level Correlation With Clinical Remission, Biomarker Normalization, and Mucosal Healing in Inflammatory Bowel Disease. *Inflamm Bowel Dis* 2019; **25**: 580-586 [PMID: 30165638 DOI: 10.1093/ibd/izy272]

59 **Levine LJ**, Gaidos JKJ, Proctor DD, Viana AV, Al-Bawardy B. Effect of obesity on vedolizumab response in inflammatory bowel disease. *Ann Gastroenterol* 2022; **35**: 275-280 [PMID: 35599926 DOI: 10.20524/aog.2022.0699]

60 **Wong ECL**, Marshall JK, Reinisch W, Narula N. Body Mass Index Does Not Impact Clinical Efficacy of Ustekinumab in Crohn's Disease: A Post Hoc Analysis of the IM-UNITI Trial. *Inflamm Bowel Dis* 2021; **27**: 848-854 [PMID: 32812022 DOI: 10.1093/ibd/izaa214]

61 **López-Sanromán A**, Esplugues JV, Domènech E. Pharmacology and safety of tofacitinib in ulcerative colitis. *Gastroenterol Hepatol* 2021; **44**: 39-48 [PMID: 32829958 DOI: 10.1016/j.gastrohep.2020.04.012]

62 **Giles JT**, Ogdie A, Gomez Reino JJ, Helliwell P, Germino R, Stockert L, Young P, Joseph W, Mundayat R, Graham D, Ritchlin C. Impact of baseline body mass index on the efficacy and safety of tofacitinib in patients with psoriatic arthritis. *RMD Open* 2021; **7** [PMID: 33452181 DOI: 10.1136/rmdopen-2020-001486]

63 **Farraye FA**, Qazi T, Kotze PG, Moore GT, Mundayat R, Lawendy N, Sharma PP, Judd DT. The impact of body mass index on efficacy and safety in the tofacitinib OCTAVE ulcerative colitis clinical programme. *Aliment Pharmacol Ther* 2021; **54**: 429-440 [PMID: 34165201 DOI: 10.1111/apt.16439]

64 **McKenna NP**, Mathis KL, Khasawneh MA, Dozois EJ, Larson DW, Pemberton JH, Lightner AL. Obese Patients Undergoing Ileal Pouch-Anal Anastomosis: Short-and Long-term Surgical Outcomes. *Inflamm Bowel Dis* 2017; **23**: 2142-2146 [PMID: 28922254 DOI: 10.1097/MIB.0000000000001238]

65 **Wahl TS**, Patel FC, Goss LE, Chu DI, Grams J, Morris MS. The Obese Colorectal Surgery Patient: Surgical Site Infection and Outcomes. *Dis Colon Rectum* 2018; **61**: 938-945 [PMID: 29994958 DOI: 10.1097/DCR.0000000000001085]

66 **Jain A**, Limketkai BN, Hutfless SJG. Mo1243 The effect of obesity on post-surgical complications during hospitalizations for inflammatory bowel disease: a nationwide analysis. *Gastroenterology* 2014; **146**: S-595 [DOI: 10.1016/S0016-5085(14)62158-2]

67 **Jiang K**, Chen B, Lou D, Zhang M, Shi Y, Dai W, Shen J, Zhou B, Hu J. Systematic review and meta-analysis: association between obesity/overweight and surgical complications in IBD. *Int J Colorectal Dis* 2022; **37**: 1485-1496 [PMID: 35641579 DOI: 10.1007/s00384-022-04190-y]

68 **Beck SJ**. Stoma issues in the obese patient. *Clin Colon Rectal Surg* 2011; **24**: 259-262 [PMID: 23204941 DOI: 10.1055/s-0031-1295689]

69 **Efron JE**, Uriburu JP, Wexner SD, Pikarsky A, Hamel C, Weiss EG, Nogueras JJ. Restorative proctocolectomy with ileal pouch anal anastomosis in obese patients. *Obes Surg* 2001; **11**: 246-251 [PMID: 11433894 DOI: 10.1381/096089201321336520]

70 **Upala S**, Sanguankeo A. Effect of lifestyle weight loss intervention on disease severity in patients with psoriasis: a systematic review and meta-analysis. *Int J Obes (Lond)* 2015; **39**: 1197-1202 [PMID: 25920774 DOI: 10.1038/ijo.2015.64]

71 **Bischoff SC**, Barazzoni R, Busetto L, Campmans-Kuijpers M, Cardinale V, Chermesh I, Eshraghian A, Kani HT, Khannoussi W, Lacaze L, Léon-Sanz M, Mendive JM, Müller MW, Ockenga J, Tacke F, Thorell A, Vranesic Bender D, Weimann A, Cuerda C. European guideline on obesity care in patients with gastrointestinal and liver diseases - Joint European Society for Clinical Nutrition and Metabolism / United European Gastroenterology guideline. *United European Gastroenterol J* 2022; **10**: 663-720 [PMID: 35959597 DOI: 10.1002/ueg2.12280]

72 **Chicco F**, Magri S, Cingolani A, Paduano D, Pesenti M, Zara F, Tumbarello F, Urru E, Melis A, Casula L, Fantini MC,

Usai P. Multidimensional Impact of Mediterranean Diet on IBD Patients. *Inflamm Bowel Dis* 2021; **27**: 1-9 [PMID: 32440680 DOI: 10.1093/ibd/izaa097]

73 **Saxena A**, Fletcher E, Larsen B, Baliga MS, Dursstine JL, Fayad R. Effect of exercise on chemically-induced colitis in adiponectin deficient mice. *J Inflamm (Lond)* 2012; **9**: 30 [PMID: 22909126 DOI: 10.1186/1476-9255-9-30]

74 **Jones PD**, Kappelman MD, Martin CF, Chen W, Sandler RS, Long MD. Exercise decreases risk of future active disease in patients with inflammatory bowel disease in remission. *Inflamm Bowel Dis* 2015; **21**: 1063-1071 [PMID: 25723616 DOI: 10.1093/MIB.0000000000000333]

75 **Yumuk V**, Tsigos C, Fried M, Schindler K, Busetto L, Micic D, Toplak H; Obesity Management Task Force of the European Association for the Study of Obesity. European Guidelines for Obesity Management in Adults. *Obes Facts* 2015; **8**: 402-424 [PMID: 26641646 DOI: 10.1159/000442721]

76 **Kuwata H**, Tsujii S, Fujita N, Okamura S, Iburi T, Mashitani T, Kitatani M, Furuya M, Hayashino Y, Ishii H. Switching from insulin to liraglutide improved glycemic control and the quality of life scores in a case of type 2 diabetes and active Crohn's disease. *Intern Med* 2014; **53**: 1637-1640 [PMID: 25088877 DOI: 10.2169/internalmedicine.53.2306]

77 **Villumson M**, Schelde AB, Jimenez-Solem E, Jess T, Allin KH. GLP-1 based therapies and disease course of inflammatory bowel disease. *EClinicalMedicine* 2021; **37**: 100979 [PMID: 34386751 DOI: 10.1016/j.eclim.2021.100979]

78 **Lie MRKL**, van der Giessen J, Fuhler GM, de Lima A, Peppelenbosch MP, van der Ent C, van der Woude CJ. Low dose Naltrexone for induction of remission in inflammatory bowel disease patients. *J Transl Med* 2018; **16**: 55 [PMID: 29523156 DOI: 10.1186/s12967-018-1427-5]

79 **Raknes G**, Simonsen P, Småbrekke L. The Effect of Low-Dose Naltrexone on Medication in Inflammatory Bowel Disease: A Quasi Experimental Before-and-After Prescription Database Study. *J Crohns Colitis* 2018; **12**: 677-686 [PMID: 29385430 DOI: 10.1093/ecco-jcc/jjy008]

80 **Kast RE**, Altschuler EL. Remission of Crohn's disease on bupropion. *Gastroenterology* 2001; **121**: 1260-1261 [PMID: 11706830 DOI: 10.1053/gast.2001.29467]

81 **Kane S**, Altschuler EL, Kast RE. Crohn's disease remission on bupropion. *Gastroenterology* 2003; **125**: 1290 [PMID: 14552325 DOI: 10.1016/j.gastro.2003.02.004]

82 **Dudley JT**, Sirota M, Shenoy M, Pai RK, Roedder S, Chiang AP, Morgan AA, Sarwal MM, Pasricha PJ, Butte AJ. Computational repositioning of the anticonvulsant topiramate for inflammatory bowel disease. *Sci Transl Med* 2011; **3**: 96ra76 [PMID: 21849664 DOI: 10.1126/scitranslmed.3002648]

83 **Crockett SD**, Schectman R, Stürmer T, Kappelman MD. Topiramate use does not reduce flares of inflammatory bowel disease. *Dig Dis Sci* 2014; **59**: 1535-1543 [PMID: 24504592 DOI: 10.1007/s10620-014-3040-7]

84 **Joshi SS**, Singh T, Newby DE, Singh J. Sodium-glucose co-transporter 2 inhibitor therapy: mechanisms of action in heart failure. *Heart* 2021; **107**: 1032-1038 [PMID: 33637556 DOI: 10.1136/heartjnl-2020-318060]

85 **Arab HH**, Al-Shorbagy MY, Saad MA. Activation of autophagy and suppression of apoptosis by dapagliflozin attenuates experimental inflammatory bowel disease in rats: Targeting AMPK/mTOR, HMGB1/RAGE and Nrf2/HO-1 pathways. *Chem Biol Interact* 2021; **335**: 109368 [PMID: 33412153 DOI: 10.1016/j.cbi.2021.109368]

86 **EIMahdy MK**, Antar SA, Elmahallawy EK, Abdo W, Hijazy HHA, Albrakati A, Khodir AE. A Novel Role of Dapagliflozin in Mitigation of Acetic Acid-Induced Ulcerative Colitis by Modulation of Monocyte Chemoattractant Protein 1 (MCP-1)/Nuclear Factor-Kappa B (NF-κB)/Interleukin-18 (IL-18). *Biomedicines* 2021; **10** [PMID: 35052720 DOI: 10.3390/biomedicines10010040]

87 **Morsy MA**, Khalaf HM, Rifaai RA, Bayoumi AMA, Khalifa EMMA, Ibrahim YF. Canagliflozin, an SGLT-2 inhibitor, ameliorates acetic acid-induced colitis in rats through targeting glucose metabolism and inhibiting NOX2. *Biomed Pharmacother* 2021; **141**: 111902 [PMID: 34328119 DOI: 10.1016/j.bioph.2021.111902]

88 **Manguso F**, Picascia S, Balzano A. Ulcerative colitis exacerbating after placement of intragastric balloon for the treatment of obesity. *Inflamm Bowel Dis* 2008; **14**: 872-873 [PMID: 18240281 DOI: 10.1002/ibd.20373]

89 **Schauer PR**, Bhatt DL, Kirwan JP, Wolski K, Brethauer SA, Navaneethan SD, Aminian A, Pothier CE, Kim ES, Nissen SE, Kashyap SR; STAMPEDE Investigators. Bariatric surgery versus intensive medical therapy for diabetes-3-year outcomes. *N Engl J Med* 2014; **370**: 2002-2013 [PMID: 24679060 DOI: 10.1056/NEJMoa1401329]

90 **Bazerbachi F**, Sawas T, Vargas EJ, Haffar S, Deepak P, Kisiel JB, Loftus EV Jr, Abu Dayyeh BK. Bariatric Surgery Is Acceptably Safe in Obese Inflammatory Bowel Disease Patients: Analysis of the Nationwide Inpatient Sample. *Obes Surg* 2018; **28**: 1007-1014 [PMID: 29019151 DOI: 10.1007/s11695-017-2955-4]

91 **Aminian A**, Andalib A, Ver MR, Corcelles R, Schauer PR, Brethauer SA. Outcomes of Bariatric Surgery in Patients with Inflammatory Bowel Disease. *Obes Surg* 2016; **26**: 1186-1190 [PMID: 26420765 DOI: 10.1007/s11695-015-1909-y]

92 **Shoar S**, Shahabuddin Hoseini S, Naderan M, Mahmoodzadeh H, Ying Man F, Shoar N, Hosseini M, Bagheri-Hariri S. Bariatric surgery in morbidly obese patients with inflammatory bowel disease: A systematic review. *Surg Obes Relat Dis* 2017; **13**: 652-659 [PMID: 27986584 DOI: 10.1016/j.sobrd.2016.10.017]

93 **Reenaers C**, de Roover A, Kohnen L, Nachury M, Simon M, Pourcher G, Trang-Poisson C, Rajca S, Msika S, Viennot S, Altwegg R, Serrero M, Seksik P, Peyrin-Biroulet L, Picon L, Bourbao Tournois C, Gontier R, Gillette C, Stefanescu C, Laharie D, Roblin X, Nahon S, Bouguen G, Carbonnel F, Attar A, Louis E, Coffin B. Bariatric Surgery in Patients With Inflammatory Bowel Disease: A Case-Control Study from the GETAID. *Inflamm Bowel Dis* 2022; **28**: 1198-1206 [PMID: 34636895 DOI: 10.1093/ibd/izab249]

94 **Hudson JL**, Barnes EL, Herfarth HH, Isaacs KL, Jain A. Bariatric Surgery Is a Safe and Effective Option for Patients with Inflammatory Bowel Diseases: A Case Series and Systematic Review of the Literature. *Inflamm Intest Dis* 2019; **3**: 173-179 [PMID: 31111033 DOI: 10.1159/000496925]

95 **Braga Neto MB**, Gregory MH, Ramos GP, Bazerbachi F, Bruining DH, Abu Dayyeh BK, Kushnir VM, Raffals LE, Ciorba MA, Loftus EV, Deepak P. Impact of Bariatric Surgery on the Long-term Disease Course of Inflammatory Bowel Disease. *Inflamm Bowel Dis* 2020; **26**: 1089-1097 [PMID: 31613968 DOI: 10.1093/ibd/izz236]

96 **Gagner M**, Hutchinson C, Rosenthal R. Fifth International Consensus Conference: current status of sleeve gastrectomy.

Surg Obes Relat Dis 2016; **12**: 750-756 [PMID: 27178618 DOI: 10.1016/j.soard.2016.01.022]

97 **Cañete F**, Mañosa M, Clos A, Cabré E, Domènec E. Review article: the relationship between obesity, bariatric surgery, and inflammatory bowel disease. *Aliment Pharmacol Ther* 2018; **48**: 807-816 [PMID: 30178869 DOI: 10.1111/apt.14956]

98 **Allin KH**, Jacobsen RK, Ungaro RC, Colombel JF, Egeberg A, Villumsen M, Jess T. Bariatric Surgery and Risk of New-onset Inflammatory Bowel Disease: A Nationwide Cohort Study. *J Crohns Colitis* 2021; **15**: 1474-1480 [PMID: 33609363 DOI: 10.1093/ecco-jcc/jjab037]

99 **Braga Neto MB**, Gregory M, Ramos GP, Loftus EV Jr, Ciorba MA, Bruining DH, Bazerbachi F, Abu Dayyeh BK, Kushnir VM, Shah M, Collazo-Clavell ML, Raffals LE, Deepak P. De-novo Inflammatory Bowel Disease After Bariatric Surgery: A Large Case Series. *J Crohns Colitis* 2018; **12**: 452-457 [PMID: 29272375 DOI: 10.1093/ecco-jcc/jjx177]

100 **Kermansaravi M**, Valizadeh R, Farazmand B, Mousavimaleki A, Taherzadeh M, Wiggins T, Singhal R. De Novo Inflammatory Bowel Disease Following Bariatric Surgery: a Systematic Review and Meta-analysis. *Obes Surg* 2022; **32**: 3426-3434 [PMID: 35906528 DOI: 10.1007/s11695-022-06226-2]

101 **Harpsøe MC**, Basit S, Andersson M, Nielsen NM, Frisch M, Wohlfahrt J, Nohr EA, Linneberg A, Jess T. Body mass index and risk of autoimmune diseases: a study within the Danish National Birth Cohort. *Int J Epidemiol* 2014; **43**: 843-855 [PMID: 24609069 DOI: 10.1093/ije/dyu045]

102 **Pérez CA**. Prescription of physical exercise in Crohn's disease. *J Crohns Colitis* 2009; **3**: 225-231 [PMID: 21172280 DOI: 10.1016/j.crohns.2009.08.006]

103 **Ng V**, Millard W, Lebrun C, Howard J. Low-intensity exercise improves quality of life in patients with Crohn's disease. *Clin J Sport Med* 2007; **17**: 384-388 [PMID: 17873551 DOI: 10.1097/JSM.0b013e31802b4fda]

104 **Klare P**, Nigg J, Nold J, Haller B, Krug AB, Mair S, Thoeringer CK, Christle JW, Schmid RM, Halle M, Huber W. The impact of a ten-week physical exercise program on health-related quality of life in patients with inflammatory bowel disease: a prospective randomized controlled trial. *Digestion* 2015; **91**: 239-247 [PMID: 25823689 DOI: 10.1159/000371795]

105 **Colombo F**, Rizzi A, Ferrari C, Frontali A, Casiraghi S, Corsi F, Sampietro GM, Foschi D. Bariatric surgery in patients with inflammatory bowel disease: an accessible path? *J Crohns Colitis* 2015; **9**: 185-190 [PMID: 25518054 DOI: 10.1093/ecco-jcc/jju011]

106 **Keidar A**, Hazan D, Sadot E, Kashtan H, Wasserberg N. The role of bariatric surgery in morbidly obese patients with inflammatory bowel disease. *Surg Obes Relat Dis* 2015; **11**: 132-136 [PMID: 25547057 DOI: 10.1016/j.soard.2014.06.022]

107 **Ungar B**, Kopylov U, Goitein D, Lahat A, Bardan E, Avidan B, Lang A, Maor Y, Eliakim R, Ben-Horin S. Severe and morbid obesity in Crohn's disease patients: prevalence and disease associations. *Digestion* 2013; **88**: 26-32 [PMID: 23816835 DOI: 10.1159/000351529]

108 **Sharma P**, McCarty TR, Njei B. Impact of Bariatric Surgery on Outcomes of Patients with Inflammatory Bowel Disease: a Nationwide Inpatient Sample Analysis, 2004-2014. *Obes Surg* 2018; **28**: 1015-1024 [PMID: 29047047 DOI: 10.1007/s11695-017-2959-0]

Submit a Manuscript: <https://www.f6publishing.com>

World J Gastroenterol 2023 March 28; 29(12): 1795-1810

DOI: 10.3748/wjg.v29.i12.1795

ISSN 1007-9327 (print) ISSN 2219-2840 (online)

REVIEW

Role of autoantibodies in the clinical management of primary biliary cholangitis

Eirini I Rigopoulou, Dimitrios P Bogdanos

Specialty type: Gastroenterology and hepatology**Provenance and peer review:**

Invited article; Externally peer reviewed.

Peer-review model: Single blind**Peer-review report's scientific quality classification**

Grade A (Excellent): 0

Grade B (Very good): B

Grade C (Good): C

Grade D (Fair): 0

Grade E (Poor): 0

P-Reviewer: Ding J, China; Mi SC, China**Received:** December 5, 2022**Peer-review started:** December 5, 2022**First decision:** December 19, 2022**Revised:** January 4, 2023**Accepted:** March 14, 2023**Article in press:** March 14, 2023**Published online:** March 28, 2023**Eirini I Rigopoulou**, Department of Medicine and Research Laboratory of Internal Medicine, National Expertise Center of Greece in Autoimmune Liver Diseases, General University Hospital of Larissa, Larissa 41110, Greece**Eirini I Rigopoulou**, European Reference Network on Hepatological Diseases (ERN RARE-LIVER), General University Hospital of Larissa, Larissa 41110, Greece**Dimitrios P Bogdanos**, Department of Rheumatology and Clinical Immunology, Faculty of Medicine, School of Health Sciences, University of Thessaly, Larissa 41110, Greece**Corresponding author:** Eirini I Rigopoulou, MD, PhD, Professor, Department of Medicine and Research Laboratory of Internal Medicine, National Expertise Center of Greece in Autoimmune Liver Diseases, General University Hospital of Larissa, Mezourlo, Larissa 41110, Greece. eirigopoulou@med.uth.gr

Abstract

Primary biliary cholangitis (PBC) is a chronic cholestatic liver disease characterized by immune-driven destruction of small intrahepatic bile ducts leading a proportion of patients to hepatic failure over the years. Diagnosis at early stages in concert with ursodeoxycholic acid treatment has been linked with prevention of disease progression in the majority of cases. Diagnosis of PBC in a patient with cholestasis relies on the detection of disease-specific autoantibodies, including anti-mitochondrial antibodies, and disease-specific anti-nuclear antibodies targeting sp100 and gp210. These autoantibodies assist the diagnosis of the disease, and are amongst few autoantibodies the presence of which is included in the diagnostic criteria of the disease. They have also become important tools evaluating disease prognosis. Herein, we summarize existing data on detection of PBC-related autoantibodies and their clinical significance. Moreover, we provide insight on novel autoantibodies and their possible prognostic role in PBC patients.

Key Words: Primary biliary cholangitis; Anti-mitochondrial antibodies; Primary biliary cholangitis-specific antinuclear antibodies; Anti-sp100; Anti-gp210; Prognosis

©The Author(s) 2023. Published by Baishideng Publishing Group Inc. All rights reserved.

Core Tip: The diagnosis of primary biliary cholangitis (PBC) relies on the detection of disease-specific autoantibodies, including anti-mitochondrial antibodies and disease-specific antinuclear antibodies targeting sp100 and gp210. In this review, we summarize existing data on detection of PBC-related autoantibodies and their clinical significance. Moreover, we provide insight on novel autoantibodies and their possible prognostic role in PBC patients.

Citation: Rigopoulou EI, Bogdanos DP. Role of autoantibodies in the clinical management of primary biliary cholangitis. *World J Gastroenterol* 2023; 29(12): 1795-1810

URL: <https://www.wjgnet.com/1007-9327/full/v29/i12/1795.htm>

DOI: <https://dx.doi.org/10.3748/wjg.v29.i12.1795>

INTRODUCTION

Primary biliary cholangitis (PBC), known until 2014 as primary biliary cirrhosis, is a chronic autoimmune cholestatic liver disease, its main features being presence of anti-mitochondrial antibodies (AMA), female predominance and progressive destruction of small intrahepatic bile ducts[1]. A proportion of PBC patients progresses over the years to fibrosis and eventually to cirrhosis leading to hepatic failure. Diagnosis at early stages in conjunction with ursodeoxycholic acid (UDCA) treatment has been linked with prevention of disease progression in the majority of cases. Over the years, significant progress has been achieved in the armamentarium used for disease diagnosis and prognostication, including autoantibody testing and on-treatment prognostic indicators[1].

Originally PBC was reported in 1851 in a woman with jaundice and xanthomata and its clinical phenotype was described in 1949[2,3]. The first association of PBC with autoantibodies was reported by Mackay[4] in 1958 in a case with high titers of circulating complement-fixing antibodies to liver, kidney and other human tissue antigens[4]. Later on, in 1965, Walker *et al*[5] have reported the presence of AMA by indirect immunofluorescence (IIFL) in patients with PBC[5].

The discovery of AMA in conjunction with advances in their diagnostic testing and increased disease awareness has led to diagnosis at earlier stages. Moreover, treatment with UDCA, which is the standard of care for naïve PBC patients has been associated with improved long-term survival. All these factors have significantly contributed to the increase in prevalence rates throughout the years[6,7]. The highest incidence and prevalence rates have been reported in Europe and the United States (incidence and prevalence rates range from 3.3 to 32 per million person-years and 19 to 402 per million respectively)[8-11]. Discrepancies between regions may reflect differences in patients' accessibility to healthcare services, increased disease awareness depending on physician's expertise and widespread use of AMA and antinuclear antibody (ANA) testing during diagnostic work-up. Still, it is debatable whether increases in prevalence and incidence rates represent true changes over the years.

PBC is considered a prototype autoimmune disease, based on the abundance of AMA, female predominance and increased rate of other autoimmune diseases. Genetic and environmental factors are regarded as key players in the induction of immune tolerance loss to biliary epithelial autoantigens, a notion well appreciated also on work performed in animal models of the disease[12-15].

Higher disease rates between family members, especially siblings, formed the initial pathogenetic link between genetics and PBC. Genome wide association studies from Europe, North America, Japan and China have identified human leukocyte antigens (HLA) and non-HLA alleles that confer susceptibility to PBC, though discrepant results between ethnicities are apparent[16]. The majority of reported loci are encoding proteins implicated in the control of immune response mechanisms, including HLA, interleukin (IL)-12 production, B and T cell activation, interferon (IFN)-γ production and production of immunoglobulins. The contribution of genetics is also emphasized by the fact that monozygotic twins display significantly higher concordance rates compared to dizygotic twins (63% vs 0%)[17]. Still, lack of remarkable concordance rates between identical twins in PBC strongly supports the implication of environmental factors and epigenetics.

Numerous studies have revealed the important contribution of environmental exposures, including chemical xenobiotics, pollutants, cosmetics and also infectious agents, in immune tolerance loss and in the initiation of disease process[18-21].

Studies on animal models of the disease have underlined the likely input of specific environmental factors in the initiation and perpetuation of disease progression, adding further support for their significant input in genetically prone individuals[15].

DIAGNOSIS OF PBC

The cornerstone for PBC diagnosis is the detection of AMA and/or PBC-specific ANA when investigating a patient with cholestasis (Table 1)[6]. It is important to stress that AMA are one of the few autoantibodies being included in diagnostic criteria of a disease[6]. Liver histology is essential when AMA are not detected in a patient with cholestasis with high suspicion of PBC, or when indications of variant forms exist[6,22].

AUTOANTIBODIES

AMA

Since their first description in 1965 by Walker *et al*[5], AMA have been uninterruptedly used as the most reliable marker for the diagnosis of PBC[5]. This landmark paper did not showcase only the close association of AMA with PBC, but provided also a straightforward technique for its detection, which has been routinely used up to this time, namely IIFL[5]. Later on, in 1968, a trypsin-sensitive antigen was identified by Berg *et al*[23] to react *in vitro* with sera from PBC patients, which was located in the inner mitochondrial membrane and was called M2[23]. The same group proposed a classification of AMA antigens from M1 to M9[24]. This nomenclature was subsequently abandoned, as several studies have failed to link PBC with any of these antigens, except for M2[25,26].

M2 antigens consist of components of the 2-oxo-acid dehydrogenase multienzyme complexes; namely, pyruvate dehydrogenase (PDC), 2-oxoglutarate (OGDC) and branched-chain 2-oxo acid (BCOADC)[27]. Each complex is formed by several copies of at least three enzymes (E1, E2 and E3) that form high molecular-weight multimers and are localized in the inner mitochondrial membrane. The E2 enzyme, based at the structural core of the complex, contains the lipoyl group, which is bound to lysine and plays significant role in the catalytic cycle[27].

The next major breakthrough was the cloning and sequencing of a 74 kDa mitochondrial autoantigen, that led to the identification of E2 subunit of PDC-E2 as the major autoantigen in PBC[27,28]. Several reports were able to establish the fine characteristics of response to antimitochondrial antigens in PBC patients[29]. In detail, up to 95% of PBC patients show reactivity to PDC-E2 and to lesser extend (50-70%) towards OGDC-E2 and BCOADC-32[29]. Few AMA positive PBC patients react only towards PDC-E2 and even less solely to OGDC-E2 or BCOADC-E2. The predominant anti-M2 reactivity is the one against the E2 component of PDC and also BCOADC and OGDC enzyme complexes, while less commonly reactivity to PDC-E1a and PDC-E1b subunits and also the dihydrolipoamide dehydrogenase (E3)-binding protein has been reported[29]. It is of interest that the E2 subunit of the OADC is highly conserved between species and also between various complexes. All immunodominant epitopes include a ExDKA motif with a lipoic acid attached to K at position 173, which is essential for T-cell antigen recognition[30].

Several studies have tried to elucidate mechanisms involved in loss of tolerance towards 2-OADC components located on the inner mitochondrial surface of biliary epithelial cells (BECs), finally leading to BECs injury and are reviewed elsewhere[31]. A multi-lineage loss of tolerance against major AMA epitopes appears to be one of the key features leading to progressive destruction of bile ducts in PBC where both CD4+ and CD8+ T cells orchestrate an immune response against the PDC-E2 complex in the liver as well as in the periphery[31]. IL-12 and IFN- γ prevail in PBC inducing Th1 immune responses at initial stages of the disease[32]. Perpetuation of liver injury during the disease process is linked with skewing towards a Th17 phenotype[31,32]. T follicular helper cells, known to assist B cell-specific antibody production, were found in increased numbers in livers of PBC patients, while T regulatory cells, that promote self-tolerance, were found numerically or functionally impaired in PBC patients[31].

Over the years, the role of BECs has been upgraded from regulators of fluidity and alkalinity of bile, to active participants of innate and adaptive immune responses contributing to bile duct injury and evolution of liver disease[1,33]. Why BECs are the targets of autoimmune attack, considering that PDC-E2 is not confined solely to these cells but is abundant in mitochondria of all nucleated cells, remains elusive. Several studies have proposed a hypothesis according to which small BECs, by undergoing apoptosis, transfer immunologically intact PDC-E2 to apoptotic bodies and form an apoptote (antigenic epitope). This apoptote in concert with macrophages and AMA can induce locally acting proinflammatory cytokines resulting in inflammation and surrounding apoptosis in PBC[14].

Methods for AMA detection

IIFL: Since its discovery, IIFL is considered the “gold” standard technique for the detection of AMA and titers above 1/40 are regarded as positive[6,22]. The preferred tissue for the detection of AMA is liver, kidney and stomach substrates, which displays a fluorescence pattern unique to AMA. AMA stains the distal tubules on kidney sections, which contain more mitochondria compared to the proximal tubules, while it produces a bright granular pattern on gastric sections and a faint cytoplasmic pattern on liver sections[34]. Alternatively, on a substrate of human larynx epithelioma cancer cell line (HEp-2) cells, AMA give a diffuse, granular cytoplasmic pattern, that is not consistent with other methods of AMA

Table 1 Autoantibodies detected in primary biliary cholangitis and their clinical significance

Autoantibodies	Method	Prevalence	Specificity	Diagnostic relevance	Clinical significance
AMA	IIFL, ELISA, Blot	90%-95%. Varies according to method used	High (90%)	Yes	AMA presence and titer not associated with severity of PBC or prognosis of PBC
Antinuclear antibodies					
Against nuclear envelope antigens: Anti-sp100; anti-PML; anti-sp140; anti-SUMO	IIFL (MND pattern), ELISA	30%-50%	Very high (approximately 98%)	Useful in AMA-negative patients	Anti-sp100 is associated with more severe disease, faster disease progression and worse outcome
Against nuclear pore complex antigens: Anti-gp210; anti-np62; anti-LBR	IIFL (Rim-like perinuclear pattern; RL/M), ELISA, Immunoblot	30%-50%	Very high. Up to 100%	Useful in AMA-negative patients	Anti-gp210 is associated with more severe disease and worse outcome
Anticentromere antibodies	IIFL	10%-30%	Low	No	Limited data on their role as prognostic factor for complications related to portal hypertension
Anti-KLHL12 antibodies	ELISA	22%-36%	Very high	Yes. Useful in AMA-negative pts	Anti-HK1 is associated with worse outcome (needs validation)
Anti-HK-1 antibodies	Immunoblot				

sp100: Nuclear body speckled 100 kDa; sp140: Nuclear body speckled 140 kDa; SUMOs: small ubiquitin-related modifiers; PML: Promyelocytic leukemia proteins; LBR: Lamin B receptor antibody; KLHL12: Anti-kelch-like 12 protein; HK-1: Anti-hexokinase 1; AMA: Anti-mitochondrial antibodies; MND: Multi nuclear dot pattern; ELISA: Enzyme-linked immunosorbent assay; IIFL: Indirect immunofluorescence; PBC: Primary biliary cholangitis.

detection (*i.e.* IIFL with triple substrate or molecular based assays) and its use as a single method for AMA detection is not recommended. Still, HEp-2 cells is recommended to be used in parallel with the triple rodent substrate for the detection of PBC-specific ANA[34].

Data from few old studies have shown that AMA are not restricted to a specific immunoglobulin (IgG subclass, though IgG3 appears to be the most predominant[35,36].

Solid phase assays: The identification of AMA molecular targets has revolutionized the diagnostic approach of patients with PBC, since new molecular-based assays have been developed, which rely on the use of recombinant or purified antigens. Amongst them are microtiter plate Enzyme-linked immunosorbent assay (ELISA), chemiluminescence and fluorescent bead-based assays[37-43]. Commercially produced ELISA's have substantially gained ground over the years, considering they offer high grade of standardization and automation and don't require skilled personnel either for their application or interpretation[44].

Gershwin's group have created a recombinant fusion protein (MIT3), consisting of the major immunodominant epitopes of the three main AMA targets (PDC-E2, BCOADCE2, OGDC-E2)[41]. An ELISA utilizing MIT3 had increased sensitivity compared to IIFL and ELISAs with conventional anti-M2, as it allowed the identification of AMA in 30%-50% of previously AMA-negative samples[39,45]. An improved technique, based on the coupling of the three recombinant mitochondrial autoantigens (PDC-E2, BCOADC-E2 and OGDC-E2) with beads, found 20% of AMA-negative by IIFL patients to be positive, while 100% of these new AMA positive patients were revealed as ANA positive[46]. The development of another assay (anti-M2-3E ELISA), which included antibodies to MIT3 and purified PDC to allow detection of additional less immunodominant mitochondrial antigens, like PDC-E1a and E1b, increased further the diagnostic accuracy of AMA compared to IIFL, conventional anti-PDC ELISA and also the anti-MIT3 ELISA[37].

Several studies have suggested that investigating individual AMA isotypes (IgG, IgM, IgA) could be of clinical relevance, as different isotypes may correlate with biochemical, clinical and histological features of the disease. As a secretory immunoglobulin, IgA is abundant in mucous membranes, while IgA AMA have been detected in bile, saliva and urine samples of PBC patients and have been suggested to contribute to bile duct injury[47,48]. Of relevance, PDC-E2 specific dimeric IgA, but not IgG resulted in induction of caspase activation in Madine-Darby canine kidney cells transfected with the human polymeric Ig receptor, in an experimental study[49]. Studies assessing the possible clinical significance of IgA AMA in PBC patients have produced conflicting results up to the present[39,50-52]. Even if we cannot recommend IgA AMA testing based on these remarks, we should stress that a minority of PBC patients (2%-3%) have only AMA of IgA isotype[39]. In this context, if a patient is suspected to have PBC based on clinical and biochemical features and IgG AMA are not detected, he should be tested for AMA of IgA isotype.

A study from China, has suggested that salivary AMA-M2, tested by ELISA is a useful biomarker for the diagnosis of PBC. It is a non-invasive method, providing high specificity, as salivary AMA-M2 were detected only in serum AMA-M2 positive PBC patients and none of the controls[53].

In PBC, SDS-PAGE followed by western blotting has been used in the past as a sensitive and specific method in identifying individual mitochondrial antigens based on their molecular weight (74 kDa band for PDC-E2, 52 kDa band for BCOADC-E2 and 48 kDa band for OGD-E2). Preparations of mitochondrial fractions of primate and/or liver or bovine heart are usually used as source of AMA antigens, though recombinant proteins are suggested to produce less background[54,55]. Immunoblotting with recombinant protein results in 91% positivity in sera from PBC patients, compared to 81% when recombinant PDC-E2 fusion protein is utilized[54]. Similar to ELISAs, the fact that a small portion of PBC patients demonstrate reactivity only to BCOADC-E2 and/or OGD-E2 could account for this variance in sensitivity. A study applying computer-assisted imaging technology showed correlation between AMA titers by IIFL and number and intensity of immunofixed 1-OADC bands in sera from PBC patients[55]. However, immunoblotting is time consuming and in routine practice its usage has been abandoned giving space for the most reliable and fully automated antigen-specific assays or automated IIFL.

Data from a recent study suggests that M2-AMA dot blot is more specific than IIF-AMA[56]. This study demonstrated increased sensitivity and specificity with increasing number of M2-AMA specificities detected.

In recent years automated particle-based multi-analyte technology (PMAT) assays have been used for the detection of autoantibodies, including those related to PBC. Data evaluating the performance of this assay have been convincing and commercial assays based on this technology are widely available, as they allow the concurrent detection of several antigen-specific autoantibodies[57].

AMA AND THEIR CLINICAL CORRELATIONS

AMA is the most characteristic feature of PBC, as up to 95% of patients are tested positive for these autoantibodies. A 2014 meta-analysis including 24 studies showed that the pooled sensitivity and specificity of AMA in the diagnosis of PBC is 84.5% and 97.8%, respectively[58]. The specificity of AMA for PBC has been initially revealed in two small longitudinal studies, where the majority of AMA positive patients with no evidence of cholestatic liver disease developed full blown PBC[59,60]. Still, recent studies have shown a small proportion of AMA positive individuals to develop PBC through the years[61,62]. These data should be interpreted with caution, as follow up duration might have been not long enough in these latter studies to allow clinical presentation of PBC that is known to progress slowly.

Data from Sun *et al*[63], though, have shown that 80% of AMA positive individuals with normal alkaline phosphatase have histological features of PBC, stressing that cholestasis is not a prerequisite for the establishment of PBC[63]. The pathogenic role of AMA is further supported by the case of two newborns where liver disease had developed after transfer of AMA from their mothers *via* the placenta, while liver pathology subsided when the autoantibodies disappeared.

However, AMA have been reported in up to 1% of healthy individuals[64,65]. Considering the substantially lower PBC prevalence, only a small percentage of those AMA positive individuals is going to advance to PBC. Moreover, longitudinal data on AMA kinetics in patients transplanted for PBC show these autoantibodies to persist, though biochemical or histological features of PBC recurrence have been reported in 36% 10 years post liver transplantation[66,67]. As autoantibodies can arise years before disease presentation only long-term observational studies spanning a period of decades will be able to elucidate this issue further.

Kisand *et al*[68] have suggested that development of PBC might arise in those who have or will develop high titer AMA overtime of various specificities and subclasses compared to AMA positive individuals with low titer antibodies of only one Ig class reactivity[68].

Whether AMA titers is a prognostic indicator for PBC needs to be assessed further, as several studies up to the present have produced conflicting data. Early studies from the 80s and 90s have shown AMA titers to correlate to disease activity and progression[69,70]. Another study demonstrated that PBC patients had significantly higher AMA titers, tested by IIFL and higher anti-PDC-E2 avidity compared to AMA positive individuals with normal biochemistry[71]. Moreover, Gabeta *et al*[39] have demonstrated IgG and IgA AMA titers to positively correlate with the Mayo risk score[39].

Whether testing by IIFL for individual IgG AMA subclasses could assist in identifying prognostic features of PBC patients remains obscure. Another study stressed that AMA of the IgG3 subclass positively correlate with more advanced liver disease, as manifested by higher frequency of cirrhosis and higher Mayo risk score[36].

Furthermore, treatment with UDCA was associated with a decrease in AMA titers in one of the first trials of UDCA in PBC patients, while in a recent study from China, response to UDCA treatment at 1 year was linked to decreased AMA titers[72,73]. However, several other studies failed to prove AMA titers or their longitudinal changes as prognostic markers of PBC progression[74-76]. In line with this, a

small study on 9 asymptomatic PBC patients with inadequate response to UDCA, who continued with combination of UDCA and fenofibrate, showed a decrease in AMA titers in 4 of these patients. These data could suggest that AMA production may be regulated by peroxisome proliferator-activated receptor α in PBC patients. Still, this is a hypothesis that needs to be confirmed in the future, as it was not reproduced by other studies[77].

Anti-M2 AMA can also occur in the context of overlapping diseases, such as the autoimmune hepatitis/PBC variant, metabolic associated fatty liver disease/PBC variant, viral hepatitis (hepatitis B virus, hepatitis C virus)/PBC variant and other rheumatic diseases, such as systemic sclerosis[6,78,79]. Their presence should be evaluated in the appropriated clinical context.

ANA IN PBC

Various ANA specificities have been reported in up to 70% of PBC patients[80]. HEp-2 cells are preferred compared to the triple tissue substrate for the detection of ANA, as large nuclei and high rate of mitosis of these cells permit the discrimination of different staining patterns[34]. A variety of staining patterns, often coinciding, have been described in PBC patients, including rim-like (RLM), nuclear dot, speckled, homogeneous and centromere staining pattern[81,82]. For diagnostic purposes, ANAs are categorized into those not specific for PBC and those specific for the disease.

According to the official categorization of ANA patterns issued by the International Consensus on ANA Patterns initiative, 2 IIFL patterns are defined as PBC-specific, namely the multiple nuclear dot (MND) pattern (AC-6) and the punctuate nuclear envelope pattern (AC-12)[83].

ANA not specific for PBC

Anticentromere antibodies (ACA) and those against extractable nuclear antigens (anti-ENA), recognizing various molecular targets, including nuclear ribonucleoproteins (nRNP), ribosomal phosphoproteins and cellular enzymes such as DNA topoisomerase I (Scl-70) and histidyl-tRNA synthetase (Jo-1) are non-specific ANA and can be detected up to 30% of PBC patients, at times indicating co-existing autoimmune rheumatic diseases[80,84].

Originally, IIFL on HEp-2 cells was used for ACA detection and counter immunoelectrophoresis on thymic and spleen extracts for anti-ENA detection. More sensitive methods, like ELISA and immunoblot were developed for the detection of various molecular targets (*i.e.* nRNP, Sm, SSB/La, SSA/Ro 60 and 52). Their application has revealed anti-ENA reactivities in up to 30% of PBC patients, anti-SSA/Ro-52kD being the most frequent one. The presence of anti-SSA/Ro-52 kD was associated with active and advanced disease in one study[84]. ACA have been reported in 20%-30% of PBC patients and 80% of patients with a PBC/Systemic Sclerosis overlap syndrome[81,84-86].

The diagnostic and clinical significance of ACA positivity in patients with PBC without SSc has recently been under investigation, though with discrepant results[86-88]. Data from two studies have suggested ACA to be a predictive factor for the development of complications related to portal hypertension in PBC patients, though not for the progression to liver failure[86,88]. As both studies were conducted in PBC patients of Asian origin, large scale data are needed to explore this hypothesis further.

PBC-specific ANA

PBC-specific ANA have been reported in up to 50% of PBC patients, with wide variation in the prevalence rate between studies depending on the method used[80]. They demonstrate high specificity, though low sensitivity for PBC and is a valuable tool during diagnostic work-up of patients with suspicion of PBC, especially in those tested negative for AMA[6,22]. Their identification is optimized when HEp-2 cells are used as a substrate, as these cells have large nuclei and during their mitotic phase ACA stain their chromosomes[34].

PBC-specific ANA display two distinct immunofluorescence patterns: A perinuclear/RLM and a MND pattern[80,83]. The RLM pattern gives a distinctive punctuated pattern of the nuclear surface that corresponds to a nuclear complex. This pattern is generated by reactivity to nuclear pore complexes (NPC), which are multi-protein structures that mediate nucleocytoplasmic transport. Gp210 is the main antigenic targets in PBC and is currently used for diagnostic purposes. Less immunodominant antigens, not incorporated in the diagnostic work-up, are those of nucleoporin p62 and lamin B receptor. The MND pattern consists of 3-20 dots scattered throughout the nucleus, but sparing the nucleoli and is produced by reactivity to the nuclear body speckled 100 kDa (sp100) protein and the promyelocytic leukemia (PML) protein, while more recently sp140 and small ubiquitin-related modifier (SUMO) protein has been reported as additional antigenic targets[80,89,90].

The visualization of ANA can be hindered by AMAs presence and other ANA specificities[34]. This could justify the perception that prevailed based on the results of early studies reporting of the presence of PBC-specific ANA especially in AMA-negative patients[81]. For example, the MND pattern can be easily mistaken with that produced by ACA; the anti-MND pattern consist of dots of various size and numbers, while the ACA pattern is characterized by dots of equal size. ACA stain the cells'

chromosome, whereas anti-MND don't.

A multicenter study showed that the diagnostic performance of the conventional IIFL improved further by the use of individual IgG (IgG1-4) isotypes instead of anti-total IgG sera, leading to increased recognition of PBC-specific ANAs[91]. In detail, 65% and 15% of PBC patients were MND and/or RLM positive using IgG isotype-specific antisera and anti-total IgG antiserum respectively[91].

The identification of the molecular targets of PBC-specific ANA has led to the development of molecular based techniques, including ELISA and immunoblot, that are more sensitive and observer-independent[80,92,93]. Accordingly, Invernizzi *et al*[92] demonstrated reactivity to NPC by immunoblotting in 22% of 105 patients known to be ANA negative by IIFL. There was no significant difference in the percentage of anti-NPC positive amongst those being AMA positive and negative PBC patients with the use of immunoblotting[92]. Similarly, Muratori *et al*[81] have reported on the increased sensitivity of ELISA in detecting PBC-specific ANAs compared to IIFL, though they were more often detected in AMA negative compared to AMA positive PBC patients[81].

Still, a major limitation of the molecular based assays is the selection of specific targets and exclusion of others that might be of potentially equal importance, especially if reactivity to those subdominant antigens is of diagnostic relevance (such is the case of single specificities).

The sensitivity of anti-gp210 has been reported between 5.71% and 55.88%, whereas specificity ranged from 61.70% to 100% depending on the method used and the population studied[94-98].

ANA AND THEIR CLINICAL CORRELATIONS

Several studies have evaluated whether PBC-specific ANAs have a prognostic role in PBC patients. Discrepant results between studies can be justified by differences in study design (*i.e.* methods to evaluate the presence of antibodies, different antigenic preparations used), as well as heterogeneity of patients investigated[86,94].

Early studies, based mainly on IIFL detection of autoantibodies, had failed to establish a link between presence of PBC-specific ANAs and disease' prognosis[99,100]. During the last 20 years, several reports relaying mostly on ELISA, western blot and line blot data, delineated the correlation of PBC-specific ANAs with more severe disease and worse outcome, though differences between studies exist. Most studies underline that positivity for anti-NPC antibodies and especially for anti-gp210 are associated with more severe disease and worst disease outcome[81,87,91,92,97,101].

One of these studies using IIFL for the identification of autoantibodies, revealed anti-RLM of the IgG3 isotype to correlate with more severe liver disease[91]. A meta-analysis encompassing 5 studies in Asian patients demonstrated anti-gp210 antibodies to be associated with worst disease outcome and suggested their use as optimal predictors of PBC prognosis at the time of diagnosis[102].

Nakamura *et al*[103] reported that persistently positive anti-gp210 antibodies during follow up in Japanese PBC patients under UDCA treatment confer a strong risk for progression to end-stage liver disease, whereas these patients had histologically more severe interface hepatitis, lobular inflammation, and ductular reaction[103]. These findings were not confirmed in a study assessing autoantibody patterns during follow up in Greek PBC patients[104].

Anti-np62 antibodies are detected in 22%-31% of PBC patients, though their significance is not well documented and their diagnostic relevance remains unclear[105,106]. A Japanese study suggested that anti-np62 antibodies are associated with advanced disease. These results need to be confirmed by other studies[105].

Anti-sp100, the most frequent amongst antibodies displaying the MND pattern, is detected in 8%-44% of PBC patients, its specificity ranging from 63.8% to 100%[81,107-109]. The pooled sensitivity of anti-sp100 for PBC has been estimated at 23.1% and the pooled specificity at 97.7%[98]. Importantly, subgroup analysis could not identify significant differences in pooled specificity across the strata of geographical regions or across various methods used for their identification[98].

The prevalence of anti-lamin B receptor antibodies have been reported in 9%-15% of PBC patients and are considered highly specific[105,110]. Given their rarity and their unknown prognostic role, they are not routinely tested in every day clinical practice.

Anti-MND and anti-sp100 antibodies tested by IIF and by ELISA respectively have been associated with more severe disease, as attested by biochemical and histological features, faster disease progression and worse outcome[91,107]. Moreover, anti-MND of the IgG3 isotype was associated with longer disease duration and more severe histological picture[91].

Autoantibodies against PML are less frequently detected in PBC patients (12%-19%), and largely co-exist with anti-sp100, though cases with single reactivity to PML have been also reported[93,107]. Double reactivity to sp100 and PML was suggested to be associated with unfavorable outcome of PBC patients[93,107]. SUMOs have been exclusively linked to presence of anti-sp100 and anti-PML, suggesting antigen spreading as a possible mechanism for anti-SUMO generation[90].

Züchner *et al*[107] reported anti-sp100 levels to remain stable during the course of the disease. Of interest, alteration in the sp100 epitope recognition pattern in some patients during the natural course of the disease was noted in a proportion of patients under UDCA treatment, which indicates that UDCA

can modify immunoglobulin expression[107]. In accordance with these findings are those from a study in 110 Greek patients, where serial determination of autoantibodies titers demonstrated that a decrease in anti-sp100 levels was associated with response to UDCA treatment and improvement of the Mayo risk score[104]. Akin to AMA, PBC-specific ANA are shown to persist after liver transplantation without signs of disease recurrence[106,111].

Few studies have suggested infectious agents to have acted as potential triggers for the development of anti-MND antibodies in PBC patients. Bogdanos *et al*[112] have demonstrated a strong correlation of anti-sp100 reactivity and presence of AMA only in those PBC patients with recurrent urinary tract infections[112]. Molecular mimicry between T-cell epitopes, first implicating mitochondrial and afterward nuclear proteins, has been proposed[113].

A study conducted in a Han Chinese population demonstrated significant genetic predisposition for sp100 but not for gp210. In detail, HLADRB1*03:01, DRB1*15:01, DRB1*01, and DPB1*03:01 alleles were associated with antibody production against sp100[114]. Whether this difference is indicative of diverse roles of anti-sp100 and anti-gp210 in PBCs pathogenesis needs to be elucidated in the future. Besides, as data of this study is confined to Chinese patients, these results need to be confirmed in other PBC cohorts.

AMA NEGATIVE PBC

The percentage of AMA negativity by IFL widely varies amongst studies, ranging from 5%-20%. Soon after the identification of the molecular targets of AMA and the development of molecular based assays, it has become apparent that such assays can considerably increase the sensitivity for AMA detection, leading to a significant drop of “true” AMA-negative cases[37,39,40,45,46,115]. By immunoblotting testing, IgG antibodies against PDC-E2 are detectable in 97% of AMA positive PBC and in 66% of AMA negative PBC[116].

Others have reported even higher prevalence of antigen-specific AMA in IFL AMA-negative PBC patients, reducing even more the percentage of AMA negative PBC[117-119]. In our hands, only 16% of IFL AMA-negative PBC patients had reactivity against mitochondrial autoantigens using a sensitive immunoblot technique[55].

Nevertheless, even when the most sensitive AMA tests are used, still a proportion of PBC patients may not have AMA. While some studies indicated that seronegative cases may convert to AMA seropositive over the years, some others have elegantly shown that there are still patients that will never develop these autoantibodies over the course of the disease. This is of fundamental importance as it implies that breaking of immunological tolerance to the mitochondrial autoantigens of AMA is not the sole cornerstone of PBC pathogenesis, and other non-mitochondrial antigen-driven mechanisms are potentially involved. It is also of diagnostic importance because it highlights the importance for the proper identification and routine use of diagnostic surrogate markers which can assist the diagnosis of PBC in AMA negative cases. It also raises the question as to whether AMA positive and AMA negative PBC are two entities with distinct characteristics or not.

It must be noted, that over the years and with the wealth of data provided, a consensus has been reached that “true” AMA-negative PBC is an entity indistinguishable from AMA-positive PBC, in terms of demographic, biochemical, clinical and histopathological features[117,118,120]. Though the total number of AMA negative cases with PBC included in various studies can be considered small, and despite the lack of multi-centre studies investigating in greater detail the features of AMA negative PBC, the current evidence supports the notion that the natural history as well as the prognosis of AMA-negative PBC is analogous to AMA-positive PBC[121,122]. Current guidelines indicate the therapeutical and clinical management of AMA negative PBC should be the same with AMA positive PBC. Early studies have reported that aside AMA status, some immunoserologic features may be different between AMA-negative and AMA-positive PBC, such as lower IgM and higher gamma globulin in the former rather than the latter group[117,118,120,123].

Several studies have published data reporting a significantly higher rate of positivity for ANA in AMA-negative compared to AMA-positive PBC. Original studies were based on IFL testing, while most recently such assays included ANA-specific antigen testing against sp100 and gp210. The wide range of ANA positivity is attributed to technical reasons, such as the sensitivity of the assay used for autoantibody detection and cohort selection bias or geographic/ethnic disparities. Early IFL studies reported the prevalence of ANA to range between 71% to 100%, in AMA-negative PBC patients, compared with 18% to 33% in AMA seropositive PBC patients[117,118,120,123].

The first point that at times is overlooked by the clinicians is that PBC-specific ANAs are not confined to AMA-negative PBC and therefore disease-specific ANA is by no means a characteristic feature of this form of the disease. It has now become apparent that this striking over-representation was due to the practical limitations imposed by IFL on tissue sections because ANA positivity could be obscured by the simultaneous presence of AMAs, which could perplex the reading by the immunodiagnostician. This is indeed true in weak AMA positive cases where ANAs become more visible and can be present in frequencies comparable to AMA negative PBC cohorts[81]. With the advent of assays using as antigenic

substrate recombinant sp100 and gp210, a more accurate estimation of the respective autoreactivities has been achieved, though great variation is still seen amongst studies. In a consecutive cohort, Muratori *et al*[81] found ANA of any pattern in 53% of patients, including 27% with anti-Sp100, and 16% with anti-gp210 antibody reactivity[81].

Most studies fail to report significant differences of anti-gp210 and anti-sp100 between AMA-positive and AMA-negative PBC cohorts[124].

The relatively recent identification of novel autoantigens in AMA negative patients with PBC has provided further hints regarding the diagnostic and clinical challenges of AMA-negative patients with PBC and their relevance to the presence of disease-specific autoantibodies.

NOVEL AUTOANTIBODIES

During the last decade, antibodies against kelch-like protein (KLHL12) and hexokinase 1 (HK-1) were proposed as novel biomarkers in PBC patients, especially those lacking AMA[125,126]. While KLHL12 is a nuclear protein that is implicated in collagen export and ubiquitination of various proteins, HK-1 is an enzyme that is localized in the outer mitochondria membrane, phosphorylates glucose and modulates susceptibility to cellular apoptosis. Both display high specificity ($\geq 95\%$), while their combination improved their overall sensitivity from 48.3% to 68.5% by ELISA and from 55% to 75% by immunoblot in AMA-negative PBC patients[125]. Recently, a study in Spanish PBC patients has confirmed the aforementioned data on the utility of these autoantibodies to diagnose AMA-negative patients by demonstrating anti-HK1 or anti-KLHL12 in a third of AMA negative and in 40% those negative for AMA, anti-gp210 and anti-sp100[127]. Furthermore, anti-HK1 positivity was associated with significantly higher possibility of liver decompensation and lower liver-related survival free of transplantation[127]. A more recent study assessed the prevalence of anti-KLHL12 and anti-HK-1 antibodies by ELISA at 5 sites within Europe and North America and documented the presence of these antibodies in patients with PBC in all geographies, irrespectively of the origin of the sera failing to identify geographic factors which could imply that the genetic make-up of the patients is responsible for the induction of these autoantibodies[128]. A Polish study reported the highest prevalence of anti-KLHL12 antibodies so far (36%) in both AMA-positive and AMA-negative patients and confirmed their high specificity for PBC diagnosis[110]. Their presence was linked to higher bilirubin levels and advanced fibrosis[110]. The prognostic significance of these autoantibodies needs to be evaluated in larger cohorts of PBC patients.

Bombaci *et al*[129] have proposed SPATA31A3 and GARP, as novel autoantigens in PBC, as PBC sera demonstrated high reactivity to these antigens irrespective of AMA and PBC-specific ANA presence [129]. Their combination with PDC-E2 assisted in discrimination of PBC from other diseases with high sensitivity and specificity. The authors offer in addition pathophysiological evidences on GARP expression in human cholangiocytes, which underlines the potential implication of this autoantigen in the induction of the disease[129].

MULTIPLEX ASSAYS

Considering that the repertoire of autoantibodies related to several autoimmune diseases is increasing, multiplex assays have become available in order to facilitate their simultaneous detection in a reliable, automated fashion, without consuming substantial amount of time. Such an example is that reported by Liu *et al*[130] in 2010 on a new PBC-screening assay that allows simultaneous detection of MIT3, sp100 and gp210 of IgG and IgA isotype by ELISA and compared these results with those from distinct IgG ELISAs[130]. Testing of 1175 PBC patients and 1232 non-PBC controls revealed sensitivity and specificity of PBC screen to be 83.8% and 94.7%, respectively, which is similar to that found from the evaluation of the combined data from individual MIT3, sp100, and gp210 IgG ELISAs[130].

Furthermore, assessment of 253 AMA-negative PBC patients by IIFL with this assay, resulted in positivity for PBC-specific autoantibodies in almost half of them (44.7%). Based on these data, PBC screen has been proposed as a reliable first line test for the diagnosis of PBC[130]. Comparable were the results from an Italian study, where examination of 100 AMA-negative PBC patients by IIFL showed reactivity in 43% of these patients with the use of the PBC screen[131].

Data from a study using a multiplex line blot assay, designed for autoimmune liver diseases, that contained AMA-M2, M2-E3 (a recombinant fusion protein including the E2 subunits of PDC, BCOADC and OGDC), as well sp100, PML and gp210 recombinant proteins had an overall sensitivity and specificity for PBC of 98.3% and 93.7% respectively. IIFL displayed lower sensitivity (86.2%), though comparable specificity (97.9%)[132]. Recently, a new automated PMAT assay on the Aptiva instrument, which includes MIT3, sp100, gp210, HK1 and KLp, facilitated the recognition of higher frequency of AMA- negative PBC patients compared to conventional immunoassays[57]. Even though multiplex technology seems to be a promising tool in the diagnosis of PBC, its use in the diagnostic algorithm of PBC needs to be further evaluated.

CONCLUSION

In conclusion, thorough discussion of the available literature reveals important aspects of the diagnostic, clinical and prognostic significance of disease-specific autoantibodies in AMA positive and AMA negative PBC patients[133]. Overall, identification of AMA and PBC-specific ANA is the cornerstone for the diagnosis of PBC. PBC-specific ANA, including anti-gp210 and anti-sp100, have a pivotal role in PBC diagnosis in AMA-negative individuals with high suspicion of the disease. Moreover, they have an established role as predictive factors for more advanced disease and worse outcome. The role of novel autoantibodies as diagnostic and prognostic tools in the management of patients with PBC needs to be assessed further.

FOOTNOTES

Author contributions: Rigopoulou EI had the original idea, wrote and revised the manuscript; Bogdanos DP wrote and revised the manuscript.

Conflict-of-interest statement: Eirini I Rigopoulou has nothing to declare; Dimitrios P Bogdanos has received lecture Honoria from Enorasis Hellas, Genesis Pharma, Novartis, Euroimmun, Menarini Hellas, Boehringer Ingelheim, Fresenius Kabi; Dimitrios P Bogdanos has received grants to support the research and educational activities of his Department from Elpen, Boehringer Ingelheim, Demo and Menarini Hellas; Dimitrios P Bogdanos has received travel bursaries to attend scientific meetings and congresses from Werfen, Hospital Line, Pfizer, Elpen, Enorasis Hellas, Novartis and IFT Hellas.

Open-Access: This article is an open-access article that was selected by an in-house editor and fully peer-reviewed by external reviewers. It is distributed in accordance with the Creative Commons Attribution NonCommercial (CC BY-NC 4.0) license, which permits others to distribute, remix, adapt, build upon this work non-commercially, and license their derivative works on different terms, provided the original work is properly cited and the use is non-commercial. See: <https://creativecommons.org/Licenses/by-nc/4.0/>

Country/Territory of origin: Greece

ORCID number: Eirini I Rigopoulou [0000-0003-1978-4602](https://orcid.org/0000-0003-1978-4602); Dimitrios P Bogdanos [0000-0002-9697-7902](https://orcid.org/0000-0002-9697-7902).

S-Editor: Fan JR

L-Editor: A

P-Editor: Fan JR

REFERENCES

- 1 **Lleo A**, Wang GQ, Gershwin ME, Hirschfield GM. Primary biliary cholangitis. *Lancet* 2020; **396**: 1915-1926 [PMID: [33308474](https://pubmed.ncbi.nlm.nih.gov/33308474/) DOI: [10.1016/S0140-6736\(20\)31607-X](https://doi.org/10.1016/S0140-6736(20)31607-X)]
- 2 **Addison T**, Gull W. On a certain affection of the skin—vitiligoidea- α -plana, β -tuberosa. *Guy's Hosp Rep* 1851; **7**: 265-276
- 3 **Ahrens EH Jr**, Kunkel HG. The relationship between serum lipids and skin xanthomata in 18 patients with primary biliary cirrhosis. *J Clin Invest* 1949; **28**: 1565-1574 [PMID: [15395959](https://pubmed.ncbi.nlm.nih.gov/15395959/) DOI: [10.1172/JCI102222](https://doi.org/10.1172/JCI102222)]
- 4 **Mackay IR**. Primary biliary cirrhosis showing a high titer of autoantibody; report of a case. *N Engl J Med* 1958; **258**: 185-188 [PMID: [13493762](https://pubmed.ncbi.nlm.nih.gov/13493762/) DOI: [10.1056/NEJM195801232580407](https://doi.org/10.1056/NEJM195801232580407)]
- 5 **Walker JG**, Doniach D, Roitt IM, Sherlock S. Serological tests in diagnosis of primary biliary cirrhosis. *Lancet* 1965; **1**: 827-831 [PMID: [14263538](https://pubmed.ncbi.nlm.nih.gov/14263538/) DOI: [10.1016/S0140-6736\(65\)91372-3](https://doi.org/10.1016/S0140-6736(65)91372-3)]
- 6 **European Association for the Study of the Liver**. EASL Clinical Practice Guidelines: The diagnosis and management of patients with primary biliary cholangitis. *J Hepatol* 2017; **67**: 145-172 [PMID: [28427765](https://pubmed.ncbi.nlm.nih.gov/28427765/) DOI: [10.1016/j.jhep.2017.03.022](https://doi.org/10.1016/j.jhep.2017.03.022)]
- 7 **Murillo Perez CF**, Goet JC, Lammers WJ, Gulamhusein A, van Buuren HR, Ponsioen CY, Carbone M, Mason A, Corpechot C, Invernizzi P, Mayo MJ, Battezzati PM, Floreani A, Pares A, Nevens F, Kowdley KV, Bruns T, Dalekos GN, Thorburn D, Hirschfield G, LaRusso NF, Lindor KD, Zachou K, Poupon R, Trivedi PJ, Verhelst X, Janssen HLA, Hansen BE; GLOBAL PBC Study Group. Milder disease stage in patients with primary biliary cholangitis over a 44-year period: A changing natural history. *Hepatology* 2018; **67**: 1920-1930 [PMID: [29220537](https://pubmed.ncbi.nlm.nih.gov/29220537/) DOI: [10.1002/hep.29717](https://doi.org/10.1002/hep.29717)]
- 8 **Boonstra K**, Beuers U, Ponsioen CY. Epidemiology of primary sclerosing cholangitis and primary biliary cirrhosis: a systematic review. *J Hepatol* 2012; **56**: 1181-1188 [PMID: [22245904](https://pubmed.ncbi.nlm.nih.gov/22245904/) DOI: [10.1016/j.jhep.2011.10.025](https://doi.org/10.1016/j.jhep.2011.10.025)]
- 9 **James OF**, Bhopal R, Howel D, Gray J, Burt AD, Metcalf JV. Primary biliary cirrhosis once rare, now common in the United Kingdom? *Hepatology* 1999; **30**: 390-394 [PMID: [10421645](https://pubmed.ncbi.nlm.nih.gov/10421645/) DOI: [10.1002/hep.510300213](https://doi.org/10.1002/hep.510300213)]
- 10 **Kim WR**, Lindor KD, Locke GR 3rd, Therneau TM, Homburger HA, Batts KP, Yawn BP, Petz JL, Melton LJ 3rd, Dickson ER. Epidemiology and natural history of primary biliary cirrhosis in a US community. *Gastroenterology* 2000; **119**: 1631-1636 [PMID: [11113084](https://pubmed.ncbi.nlm.nih.gov/11113084/) DOI: [10.1053/gast.2000.20197](https://doi.org/10.1053/gast.2000.20197)]

- 11 **Gatselis NK**, Zachou K, Lygoura V, Azariadis K, Arvaniti P, Spyrou E, Papadamou G, Koukoulis GK, Dalekos GN, Rigopoulou EI. Geoepidemiology, clinical manifestations and outcome of primary biliary cholangitis in Greece. *Eur J Intern Med* 2017; **42**: 81-88 [PMID: 28535947 DOI: 10.1016/j.ejim.2017.05.006]
- 12 **Hirschfield GM**, Gershwin ME. The immunobiology and pathophysiology of primary biliary cirrhosis. *Annu Rev Pathol* 2013; **8**: 303-330 [PMID: 23347352 DOI: 10.1146/annurev-pathol-020712-164014]
- 13 **Webb GJ**, Siminovitch KA, Hirschfield GM. The immunogenetics of primary biliary cirrhosis: A comprehensive review. *J Autoimmun* 2015; **64**: 42-52 [PMID: 26250073 DOI: 10.1016/j.jaut.2015.07.004]
- 14 **Lleo A**, Maroni L, Glaser S, Alpini G, Marziani M. Role of cholangiocytes in primary biliary cirrhosis. *Semin Liver Dis* 2014; **34**: 273-284 [PMID: 25057951 DOI: 10.1055/s-0034-1383727]
- 15 **Wakabayashi K**, Lian ZX, Leung PS, Moritoki Y, Tsuneyama K, Kurth MJ, Lam KS, Yoshida K, Yang GX, Hibi T, Ansari AA, Ridgway WM, Coppel RL, Mackay IR, Gershwin ME. Loss of tolerance in C57BL/6 mice to the autoantigen E2 subunit of pyruvate dehydrogenase by a xenobiotic with ensuing biliary ductular disease. *Hepatology* 2008; **48**: 531-540 [PMID: 18563844 DOI: 10.1002/hep.22390]
- 16 **Tanaka A**, Leung PSC, Gershwin ME. The Genetics and Epigenetics of Primary Biliary Cholangitis. *Clin Liver Dis* 2018; **22**: 443-455 [PMID: 30259846 DOI: 10.1016/j.cld.2018.03.002]
- 17 **Selmi C**, Mayo MJ, Bach N, Ishibashi H, Invernizzi P, Gish RG, Gordon SC, Wright HI, Zweibaum B, Podda M, Gershwin ME. Primary biliary cirrhosis in monozygotic and dizygotic twins: genetics, epigenetics, and environment. *Gastroenterology* 2004; **127**: 485-492 [PMID: 15300581 DOI: 10.1053/j.gastro.2004.05.005]
- 18 **Gershwin ME**, Selmi C, Worman HJ, Gold EB, Watnik M, Utts J, Lindor KD, Kaplan MM, Vierling JM; USA PBC Epidemiology Group. Risk factors and comorbidities in primary biliary cirrhosis: a controlled interview-based study of 1032 patients. *Hepatology* 2005; **42**: 1194-1202 [PMID: 16250040 DOI: 10.1002/hep.20907]
- 19 **Parikh-Patel A**, Gold EB, Worman H, Krivy KE, Gershwin ME. Risk factors for primary biliary cirrhosis in a cohort of patients from the united states. *Hepatology* 2001; **33**: 16-21 [PMID: 11124815 DOI: 10.1053/jhep.2001.21165]
- 20 **Prince MI**, Ducker SJ, James OF. Case-control studies of risk factors for primary biliary cirrhosis in two United Kingdom populations. *Gut* 2010; **59**: 508-512 [PMID: 20332522 DOI: 10.1136/gut.2009.184218]
- 21 **Corpechot C**, Chrétien Y, Chazouillères O, Poupon R. Demographic, lifestyle, medical and familial factors associated with primary biliary cirrhosis. *J Hepatol* 2010; **53**: 162-169 [PMID: 20471130 DOI: 10.1016/j.jhep.2010.02.019]
- 22 **Hirschfield GM**, Dyson JK, Alexander GJM, Chapman MH, Collier J, Hübscher S, Patanwala I, Pereira SP, Thain C, Thorburn D, Tiniakos D, Walmsley M, Webster G, Jones DEJ. The British Society of Gastroenterology/UK-PBC primary biliary cholangitis treatment and management guidelines. *Gut* 2018; **67**: 1568-1594 [PMID: 29593060 DOI: 10.1136/gutjnl-2017-315259]
- 23 **Berg PA**, Doniach D, Roitt IM. Mitochondrial antibodies in primary biliary cirrhosis. I. Localization of the antigen to mitochondrial membranes. *J Exp Med* 1967; **126**: 277-290 [PMID: 4165742 DOI: 10.1084/jem.126.2.277]
- 24 **Berg PA**, Klein R. Antimitochondrial antibodies in primary biliary cirrhosis and other disorders: definition and clinical relevance. *Dig Dis* 1992; **10**: 85-101 [PMID: 1530697 DOI: 10.1159/000171347]
- 25 **Davis PA**, Leung P, Manns M, Kaplan M, Munoz SJ, Gorin FA, Dickson ER, Krawitt E, Coppel R, Gershwin ME. M4 and M9 antibodies in the overlap syndrome of primary biliary cirrhosis and chronic active hepatitis: epitopes or epiphenomena? *Hepatology* 1992; **16**: 1128-1136 [PMID: 1330864]
- 26 **Palmer JM**, Yeaman SJ, Bassendine MF, James OF. M4 and M9 autoantigens in primary biliary cirrhosis--a negative study. *J Hepatol* 1993; **18**: 251-254 [PMID: 7691927 DOI: 10.1016/s0168-8278(05)80253-3]
- 27 **Gershwin ME**, Mackay IR, Sturgess A, Coppel RL. Identification and specificity of a cDNA encoding the 70 kd mitochondrial antigen recognized in primary biliary cirrhosis. *J Immunol* 1987; **138**: 3525-3531 [PMID: 3571977]
- 28 **Van de Water J**, Gershwin ME, Leung P, Ansari A, Coppel RL. The autoepitope of the 74-kD mitochondrial autoantigen of primary biliary cirrhosis corresponds to the functional site of dihydrolipoamide acetyltransferase. *J Exp Med* 1988; **167**: 1791-1799 [PMID: 2455013 DOI: 10.1084/jem.167.6.1791]
- 29 **Leung PS**, Coppel RL, Ansari A, Munoz S, Gershwin ME. Antimitochondrial antibodies in primary biliary cirrhosis. *Semin Liver Dis* 1997; **17**: 61-69 [PMID: 9089911 DOI: 10.1055/s-2007-1007183]
- 30 **Shimoda S**, Van de Water J, Ansari A, Nakamura M, Ishibashi H, Coppel RL, Lake J, Keeffe EB, Roche TE, Gershwin ME. Identification and precursor frequency analysis of a common T cell epitope motif in mitochondrial autoantigens in primary biliary cirrhosis. *J Clin Invest* 1998; **102**: 1831-1840 [PMID: 9819369 DOI: 10.1172/JCI4213]
- 31 **Gulamhusein AF**, Hirschfield GM. Primary biliary cholangitis: pathogenesis and therapeutic opportunities. *Nat Rev Gastroenterol Hepatol* 2020; **17**: 93-110 [PMID: 31819247 DOI: 10.1038/s41575-019-0226-7]
- 32 **Yang CY**, Ma X, Tsuneyama K, Huang S, Takahashi T, Chalasani NP, Bowlus CL, Yang GX, Leung PS, Ansari AA, Wu L, Coppel RL, Gershwin ME. IL-12/Th1 and IL-23/Th17 biliary microenvironment in primary biliary cirrhosis: implications for therapy. *Hepatology* 2014; **59**: 1944-1953 [PMID: 24375552 DOI: 10.1002/hep.26979]
- 33 **Ronca V**, Mancuso C, Milani C, Carbone M, Oo YH, Invernizzi P. Immune system and cholangiocytes: A puzzling affair in primary biliary cholangitis. *J Leukoc Biol* 2020; **108**: 659-671 [PMID: 32349179 DOI: 10.1002/JLB.5MR0320-200R]
- 34 **Bogdanos DP**, Invernizzi P, Mackay IR, Vergani D. Autoimmune liver serology: current diagnostic and clinical challenges. *World J Gastroenterol* 2008; **14**: 3374-3387 [PMID: 18528935 DOI: 10.3748/wjg.14.3374]
- 35 **Riggione O**, Stokes RP, Thompson RA. Predominance of IgG3 subclass in primary cirrhosis. *Br Med J (Clin Res Ed)* 1983; **286**: 1015-1016 [PMID: 6403174 DOI: 10.1136/bmjj.286.6370.1015-a]
- 36 **Rigopoulou EI**, Davies ET, Bogdanos DP, Liaskos C, Mytilinaiou M, Koukoulis GK, Dalekos GN, Vergani D. Antimitochondrial antibodies of immunoglobulin G3 subclass are associated with a more severe disease course in primary biliary cirrhosis. *Liver Int* 2007; **27**: 1226-1231 [PMID: 17919234 DOI: 10.1111/j.1478-3231.2007.01586.x]
- 37 **Dähnrich C**, Pares A, Caballeria L, Rosemann A, Schlumberger W, Probst C, Mytilinaiou M, Bogdanos D, Vergani D, Stöcker W, Komorowski L. New ELISA for detecting primary biliary cirrhosis-specific antimitochondrial antibodies. *Clin Chem* 2009; **55**: 978-985 [PMID: 19264849 DOI: 10.1373/clinchem.2008.118299]
- 38 **Kaplan MM**, Gandolfo JV, Quaroni EG. An enzyme-linked immunosorbent assay (ELISA) for detecting

antimitochondrial antibody. *Hepatology* 1984; **4**: 727-730 [PMID: 6378751 DOI: 10.1002/hep.1840040428]

39 **Gabeta S**, Norman GL, Liaskos C, Papamichalis PA, Zografos T, Garagounis A, Rigopoulou EI, Dalekos GN. Diagnostic relevance and clinical significance of the new enhanced performance M2 (MIT3) ELISA for the detection of IgA and IgG antimitochondrial antibodies in primary biliary cirrhosis. *J Clin Immunol* 2007; **27**: 378-387 [PMID: 17514501 DOI: 10.1007/s10875-007-9092-0]

40 **Kadokawa Y**, Omagari K, Hazama H, Ohba K, Masuda J, Kinoshita H, Hayashida K, Isomoto H, Mizuta Y, Murase K, Murata I, Kohno S. Evaluation of newly developed ELISA using "MESACUP-2 test mitochondrial M2" kit for the diagnosis of primary biliary cirrhosis. *Clin Biochem* 2003; **36**: 203-210 [PMID: 12726929 DOI: 10.1016/s0009-9120(02)00439-3]

41 **Moteki S**, Leung PS, Coppel RL, Dickson ER, Kaplan MM, Munoz S, Gershwin ME. Use of a designer triple expression hybrid clone for three different lipoyl domain for the detection of antimitochondrial autoantibodies. *Hepatology* 1996; **24**: 97-103 [PMID: 8707289 DOI: 10.1002/hep.510240117]

42 **Bargou I**, Mankař A, Jamaa A, Ben Jazia I, Skandrani K, Sfar H, Baccouche A, Ajmi S, Letaief A, Fabien N, Jedd M, Ghedira I. Detection of M2 antimitochondrial antibodies by dot blot assay is more specific than by enzyme linked immunosorbent assay. *Pathol Biol (Paris)* 2008; **56**: 10-14 [PMID: 17604571 DOI: 10.1016/j.pathbio.2007.05.001]

43 **Meyer W**, Schepet T, Janssen N, Komorowski L, Probst C, Schlumberger W, Bogdanos D, Stöcker W. A comprehensive line immunoassay for the detection of autoantibodies in primary biliary cirrhosis. In: Conrad K, Chan EK, Fritzler MJ, Sack U, Shoenfeld Y, Wiik A, editors. From Etiopathogenesis to the Prediction of Autoimmune Diseases: Relevance of Autoantibodies. Report on the 8th Dresden Symposium on Autoantibodies. 5ed. Dresden: Pabst Science Publishers, 2007: 323-325

44 **Bogdanos DP**, Komorowski L. Disease-specific autoantibodies in primary biliary cirrhosis. *Clin Chim Acta* 2011; **412**: 502-512 [PMID: 21185272 DOI: 10.1016/j.cca.2010.12.019]

45 **Muratori P**, Muratori L, Gershwin ME, Czaja AJ, Pappas G, MacCariello S, Granito A, Cassani F, Loria P, Lenzi M, Bianchi FB. 'True' antimitochondrial antibody-negative primary biliary cirrhosis, low sensitivity of the routine assays, or both? *Clin Exp Immunol* 2004; **135**: 154-158 [PMID: 14678277 DOI: 10.1111/j.1365-2249.2004.02332.x]

46 **Oertelt S**, Rieger R, Selmi C, Invernizzi P, Ansari AA, Coppel RL, Poddar M, Leung PS, Gershwin ME. A sensitive bead assay for antimitochondrial antibodies: Chipping away at AMA-negative primary biliary cirrhosis. *Hepatology* 2007; **45**: 659-665 [PMID: 17326160 DOI: 10.1002/hep.21583]

47 **Nishio A**, Van de Water J, Leung PS, Joplin R, Neuberger JM, Lake J, Björkland A, Tötterman TH, Peters M, Worman HJ, Ansari AA, Coppel RL, Gershwin ME. Comparative studies of antimitochondrial autoantibodies in sera and bile in primary biliary cirrhosis. *Hepatology* 1997; **25**: 1085-1089 [PMID: 9141421 DOI: 10.1002/hep.510250506]

48 **Floreani A**, Baragiotta A, Pizzuti D, Martines D, Cecchetto A, Chiarelli S. Mucosal IgA defect in primary biliary cirrhosis. *Am J Gastroenterol* 2002; **97**: 508-510 [PMID: 11866313 DOI: 10.1111/j.1572-0241.2002.05521.x]

49 **Matsumura S**, Van De Water J, Leung P, Odin JA, Yamamoto K, Gores GJ, Mostov K, Ansari AA, Coppel RL, Shiratori Y, Gershwin ME. Caspase induction by IgA antimitochondrial antibody: IgA-mediated biliary injury in primary biliary cirrhosis. *Hepatology* 2004; **39**: 1415-1422 [PMID: 15122771 DOI: 10.1002/hep.20175]

50 **Kisand KE**, Kisand KV, Karvonen AL, Vuoristo M, Mattila J, Mäkinen J, Uibo R. Antibodies to pyruvate dehydrogenase in primary biliary cirrhosis: correlation with histology. *APMIS* 1998; **106**: 884-892 [PMID: 9808415 DOI: 10.1111/j.1699-0463.1998.tb00235.x]

51 **Tanaka A**, Nezu S, Uegaki S, Mikami M, Okuyama S, Kawamura N, Aiso M, Gershwin ME, Takahashi S, Selmi C, Takikawa H. The clinical significance of IgA antimitochondrial antibodies in sera and saliva in primary biliary cirrhosis. *Ann N Y Acad Sci* 2007; **1107**: 259-270 [PMID: 17804554 DOI: 10.1196/annals.1381.028]

52 **Masuda J**, Omagari K, Ohba K, Hazama H, Kadokawa Y, Kinoshita H, Hayashida K, Ishibashi H, Nakanuma Y, Kohno S. Correlation between histopathological findings of the liver and IgA class antibodies to 2-oxo-acid dehydrogenase complex in primary biliary cirrhosis. *Dig Dis Sci* 2003; **48**: 932-938 [PMID: 12772793 DOI: 10.1023/a:1023055714208]

53 **Lu C**, Hou X, Li M, Wang L, Zeng P, Jia H, Chen J, Wei Y, He H, Liu X, Diao H. Detection of AMA-M2 in human saliva: Potentials in diagnosis and monitoring of primary biliary cholangitis. *Sci Rep* 2017; **7**: 796 [PMID: 28400582 DOI: 10.1038/s41598-017-00906-1]

54 **Leung PS**, Choi J, Yang G, Woo E, Kenny TP, Gershwin ME. A contemporary perspective on the molecular characteristics of mitochondrial autoantigens and diagnosis in primary biliary cholangitis. *Expert Rev Mol Diagn* 2016; **16**: 697-705 [PMID: 26953925 DOI: 10.1586/14737159.2016.1164038]

55 **Rigopoulou EI**, Bogdanos DP, Liaskos C, Koutsoumpas A, Baum H, Vergani D, Dalekos GN. Anti-mitochondrial antibody immunofluorescent titres correlate with the number and intensity of immunoblot-detected mitochondrial bands in patients with primary biliary cirrhosis. *Clin Chim Acta* 2007; **380**: 118-121 [PMID: 17321509 DOI: 10.1016/j.cca.2007.01.023]

56 **Poyatos E**, Morandeira F, Climent J, Mas V, Castellote J, Bas J. Detection of anti-mitochondrial 2-oxoacid dehydrogenase complex subunit's antibodies for the diagnosis of primary biliary cholangitis. *Clin Immunol* 2021; 108749 [PMID: 33945872 DOI: 10.1016/j.clim.2021.108749]

57 **Villalta D**, Seaman A, Tiengson M, Warren C, Bentow C, Bizzaro N, Alessio MG, Porcelli B, Norman GL, Mahler M. Evaluation of a novel extended automated particle-based multi-analyte assay for the detection of autoantibodies in the diagnosis of primary biliary cholangitis. *Clin Chem Lab Med* 2020; **58**: 1499-1507 [PMID: 32286240 DOI: 10.1515/cclm-2020-0122]

58 **Hu S**, Zhao F, Wang Q, Chen WX. The accuracy of the anti-mitochondrial antibody and the M2 subtype test for diagnosis of primary biliary cirrhosis: a meta-analysis. *Clin Chem Lab Med* 2014; **52**: 1533-1542 [PMID: 24501161 DOI: 10.1515/cclm-2013-0926]

59 **Metcalf JV**, Mitchison HC, Palmer JM, Jones DE, Bassendine MF, James OF. Natural history of early primary biliary cirrhosis. *Lancet* 1996; **348**: 1399-1402 [PMID: 8937278 DOI: 10.1016/S0140-6736(96)04410-8]

60 **Mitchison HC**, Bassendine MF, Hendrick A, Bennett MK, Bird G, Watson AJ, James OF. Positive antimitochondrial antibody but normal alkaline phosphatase: is this primary biliary cirrhosis? *Hepatology* 1986; **6**: 1279-1284 [PMID: 3530311 DOI: 10.1002/hep.510060311]

3793004 DOI: 10.1002/hep.1840060609]

61 **Zandanel S**, Strasser M, Feldman A, Tevini J, Strebinger G, Niederseer D, Pohla-Gubo G, Huber-Schönauer U, Ruhaltinger S, Paulweber B, Datz C, Felder TK, Aigner E. Low rate of new-onset primary biliary cholangitis in a cohort of anti-mitochondrial antibody-positive subjects over six years of follow-up. *J Intern Med* 2020; **287**: 395-404 [PMID: 31802567 DOI: 10.1111/joim.13005]

62 **Dahlqvist G**, Gaour F, Carrat F, Meurisse S, Chazouillères O, Poupon R, Johanet C, Corpechot C; French network of Immunology Laboratories. Large-scale characterization study of patients with antimitochondrial antibodies but nonestablished primary biliary cholangitis. *Hepatology* 2017; **65**: 152-163 [PMID: 27688145 DOI: 10.1002/hep.28859]

63 **Sun C**, Xiao X, Yan L, Sheng L, Wang Q, Jiang P, Lian M, Li Y, Wei Y, Zhang J, Chen Y, Li B, Huang B, Peng Y, Chen X, Fang J, Qiu D, Hua J, Tang R, Leung P, Gershwin ME, Miao Q, Ma X. Histologically proven AMA positive primary biliary cholangitis but normal serum alkaline phosphatase: Is alkaline phosphatase truly a surrogate marker? *J Autoimmun* 2019; **99**: 33-38 [PMID: 30709684 DOI: 10.1016/j.jaut.2019.01.005]

64 **Turchany JM**, Uibo R, Kivik T, Van de Water J, Prindiville T, Coppel RL, Gershwin ME. A study of antimitochondrial antibodies in a random population in Estonia. *Am J Gastroenterol* 1997; **92**: 124-126 [PMID: 8995951]

65 **Mattalia A**, Quaranta S, Leung PS, Bauducco M, Van de Water J, Calvo PL, Danielle F, Rizzetto M, Ansari A, Coppel RL, Rosina F, Gershwin ME. Characterization of antimitochondrial antibodies in health adults. *Hepatology* 1998; **27**: 656-661 [PMID: 9500690 DOI: 10.1002/hep.510270303]

66 **Dubel L**, Farges O, Bismuth H, Sebagh M, Homberg JC, Johanet C. Kinetics of anti-M2 antibodies after liver transplantation for primary biliary cirrhosis. *J Hepatol* 1995; **23**: 674-680 [PMID: 8750166 DOI: 10.1016/0168-8278(95)80033-6]

67 **Montano-Loza AJ**, Hansen BE, Corpechot C, Roccarina D, Thorburn D, Trivedi P, Hirschfield G, McDowell P, Poupon R, Dumortier J, Bosch A, Giostra E, Conti F, Parés A, Reig A, Floreani A, Russo FP, Goet JC, Harms MH, van Buuren H, Van den Ende N, Nevens F, Verhelst X, Donato MF, Malinverno F, Ebadi M, Mason AL; Global PBC Study Group. Factors Associated With Recurrence of Primary Biliary Cholangitis After Liver Transplantation and Effects on Graft and Patient Survival. *Gastroenterology* 2019; **156**: 96-107.e1 [PMID: 30296431 DOI: 10.1053/j.gastro.2018.10.001]

68 **Kisand KE**, Metsküla K, Kisand KV, Kivik T, Gershwin ME, Uibo R. The follow-up of asymptomatic persons with antibodies to pyruvate dehydrogenase in adult population samples. *J Gastroenterol* 2001; **36**: 248-254 [PMID: 11324728 DOI: 10.1007/s005350170111]

69 **Heseltine L**, Turner IB, Fussey SP, Kelly PJ, James OF, Yeaman SJ, Bassendine MF. Primary biliary cirrhosis. Quantitation of autoantibodies to purified mitochondrial enzymes and correlation with disease progression. *Gastroenterology* 1990; **99**: 1786-1792 [PMID: 2227292 DOI: 10.1016/0016-5085(90)90488-m]

70 **Christensen E**, Crowe J, Doniach D, Popper H, Ranek L, Rodés J, Tygstrup N, Williams R. Clinical pattern and course of disease in primary biliary cirrhosis based on an analysis of 236 patients. *Gastroenterology* 1980; **78**: 236-246 [PMID: 7350046]

71 **Dellavance A**, Cançado EL, Abrantes-Lemos CP, Harriz M, Marvulle V, Andrade LE. Humoral autoimmune response heterogeneity in the spectrum of primary biliary cirrhosis. *Hepatol Int* 2013; **7**: 775-784 [PMID: 23853697 DOI: 10.1007/s12072-012-9413-0]

72 **Poupon RE**, Balkau B, Eschwège E, Poupon R. A multicenter, controlled trial of ursodiol for the treatment of primary biliary cirrhosis. UDCA-PBC Study Group. *N Engl J Med* 1991; **324**: 1548-1554 [PMID: 1674105 DOI: 10.1056/NEJM199105303242204]

73 **Chang ML**, Chen WT, Chan TM, Lin CY, Chang MY, Chen SC, Chien RN. Anti-Mitochondrial Antibody Titers Decrease Over Time in Primary Biliary Cholangitis Patients With Ursodeoxycholic Acid Therapeutic Response: A Cohort Study Followed Up to 28 Years. *Front Immunol* 2022; **13**: 869018 [PMID: 35663951 DOI: 10.3389/fimmu.2022.869018]

74 **Tana MM**, Shums Z, Milo J, Norman GL, Leung PS, Gershwin ME, Noureddin M, Kleiner DE, Zhao X, Heller T, Hoofnagle JH. The Significance of Autoantibody Changes Over Time in Primary Biliary Cirrhosis. *Am J Clin Pathol* 2015; **144**: 601-606 [PMID: 26386081 DOI: 10.1309/AJCPQV4A7QAEFEV]

75 **Van Norstrand MD**, Malinchoc M, Lindor KD, Therneau TM, Gershwin ME, Leung PS, Dickson ER, Homburger HA. Quantitative measurement of autoantibodies to recombinant mitochondrial antigens in patients with primary biliary cirrhosis: relationship of levels of autoantibodies to disease progression. *Hepatology* 1997; **25**: 6-11 [PMID: 8985257 DOI: 10.1002/hep.510250103]

76 **Feng L**, Dong K, Zhang X, Ma B, Chen L, Yang Q, Chen Q, Wen X, Jin Q. Clinical significance of IgG antimitochondrial M2 antibody levels in primary biliary cholangitis: A single center study from China. *PLoS One* 2020; **15**: e0242164 [PMID: 33180817 DOI: 10.1371/journal.pone.0242164]

77 **Dohmen K**, Mizuta T, Nakamura M, Shimohashi N, Ishibashi H, Yamamoto K. Fenofibrate for patients with asymptomatic primary biliary cirrhosis. *World J Gastroenterol* 2004; **10**: 894-898 [PMID: 15040040 DOI: 10.3748/wjg.v10.i6.894]

78 **European Association for the Study of the Liver**. EASL Clinical Practice Guidelines: Autoimmune hepatitis. *J Hepatol* 2015; **63**: 971-1004 [PMID: 26341719 DOI: 10.1016/j.jhep.2015.06.030]

79 **Rigopoulou EI**, Zachou K, Gatselis NK, Papadamou G, Koukoulis GK, Dalekos GN. Primary biliary cirrhosis in HBV and HCV patients: Clinical characteristics and outcome. *World J Hepatol* 2013; **5**: 577-583 [PMID: 24179617 DOI: 10.4254/wjh.v5.i10.577]

80 **Rigopoulou EI**, Dalekos GN. Molecular diagnostics of primary biliary cirrhosis. *Expert Opin Med Diagn* 2008; **2**: 621-634 [PMID: 23495774 DOI: 10.1517/17530059.2.6.621]

81 **Muratori P**, Muratori L, Ferrari R, Cassani F, Bianchi G, Lenzi M, Rodrigo L, Linares A, Fuentes D, Bianchi FB. Characterization and clinical impact of antinuclear antibodies in primary biliary cirrhosis. *Am J Gastroenterol* 2003; **98**: 431-437 [PMID: 12591064 DOI: 10.1111/j.1572-0241.2003.07257.x]

82 **Marasini B**, Gagetta M, Rossi V, Ferrari P. Rheumatic disorders and primary biliary cirrhosis: an appraisal of 170 Italian patients. *Ann Rheum Dis* 2001; **60**: 1046-1049 [PMID: 11602476 DOI: 10.1136/ard.60.11.1046]

83 **Damoiseaux J**, Andrade LEC, Carballo OG, Conrad K, Francescantonio PLC, Fritzler MJ, Garcia de la Torre I, Herold

M, Klotz W, Cruvinel WM, Mimori T, von Muhlen C, Satoh M, Chan EK. Clinical relevance of HEp-2 indirect immunofluorescent patterns: the International Consensus on ANA patterns (ICAP) perspective. *Ann Rheum Dis* 2019; **78**: 879-889 [PMID: 30862649 DOI: 10.1136/annrheumdis-2018-214436]

84 **Granito A**, Muratori P, Muratori L, Pappas G, Cassani F, Worthington J, Ferri S, Quarneri C, Cipriano V, de Molo C, Lenzi M, Chapman RW, Bianchi FB. Antibodies to SS-A/Ro-52kD and centromere in autoimmune liver disease: a clue to diagnosis and prognosis of primary biliary cirrhosis. *Aliment Pharmacol Ther* 2007; **26**: 831-838 [PMID: 17767467 DOI: 10.1111/j.1365-2036.2007.03433.x]

85 **Rigamonti C**, Shand LM, Feudjo M, Bunn CC, Black CM, Denton CP, Burroughs AK. Clinical features and prognosis of primary biliary cirrhosis associated with systemic sclerosis. *Gut* 2006; **55**: 388-394 [PMID: 16150855 DOI: 10.1136/gut.2005.075002]

86 **Nakamura M**, Kondo H, Mori T, Komori A, Matsuyama M, Ito M, Takii Y, Koyabu M, Yokoyama T, Migita K, Daikoku M, Abiru S, Yatsuhashi H, Takezaki E, Masaki N, Sugi K, Honda K, Adachi H, Nishi H, Watanabe Y, Nakamura Y, Shimada M, Komatsu T, Saito A, Saoshiro T, Harada H, Sodeyama T, Hayashi S, Masumoto A, Sando T, Yamamoto T, Sakai H, Kobayashi M, Muro T, Koga M, Shums Z, Norman GL, Ishibashi H. Anti-gp210 and anti-centromere antibodies are different risk factors for the progression of primary biliary cirrhosis. *Hepatology* 2007; **45**: 118-127 [PMID: 17187436 DOI: 10.1002/hep.21472]

87 **Yang WH**, Yu JH, Nakajima A, Neuberg D, Lindor K, Bloch DB. Do antinuclear antibodies in primary biliary cirrhosis patients identify increased risk for liver failure? *Clin Gastroenterol Hepatol* 2004; **2**: 1116-1122 [PMID: 15625657 DOI: 10.1016/s1542-3565(04)00465-3]

88 **Gao L**, Tian X, Liu B, Zhang F. The value of antinuclear antibodies in primary biliary cirrhosis. *Clin Exp Med* 2008; **8**: 9-15 [PMID: 18385935 DOI: 10.1007/s10238-008-0150-6]

89 **Invernizzi P**, Selmi C, Ranftler C, Podda M, Wesierska-Gadek J. Antinuclear antibodies in primary biliary cirrhosis. *Semin Liver Dis* 2005; **25**: 298-310 [PMID: 16143945 DOI: 10.1055/s-2005-916321]

90 **Janka C**, Selmi C, Gershwin ME, Will H, Sternsdorf T. Small ubiquitin-related modifiers: A novel and independent class of autoantigens in primary biliary cirrhosis. *Hepatology* 2005; **41**: 609-616 [PMID: 15726652 DOI: 10.1002/hep.20619]

91 **Rigopoulou EI**, Davies ET, Pares A, Zachou K, Liaskos C, Bogdanos DP, Rodes J, Dalekos GN, Vergani D. Prevalence and clinical significance of isotype specific antinuclear antibodies in primary biliary cirrhosis. *Gut* 2005; **54**: 528-532 [PMID: 15753539 DOI: 10.1136/gut.2003.036558]

92 **Invernizzi P**, Podda M, Battezzati PM, Crosignani A, Zuin M, Hitchman E, Maggioni M, Meroni PL, Penner E, Wesierska-Gadek J. Autoantibodies against nuclear pore complexes are associated with more active and severe liver disease in primary biliary cirrhosis. *J Hepatol* 2001; **34**: 366-372 [PMID: 11322196 DOI: 10.1016/s0168-8278(00)00040-4]

93 **Mytilinaiou MG**, Meyer W, Scheper T, Rigopoulou EI, Probst C, Koutsoumpas AL, Abeles D, Burroughs AK, Komorowski L, Vergani D, Bogdanos DP. Diagnostic and clinical utility of antibodies against the nuclear body promyelocytic leukaemia and Sp100 antigens in patients with primary biliary cirrhosis. *Clin Chim Acta* 2012; **413**: 1211-1216 [PMID: 22503841 DOI: 10.1016/j.cca.2012.03.020]

94 **Bogdanos DP**, Liaskos C, Pares A, Norman G, Rigopoulou EI, Caballeria L, Dalekos GN, Rodes J, Vergani D. Anti-gp210 antibody mirrors disease severity in primary biliary cirrhosis. *Hepatology* 2007; **45**: 1583; author reply 1583-1583; author reply 1584 [PMID: 17538935 DOI: 10.1002/hep.21678]

95 **Mattalia A**, Lüttig B, Rosina F, Leung PS, Van de Water J, Bauducci M, Ciancio A, Böker KH, Worman H, Cooper RL, Manns M, Ansari A, Rizzetto M, Gershwin ME. Persistence of autoantibodies against recombinant mitochondrial and nuclear pore proteins after orthotopic liver transplantation for primary biliary cirrhosis. *J Autoimmun* 1997; **10**: 491-497 [PMID: 9376077 DOI: 10.1006/jaut.1997.0156]

96 **Bandin O**, Courvalin JC, Poupon R, Dubel L, Homberg JC, Johanet C. Specificity and sensitivity of gp210 autoantibodies detected using an enzyme-linked immunosorbent assay and a synthetic polypeptide in the diagnosis of primary biliary cirrhosis. *Hepatology* 1996; **23**: 1020-1024 [PMID: 8621127 DOI: 10.1002/hep.510230512]

97 **Itoh S**, Ichida T, Yoshida T, Hayakawa A, Uchida M, Tashiro-Itoh T, Matsuda Y, Ishihara K, Asakura H. Autoantibodies against a 210 kDa glycoprotein of the nuclear pore complex as a prognostic marker in patients with primary biliary cirrhosis. *J Gastroenterol Hepatol* 1998; **13**: 257-265 [PMID: 9570238 DOI: 10.1111/j.1440-1746.1998.01553.x]

98 **Hu SL**, Zhao FR, Hu Q, Chen WX. Meta-analysis assessment of GP210 and SP100 for the diagnosis of primary biliary cirrhosis. *PLoS One* 2014; **9**: e101916 [PMID: 25010534 DOI: 10.1371/journal.pone.0101916]

99 **Lozano F**, Parés A, Borche L, Plana M, Gallart T, Rodés J, Vives J. Autoantibodies against nuclear envelope-associated proteins in primary biliary cirrhosis. *Hepatology* 1988; **8**: 930-938 [PMID: 3292364 DOI: 10.1002/hep.1840080438]

100 **Lassoued K**, Brenard R, Degos F, Courvalin JC, Andre C, Danon F, Brouet JC, Zine-el-Abidine Y, Degott C, Zafrani S. Antinuclear antibodies directed to a 200-kilodalton polypeptide of the nuclear envelope in primary biliary cirrhosis. A clinical and immunological study of a series of 150 patients with primary biliary cirrhosis. *Gastroenterology* 1990; **99**: 181-186 [PMID: 2188869 DOI: 10.1016/0016-5085(90)91246-3]

101 **Sfakianaki O**, Koulentaki M, Tzardi M, Tsangaridou E, Theodoropoulos PA, Castanas E, Kouroumalis EA. Peri-nuclear antibodies correlate with survival in Greek primary biliary cirrhosis patients. *World J Gastroenterol* 2010; **16**: 4938-4943 [PMID: 20954280 DOI: 10.3748/wjg.v16.i39.4938]

102 **Huang C**, Han W, Wang C, Liu Y, Chen Y, Duan Z. Early Prognostic Utility of Gp210 Antibody-Positive Rate in Primary Biliary Cholangitis: A Meta-Analysis. *Dis Markers* 2019; **2019**: 9121207 [PMID: 31737133 DOI: 10.1155/2019/9121207]

103 **Nakamura M**, Shimizu-Yoshida Y, Takii Y, Komori A, Yokoyama T, Ueki T, Daikoku M, Yano K, Matsumoto T, Migita K, Yatsuhashi H, Ito M, Masaki N, Adachi H, Watanabe Y, Nakamura Y, Saoshiro T, Sodeyama T, Koga M, Shimoda S, Ishibashi H. Antibody titer to gp210-C terminal peptide as a clinical parameter for monitoring primary biliary cirrhosis. *J Hepatol* 2005; **42**: 386-392 [PMID: 15710222 DOI: 10.1016/j.jhep.2004.11.016]

104 **Gatselis NK**, Zachou K, Norman GL, Gabeta S, Papamichalis P, Koukoulis GK, Dalekos GN. Clinical significance of the fluctuation of primary biliary cirrhosis-related autoantibodies during the course of the disease. *Autoimmunity* 2013; **46**:

471-479 [PMID: 23777462 DOI: 10.3109/08916934.2013.801461]

105 **Miyachi K**, Hankins RW, Matsushima H, Kikuchi F, Inomata T, Horigome T, Shibata M, Onozuka Y, Ueno Y, Hashimoto E, Hayashi N, Shibuya A, Amaki S, Miyakawa H. Profile and clinical significance of anti-nuclear envelope antibodies found in patients with primary biliary cirrhosis: a multicenter study. *J Autoimmun* 2003; **20**: 247-254 [PMID: 12753810 DOI: 10.1016/s0896-8411(03)00033-7]

106 **Wesierska-Gadek J**, Hohenuer H, Hitchman E, Penner E. Autoantibodies against nucleoporin p62 constitute a novel marker of primary biliary cirrhosis. *Gastroenterology* 1996; **110**: 840-847 [PMID: 8608894 DOI: 10.1053/gast.1996.v110.pm8608894]

107 **Züchner D**, Sternsdorf T, Szostecki C, Heathcote EJ, Cauch-Dudek K, Will H. Prevalence, kinetics, and therapeutic modulation of autoantibodies against Sp100 and promyelocytic leukemia protein in a large cohort of patients with primary biliary cirrhosis. *Hepatology* 1997; **26**: 1123-1130 [PMID: 9362351 DOI: 10.1002/hep.510260506]

108 **Muratori P**, Muratori L, Cassani F, Terlizzi P, Lenzi M, Rodrigo L, Bianchi FB. Anti-multiple nuclear dots (anti-MND) and anti-SP100 antibodies in hepatic and rheumatological disorders. *Clin Exp Immunol* 2002; **127**: 172-175 [PMID: 11882049 DOI: 10.1046/j.1365-2249.2002.01719.x]

109 **Bauer A**, Habior A, Kraszewska E. Detection of anti-SP100 antibodies in primary biliary cirrhosis. Comparison of ELISA and immunofluorescence. *J Immunoassay Immunochem* 2013; **34**: 346-355 [PMID: 23859785 DOI: 10.1080/15321819.2012.741088]

110 **Bauer A**, Habior A, Gawel D. Diagnostic and Clinical Value of Specific Autoantibodies against Kelch-like 12 Peptide and Nuclear Envelope Proteins in Patients with Primary Biliary Cholangitis. *Biomedicines* 2022; **10** [PMID: 35453551 DOI: 10.3390/biomedicines10040801]

111 **Luettig B**, Boeker KH, Schoessler W, Will H, Loges S, Schmidt E, Worman HJ, Gershwin ME, Manns MP. The antinuclear autoantibodies Sp100 and gp210 persist after orthotopic liver transplantation in patients with primary biliary cirrhosis. *J Hepatol* 1998; **28**: 824-828 [PMID: 9625318 DOI: 10.1016/s0168-8278(98)80233-x]

112 **Bogdanos DP**, Baum H, Butler P, Rigopoulou EI, Davies ET, Ma Y, Burroughs AK, Vergani D. Association between the primary biliary cirrhosis specific anti-sp100 antibodies and recurrent urinary tract infection. *Dig Liver Dis* 2003; **35**: 801-805 [PMID: 14674671 DOI: 10.1016/s1590-8658(03)00466-3]

113 **Shimoda S**, Nakamura M, Ishibashi H, Kawano A, Kamihira T, Sakamoto N, Matsushita S, Tanaka A, Worman HJ, Gershwin ME, Harada M. Molecular mimicry of mitochondrial and nuclear autoantigens in primary biliary cirrhosis. *Gastroenterology* 2003; **124**: 1915-1925 [PMID: 12806624 DOI: 10.1016/s0016-5085(03)00387-1]

114 **Wang C**, Zheng X, Jiang P, Tang R, Gong Y, Dai Y, Wang L, Xu P, Sun W, Han C, Jiang Y, Wei Y, Zhang K, Wu J, Shao Y, Gao Y, Yu J, Hu Z, Zang Z, Zhao Y, Wu X, Dai N, Liu L, Nie J, Jiang B, Lin M, Li L, Li Y, Chen S, Shu L, Qiu F, Wu Q, Zhang M, Chen R, Jawed R, Zhang Y, Shi X, Zhu Z, Pei H, Huang L, Zhao W, Tian Y, Zhu X, Qiu H, Gershwin ME, Chen W, Seldin MF, Liu X, Sun L, Ma X. Genome-wide Association Studies of Specific Antinuclear Autoantibody Subphenotypes in Primary Biliary Cholangitis. *Hepatology* 2019; **70**: 294-307 [PMID: 30854688 DOI: 10.1002/hep.30604]

115 **Vergani D**, Bogdanos DP. Positive markers in AMA-negative PBC. *Am J Gastroenterol* 2003; **98**: 241-243 [PMID: 12591035 DOI: 10.1111/j.1572-0241.2003.07270.x]

116 **Miyakawa H**, Tanaka A, Kikuchi K, Matsushita M, Kitazawa E, Kawaguchi N, Fujikawa H, Gershwin ME. Detection of antimitochondrial autoantibodies in immunofluorescent AMA-negative patients with primary biliary cirrhosis using recombinant autoantigens. *Hepatology* 2001; **34**: 243-248 [PMID: 11481607 DOI: 10.1053/jhep.2001.26514]

117 **Michieletti P**, Wanless IR, Katz A, Scheuer PJ, Yeaman SJ, Bassendine MF, Palmer JM, Heathcote EJ. Antimitochondrial antibody negative primary biliary cirrhosis: a distinct syndrome of autoimmune cholangitis. *Gut* 1994; **35**: 260-265 [PMID: 8307480 DOI: 10.1136/gut.35.2.260]

118 **Nakajima M**, Shimizu H, Miyazaki A, Watanabe S, Kitami N, Sato N. Detection of IgA, IgM, and IgG subclasses of anti-M2 antibody by immunoblotting in autoimmune cholangitis: is autoimmune cholangitis an early stage of primary biliary cirrhosis? *J Gastroenterol* 1999; **34**: 607-612 [PMID: 10535489 DOI: 10.1007/s005350050380]

119 **Kitami N**, Komada T, Ishii H, Shimizu H, Adachi H, Yamaguchi Y, Kitamura T, Oide H, Miyazaki A, Ishikawa M. Immunological study of anti-M2 in antimitochondrial antibody-negative primary biliary cirrhosis. *Intern Med* 1995; **34**: 496-501 [PMID: 7549131 DOI: 10.2169/internalmedicine.34.496]

120 **Invernizzi P**, Crosignani A, Battezzati PM, Covini G, De Valle G, Larghi A, Zuin M, Podda M. Comparison of the clinical features and clinical course of antimitochondrial antibody-positive and -negative primary biliary cirrhosis. *Hepatology* 1997; **25**: 1090-1095 [PMID: 9141422 DOI: 10.1002/hep.510250507]

121 **Juliusson G**, Imam M, Björnsson ES, Talwalkar JA, Lindor KD. Long-term outcomes in antimitochondrial antibody negative primary biliary cirrhosis. *Scand J Gastroenterol* 2016; **51**: 745-752 [PMID: 26776319 DOI: 10.3109/00365521.2015.1132337]

122 **Jin Q**, Moritoki Y, Lleo A, Tsuneyama K, Invernizzi P, Moritoki H, Kikuchi K, Lian ZX, Hirschfield GM, Ansari AA, Coppel RL, Gershwin ME, Niu J. Comparative analysis of portal cell infiltrates in antimitochondrial autoantibody-positive vs antimitochondrial autoantibody-negative primary biliary cirrhosis. *Hepatology* 2012; **55**: 1495-1506 [PMID: 22135136 DOI: 10.1002/hep.25511]

123 **Lacerda MA**, Ludwig J, Dickson ER, Jorgensen RA, Lindor KD. Antimitochondrial antibody-negative primary biliary cirrhosis. *Am J Gastroenterol* 1995; **90**: 247-249 [PMID: 7847294]

124 **Liu B**, Shi XH, Zhang FC, Zhang W, Gao LX. Antimitochondrial antibody-negative primary biliary cirrhosis: a subset of primary biliary cirrhosis. *Liver Int* 2008; **28**: 233-239 [PMID: 18251980 DOI: 10.1111/j.1478-3231.2007.01651.x]

125 **Norman GL**, Yang CY, Ostendorff HP, Shums Z, Lim MJ, Wang J, Awad A, Hirschfield GM, Milkiewicz P, Bloch DB, Rothschild KJ, Bowlus CL, Adamopoulos IE, Leung PS, Janssen HJ, Cheung AC, Coltescu C, Gershwin ME. Anti-kelch-like 12 and anti-hexokinase 1: novel autoantibodies in primary biliary cirrhosis. *Liver Int* 2015; **35**: 642-651 [PMID: 25243383 DOI: 10.1111/liv.12690]

126 **Hu CJ**, Song G, Huang W, Liu GZ, Deng CW, Zeng HP, Wang L, Zhang FC, Zhang X, Jeong JS, Blackshaw S, Jiang LZ, Zhu H, Wu L, Li YZ. Identification of new autoantigens for primary biliary cirrhosis using human proteome microarrays.

Mol Cell Proteomics 2012; **11**: 669-680 [PMID: 22647870 DOI: 10.1074/mcp.M111.015529]

127 **Reig A**, Norman GL, Garcia M, Shums Z, Ruiz-Gaspà S, Bentow C, Mahler M, Romera MA, Vinas O, Pares A. Novel Anti-Hexokinase 1 Antibodies Are Associated With Poor Prognosis in Patients With Primary Biliary Cholangitis. *Am J Gastroenterol* 2020; **115**: 1634-1641 [PMID: 32467507 DOI: 10.14309/ajg.00000000000000690]

128 **Norman GL**, Reig A, Viñas O, Mahler M, Wunsch E, Milkiewicz P, Swain MG, Mason A, Stinton LM, Aparicio MB, Aldegunde MJ, Fritzler MJ, Parés A. The Prevalence of Anti-Hexokinase-1 and Anti-Kelch-Like 12 Peptide Antibodies in Patients With Primary Biliary Cholangitis Is Similar in Europe and North America: A Large International, Multi-Center Study. *Front Immunol* 2019; **10**: 662 [PMID: 31001269 DOI: 10.3389/fimmu.2019.00662]

129 **Bombaci M**, Pesce E, Torri A, Carpi D, Crosti M, Lanzafame M, Cordigliero C, Sinisi A, Moro M, Bernuzzi F, Gerussi A, Geginat J, Muratori L, Terracciano LM, Invernizzi P, Abrignani S, Grifantini R. Novel biomarkers for primary biliary cholangitis to improve diagnosis and understand underlying regulatory mechanisms. *Liver Int* 2019; **39**: 2124-2135 [PMID: 31033124 DOI: 10.1111/liv.14128]

130 **Liu H**, Norman GL, Shums Z, Worman HJ, Krawitt EL, Bizzaro N, Vergani D, Bogdanos DP, Dalekos GN, Milkiewicz P, Czaja AJ, Heathcote EJ, Hirschfield GM, Tan EM, Miyachi K, Bignotto M, Battezzati PM, Lleo A, Leung PS, Podda M, Gershwin ME, Invernizzi P. PBC screen: an IgG/IgA dual isotype ELISA detecting multiple mitochondrial and nuclear autoantibodies specific for primary biliary cirrhosis. *J Autoimmun* 2010; **35**: 436-442 [PMID: 20932720 DOI: 10.1016/j.jaut.2010.09.005]

131 **Bizzaro N**, Covini G, Rosina F, Muratori P, Tonutti E, Villalta D, Pesente F, Alessio MG, Tampoaia M, Antico A, Platzgummer S, Porcelli B, Terzuoli L, Liguori M, Bassetti D, Brusca I, Almasio PL, Tarantino G, Bonaguri C, Agostinis P, Bredi E, Tozzoli R, Invernizzi P, Selmi C. Overcoming a "probable" diagnosis in antimitochondrial antibody negative primary biliary cirrhosis: study of 100 sera and review of the literature. *Clin Rev Allergy Immunol* 2012; **42**: 288-297 [PMID: 21188646 DOI: 10.1007/s12016-010-8234-y]

132 **Villalta D**, Sorrentino MC, Girolami E, Tampoaia M, Alessio MG, Brusca I, Daves M, Porcelli B, Barberio G, Bizzaro N; Study Group on Autoimmune Diseases of the Italian Society of Laboratory Medicine. Autoantibody profiling of patients with primary biliary cirrhosis using a multiplexed line-blot assay. *Clin Chim Acta* 2015; **438**: 135-138 [PMID: 25172039 DOI: 10.1016/j.cca.2014.08.024]

133 **Leung KK**, Hirschfield GM. Autoantibodies in Primary Biliary Cholangitis. *Clin Liver Dis* 2022; **26**: 613-627 [PMID: 36270719 DOI: 10.1016/j.cld.2022.06.004]

Artificial intelligence as a noninvasive tool for pancreatic cancer prediction and diagnosis

Alexandra Corina Faur, Daniela Cornelia Lazar, Laura Andreea Ghenciu

Specialty type: Gastroenterology and hepatology

Provenance and peer review:
Invited article; Externally peer reviewed.

Peer-review model: Single blind

Peer-review report's scientific quality classification

Grade A (Excellent): 0

Grade B (Very good): B

Grade C (Good): C

Grade D (Fair): D

Grade E (Poor): 0

P-Reviewer: Charalampopoulou A, Italy; Chen G, China; Yang Y, China

Received: November 15, 2022

Peer-review started: November 15, 2022

First decision: December 11, 2022

Revised: December 23, 2022

Accepted: March 15, 2023

Article in press: March 15, 2023

Published online: March 28, 2023



Alexandra Corina Faur, Department of Anatomy and Embriology, "Victor Babeș" University of Medicine and Pharmacy Timișoara, Timișoara 300041, Timiș, Romania

Daniela Cornelia Lazar, Department V of Internal Medicine I, Discipline of Internal Medicine IV, University of Medicine and Pharmacy "Victor Babes" Timișoara, Timișoara 300041, Timiș, Romania

Laura Andreea Ghenciu, Department III, Discipline of Pathophysiology, "Victor Babeș" University of Medicine and Pharmacy, Timișoara 300041, Timiș, Romania

Corresponding author: Alexandra Corina Faur, PhD, Additional Professor, Department of Anatomy and Embriology, "Victor Babeș" University of Medicine and Pharmacy Timișoara, Eftimie Murgu Sq. no. 2, Timișoara 300041, Timiș, Romania. faur.alexandra@umft.ro

Abstract

Pancreatic cancer (PC) has a low incidence rate but a high mortality, with patients often in the advanced stage of the disease at the time of the first diagnosis. If detected, early neoplastic lesions are ideal for surgery, offering the best prognosis. Preneoplastic lesions of the pancreas include pancreatic intraepithelial neoplasia and mucinous cystic neoplasms, with intraductal papillary mucinous neoplasms being the most commonly diagnosed. Our study focused on predicting PC by identifying early signs using noninvasive techniques and artificial intelligence (AI). A systematic English literature search was conducted on the PubMed electronic database and other sources. We obtained a total of 97 studies on the subject of pancreatic neoplasms. The final number of articles included in our study was 44, 34 of which focused on the use of AI algorithms in the early diagnosis and prediction of pancreatic lesions. AI algorithms can facilitate diagnosis by analyzing massive amounts of data in a short period of time. Correlations can be made through AI algorithms by expanding image and electronic medical records databases, which can later be used as part of a screening program for the general population. AI-based screening models should involve a combination of biomarkers and medical and imaging data from different sources. This requires large numbers of resources, collaboration between medical practitioners, and investment in medical infrastructures.

Key Words: Pancreatic cancer; Early pancreatic lesions; Pancreatic neoplasia; Artificial intelligence; Deep learning; Machine learning; Radiomics; Diagnosis; Pancreas

Core Tip: To improve the clinical management and prognosis for patients with pancreatic cancer (PC), new diagnostic methods should be developed to identify precursor lesions. Artificial intelligence (AI) is a tool that can offer a personalized approach in this regard by analyzing a large quantity of heterogeneous data and can also help in decision-making, increasing the prediction accuracy for an early diagnosis. The aim of this study was to provide a comprehensive overview of the advances in detecting PC noninvasively with an emphasis on early lesions and AI.

Citation: Faur AC, Lazar DC, Ghenciu LA. Artificial intelligence as a noninvasive tool for pancreatic cancer prediction and diagnosis. *World J Gastroenterol* 2023; 29(12): 1811-1823

URL: <https://www.wjgnet.com/1007-9327/full/v29/i12/1811.htm>

DOI: <https://dx.doi.org/10.3748/wjg.v29.i12.1811>

INTRODUCTION

The World Health Organization estimates that early cancer detection will result in 30% greater cure rates for most cancer types[1]. Pancreatic cancer (PC) has a low incidence but is currently the 4th leading cause of all cancer deaths. The 5-year survival rate for PC is between 7% and 20%, with the best prognosis obtained for pancreatic neoplasms diagnosed in early stages[2-4]. Studies have reported that the 5-year survival rate can be as high as 39.9% in localized pancreatic tumors, but in patients who develop metastatic disease, the rate drops significantly to 2.9%[2-4].

There are two main types of PC, exocrine carcinomas and neuroendocrine neoplasms, with the former accounting for more than 95% of pancreatic tumors[5]. Patients with exocrine tumors compared with those with endocrine ones have a median survival of approximately 4 mo vs 27 mo[6]. Approximately 90% of exocrine PC cases are pancreatic ductal adenocarcinoma (PDAC); 80% of PDAC patients are in the advanced stage of the disease at the time of the first diagnosis[4,7]. A total of 49.6% of PDAC patients are diagnosed with distant metastases, and only approximately 15% have a surgically resectable tumor[1,2,4,7]. By 2030, PDAC is expected to become the second most common cause of cancer-related death in Western countries[8]. An important aspect in the diagnosis of PC is the size of the tumor, which correlates with outcome. For early-stage PDAC with node-negative, small tumors (< 2 cm), the survival rate can be as high as 80%[8]. Less than 2% of PCs are pancreatic neuroendocrine tumors (PNT). Current data have shown that an earlier diagnosis of PNTs is not associated with an improved survival rate. Compared with PDACs, PNTs have a better prognosis[9,10].

Preneoplastic lesions that frequently arise in the exocrine pancreas include pancreatic intraepithelial neoplasia (PanIN), mucinous cystic neoplasms (MCN), and intraductal papillary mucinous neoplasms (IPMNs)[11]. Low-grade PanIN is quite common (present in 40%-75% of adults), especially after the age of 40[12]. The progression from low-grade PanIN to invasive tumors is unknown, and currently, identifying this type of lesion is not sufficient to justify surgical intervention. However, if high-grade PanIN is detected, surgery is highly indicated[1]. MCNs of the pancreas rarely progress to PC[11], while IPMNs are fairly common and, if left untreated, can progress to cancer[13]. An association between PDAC and IPMN has been reported in 11%-80% of cases[14]. Identifying high-risk IPMNs before surgical intervention enables patients in the low-risk category to avoid unnecessary surgery for benign disease. At this time, there are no accurate methods for the preoperative discrimination between high- and low-risk IPMNs[3,15].

Pancreatitis and cystic lesions of the pancreas are considered risk factors for developing PDAC. Chronic pancreatitis was identified in patients with PDAC 10 to 20 years earlier and acute pancreatitis 1 to 2 years before tumor diagnosis. Studies have shown that less than 5% of patients with chronic pancreatitis also develop PDAC. Cystic precursor lesions of PC include IPMN and MCNs, with IPMN being the most commonly diagnosed[1,14]. Pancreatic cyst fluid cytologic analysis is a candidate method for identifying progression to high-grade PanIN or cancer with a 25%-88% sensitivity in detecting pancreatic malignancy[1,16].

A challenge in the early diagnosis PC is the absence of specific symptoms or clinical data for patients with pancreatic tumors. The symptoms of PC, if present, are not specific and manifest approximately 6 mo after the identification of PDAC. Patients with symptoms from PC complain of abdominal pain and unexplained weight loss and are often found to have jaundice[4]. The majority of patients are asymptomatic, however[14].

Initial tests for evaluating patients suspected of having PC include serological investigation and abdominal imaging[5]. The latter is often performed using magnetic resonance imaging (MRI), MRI cholangiopancreatography, computed tomography (CT), endoscopic ultrasound (EUS), endoscopic

retrograde cholangiopancreatography (ERCP), and positron emission tomography[5,14,17]. One of the newest techniques in MRI involves diffusion-weighted imaging, which is capable of discriminating between PC and pancreatitis[17]. Certain features can be indicative of malignancy on imaging studies of early lesions for PC, including internal septation, mural nodularity, solid masses, duct dilatation, and vascular invasion. In 36%-70% of IPMN-associated cancers, mural nodules are diagnosed[14]. CT and MRI have a 56%-88% accuracy in detecting IPMN, but EUS has a higher resolution[14]. Pancreatic cysts are found in 3% of CT scans and 20% of MRI scans and can reach a 40% incidence in patients over 80 years old[14]. The most common imaging methods used, however, are EUS and CT. New EUS techniques (contrast-enhanced EUS and elastography) and the use of two or more imaging methods can enhance the diagnostic accuracy[7].

Additional methods implemented for PC include the analysis of personal data, biomarkers, and genomic features. Conditions such as family history of PC, body mass index, smoking, and alcohol abuse are epidemiologically associated with PC[18]. A total of 75%-80% of PCs are found in the head of the pancreas[14]. Diabetes is identified in 10%-40% of cases with IPMN, and a strong association between insulin and the risk of IPMN has been reported[14]. Patients with Peutz-Jegher syndrome, McCum-Albright syndrome, and familial adenomatous polyposis have also been diagnosed with IPMN [12,14]. MicroRNAs are biomarkers that have shown potential as a diagnostic tool for PDAC because of their high expression in the plasma of these patients[2]. MUC4, MUC16, differentially methylated DNA, telomerase protease expression, and overexpression of Das-1 biomarkers are associated with PDACs and are currently being validated for clinical use[1,14]. Elevated levels of carbohydrate antigen (CA)19-9 and carcinoembryonic antigen (CEA) and the identification of a new protein (cell migration-inducing hyaluronan-binding protein) are considered useful in PC prediction[14,19]. High concentrations of CEA are reported in mucinous pancreatic cysts but lack the potential to differentiate between IPMNs and PDACs[14]. The only biomarker for PDAC commonly considered reliable is CA19-9, but in the early stage disease, it has a sensitivity between 25% and 50% and is present in 51.1% of patients with PC stage I and 44.1% of patients with stage II[1,5].

Specific genomic features have been described for PDAC[1]. The top genes targeted during pancreatic carcinogenesis include KRAS, CDKN2A, TP53, and SMAD4. In patients with hereditary pancreatitis, mutation of the PRSS1 gene is associated with a higher risk of PC[12]. In early lesions of low-grade PanIN, KRAS mutations have identified, while inactivation of CDK2A and alterations in TP53, SMAD4, and BRCA2 occur in high-grade PanIN. Patients with these gene alterations can be classified as high-risk PDAC cohorts and considered for PC screening. These cohorts can also include patients with pancreatic cysts, pancreatitis, and new-onset diabetes who are 60 to 75 years of age[1]. KRAS, GNAS, TP53, SMAD4, PIK3CR, PTEN, and AKT1 mutations have been reported in IPMN-associated neoplasms with a 32%-89% sensitivity and 96%-100% specificity[14]. However, screening for PC asymptomatic subjects without a well-defined high-risk group is currently considered cost prohibitive[1].

Surgery is seen as a potentially curative treatment for PC if the patient is diagnosed in the early stage. For these patients, the pancreatic tumor can be completely resected, and by doing so, the survival rate significantly increases to 50%[4]. Treatment for the advanced state of PC typically includes partial resection, which is associated with tumor recurrence and a 5-year survival rate of less than 10%[4]. Unfortunately, pancreatic resection for PC has a high morbidity rate of up to 60%. Postoperative pancreatic fistula, stroke, cardiac arrest, wound dehiscence, infection, hemorrhage, and renal failure have been reported in patients the first month after pancreatic surgery[20]. Considering these factors, predicting PC by diagnosing early lesions and implementation of a screening program for PC becomes a matter of paramount importance. Artificial intelligence (AI) models integrating multisource risk factors are the future of early PC diagnosis.

Machine learning (ML), deep learning (DL) and the ability of computers to independently solve problems by using specific algorithms, is known today as AI. Although the terms ML and AI are commonly used interchangeably, ML is a subfield of AI. ML is based on developing mathematical algorithms for the analysis of data with the goal of creating a prediction model by recognizing patterns in these data. The algorithms can produce a machine-based diagnostic outcome for a specific disease. ML algorithms can be supervised or unsupervised and represented by support vector machines (SVMs), Bayesian interference, regressions, ensemble methods, decision trees, k-nearest neighbors, linear discriminants, and neural networks[16,21]. Supervised algorithms are based on data previously known by the computer, meaning that the computer is first trained with datasets from the domain of interest to later accurately analyze new datasets with the same subject and produce the desired mathematical outcome. In unsupervised algorithms, the computer sorts the input data and identifies features that are grouped into clusters or associations and analyzes them to reach a desired outcome[22]. Reinforcement learning is an advanced type of ML that is used to develop models that will help in the prediction of cancer but also facilitate the decision-making process[23]. Deep reinforcement learning is the combined process of reinforcement learning with DL. DL methods are trained to analyze large datasets through multilayer neural networks[24]. Developing algorithms by using AI methods helps in analyzing large amounts of data at the same time and integrating data obtained from different sources. Therefore, the results of clinical tests, imaging, personal data, biomarkers, and genomic features can be quickly analyzed, compared with existing knowledge, and used to reach an initial machine-made diagnosis. The purpose of our study was to identify the current diagnostic methods for detecting PC by using

noninvasive techniques with an emphasis on early lesions and AI.

METHODS

English-language literature published in the last 10 years covering diagnosing PC was searched by accessing the PubMed electronic database and other sources. The following key words were used for the search: "Pancreatic cancer", "early pancreatic lesions", "predicting pancreatic neoplasia", "artificial intelligence", "deep learning", "machine learning", "radiomics", "diagnosis", and "pancreas". We obtained a database of 97 studies on pancreatic neoplasms, including both single studies and reviews. We then removed duplicates, resulting in 86 papers. We excluded abstracts, reviews with insufficiently explained results, and articles not in the field of interest/irrelevant topics or with repetitive information. The final number of articles included was 44. The article selection algorithm for the study is depicted in [Figure 1](#). We divided the remaining articles into two datasets. One contained the newest review articles and studies on obtaining information about current knowledge in assessing PC (10), and the other included studies that explored the use of AI algorithms in the diagnosis of pancreatic lesions (34). This second dataset included 24 studies on the current status of AI diagnostic methods for PC and 10 studies discussing the implications for early PC and prediction of the use of AI algorithms. The obtained data from the two datasets are presented narratively. The results of our analysis on the PC prediction methods for diagnosing early lesions are summarized in [Table 1](#) and [Figure 2](#).

BRIEF DESCRIPTION OF AI IN MEDICINE

ML in medicine is based on analyzing digital medical images from CT, MRI, and EUS and extracting image features in a process called radiomics. These radiomics features are converted into data that can be subjected to statistical analysis. In supervised methods, a human operator selects and labels the lesion in an image that will constitute the input data before an ML algorithm analyses these data. Unsupervised algorithms use a large amount of data for training and learn how to extract the region that will be later subjected to analysis. These mathematical algorithms will then examine the input data through a network similar to the neuronal network of the human brain. The human central nervous system receives input through various receptors, and then sends this information to the brain *via* the ascending pathway, where the data is then examined before a specific response is delivered through descending pathways to the intended receiver organs. There are similarities between the AI network and the human model of neural processing. We can consider humans as receptors of patient information, the input data as the ascending pathways, computers organized in layers as the brain, and output data as the descending pathways reaching the desired outcome as the receiver. Deep neural network or DL models are composed of sets of so-called hidden layers capable of studying a large amount of data. Each of the layers selects and amplifies certain features of the input information. For example, the first layer identifies a specific region and its length, the next layer analyzes the depth, another layer detects the pattern, and the subsequent layers compare the input with known or trained patterns so that when the information is clear, it is transformed into the output represented by the feature that best characterizes a specific type of lesion. In this way, AI is similar to humans but with significantly reduced human intervention and fewer human errors[25].

The interest in AI in healthcare is growing. The SVM algorithm has been used to classify breast cancer and has achieved a lower error rate than K-nearest neighbor, naïve Bayes, and C4.5 algorithms[22,26, 27]. Electronic phenotyping algorithms have been built by researchers for predicting a disease correctly by using the electronic health records of the patients[22]. A convolutional neural network (CNN) has been used to prognosticate rectum toxicity in cervical cancer subjects with data provided from beam radiotherapy and brachytherapy. An alternative to surgery for the treatment of PC is radiation therapy. Given the challenging anatomy of the pancreas, sometimes the target area for treatment is difficult to identify. For these patients, metallic fiducials are implanted into the tumor target. These fiducials, however, can cause metal artifacts, obscure the tumor target, or be a source of complications such as pancreatitis or infections, all leading to delayed treatment. Therefore, developing mathematical algorithms for PC radiation therapy is a current subject of research. AI models using CT image data to localize the target PC for radiation therapy and calculate the dose of stereotactic body radiation have been reported with encouraging results[16,25]. DL algorithms have analyzed the mitotic rate of neoplastic cells to classify tumors. DL involves up to 150 hidden layers in the neural network, while traditional neural networks contain 2-3 layers. Some authors have suggested that tumors can be characterized by using computer aided design tools with supervised and unsupervised DL algorithms using CNN and transfer learning techniques. CNNs can be trained to automatically extract relevant features from images and classify the objects in the images with acceptable accuracy[22]. For AI-driven technologies to see further development in healthcare, ethical concerns must be addressed. Because AI algorithms require large datasets for training and for validation, data collection, storage, processing, confidentiality, and sharing must be considered[23].

Table 1 Studies exploring artificial intelligence algorithms for the diagnosis of early lesions and prediction of pancreatic cancer

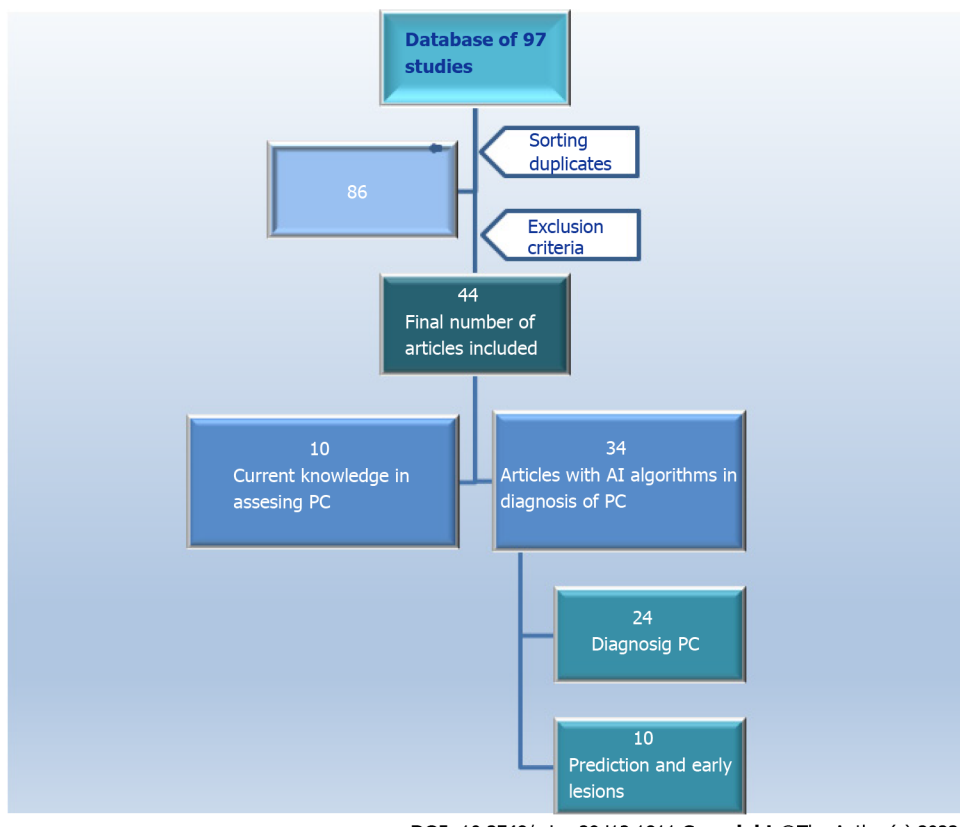
Ref.	Purpose of the model	Type of study	Type of model	Input data	Type of validation	No. cases
Qureshi <i>et al</i> [19], 2022	Identifying predictive features on prediagnostic CT scans for PDAC	Retrospective	NB	4000 radiomics from CT	External	72 (36 with PC)
Sekaran <i>et al</i> [22], 2020	Predicting PC	Retrospective	CNN	19000 images from CT	Internal	80 (NS)
Chen <i>et al</i> [36], 2018	Identification and classification methods for PC on MRI	Retrospective	CNN	863 images from MRI	Internal	40 (20 with PC)
Muhammad <i>et al</i> [18], 2019	Prediction of PC risk	Retrospective	CNN	18 features of epidemiologic and clinical data	External	800144 (898 with PC)
Alves <i>et al</i> [8], 2022	Detection and localization of small PDAC lesions on contrast-enhanced CT	Retrospective	DL	242 images from CT-CE	External	242 (119 with PC)
Kuwahara <i>et al</i> [35], 2019	Investigate the value of EUS in predicting malignancy in IPMN	Retrospective	CNN	3970 radiomics from EUS	Internal	50 (23 malignant)
Hussein <i>et al</i> [3], 2019	Identification of IPMN	Retrospective	CAD	171 MRI images	Internal	171 (133 IPMN)
Chakraborty <i>et al</i> [15], 2018	Identification of high-risk IPMN	Retrospective	SVM	103 CT images	Internal	103 (27 high-risk IPMN)
Liu <i>et al</i> [28], 2020	Classifying images as cancerous or noncancerous PC	Retrospective	CNN	21105 CT images	Internal and external	1242 (752 with PC)
Lee <i>et al</i> [44], 2022	Prediction of risk for PC	Retrospective	DNN	9 factors	Internal and external	2952 (738 with PC)

NB: Naïve Bayes; CT: Computed tomography; CNN: Convolved neural network; PDAC: Pancreatic ductal adenocarcinoma; PC: Pancreatic cancer; NS: No specification; DL: Deep learning; EUS: Endoscopic ultrasound; IPMN: Intraductal papillary mucinous neoplasms; CAD: Computer-aided diagnosis; SVM: Support vector machine; MRI: Magnetic resonance imaging; DNN: Deep neural network.

NONINVASIVE METHODS FOR DIAGNOSING PC

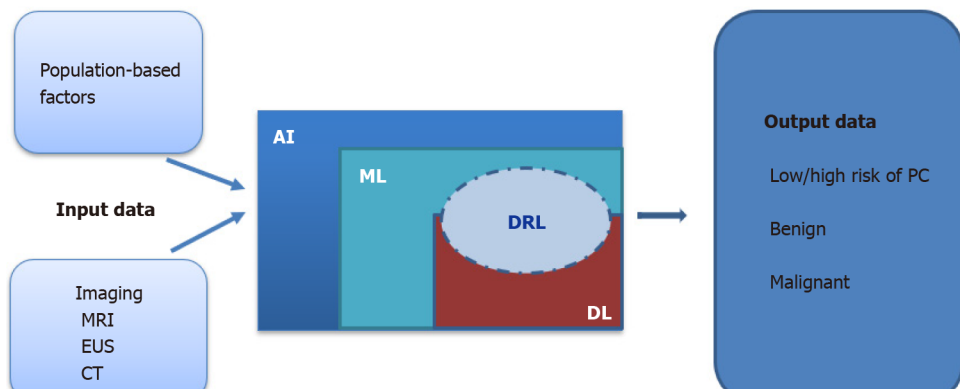
The potential of CNNs has been explored in the diagnosis of skin neoplasms, diabetic retinopathy, and liver tumors, but its utility in the detection of PC remains to be fully determined. CNN algorithms have been used for segmentation of the pancreas, risk stratification for IPMN, assessment of the grade (G) of pancreatic neuroendocrine neoplasm, targeting PC for radiotherapy, and classification of the pancreatic cysts[28].

In the diagnosis of PCs, AI is used for the analysis of radiomics features from CT, MRI, and EUS, of images from histopathological slides, and of tumor markers[29] (Figure 3). Because CT is commonly performed when investigating patients, it is currently the most explored imaging modality with AI. In the United States, approximately 7 million patients per year present to the emergency room with abdominal pain, for which a CT scan analysis is required by hospital protocols. These protocols offer a database that can be consulted for patients who later develop PC[1,19]. In identifying PC, contrast-enhanced CT has a sensitivity of 70%-100%, and the usual CT scan has an accuracy of 83.3%, sensitivity of 81.4%, and specificity of 43%. In the detection of PDAC, CT has a sensitivity of 76%-96% and offers information about the location, size, and morphology of the pancreatic mass[1,2,25]. According to Qureshi *et al*[19], healthy cells transforming into neoplastic cells appear darker on a CT scan. Even with these results, CT scan-based analysis is not taken into consideration as a screening method for early pancreatic lesions because of the constant exposure of the patient to radiation[1,2,25]. MRI techniques identify early modifications in the pancreatic parenchyma, such as fibrosis and inflammation, with enhanced resolution. New developments in these techniques have allowed the evaluation of tissue vascularization[3]. PDAC can be diagnosed on MRI with an accuracy of 89.1%, sensitivity of 89.5%, and specificity of 63.4%. EUS has demonstrated the highest precision in tumor detection for pancreatic lesions, with a sensitivity as high as 74%-94%[1,25]; in the detection of PCs, an endoscopist analyzing EUS images can reach a sensitivity of 94%[1,29-31]. Some studies have shown that even though PDAC is the most commonly identified histopathological type of PC, PNTs have a higher predominance in small pancreatic lesions. The differential diagnosis between PNTs and other types of PC can be made using EUS because of the better contrast offered by their rich vascularization[30]. In neuroendocrine tumors,



DOI: 10.3748/wjg.v29.i12.1811 Copyright ©The Author(s) 2023.

Figure 1 Article selection algorithm for the study. A total of 97 studies and reviews were identified with key words; 86 papers remained after removing duplicates; 34 eligible studies were finally included: 24 on the current status of artificial intelligence (AI) diagnostic methods for pancreatic cancer (PC) and 10 discussing the implications of AI algorithms in early PC and prediction. AI: Artificial intelligence; PC: Pancreatic cancer.

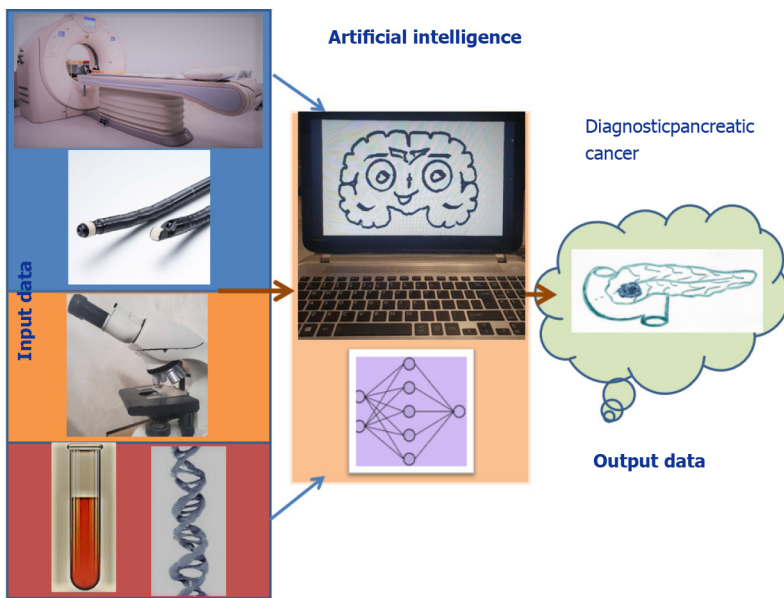


DOI: 10.3748/wjg.v29.i12.1811 Copyright ©The Author(s) 2023.

Figure 2 Pancreatic cancer prediction methods for diagnosing early lesions. AI: Artificial intelligence; ML: Machine learning; DL: Deep learning; DRL: Deep reinforcement learning; PC: Pancreatic cancer; CT: Computed tomography; EUS: Endoscopic ultrasound; MRI: Magnetic resonance imaging.

EUS has a 75%-97% detection rate for PNTs but gives the best results when combined with MRI studies in the initial assessment[30]. By using AI algorithms in EUS for detecting PC, the sensitivity increases to 83%-100% with an overall accuracy of 80%-97%[1,21]. However, there are limitations to using EUS as a common analytical method for clinical diagnosis; although it is more cost-effective than MRI, EUS is limited by: (1) The need for patient sedation; (2) The need for a technician with suitable knowledge and experience in performing the method; and (3) The narrow field investigated, as EUS cannot visualize extrapancreatic organs[1]. The sensitivity of EUS in diagnosing PC ranges from 54%-98%; hence, new techniques, such as ML algorithms, are needed[16,25].

Diagnosing PC is often difficult due to the lack of well-defined radiographic images and symptoms of the disease in early lesions as well as mimickers of neoplasia[4]. In performing CT segmentation, a radiologist must analyze approximately 300 images containing visual information for each patient, so a



DOI: 10.3748/wjg.v29.i12.1811 Copyright ©The Author(s) 2023.

Figure 3 Artificial intelligence leading concepts for pancreatic cancer diagnosis. Input data: Imaging, endoscopic, and histopathologic data and tumor markers; artificial intelligence with machine learning and deep learning; output data: Diagnosing pancreatic cancer.

mathematical algorithm developed for the analysis of data extracted from a CT scan of the patients listed as high-risk in a screening program would increase efficiency[1]. Even though the image of a neoplasm can be identified months before the time of diagnosis, the sensitivity for PC is low, so a screening method involving AI algorithms could help predict and identify early stages of PC. On CT scans, PC presents with irregular contours and poorly defined margins. Early lesion studies have shown that on CT, alterations are present in the pancreas 18 mo before the diagnosis of PDAC but with a sensitivity of about 15%[1,2,25]. In early disease stages, when the lesions are small, these masses can be overlooked by radiologists[31]. Typically, pancreatic tumors smaller than 2 cm are difficult to identify from the surrounding tissue, and the gland itself represents approximately 1.3% of a CT image, offering only a small amount of data[1,2,31]. Lesions that can alter the depiction of the pancreas on a CT scan by causing shape and size deformations and that appear similar to PC include parenchymal atrophy, IPMN, lithiasis, pancreatitis, and pancreatic duct ectasia. These lesions increase the tissue heterogeneity of the pancreas on CT, making the diagnosis of PC difficult[4]. One report showed that in 90% of cases, the misdiagnosis of PC on imaging was due to inflammation that obscured the underlying tumor mass [23]. Studies of PC with AI have been conducted to help classify PNTs by analyzing preoperative CT and MRI accurately and showed that these AI algorithms can be useful in differentiating exocrine from endocrine PC in complicated cases. Commonly, there are different patterns in the vascularization of PNT and pancreatic adenocarcinomas, but there are small proportions of cases with atypical findings that make the differential diagnosis difficult, and for these situations, a histogram analysis on CT can be used[31]. Studies have assessed tumor grade, with results showing that DL methods applied to MRI can differentiate between histological aspects of PNT by classifying G1 from G2 and G3 neoplasms and G1 and G2 from G3[31,32].

AI algorithms for EUS, MRI, and CT images in PC diagnosis

EUS has an elevated detection rate for IPMN and *in situ* PC (stage 0)[33]. Digital image analysis of EUS images using computers with SVM- and artificial neural network (ANN)-based methods has demonstrated high accuracy[25,34]. The overall accuracy in using ANNs on EUS for the diagnosis of PC ranges between 89%-94%. Elastography performed during EUS is reported to have an accuracy of 83%-90%; this imaging technique can differentiate the consistency of the issue on an EUS image by color coding, with red indicating softer tissue and blue indicating harder areas[25]. Better results of EUS analysis with AI techniques have been obtained by studying an extended neural network of EUS elastography images with an accuracy of 89.7% in differentiating between malignant and benign pancreatic lesions. Additionally, contrast-enhanced EUS and contrast-enhanced harmonic EUS have been shown to be useful in identifying focal pancreatic masses together with a diagnosis of a benign or malignant lesion. In contrast-enhanced EUS, contrast agents are intravenously injected for better identification of focal pancreatic lesions[21]. Preoperative AI sorting of EUS images of IPMNs presented a higher accuracy in predicting the malignant component than a human technician (94% vs 56%, respectively). A study performed with a DL back propagation master for EUS training and quality control, which had both internal and external validation, achieved an accuracy ranging from 82.4% to

94.2% in detecting PC. The decision tree method, implemented for patients who underwent ERCP, precisely identified PC with an 87%-91% sensitivity and 80% specificity[16].

A meta-analysis of published data aiming to investigate the diagnostic value of AI EUS in PC showed a very good diagnostic accuracy. The meta-analysis extracted data from 10 studies that included 1871 patients with AI algorithms based on a CNN, ANN, and SVM. The ANN model had the best accuracy in detecting PC, with a sensitivity in detecting small pancreatic tumors of 93% for EUS, 53% for CT, and 67% for MRI. However, the authors stated that the results of these 10 studies did not have a general utility because the data were evaluated only with internal validation, and thus the results could have been overestimated. To be relevant for patients from different populations, the sources used for validation must be diverse, external, and from more than one center[24]. Studies have reported that ML models such as ANNs and CNNs can be trained to extract quantitative data that can be correlated with the histological type of PC but also with the survival rates and the response to chemotherapy[11,25,31].

A retrospective study was performed by Kuwahara *et al*[35] on 50 patients diagnosed surgically with IPMN. A total of 3970 radiomics features from EUS were investigated with a CNN algorithm. After augmenting the data, the sample fully investigated was composed of 508160 images. The author's goal was then to classify IPMNs as benign or malignant. For this, the ability to predict early lesions was investigated by comparing AI methods with physicians. The AI methods demonstrated an accuracy of 94.0% in predicting malignancy, while the humans achieved an accuracy of 56.0%. This study had a number of limitations; however, it was retrospective, had a small sample of cases, only performed internal validation, and used data from only one center. Additionally, all the patients included in the study were surgically investigated, and for IPMNs, the recommendation was surveillance[35].

Chen *et al*[36] implemented a number of 3D CNNs, including ResNet18, ResNet34, ResNet52, and Inception-ResNet, to classify pancreatic tumors from MRI images. These authors used the MRI images of 20 normal patients and 20 patients with tumors, from whom 77 benign MRI images and 38 malignant MRI images were obtained, and through data augmentation, 442 benign MRI images and 421 malignant MRI images were finally analyzed[36]. Data augmentation oversamples images to generate synthetic data in cases with small sample sizes and limited availability of image data, such as rare cancers and PCs[31]. The ResNet18 method achieved an accuracy of 91% in classifying benign and malignant lesions. Other studies have reported analyses with 3 DCNN using MRI for Alzheimer's disease diagnosis and the classification of lung, brain, and prostate lesions[25,31,36].

Hussein *et al*[3] used the MRI data from 171 subjects to identify IPMN, including 38 normal subjects and 133 diagnosed with IPMN. Two-dimensional axial slices were used to generate regions of interest, and supervised and unsupervised learning was used in computer-aided diagnosis. The authors used unsupervised DL features for image classification with a CNN, and the highest accuracy in classifying the IPMN was obtained with nonlinearity clustering and implementation of a VGG-fc7 layer. In supervised learning, the deep network associated with adaptive synthetic sampling performed better on small datasets[3].

Chakraborty *et al*[15] studied CT images from 103 patients confirmed with IPMN using SVM and random forest methods. The random forest algorithm had better results in extracting the features of the IPMN lesions. These authors experimentally developed an architecture designed for predicting high-risk patients with IPMN, but their method lacked independent validation. Additional limitations include its retrospective nature, the need for manual segmentation of the lesion and the pancreas, and the use of small datasets. Pancreatic cystic lesions were identified on 2.6% of the abdominal CT scans, with 25% of all lesions being diagnosed as IPMN and approximately one-third being associated with invasive carcinoma. The criteria for establishing whether IPMNs are at low or high risk of harboring malignancy are limited. Distinguishing between these two lesions is important, as low-risk patients are recommended to undergo surveillance, while high-risk patients should undergo surgical resection[1,16].

Alves *et al*[8] performed a study on the contrast-enhanced CT scans from 119 PDAC patients and 123 patients without PDAC. PDAC was detected using a self-configuring framework for medical segmentation, NNU net, focusing on small lesions and assigning a label of tumor or nontumor. Their results showed that DL models can diagnose early PDAC lesions, but the study included only tumors of the pancreatic head and required resources for the manual labeling of PDAC images[8].

In an attempt to use AI as a prediction model for early PDAC diagnosis, Qureshi *et al*[4] used three types of radiomics features from CT scans. Two types belonged to the same patients but were executed (one before and one after the diagnosis was histopathologically confirmed) and another type was extracted from normal subjects. The prediagnostic CT scans of the patients were obtained 6 mo to 3 years before the PC was identified. In their study, Qureshi *et al*[4] analyzed 108 CT scans from 72 patients classified into two datasets, an internal dataset consisting of 66 contrast-enhanced abdominal CT scans for building the model, and an external dataset consisting of 42 scans for validation. A naïve Bayes classifier was trained to perform automatic classification of the CT scans of two groups, one representing the healthy control group and the other the prediagnostic group. A total of 4000 radiomics features were extracted from each of the 66 scans with the aim of identifying patterns in the images obtained before and after the PC diagnosis. The study concluded that prediagnostic CT images provided sufficient information to validate the contribution of AI in predicting patients at risk of PDAC, but further studies are needed to address the potential overfitting due to the limited dataset used[4].

A retrospective study on 6084 contrast-enhanced CT images in patients with histopathologically confirmed PDAC used a Faster R-CNN model to develop an automatic system for automatically diagnosing PC. The AI produced its diagnoses in 3 s, shorter than the 8 min required by the image specialist. The limitations of this study were as follows: It was a retrospective study of patients with PC diagnosis pathologically confirmed from a single center, normal patients and those with benign lesions were excluded, and it did not have external validation[37].

Sekaran *et al*[22] proposed a DL network by analyzing a dataset consisting of 19000 radiomics features from 82 abdominal CT images. The method involved a Gaussian mixture model with an EM algorithm and a DL CNN. They proposed a lump recognition algorithm, with the input or region of interest being the area in which the growth of a lump is detected. Each layer of the CNN extracts features of this region to build a model for assessing the features of the lump in terms of size, shape, and weight. Their results were able to help the patients by identifying the rate of spread of the tumor in the head of the pancreas after diagnosis and treatment. This study was limited by the fact that the tumors were analyzed in only one part of the pancreas, the head.

Liu *et al*[28] used two datasets, one consisting of 471 patients, 355 with histopathologically diagnosed or cytologically confirmed PC, and the other for external and internal validation. The control set participants had no pancreatic lesions at the time when the CT scan was performed. The study was conducted in the patch and patient levels. In the patch-based analysis, the region of interest was processed into patches, and the patients were classified as having or not having PC using a modified CNN model from the Visual Geometry Group. For the patient-based approach, age, sex, and tumor stage and size were taken into consideration. This study designed a CNN-based algorithm for classifying patients with or without PC by using CT scans, with an accuracy of 99%. Additionally, their method ensured avoidance of overfitting by using training and validation datasets that were sufficiently different but included patients of different races and ethnicities, preprocessing CT images into patches, and using data augmentation methods such as moving windows and flipping. Radiologists were provided with the clinical data of the PC patients, and the CNN had no information. The patches used for training the CNN were segmented by the radiologists. The limitations of these results were manual labeling of pancreatic images with a modest sample size and only Asian participants from a single institution.

Cardobi *et al*[38] found that a CNN-based analysis on CT images for identifying malignancies in IPMNs showed a sensitivity, specificity, and accuracy in the classification of tumors of 95.7%, 92.6%, and 94.0%, respectively. Additionally, AI algorithm models built for the segmentation of the pancreas and used to determine the pancreas volume in autoimmune pancreatitis were 2.38 times faster than manual approaches[38].

AI algorithms for diagnosing PC using tumor markers, images from histopathological slides, and epidemiologic data

Studies using neural networks for the analysis of tumor markers for PC diagnosis have shown that the diagnostic performance of a single marker is lower than that of the AI model multiple for tumor marker analysis. Detecting the values of only one of CA19-9, CEA, and CA125 for PC diagnosis with AI has a low sensitivity[39]. In a mouse model, Serrao *et al*[39] measured the concentrations of alanine and lactate and the activities of lactate dehydrogenase and alanine aminotransferase in the pancreas of animals with different lesions ranging from pancreatitis to tumors. Their method used metabolic magnetic resonance spectroscopic imaging with hyperpolarized [1-13C] pyruvate for detecting and monitoring the progression of PC precursor lesions. Their results were able to distinguish pancreases with predominantly low-grade PanIN from tissue with high-grade PanIN and tumors. However, the studied animals had a small pancreas, and the high-grade PanINs occupied approximately 40% of the tissue. The human pancreas is larger than that of mice, and these lesions are usually small, so additional data are needed before this method can be used for human patients[18,32]. A new field of liquid biopsies offers data available from biomarkers such as exosomes, proteomes, proteins, cell-free DNA, and circulating microRNA that can be analyzed using AI methods for the early diagnosis of PC[24].

With the development of ML, digital medical imaging can play a role in assisting with diagnosis based on histopathological images. Today, it is possible to digitize glass slides using whole-slide imaging. AI techniques have been applied in pathology slide analysis for prostate and breast cancers. For these methods, a high-resolution digital image of the tissue from the glass slide is obtained by using a specialized scanner; the images are then analyzed by AI methods. Currently, however, only a few studies have investigated the use of AI on physical PC specimens. With an ANN algorithm, an overall accuracy of 77% was obtained in the reclassification of specimens as malignant or benign[25]. A study using a deep CNN on histopathological images of PDAC achieved a 95.3% classification accuracy by examining a total of 231 tissue samples from 171 PC and 60 normal pancreas slides using whole-slide imaging and image augmentation techniques[40]. Sehmi *et al*[41] developed DL models for grading PC from pathology slides that had a 95.61% classification accuracy. Naito *et al*[42] trained a DL method to assess PDAC on endoscopic ultrasonography-guided fine-needle biopsies and obtained a model that was able to detect small amounts of cancer cells in difficult cases. Cutting-edge digital pathology tools that can scan, analyze, and store data from an entire tissue sample continue to be developed[23].

Si *et al*[43] proposed a fully end-to-end deep-learning-based (FEE-DL) algorithm for the automatic diagnosis of different types of PCs. A total of 284 PCs, such as IPMN, PNET, serous cystic neoplasms, and a group labeled "other"-represented by gallbladder tumors, cholangiocarcinoma, ampullary carcinomas, duodenal cancer and metastasis-was investigated. The dataset was augmented using random elastic brightness, random contrast, random elastic transformation, and random cropping. The FEE-DL consisted of a tree connected subnetwork: ResNet18 for recognizing images containing the pancreas, U-Net-32 for making predictions on each image for pancreas segmentation, and ResNet34 for diagnosing pancreatic tumors. This model had an average accuracy of 82.7% for all tumor types, with a 100% accuracy in identifying IPMN and 87.6% for PDAC on a dataset that included 347 patients following four stages: Image screening, pancreas location, pancreas segmentation, and PC diagnosis. The FEE-DL algorithm independently identified different histologic types of PC with precise results in detecting PDAC and IPMN.

Muhammad *et al*[18] designed an ANN method to predict PC based on a study of a total of 18 personal health features (age, diabetes, smoking, exercise status, alcohol consumption, and family history of PC) from 800114 participants, including 898 with PC. Their results showed that the risk of PC can be predicted and stratified using an ANN that analyzes easily obtainable personal health features with an 80.7% sensitivity and 80.7% specificity. This study used two broad data sources: The National Health Interview Survey, established in the United States to monitor the general health status of the population with 131 PC patients from 645217 respondents, and the Prostate, Lung, Colorectal and Ovarian screening program, including 797 PC patients from 154897 participants[18].

Lee *et al*[44] developed a CNN predictive model for PC using data from the Taiwan Health Insurance database, which covers 99.98% of the population of the region. A total of 3690 subjects were selected, 2952 of whom presented with risk factors associated with PC, including pancreatitis, diabetes, peptic ulcer, cholangitis, hepatitis, periodontal disease, sleep disorders, and fasciitis, but factors obtained from the subjects' medical history were further added. Finally, 74 candidate factors were included in this study; 738 patients had PC, and 2214 subjects representing the control group were cancer-free. This study constructed a PC prediction model with an accuracy higher than that of previous studies using nine key independent predictors: Abdominal pain, peptic ulcer, flatulence, gastritis, abnormal gastric function, hepatitis, sleep disorders, cholangitis, and pancreatitis.

FUTURE PERSPECTIVES

For PC, a cost-effective screening method for early lesions is needed. AI models developed for a diverse group of patients from high-risk PDAC cohorts belonging to broad datasets from different sources can be of great use for improving PDAC treatment outcomes and enhancing diagnostic precision. AI methods represent a needed step to reach a standardized interpretation of patient data and investigations while reducing human bias or error. For this, a wide range of data from different sources is necessary. All of these data have a central role in training AI methods in diagnosing PC and establishing the most accurate algorithm to be used for such a diagnosis. Correlations can be made through AI algorithms by expanding the image and electronic medical record databases, which will significantly improve the diagnostic accuracy and provide an early diagnosis for PC patients, thereby producing a better prognosis and more effective therapy. AI creates a common ground in diagnosing PC that can be standardized and used for the general population. Such an AI model should contain a combination of biomarkers, medical data, and imaging data obtained by alternating CT, EUS, and MRI testing so that maximized accuracy and early diagnosis with noninvasive techniques can be achieved.

The coronavirus disease 2019 pandemic has produced a model for forming an international infrastructure that can be studied with AI algorithms and even used for predicting and early diagnosing cancers. The collaboration between scientists and academic centers has shown that humans from different countries and continents can work together to share information in a common attempt to save lives while creating a vast database. This will require resources, global solidarity, and support investment in medical infrastructures worldwide. However, the need to develop health infrastructure and multidisciplinary research studies is crucial, as the pandemic situation has already shown.

CONCLUSION

Our analysis of the current diagnostic methods for detecting PC noninvasively with an emphasis on early lesions has revealed a series of common features and limitations: Published studies about predicting early lesions in PC are lacking. For PC diagnosis, noninvasive tests such as imaging, tumor marker analysis, and population-based studies can be used to train AI algorithms to identify features, patterns, and subtle changes that can help classify pancreatic lesions and build predictive models that can improve the awareness of the risk of pancreatic neoplasia. Published studies typically included only small samples from a limited number of cases. The analysis of these studies focused mostly on just one type of investigation (radiomics features, personal data, biomarkers, or genomic features without

making correlations between all the data that a physician analyses for a diagnosis of PC in a specific patient). A high percentage of the studies only performed internal validation, so bias and overfitting can constitute a problem when generalizing their conclusions. Commonly, for machine diagnosis, the mechanism that generates the output is not clearly explained, so assessing how a specific AI algorithm makes its final diagnosis remains controversial. AI algorithms for assessing pancreatic volumes with and without tumors are time- and cost-consuming that are usually run manually and in direct relation with the radiologist's experience. Finding an AI-driven automated volumetric segmentation algorithm is difficult because of the variations in shape, the shallowness of the boundaries, and the small size of the pancreas. Pancreatic tumors smaller than 2 cm frequently have inconspicuous borders with high similarity to the surrounding tissues on radiomics analysis, making early lesion diagnosis challenging. However, AI methods have the potential to improve accuracy and support clinical decisions for the preoperative diagnosis of pancreatic lesions and to aid in the surgical management and prognosis of PC.

FOOTNOTES

Author contributions: Faur AC and Lazar DC contributed to manuscript drafting and writing; Faur AC, Lazar DC, and Ghenciu LA were involved in literature search; Faur AC and Ghenciu LA participated in study conceptualization and design; Faur AC and Lazar DC supervised the manuscript; and all authors have read and agreed to the final version of the manuscript.

Conflict-of-interest statement: All the authors report no relevant conflicts of interest for this article.

Open-Access: This article is an open-access article that was selected by an in-house editor and fully peer-reviewed by external reviewers. It is distributed in accordance with the Creative Commons Attribution NonCommercial (CC BY-NC 4.0) license, which permits others to distribute, remix, adapt, build upon this work non-commercially, and license their derivative works on different terms, provided the original work is properly cited and the use is non-commercial. See: <https://creativecommons.org/Licenses/by-nc/4.0/>

Country/Territory of origin: Romania

ORCID number: Alexandra Corina Faur [0000-0001-8953-5076](https://orcid.org/0000-0001-8953-5076); Daniela Cornelia Lazar [0000-0002-6984-0046](https://orcid.org/0000-0002-6984-0046); Laura Andreea Ghenciu [0000-0002-5326-5438](https://orcid.org/0000-0002-5326-5438).

S-Editor: Wang JJ

L-Editor: Wang TQ

P-Editor: Wang JJ

REFERENCES

- 1 **Kenner B**, Chari ST, Kelsen D, Klimstra DS, Pandol SJ, Rosenthal M, Rustgi AK, Taylor JA, Yala A, Abul-Husn N, Andersen DK, Bernstein D, Brunak S, Canto MI, Eldar YC, Fishman EK, Fleshman J, Go VLW, Holt JM, Field B, Goldberg A, Hoos W, Iacobuzio-Donahue C, Li D, Lidgard G, Maitra A, Matisian LM, Poblete S, Rothschild L, Sander C, Schwartz LH, Shalit U, Srivastava S, Wolpin B. Artificial Intelligence and Early Detection of Pancreatic Cancer: 2020 Summative Review. *Pancreas* 2021; **50**: 251-279 [PMID: [33835956](https://pubmed.ncbi.nlm.nih.gov/33835956/) DOI: [10.1097/MPA.0000000000001762](https://doi.org/10.1097/MPA.0000000000001762)]
- 2 **Hayashi H**, Uemura N, Matsumura K, Zhao L, Sato H, Shiraishi Y, Yamashita YI, Baba H. Recent advances in artificial intelligence for pancreatic ductal adenocarcinoma. *World J Gastroenterol* 2021; **27**: 7480-7496 [PMID: [34887644](https://pubmed.ncbi.nlm.nih.gov/34887644/) DOI: [10.3748/wjg.v27.i43.7480](https://doi.org/10.3748/wjg.v27.i43.7480)]
- 3 **Hussein S**, Kandel P, Bolan CW, Wallace MB, Bagci U. Lung and Pancreatic Tumor Characterization in the Deep Learning Era: Novel Supervised and Unsupervised Learning Approaches. *IEEE Trans Med Imaging* 2019; **38**: 1777-1787 [PMID: [30676950](https://pubmed.ncbi.nlm.nih.gov/30676950/) DOI: [10.1109/TMI.2019.2894349](https://doi.org/10.1109/TMI.2019.2894349)]
- 4 **Qureshi TA**, Gaddam S, Wachsman AM, Wang L, Azab L, Asadpour V, Chen W, Xie Y, Wu B, Pandol SJ, Li D. Predicting pancreatic ductal adenocarcinoma using artificial intelligence analysis of pre-diagnostic computed tomography images. *Cancer Biomark* 2022; **33**: 211-217 [PMID: [35213359](https://pubmed.ncbi.nlm.nih.gov/35213359/) DOI: [10.3233/CBM-210273](https://doi.org/10.3233/CBM-210273)]
- 5 **Gheorghe G**, Bungau S, Ilie M, Behl T, Vesa CM, Brisc C, Bacalbasa N, Turi V, Costache RS, Diaconu CC. Early Diagnosis of Pancreatic Cancer: The Key for Survival. *Diagnostics (Basel)* 2020; **10** [PMID: [33114412](https://pubmed.ncbi.nlm.nih.gov/33114412/) DOI: [10.3390/diagnostics10110869](https://doi.org/10.3390/diagnostics10110869)]
- 6 **Casà C**, Piras A, D'Aviero A, Preziosi F, Mariani S, Cusumano D, Romano A, Boskoski I, Lenkowicz J, Dinapoli N, Cellini F, Gambacorta MA, Valentini V, Mattiucci GC, Boldrini L. The impact of radiomics in diagnosis and staging of pancreatic cancer. *Ther Adv Gastrointest Endosc* 2022; **15**: 26317745221081596 [PMID: [35342883](https://pubmed.ncbi.nlm.nih.gov/35342883/) DOI: [10.1177/26317745221081596](https://doi.org/10.1177/26317745221081596)]
- 7 **Mahmoudi T**, Kouzahkanan ZM, Radmard AR, Kafieh R, Salehnia A, Davarpanah AH, Arabalibeik H, Ahmadian A. Segmentation of pancreatic ductal adenocarcinoma (PDAC) and surrounding vessels in CT images using deep convolutional neural networks and texture descriptors. *Sci Rep* 2022; **12**: 3092 [PMID: [35197542](https://pubmed.ncbi.nlm.nih.gov/35197542/) DOI: [10.1038/s41598-022-07111-9](https://doi.org/10.1038/s41598-022-07111-9)]
- 8 **Alves N**, Schuurmans M, Litjens G, Bosma JS, Hermans J, Huisman H. Fully Automatic Deep Learning Framework for

Pancreatic Ductal Adenocarcinoma Detection on Computed Tomography. *Cancers (Basel)* 2022; **14** [PMID: 35053538 DOI: 10.3390/cancers14020376]

- 9 **Philips S**, Shah SN, Vikram R, Verma S, Shanbhogue AK, Prasad SR. Pancreatic endocrine neoplasms: a current update on genetics and imaging. *Br J Radiol* 2012; **85**: 682-696 [PMID: 22253347 DOI: 10.1259/bjr/85014761]
- 10 **Halfdanarson TR**, Rabe KG, Rubin J, Petersen GM. Pancreatic neuroendocrine tumors (PNETs): incidence, prognosis and recent trend toward improved survival. *Ann Oncol* 2008; **19**: 1727-1733 [PMID: 18515795 DOI: 10.1093/annonc/mdn351]
- 11 **Chidambaram S**, Kawka M, Gall TM, Cunningham D, Jiao LR. Can we predict the progression of premalignant pancreatic cystic tumors to ductal adenocarcinoma? *Future Oncol* 2022; **18**: 2605-2612 [PMID: 35730473 DOI: 10.2217/fon-2021-1545]
- 12 **Del Chiaro M**, Segersvärd R, Lohr M, Verbeke C. Early detection and prevention of pancreatic cancer: is it really possible today? *World J Gastroenterol* 2014; **20**: 12118-12131 [PMID: 25232247 DOI: 10.3748/wjg.v20.134.12118]
- 13 **Legrand T**, Salleron J, Conroy T, Marchal F, Thomas J, Monard L, Biagi JJ, Lambert A. Preneoplastic Lesions in Surgical Specimens Do Not Worsen the Prognosis of Patients Who Underwent Surgery for Pancreatic Adenocarcinoma: Post-Hoc Analysis of the PRODIGE 24-CCTG PA 6 Trial. *Cancers (Basel)* 2022; **14** [PMID: 36010938 DOI: 10.3390/cancers14163945]
- 14 **Singhi AD**, Koay EJ, Chari ST, Maitra A. Early Detection of Pancreatic Cancer: Opportunities and Challenges. *Gastroenterology* 2019; **156**: 2024-2040 [PMID: 30721664 DOI: 10.1053/j.gastro.2019.01.259]
- 15 **Chakraborty J**, Midya A, Gazit L, Attiyeh M, Langdon-Embry L, Allen PJ, Do RKG, Simpson AL. CT radiomics to predict high-risk intraductal papillary mucinous neoplasms of the pancreas. *Med Phys* 2018; **45**: 5019-5029 [PMID: 30176047 DOI: 10.1002/mp.13159]
- 16 **Goyal H**, Mann R, Gandhi Z, Perisetti A, Zhang Z, Sharma N, Saligram S, Inamdar S, Tharian B. Application of artificial intelligence in pancreaticobiliary diseases. *Ther Adv Gastrointest Endosc* 2021; **14**: 2631774521993059 [PMID: 33644756 DOI: 10.1177/2631774521993059]
- 17 **Chen W**, Butler RK, Zhou Y, Parker RA, Jeon CY, Wu BU. Prediction of Pancreatic Cancer Based on Imaging Features in Patients With Duct Abnormalities. *Pancreas* 2020; **49**: 413-419 [PMID: 32132511 DOI: 10.1097/MPA.0000000000001499]
- 18 **Muhammad W**, Hart GR, Nartowt B, Farrell JJ, Johung K, Liang Y, Deng J. Pancreatic Cancer Prediction Through an Artificial Neural Network. *Front Artif Intell* 2019; **2**: 2 [PMID: 33733091 DOI: 10.3389/frai.2019.00002]
- 19 **Qureshi TA**, Javed S, Sarmadi T, Pandol SJ, Li D. Artificial intelligence and imaging for risk prediction of pancreatic cancer: a narrative review. *Chin Clin Oncol* 2022; **11**: 1 [PMID: 35144387 DOI: 10.21037/cco-21-117]
- 20 **Schlanger D**, Graur F, Popa C, Moiș E, Al Hajjar N. The role of artificial intelligence in pancreatic surgery: a systematic review. *Updates Surg* 2022; **74**: 417-429 [PMID: 35237939 DOI: 10.1007/s13304-022-01255-z]
- 21 **Laoveeravat P**, Abhyankar PR, Brenner AR, Gabr MM, Habr FG, Atsawarungruangkit A. Artificial intelligence for pancreatic cancer detection: Recent development and future direction. *Artif Intell Gastroenterol* 2021; **2**: 56-68 [DOI: 10.35712/aig.v2.i2.56]
- 22 **Sekaran K**, Chandana P, Krishna MN, Kadry S. Deep learning convolutional neural network (CNN) with Gaussian mixture model for predicting pancreatic cancer. *Multimed Tools Appl* 2020; **79**: 10233-10247 [DOI: 10.1007/s11042-019-7419-5]
- 23 **Hameed BS**, Krishnan UM. Artificial Intelligence-Driven Diagnosis of Pancreatic Cancer. *Cancers (Basel)* 2022; **14** [PMID: 36358800 DOI: 10.3390/cancers14215382]
- 24 **Huang B**, Huang H, Zhang S, Zhang D, Shi Q, Liu J, Guo J. Artificial intelligence in pancreatic cancer. *Theranostics* 2022; **12**: 6931-6954 [PMID: 36276650 DOI: 10.7150/thno.77949]
- 25 **Mendoza Ladd A**, Diehl DL. Artificial intelligence for early detection of pancreatic adenocarcinoma: The future is promising. *World J Gastroenterol* 2021; **27**: 1283-1295 [PMID: 33833482 DOI: 10.3748/wjg.v27.113.1283]
- 26 **Asri H**, Mousannif H, Al Moatassime H, Noel T. Using machine learning algorithms for breast cancer risk prediction and diagnosis. *Proc Com Sci* 2016; **83**: 1064-1069 [DOI: 10.1016/j.procs.2016.04.224]
- 27 **Bakasa W**, Viriri S. Pancreatic Cancer Survival Prediction: A Survey of the State-of-the-Art. *Comput Math Methods Med* 2021; **2021**: 1188414 [PMID: 34630626 DOI: 10.1155/2021/1188414]
- 28 **Liu KL**, Wu T, Chen PT, Tsai YM, Roth H, Wu MS, Liao WC, Wang W. Deep learning to distinguish pancreatic cancer tissue from non-cancerous pancreatic tissue: a retrospective study with cross-racial external validation. *Lancet Digit Health* 2020; **2**: e303-e313 [PMID: 33328124 DOI: 10.1016/S2589-7500(20)30078-9]
- 29 **Dumitrescu EA**, Ungureanu BS, Cazacu IM, Florescu LM, Streba L, Croitoru VM, Sur D, Croitoru A, Turcu-Stirolica A, Lungulescu CV. Diagnostic Value of Artificial Intelligence-Assisted Endoscopic Ultrasound for Pancreatic Cancer: A Systematic Review and Meta-Analysis. *Diagnostics (Basel)* 2022; **12** [PMID: 35204400 DOI: 10.3390/diagnostics12020309]
- 30 **Deguelte S**, de Mestier L, Hentic O, Cros J, Lebtahi R, Hammel P, Kianmanesh R. Preoperative imaging and pathologic classification for pancreatic neuroendocrine tumors. *J Visc Surg* 2018; **155**: 117-125 [PMID: 29397338 DOI: 10.1016/j.jviscsurg.2017.12.008]
- 31 **Thomasian NM**, Kamel IR, Bai HX. Machine intelligence in non-invasive endocrine cancer diagnostics. *Nat Rev Endocrinol* 2022; **18**: 81-95 [PMID: 34754064 DOI: 10.1038/s41574-021-00543-9]
- 32 **Gao X**, Wang X. Deep learning for World Health Organization grades of pancreatic neuroendocrine tumors on contrast-enhanced magnetic resonance images: a preliminary study. *Int J Comput Assist Radiol Surg* 2019; **14**: 1981-1991 [PMID: 31555998 DOI: 10.1007/s11548-019-02070-5]
- 33 **Kurihara K**, Hanada K, Shimizu A. Endoscopic Ultrasonography Diagnosis of Early Pancreatic Cancer. *Diagnostics (Basel)* 2020; **10** [PMID: 33327420 DOI: 10.3390/diagnostics10121086]
- 34 **Arulmozhi S**, Shankar R, Duraisamy S. A review: deep learning techniques for image classification of pancreatic tumor. *Int J Video Proc* 2020; **11**: 2217-2223
- 35 **Kuwahara T**, Hara K, Mizuno N, Okuno N, Matsumoto S, Obata M, Kurita Y, Koda H, Toriyama K, Onishi S, Ishihara M, Tanaka T, Tajika M, Niwa Y. Usefulness of Deep Learning Analysis for the Diagnosis of Malignancy in Intraductal Papillary Mucinous Neoplasms of the Pancreas. *Clin Transl Gastroenterol* 2019; **10**: 1-8 [PMID: 31117111 DOI: 10.2217/fon-2021-1545]

10.14309/ctg.00000000000000045]

36 **Chen X**, Chen Y, Ma C, Liu X, Tang X. Classification of pancreatic tumors based on MRI images using 3D convolutional neural networks. Proceedings of the 2nd International Symposium on Image and Computing and Digital Medicine; 2018 Oct 13-14; Chengdu, China. New York: Association for Computing Machinery, 2018: 92-96

37 **Liu SL**, Li S, Guo YT, Zhou YP, Zhang ZD, Lu Y. Establishment and application of an artificial intelligence diagnosis system for pancreatic cancer with a faster region-based convolutional neural network. *Chin Med J (Engl)* 2019; **132**: 2795-2803 [PMID: 31856050 DOI: 10.1097/CM9.0000000000000544]

38 **Cardobi N**, Dal Palù A, Pedrini F, Beleù A, Nocini R, De Robertis R, Ruzzenente A, Salvia R, Montemezzi S, D'Onofrio M. An Overview of Artificial Intelligence Applications in Liver and Pancreatic Imaging. *Cancers (Basel)* 2021; **13** [PMID: 33946223 DOI: 10.3390/cancers13092162]

39 **Serrao EM**, Kettunen MI, Rodrigues TB, Dzien P, Wright AJ, Gopinathan A, Gallagher FA, Lewis DY, Frese KK, Almeida J, Howat WJ, Tuveson DA, Brindle KM. MRI with hyperpolarised [1-13C]pyruvate detects advanced pancreatic preneoplasia prior to invasive disease in a mouse model. *Gut* 2016; **65**: 465-475 [PMID: 26347531 DOI: 10.1136/gutjnl-2015-310114]

40 **Fu H**, Mi W, Pan B, Guo Y, Li J, Xu R, Zheng J, Zou C, Zhang T, Liang Z, Zou J, Zou H. Automatic Pancreatic Ductal Adenocarcinoma Detection in Whole Slide Images Using Deep Convolutional Neural Networks. *Front Oncol* 2021; **11**: 665929 [PMID: 34249702 DOI: 10.3389/fonc.2021.665929]

41 **Sehmi MNM**, Fauzi MFA, Ahmad WSHMW, Chang EWL. Pancreatic cancer grading in pathological images using deep learning convolutional neural network. *F1000 Res* 2021; **10**: 1057 [DOI: 10.12688/f1000research.73161.1]

42 **Naito Y**, Tsuneki M, Fukushima N, Koga Y, Higashi M, Notohara K, Aishima S, Ohike N, Tajiri T, Yamaguchi H, Fukumura Y, Kojima M, Hirabayashi K, Hamada Y, Norose T, Kai K, Omori Y, Sukeda A, Noguchi H, Uchino K, Itakura J, Okabe Y, Yamada Y, Akiba J, Kanavati F, Oda Y, Furukawa T, Yano H. A deep learning model to detect pancreatic ductal adenocarcinoma on endoscopic ultrasound-guided fine-needle biopsy. *Sci Rep* 2021; **11**: 8454 [PMID: 33875703 DOI: 10.1038/s41598-021-87748-0]

43 **Si K**, Xue Y, Yu X, Zhu X, Li Q, Gong W, Liang T, Duan S. Fully end-to-end deep-learning-based diagnosis of pancreatic tumors. *Theranostics* 2021; **11**: 1982-1990 [PMID: 33408793 DOI: 10.7150/thno.52508]

44 **Lee HA**, Chen KW, Hsu CY. Prediction Model for Pancreatic Cancer-A Population-Based Study from NHIRD. *Cancers (Basel)* 2022; **14** [PMID: 35205630 DOI: 10.3390/cancers14040882]

New uses for an old remedy: Digoxin as a potential treatment for steatohepatitis and other disorders

Fatima Jamshed, Farzaneh Dashti, Xinshou Ouyang, Wajahat Z Mehal, Bubu A Banini

Specialty type: Gastroenterology and hepatology

Fatima Jamshed, Farzaneh Dashti, Xinshou Ouyang, Wajahat Z Mehal, Bubu A Banini, Section of Digestive Diseases, Yale School of Medicine, New Haven, CT 06510, United States

Provenance and peer review:

Invited article; Externally peer reviewed.

Fatima Jamshed, Griffin Hospital-Yale University, Derby, CT 06418, United States

Peer-review model: Single blind

Wajahat Z Mehal, West Haven Veterans Medical Center, West Haven, CT 06516, United States

Peer-review report's scientific quality classification

Corresponding author: Bubu A Banini, MD, PhD, Assistant Professor, Section of Digestive Diseases, Yale School of Medicine, 40 Temple St, Suite 1A, New Haven, CT 06510, United States. bubu.banini@yale.edu

Grade A (Excellent): 0

Grade B (Very good): B

Grade C (Good): C, C

Grade D (Fair): 0

Grade E (Poor): 0

P-Reviewer: Ratajewski M, Poland; Savari F, Iran

Received: November 19, 2022

Peer-review started: November 19, 2022

First decision: December 10, 2022

Revised: January 12, 2023

Accepted: March 14, 2023

Article in press: March 14, 2023

Published online: March 28, 2023

Abstract

Repurposing of the widely available and relatively cheap generic cardiac glycoside digoxin for non-cardiac indications could have a wide-ranging impact on the global burden of several diseases. Over the past several years, there have been significant advances in the study of digoxin pharmacology and its potential non-cardiac clinical applications, including anti-inflammatory, antineoplastic, metabolic, and antimicrobial use. Digoxin holds promise in the treatment of gastrointestinal disease, including nonalcoholic steatohepatitis and alcohol-associated steatohepatitis as well as in obesity, cancer, and treatment of viral infections, among other conditions. In this review, we provide a summary of the clinical uses of digoxin to date and discuss recent research on its emerging applications.

Key Words: Digoxin; Cardiac glycosides; Oxidative stress; Nonalcoholic steatohepatitis; Alcohol-associated steatohepatitis; Sterile inflammation

©The Author(s) 2023. Published by Baishideng Publishing Group Inc. All rights reserved.



Core Tip: Digoxin has been used primarily as a cardiac drug for treatment of arrhythmias and heart failure. Preclinical work supports the repurposing of digoxin as therapy for non-cardiac conditions, including alcohol-associated steatohepatitis, nonalcoholic steatohepatitis, obesity and metabolic disorders, autoimmune and inflammatory conditions, malignancy, and viral infections, among others. Here, we provide an overview of findings to date on the potential clinical applications of digoxin and mechanisms of action in steatohepatitis and other non-cardiac disorders. We discuss evidence on the differential action of digoxin at high vs low concentrations and identify areas of further research necessary to harness its promising multifunctional use.

Citation: Jamshed F, Dashti F, Ouyang X, Mehal WZ, Banini BA. New uses for an old remedy: Digoxin as a potential treatment for steatohepatitis and other disorders. *World J Gastroenterol* 2023; 29(12): 1824-1837

URL: <https://www.wjgnet.com/1007-9327/full/v29/i12/1824.htm>

DOI: <https://dx.doi.org/10.3748/wjg.v29.i12.1824>

INTRODUCTION

Digoxin in a nutshell: An overview of 200 years

Digoxin (also known by the broader term digitalis) is derived from the purple foxglove, a medicinal plant that can be traced to Irish monks and Germans and was cultivated during the time of Charles the Great (700s-800s). Its Latin scientific name *Digitalis purpurea* was coined by Leonard Fuchs in 1542 based on the translation of the German word describing the shape of the flower as a fingerhut or thimble. Digitalis was mentioned in herbal remedies in England in the 1500s and 1600s for several purposes, including epilepsy, vertigo, swelling/fluid accumulation, tuberculosis, and skin diseases[1]. Subsequently, digitalis fell out of favor due to reports of its toxicity. Animal experiments involving the administration of digoxin leaves to turkeys and roosters resulted in fits and death[1].

In the late 1700s, Withering[2], an English botanist and physician, heard about a family recipe containing over twenty different herbs used in the cure of fluid overload, referred to as dropsy[2]. After realizing that the active ingredient in the herbal remedy was likely from the foxglove plant, Withering [2] administered foxglove tea as a cure to a patient with dropsy. That patient did well, and over the ensuing decade he performed a comprehensive case series of digitalis by administering a decoction prepared from dried foxglove leaves to 163 patients with fluid retention, of whom 101 experienced relief. He noted that digitalis was especially helpful for patients with dropsy after having scarlet fever or bad sore throats. Withering's work inspired other physicians to try digitalis as a therapy in dropsy[2]. For further information on the evolution of digoxin as a medical therapy, the reader is referred to an excellent review by Wray *et al*[1].

The molecular formula of digoxin is $C_{41}H_{64}O_{14}$, and its molecular weight is 780.9 g/mol. Similar to other cardiac glycosides (CG), digoxin increases the force of contraction of the heart by reversibly inhibiting the activity of the myocardial Na-K ATPase pump, an enzyme that controls the movement of potassium ions into the heart[3-5]. The most common cardiac uses of digoxin include heart failure and supraventricular arrhythmia. Its role in heart failure is due to its inotropic properties, inhibiting the Na-K ATPase pump thus increasing the intercellular calcium concentration[6]. This lengthens the cardiac action potential, lowering the heart rate and increasing myocardial contractility. The American College of Cardiology/American Heart Association guidelines recommend that digoxin be added to the heart failure medication regimen in patients with left ventricular systolic dysfunction when symptoms persist despite optimization of treatment with an angiotensin-converting enzyme inhibitor, a β -blocker, and/or a diuretic[7-9]. The digoxin effect in treatment of supraventricular arrhythmia occurs through its parasympathomimetic stimulation *via* the vagus nerve, reducing automaticity of the sinoatrial node and slowing atrioventricular conduction[10].

Current clinical use of digoxin is limited to the cardiac arena. Oral digoxin is available as a solution (0.05 mg/mL) or as tablets (0.0625 mg, 0.125 mg, 0.1875 mg, and 0.25 mg). Dosing is typically maintained between 0.125 to 0.25 mg daily, with lower doses considered in patients 70 years of age or older[11]. The steady-state volume of distribution of digoxin is decreased in chronic renal failure; therefore, both loading and maintenance dosing should be decreased in such patients[12]. Digoxin has a narrow therapeutic window, with the rate of toxicity increasing as serum concentration reaches over 2.0 ng/mL. However, toxicity can also occur at levels below 2.0 ng/mL in the setting of risk factors such as age, decreased renal function, hypokalemia or other electrolyte abnormalities, or interacting medications[13]. The narrow therapeutic window of digoxin necessitates monitoring of serum digoxin levels, particularly in patients with chronic renal dysfunction or varying renal function.

With the discovery of many effective cardiac drugs for heart failure and supraventricular arrhythmias over the past few decades and difficulty maintaining the narrow digoxin therapeutic index, the use of digoxin in cardiac disease has been waning. During this period, however, there have been several

advances in basic and preclinical work toward the potential repurposing of digoxin and other CGs for non-cardiac conditions. These studies indicate that the biological effects of CG are not limited to the inhibition of Na, K-ATPase but include various signal transduction pathways including nuclear receptors (NRs) involved in hormonal signaling, immune response, and carcinogenesis, among others [14-19].

DIGOXIN IN STEATOHEPATITIS

Overnutrition and obesity impair metabolic homeostasis and trigger sterile-type inflammation[20-23], contributing to the development of nonalcoholic fatty liver disease (NAFLD) and nonalcoholic steatohepatitis (NASH). The amplitude of sterile inflammation triggered by metabolic stress in the liver has major clinical consequences. Sterile inflammation is responsible for increasing amounts of liver damage and cell death in NASH[24]. NASH, as well as other diseases associated with sterile inflammation of the liver, lacks effective treatments. This is due to the relatively poor understanding of the initiating steps in sterile inflammation and the dysregulation of a wide range of pathways, making it difficult to know which ones to target.

Identification of hypoxia-inducible factor 1-alpha (HIF-1 α) pathway activation in macrophages for sustained inflammatory responses provided HIF-1 α with a key role in the core regulatory machinery for the transition from acute self-limiting to sustained chronic inflammation[25]. These mechanistic insights into the role of the HIF-1 α pathway in sterile inflammation may have great clinical relevance due to the ability of digoxin to inhibit HIF-1 α activation[26]. Digoxin (1.0-0.05 mg/kg) effectively prevents acute and chronic hepatic damage, steatosis, and inflammation in both lipopolysaccharide- and high-fat diet-driven animal models[27].

Digoxin reduces oxidative stress during liver injury by maintaining cellular redox homeostasis and protects the liver from a wide variety of insults[27,28]. Digoxin reduces HIF-1 α transcriptional activity, thus disrupting HIF-1 α -mediated antioxidant pathways. Digoxin induced significant changes in gene transcripts related to HIF-1 α in metabolic processes and nucleic acid binding[27]. To understand the direct molecular mechanisms responsible for the digoxin effect on HIF-1 α transcription, pyruvate kinase M2 (PKM2) was identified as the major digoxin binding protein using a novel approach of digoxin-immunized agarose beads coupled with liquid chromatography with tandem mass spectrometry analysis[27]. The ability of digoxin to bind to PKM2 was an unexpected finding and provided novel insights into PKM2 biology and the role of PKM2 in sterile inflammatory liver diseases. PKM2 is best known as the rate-limiting glycolytic enzyme that catalyzes the conversion of phosphoenol pyruvate and adenosine diphosphate to pyruvate and ATP[29].

In addition to its pyruvate kinase function, PKM2 interacts with HIF-1 α in the nucleus and functions as a transcriptional coactivator for HIF-1 α , resulting in the stimulation of HIF-1 α responsive genes[30]. Interestingly, the interaction of digoxin with PKM2 did not alter its pyruvate kinase ability or reduce its nuclear translocation. Digoxin, however, reduced the ability of PKM2 to upregulate the transcription of HIF-1 α and its downstream genes, such as inflammatory genes and genes involved in oxidative stress (Figure 1). Further, digoxin reduced the binding of PKM2 to histones, suggesting that digoxin suppressed PKM2-mediated transactivation of HIF-1 α through chromatin modifications[27].

Oral digoxin significantly reduced high-fat diet-induced hepatic damage, steatosis, and liver inflammation across a wide dosage range[27]. The lowest dose of digoxin (0.125 mg/kg) showed significant protective effects against liver injury and sterile inflammation. Interestingly, digoxin had direct effects on the inhibition of inflammasome activation. Digoxin had a small effect on typical inflammasome activity while strongly inhibiting the HIF-1 α pathway-sustained inflammasome activity in macrophages. Despite the importance of PKM2-HIF1 α pathway activation in immune cells during NASH development [27], its direct effect on hepatocytes was unclear. PKM2 levels in healthy human liver cells were very low, but they were significantly elevated in NAFLD and NASH. Pyruvate kinase L/R, the major isoform of pyruvate kinase in the liver, was unchanged. Digoxin treatment directly inhibited PKM2 transactivation leading to the improvement of hepatocyte mitochondrial dysfunction, steatosis, and hepatocellular injury in the obese mouse model (Table 1).

NRs are ligand-activated transcription factors that are involved in a wide array of physiological processes. These transcription factors typically have different domains responsible for ligand-independent interactions with corepressors and coactivators, recognition and binding of response elements within target genes, interaction with other proteins or facilitation of protein translocation, as well as ligand-dependent functions[31-37]. The involvement of NRs in the regulation of a variety of metabolic and physiological processes makes them interesting pharmacological targets.

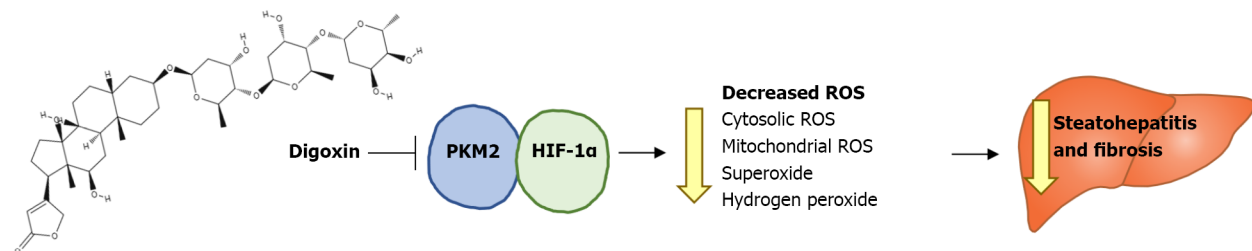
The NR gene retinoic acid-related orphan receptor C gene encodes two protein products, the retinoid-related orphan receptor-gamma (ROR γ) and ROR γ T isoforms, which differ by 21 amino acids in their N-terminal A/B domains. The ROR γ isoform is broadly expressed[38] and is involved in the regulation of genes in the circadian cycle and metabolism[37,39,40]. The ROR γ T isoform is expressed exclusively in T helper 17 (Th17) cells and regulates expression of interleukins (IL)-17A and IL-17F[41,42] involved in autoimmune disease[43-45]. Pivotal evidence for digoxin involvement in the regulation of ROR γ T

Table 1 Summary of the main findings from key original articles investigating non-cardiac applications of digoxin and other cardiac glycosides

Manuscript title	Publication year	Main biomedical/molecular findings	Main histological findings	Ref.
Cardiac glycosides inhibit p53 synthesis by a mechanism relieved by Src or MAPK inhibition	2009	Activation of Src/MAPK signaling pathways, resulting in reduction of p53 protein synthesis	NA	[72]
Human cytomegalovirus inhibition by cardiac glycosides: Evidence for involvement of the <i>HERG</i> gene	2012	CG reduced expression of the potassium channel gene, <i>hERG</i> , and reduced NF- κ B levels	NA	[85]
Digoxin Suppresses HIV-1 Replication by Altering Viral RNA Processing	2013	Reduction in HIV-1 viral mRNAs encoding structural proteins, with reduced synthesis of HIV-1 structural protein; altered viral RNA splice site use leading to loss of essential viral factor Rev; changed activity of CLK family of SR protein kinases and modification of SR proteins	NA	[91]
A novel cell-based high-throughput screen for inhibitors of HIV-1 gene expression and budding identifies the cardiac glycosides	2014	Na-K ATPase- dependent but intracellular Ca ²⁺ - independent inhibition of HIV-1 gene expression at the post-integration stage of the viral life cycle	NA	[90]
Digoxin Suppresses Tumor Malignancy through Inhibiting Multiple Src-Related Signaling Pathways in Non-Small Cell Lung Cancer	2015	Inhibition of proliferation, invasion, migration, and colony formation of A549 lung cancer cells; suppression of Src and related protein activity; reduced EGFR and STAT3 activity	NA	[75]
Synergistic effects of ion transporter and MAP kinase pathway inhibitors in melanoma	2016	Inhibition of the ATP1A1 Na ⁺ /K ⁺ pump, which is highly expressed in melanoma, resulting in selective toxicity to melanoma cells. Digoxin was also additive or synergistic with MEK inhibitor and/or BRAF inhibitor to induce cell death in melanoma cells; increased intracellular acidification, mitochondrial calcium dysregulation, and ATP depletion in melanoma cells	NA	[79]
Small-molecule TFEB pathway agonists that ameliorate metabolic syndrome in mice and extend <i>C. elegans</i> lifespan	2017	Activated TFEB, conferred hepatoprotection against diet-induced steatosis in mice, and extended lifespan of <i>Caenorhabditis elegans</i>	Amelioration of high-fat diet-induced steatosis, reversal of hepatocyte p62/SQSTM1 accumulation, suggesting enhanced autophagic flux	[62]
Targeting Intracellular Ion Homeostasis for the Control of Respiratory Syncytial Virus	2018	Findings suggested digoxin-mediated inhibition of RSV transcription and/or replication, likely dependent on changes in intracellular Na ⁺ and K ⁺	NA	[82]
Digoxin Suppresses PKM2 Promoted HIF-1 α Transactivation in Steatohepatitis	2018	Binding of PKM2 by digoxin downregulated HIF-1 α transactivation to decrease sterile inflammation in the liver. Digoxin suppressed ROS production both <i>in vivo</i> and <i>in vitro</i> from hepatocytes and immune cells	Reduction in hepatic damage, steatosis, and inflammation induced by endotoxin, high fat diet, or alcohol	[27]
Digoxin improves steatohepatitis with differential involvement of liver cell subsets in mice through inhibition of PKM2 transactivation	2019	Digoxin downregulated PKM2-PKM2-HIF-1 α axis and attenuated inflammasome activity in macrophages and hepatic oxidative stress response	Reduction of high fat diet-induced hepatic damage, steatosis, and liver inflammation	[28]
Antiviral activity of digoxin and ouabain against SARS-CoV-2 infection and its implication for COVID-19	2020	Inhibition of viral mRNA expression, copy number, and viral protein expression at the post entry stage of the viral life cycle	NA	[81]
Classical Drug Digitoxin Inhibits Influenza Cytokine Storm, With Implications for COVID-19 therapy	2020	Suppression of levels of the cytokines TNF- α , GRO/KC, MIP2, MCP1, and IFN- γ during cytokine storm	No difference in density of immune cells in rat lung sections, comparing digitoxin-treated and control lungs	[84]
Inhibition of the IL-17A axis in adipocytes suppresses diet-induced obesity and metabolic	2021	Digoxin inhibition of ROR γ T activity suppressed the IL-17A axis, thus preventing diet-induced obesity, metabolic alterations, and liver injury	Prevention of high fat diet-induced hepatic lipid accumulation, reduced	[59]

disorders in mice	fibrosis, increased browning of adipose tissue
-------------------	--

TFEB: Transcription factor EB; PKM2: Pyruvate kinase M2; IL-17A: Interleukin-17A; MAPK: Mitogen-activated protein kinase; CG: Cardiac glycoside; NF- κ B: Nuclear factor- κ B; CLK: Cdc2-like kinases; SR: Serine-arginine; EGFR: Epidermal growth factor receptor; MEK: MAP kinase kinase; RSV: Respiratory syncytial virus; HIF-1 α : Hypoxia-inducible factor 1-alpha; SARS-CoV-2: Severe acute respiratory syndrome coronavirus 2; COVID-19: Coronavirus disease 2019; TNF- α : Tumor necrosis factor-alpha; GRO/KC: Growth-regulated oncogene/keratinocyte chemoattractant; MIP2: Macrophage inflammatory protein 2; MCP1: Monocyte chemoattractant protein-1; IFNy: Interferon-gamma; ROR γ T: Retinoid-related orphan receptor-gamma; NA: No application; ROS: Reactive oxygen species; STAT3: Signal transducer and activator of transcription 3.



DOI: 10.3748/wjg.v29.i12.1824 Copyright ©The Author(s) 2023.

Figure 1 Digoxin reduces steatohepatitis by suppressing pyruvate kinase M2 dependent hypoxia-inducible factor 1-alpha activity and inhibiting reactive oxygen species production[27,28]. Digoxin structure derived from MolView. HIF-1 α : Hypoxia-inducible factor 1-alpha; PKM2: Pyruvate kinase M2; ROS: Reactive oxygen species.

activity was provided by Huh *et al*[46] in 2011 when they showed that digoxin inhibits the transcriptional activity of ROR γ T[46]. Inhibition of ROR γ T by digoxin or its non-toxic derivatives selectively inhibits Th17 differentiation, delaying the onset and severity of autoimmune reactions in murine models [46]. More recently, Karaš *et al*[47,48] reported opposing findings with CGs activating ROR γ in HepG2 cells and ROR γ T in Th17 lymphocytes[47,48] when these compounds were used at much lower doses than originally used by Huh *et al*[46]. Thus, it appears that digoxin-mediated inhibition *vs* activation of ROR γ T may be dependent of the dose utilized[49].

ROR γ directly regulates glucose-6 phosphatase (G6Pase) and a number of genes involved in glucose regulation and insulin sensitivity. G6Pase facilitates glucose-6 phosphate hydrolysis into inorganic phosphate and free glucose[50-52], with suppression of hepatic G6Pase resulting in accumulation of glucose-6 phosphate and metabolic reprogramming involving increased carbohydrate response element binding protein activity and gene expression that lead to hepatic steatosis[53-56]. Digoxin-mediated activation of ROR γ upregulates G6Pase, resulting in improved glucose homeostasis and decreased NAFLD phenotype.

In many respects, the pathophysiological changes seen in alcohol-associated steatohepatitis (ASH) are similar to those seen in NASH, including increased oxidative stress and sterile inflammation manifested as steatohepatitis[57]. The ability of digoxin to improve ASH was tested in a well-accepted Lieber-Decarli ethanol liquid diet (5% ethanol) plus a single ethanol binge mouse model during chronic feeding [58]. Digoxin (0.2-1.0 mg/kg) dose-dependently improved hepatic steatosis, neutrophil infiltration, and hepatocellular damage in ASH. The effect of digoxin was confirmed in human liver tissues, which showed a greater degree of upregulation of HIF-1 α and HIF-1 α -dependent genes in severe ASH compared to mild disease. It was concluded that long-term treatment with digoxin reduced chronic liver damage, inflammation, and steatosis in experimental models of NASH and ASH without affecting cardiac chronotropic and inotropy.

Digoxin is notable for producing cardiotoxicity at concentrations that are close to its effective concentration. Remarkably, however, digoxin did not have any cardiac or other toxicity at lower doses. These studies identified an entirely novel application of this old drug at doses significantly below the dose required for the cardiac effect. Digoxin showed the potential to therapeutically inhibit liver injury in both ASH and NASH through the regulation of PKM2-HIF-1 α pathway activation with the involvement of multiple cell types. Because of the large clinical experience with oral digoxin, this may have significant clinical applicability in human ASH and NASH. Digoxin is currently being investigated in a phase II pilot study in patients with ASH (NCT05014087) (Table 2).

DIGOXIN IN OBESITY AND METABOLIC DISORDERS

Overnutrition, inadequate physical activity, genetic and epigenetic factors, and other risk factors can

Table 2 Ongoing clinical trials of digoxin in non-cardiac diseases

Study title	Medication doses	Current status	Estimated study completion date	Clinical Trials.gov number	Number of participants	Country of trial
Phase 1						
Inhibition of Sterile Inflammation by Digoxin	Digoxin 3.00 mcg/Kg/day vs Digoxin 0.15 mcg/Kg/day vs placebo	Recruiting	July 2023	NCT03559868	45	United States
Phase IB Trial of Metformin, Digoxin, Simvastatin in Subjects With Advanced Pancreatic Cancer and Other Advanced Solid Tumors	Metformin 850 mg po/day, Simvastatin 5 mg po/day, Digoxin 0.0625 mg po/day vs Metformin 850 mg po/day then 1700 mg po/day, Simvastatin 20 mg po/day, Digoxin 0.25 mg po/day vs Metformin 850 mg po/day then 1700 mg po/day Simvastatin 40 mg po/day, Digoxin 0.25 mg po/day then 0.375 mg po/day	Recruiting	December 2023	NCT03889795	15	United States
Effect of Digoxin on Clusters of Circulating Tumor Cells in Breast Cancer Patients	Digoxin 0.125 mg or 0.250 mg digoxin based on renal function and target serum digoxin concentration	Recruiting	June 2022	NCT03928210	9	Switzerland
Phase 2						
Digoxin In Treatment of Alcohol Associated Hepatitis	Digoxin titration to goal 0.5 and 1.1 ng/mL vs no digoxin	Recruiting	August 2024	NCT05014087	60	United States
Evaluating the Effect of Digoxin and Ursodeoxycholic Acid in Patients With Rheumatoid Arthritis	Digoxin 0.25 mg + DMARDs vs UCDA 500 mg + DMARDs vs placebo + DMARDs	Recruiting	July 2022	NCT04834557	90	Egypt
FOLFIRINOX With Digoxin in Patients With Resectable Pancreatic Cancer	FOLFIRINOX + digoxin 0.125 or 0.250 mg for target digoxin level 0.8 to 1.2 ng/mL	Recruiting	February 2025	NCT04141995	20	United States
Topical Ionic Contra-Viral Therapy in Actinic Keratosis	Digoxin topical gel 0.125% vs furosemide topical gel 0.125% vs digoxin and furosemide gel 0.125% vs vehicle gel	Unknown	September 2019	NCT03684772	32	Netherlands
Phase II Multicentric Study of Digoxin Per os in Classic or Endemic Kaposi's Sarcoma (KADIG 01)	Digoxin goal 0.6 to 1.2 ng/mL for age < 75 yr; Digoxin goal 0.5-0.8 ng/mL for age > 75 yr	Unknown	September 2019	NCT02212639	17	France

DMARDs: Disease-modifying antirheumatic drug; FOLFIRINOX: FOLinic acid, 5-Fluorouracil, IRINotecan and Oxaliplatin; UCDA: Ursodeoxycholic acid.

predispose individuals to metabolic syndrome[59] with associated comorbidities[60]. Inhibition of ROR γ T-mediated IL-17A production by digoxin abolishes the IL-17A axis[46], suppressing diet-induced obesity and leading to increased brown adipose tissue[61]. Brown adipose tissue is an essential site for thermogenesis and critical for maintaining body temperature regulated by mitochondria uncoupling protein-1[61]. The metabolic effects observed with digoxin can also be achieved by the ubiquitous deletion of IL-17 receptor A. Modulation of IL-17A signaling may thus serve as a strategy to inhibit obesity and related complications[59].

Metabolic disorders, including obesity, liver steatosis, and aging, may be improved by caloric restriction or starvation, which activates the transcription factor EB (TFEB) that regulates lipid metabolism and the biogenesis of lysosomes. Agents that activate TFEB can confer metabolic changes resembling starvation and thus have utility in the treatment of these metabolic disorders. Recently through a nanotechnology-enabled high-throughput screening of various small molecules, digoxin was one of three small molecules identified that activate TFEB[62]. This activation occurs through distinct calcium-dependent mechanisms and by promoting autophagolysosomal activity, an adaptive catabolic process that generates nutrients and energy during starvation[62]. Calcium is stored in cells in three different compartments, including lysosomes, mitochondria, and the endoplasmic reticulum[63], and TFEB activators can differentially affect calcium stores in these compartments. Digoxin induces lysosomal calcium release through mucolipin 1, leading to activation of TFEB with resultant anti-obesity effects[59].

CGs also appear to hold promise for heritable metabolic disorders. Familial hypercholesterolemia, characterized by elevated serum low-density lipoprotein-cholesterol, is a genetic disorder caused primarily by mutations in the low-density lipoprotein receptor. Patients with compound heterozygous

or homozygous mutations in the low-density lipoprotein receptor have low-density lipoprotein-cholesterol levels > 500 mg/dL, leading to the formation of xanthomas, severe cardiovascular disease, and early death[64]. Hepatocyte-like cells derived from induced pluripotent stem cells from patients with homozygous familial hypercholesterolemia have been used to screen for potential pharmacological therapies[65]. CGs reduced apoB, the crucial protein component of very-low-density lipoprotein and low-density lipoprotein particles, in human hepatocytes as well as in the serum of mice with humanized livers. The mechanism through which CG-mediated reduction of apoB and improvement of hypercholesterolemia occurred did not appear to involve the expression of the *APOB* gene or the synthesis of apoB protein but rather the enhancement of proteolytic turnover of the apoB protein[65].

DIGOXIN IN AUTOIMMUNE AND INFLAMMATORY CONDITIONS

Th17 cells are an independent subset of T helper cells that produce IL-17 and are involved in the induction of inflammation and autoimmune disease. These cells have a unique transcription factor, ROR γ T[41], and are activated by IL-6 and transforming growth factor-beta 1. Because Th17 cells are inducers of inflammation and autoimmune disease, specific targeting of these cells can reduce inflammation. Digoxin downregulates Th17 differentiation through suppression of ROR γ T transcriptional activity without effect on the differentiation of T cell lineages[66].

Th17 and T1 play a crucial role in rheumatoid arthritis, a systemic autoimmune inflammatory disorder characterized by hyperplasia of the synovial membrane along with persistent inflammation of joints. In one study assessing the effect of digoxin on the peripheral blood mononuclear cells of 30 rheumatoid arthritis patients and 10 healthy controls, there was a significant reduction in the population of Th17 cells through suppression of the transcription factor ROR γ T and a decrease in the levels of IL-1 β , IL-6, IL-17, and IL-23 cytokines[67]. Digoxin treatment did not modify the expression of transforming growth factor-beta 1 and interferon-gamma (IFN- γ) at the level of mRNA and protein.

Psoriasis is another chronic inflammatory disease involving IL-17-producing Th17 cells[68]. The toll-like receptor 7 agonist imiquimod creates psoriasis-like lesions on the ear or back skin of mice through an IL-17-dependent mechanism. Intraperitoneal digoxin differentially affects these skin lesions, reducing those on the ear and exacerbating those on the back[68]. This differential effect of digoxin may relate to differences in target tissues, the imiquimod application dose, and digoxin bioavailability in different sites.

Digoxin might also be effective for managing pain[69]. Digoxin is a potent inhibitor of soluble epoxide hydrolase enzyme, which breaks down endogenous lipid mediators like epoxyeicosatrienoic acids that are known to have cardiovascular effects including vasodilation, anti-migratory actions on vascular smooth muscle cells, and anti-inflammatory actions[70]. Digoxin has antipyretic activity in rats and inhibits neutrophil infiltration and alveolar septal thickening in lung tissue[69]. Administration of digoxin at a low dose can reduce pain and allodynia and decrease edema and abdominal contraction [69].

DIGOXIN IN CANCER

In a study investigating potential new drugs for prostate cancer, digoxin was found to be highly potent in inhibiting prostate cancer cell growth *in vitro*[71]. Regular digoxin use, especially over 10 years, was found to be associated with a 25% lower risk of prostate cancer[71]. Although the methods through which digoxin reduced prostate cancer risk are unclear, one potential mechanism involves the increased influx of intracellular calcium into prostate cancer cells triggering apoptosis through the cyclin-dependent kinase 5/p25 pathway. Activated Src/mitogen-activated protein kinase (MAPK) signaling results in inhibition of p53 synthesis, suggesting that CGs may have utility in the treatment of cancers with gain of function *P53* mutations[72]. Other mechanisms proposed for the anticancer effects of digoxin include inhibition of Na⁺/K⁺-ATPase and topoisomerase[73], alterations of calcium signaling [74], and inhibition of HIF-1 α synthesis[26]. The DIG-HIF-1 pharmacodynamic trial, which sought to test whether digoxin can reduce the expression of HIF-1 α protein in surgically resected breast cancer tissue, was terminated early due to difficulty with accrual (NCT01763931). We hope that there will be subsequent studies that will shed light on this important question.

When given together with the anti-neoplastic drug adriamycin, digoxin enhanced anti-cancer effects *in vitro* on non-small cell lung cancer by inhibiting both DNA double-strand break and single-strand break repair and reducing the cardiotoxicity of adriamycin[72]. Cotreatment with digoxin blocked the adriamycin-induced reduction in cardiomyocyte size, suggesting that digoxin can ameliorate the reduction of heart weight/body weight ratio by adriamycin.

Digoxin suppresses lung cancer progression by inhibiting Src activation and related pathways[75]. In digoxin-treated cells, the phosphorylation of Src and its related proteins was inhibited, suppressing lung cancer cell proliferation, migration, and invasion through inhibition of phosphatidylinositol 3-kinase, focal adhesion kinase, stress-activated protein kinases/Jun amino-terminal kinases, paxillin, and

p130Cas activities. Digoxin also reduces mRNA expression of Src and related protein kinases[75]. Digoxin was also found to have effects on glioblastoma, a highly aggressive and lethal brain tumor, by enhancing apoptosis and reducing the levels of the anti-apoptotic protein through its proteasomal degradation[76].

A screen of 200000 small molecules for inhibitory effect against primary human melanoma cells showed that several CGs, including digoxin, demonstrated toxicity against melanoma cells *vs* normal human melanocytes[77]. This effect involves inhibition of the ATP1A1 Na⁺/K⁺ pump that is crucial for the maintenance of ion gradients across the plasma membrane for substrate transport. Although CGs alone were insufficient to cause melanoma regression in patient-derived xenografts, they showed synergistic effects with inhibitors of MAPK pathway to mediate regression in both *BRAF* wildtype and *BRAF* mutant melanomas[77]. Polarization of CD4+ T cells into the Th17 subtype in a transgenic mouse model resulted in destruction of advanced B16 murine melanoma through IFN- γ dependent mechanisms[78]. A recent phase 1B clinical trial of digoxin and trametinib, a MAP kinase kinase inhibitor, in patients with *BRAF* wildtype metastatic melanoma who were refractory or intolerant to immune checkpoint blockade showed that 13 out of 20 patients (65%) achieved disease control (NCT28278423)[79]. The results of this early study are encouraging and need to be expanded.

Digoxin is currently being studied in a phase 1B combination drug trial in pancreatic cancer and other advanced solid tumors (NCT03889795) (Table 2). It is also being studied for feasibility and safety when combined with folinic acid, 5-fluorouracil, irinotecan, and oxaliplatin in patients with resectable pancreatic cancer (NCT04141995).

DIGOXIN IN VIRAL INFECTION

Digoxin inhibits coronaviruses and other viruses[80]. It inhibits the cytokine storm generated by severe acute respiratory syndrome coronavirus 2 (SARS-CoV-2) infection and blocks viral cell penetration and infectivity[81]. After single-dose digoxin treatment, SARS-CoV-2 titers were the same as achieved with treatment by remdesivir, with > 99% viral inhibition compared to controls or patients on chloroquine at 48 h post-infection[81]. In other cases, digoxin suppressed viral mRNA expression (99%) more effectively than remdesivir (> 60%) or chloroquine (> 30%)[82]. Host cell entry by Middle East respiratory syndrome and SARS-CoV is inhibited through the silencing or inhibition of the Na₊ K₊-ATPase α 1-subunit by low doses of CG. This disruption of cell entry occurs at an early stage by interfering with endocytosis through a non-elucidated pathway[80,83]. In the post-entry stage, digoxin significantly inhibits viral mRNA expression, copy number, and viral protein expression at half-maximal inhibitory concentration of 0.043 nM[81].

In rat models infected with influenza virus, administration of digoxin analog digitoxin suppressed cytokine levels, including tumor necrosis factor-alpha, growth-regulated oncogene/keratinocyte chemoattractant, macrophage inflammatory protein 2, monocyte chemoattractant protein-1, and IFN- γ in the rat lung[84]. The inhibition of Na-K-ATPase by CGs decreased intracellular potassium, inhibiting the host cell translational machinery and decreasing influenza virus replication[80].

Digoxin and other CGs also inhibit replication of cytomegalovirus, a herpesvirus pathologic agent of important human diseases, at nanomolar concentrations, with an additive effect when combined with antiviral drugs for cytomegalovirus such as ganciclovir[80]. CGs reduced the levels of viral proteins and cellular nuclear factor-kappaB, with the activity of CGs correlating with the expression of *hERG*, a potassium channel gene[85].

Human papillomaviruses (HPVs) rely on potassium ion influx for replication[86]. Cutaneous warts (including plantar warts or common warts) are typically caused by HPV 1, 2, 27, and 57[87,88], while genital warts are typically caused by HPV 6 and 11. CGs such as digoxin and the loop diuretic furosemide interact with the cell-membrane ion cotransporters Na⁺/K⁺-ATPase and Na-K-Cl and inhibit potassium flux thus inhibiting HPV replication[86]. The inhibitory effect on DNA replication appears most potent when digoxin and furosemide are combined; the term ionic contra-viral therapy (ICVT) describes the topical application of these drugs in combination. A phase 1/2 open-label study of ICVT was safe and efficacious in 12 healthy patients with common warts[89]. A follow-up randomized, double-blind, placebo-controlled phase 2A proof-of-concept study assessed the efficacy, safety, and tolerability of ICVT in adults with cutaneous warts. Eighty adult patients were randomized to digoxin or furosemide alone, ICVT or placebo (NCT02333643)[87]. Reduction in HPV load and wart size was achieved in all active treatment groups but not in placebo, with a statistically significant reduction in wart diameter in those treated with ICVT *vs* placebo. On the contrary, a phase 2 study of ICVT for HPV-related genital lesions was terminated early due to a lack of effect on interim analysis (NCT03334240). Overall, digoxin appears promising for the treatment of HPV-induced lesions, especially the cutaneous subtype, and warrants further investigation in large multicenter studies.

A cell-based screen performed on cells transfected with proviral DNA constructs uncovered a number of compounds that inhibit HIV-1 virion production, including numerous CGs[90]. Digoxin selectively impaired HIV-1 replication at two levels: (1) Through global alterations in the efficiency of HIV-1 RNA processing; and (2) By blocking the export of incompletely spliced viral RNAs to the

cytoplasm[91]. The cardenolides and the bufadienolides, both subclasses of CGs, inhibited the late stages of the HIV-1 replication cycle. Although both are C(23) steroids, they differ in that cardenolides contain a five-membered lactone ring at C-17, whereas bufadienolides contain a six-membered lactone ring. Members of both classes of CGs inhibited late stages of HIV-1 production, and changes in structure resulted in changes in inhibition. Digoxin (and potentially the CG family of drugs) represents a novel HIV-1 inhibitor with the potential for rapid development into antiretroviral therapy. The dose-limiting toxicities observed with CGs in humans are typically related to toxic increases in cardiac contractility driven by increases in intracellular calcium. As the mechanism of CG inhibition of HIV-1 appears to be independent of such calcium increases, it is possible that structural modification of the CGs could avoid cardiac toxicity while maintaining HIV-1 inhibition.

DIGOXIN IN NON-CARDIAC GENETIC DISORDERS

CGs or their derivatives, including digoxin, also appear promising for treating certain genetic diseases, such as cystic fibrosis and Duchenne's muscular dystrophy, wherein truncated protein products encoded by the corresponding nonsense mRNAs are fully or partially functional[92,93]. The nonsense-mediated mRNA decay (NMD) pathway selectively eliminates aberrant transcripts containing premature translation termination codons and regulates the levels of a number of physiological mRNAs. NMD modulates the clinical outcome of a variety of human diseases, including cancer and several genetic disorders. Using a dual-color bioluminescence-based NMD reporter system, Nickless *et al*[94] performed a high-throughput screen to identify drug candidates that can alter NMD activity in human cells[94]. The effects of seven of the inhibitor hits were found, and each validated compound inhibited NMD in a dose-dependent manner. Notably, the top five verified hits, including digitoxin, digoxin, lanatoside C, proscillarin, and ouabain, are all CGs[95]. It should be noted that the concentrations of CGs used in this study to achieve more complete NMD inhibition without causing significant cellular toxicity (for example, 500 nM for digoxin and 175 nM for ouabain) are much higher than standard clinical doses used for the treatment of cardiac failure. Thus, acute use of these drugs at the experimental working concentrations cannot directly translate to the clinic owing to *in vivo* toxic effects. However, the benefits of partial NMD inhibition with chronic treatment at clinically relevant doses may potentially be efficacious, but this will require further clinical pharmacology studies.

CONCLUSION

Until now, most of our knowledge and experience with digoxin pertains to its use in the cardiac field. However, in the past decade, digoxin has emerged as a potential pharmacologic agent in the management of several conditions, including steatohepatitis in the context of nonalcohol and alcohol-associated fatty liver disease, obesity and other metabolic disorders, autoimmune conditions, malignancy, and viral infection, among others. Clinical trials on the repurposing of digoxin for therapeutic use in a variety of non-cardiac conditions are still in their early stages but appear promising.

At relatively high concentrations (hundreds of nM), digoxin and other CGs inhibit the Na-K ATPase pump, leading to accumulation of sodium ions in the cytosol that drives an influx of calcium into the heart, increasing contractility[96]. At lower doses (picomolar to low nanomolar), digoxin induces the Na-K ATPase to act as a receptor that can modulate a variety of pathways[5,96], including the Src/MAPK pathway, which regulates a number of downstream signaling pathways. Also at high doses, digoxin binding to the ligand-binding domain of the NR ROR γ T inhibits its transcriptional activity, leading to inhibition of Th17 activity and IL-17 release[59] and suppressing nuclear factor- κ B activity[85], altogether reducing the inflammatory response. At lower doses, digoxin activates ROR γ T signaling, leading to induction of several Th17-specific genes, suggesting a potential role of digoxin in adoptive cell therapy[14,47,48].

Several questions remain to be clarified in the quest towards repurposing of digoxin including: the structure-activity relationships that direct its molecular targeting in specific disease settings; whether dosing/concentration alone determines its activity as an inhibitor *vs* activator or whether other factors affect its action; and the ideal potency that can be utilized for pharmacologic intervention in a particular tissue while optimizing its safety profile. Indeed, the decline of digoxin in the cardiac arena is largely attributable to its narrow therapeutic index and potential toxicity, thus it is very exciting that recent studies show potent biological activity of much smaller doses of digoxin than used historically in the clinical setting. Digoxin is commercially available as a relatively cheap generic drug, thus further elucidation of its biological effects and mechanisms of action especially at low non-toxic doses will facilitate its rapid therapeutic repurposing.

FOOTNOTES

Author contributions: The manuscript was outlined and proposed by Banini BA; The literature search, critical assessment of the literature, and writing of the manuscript were performed by Jamshed F, Dashti F, Ouyang X, Mehal WZ, and Banini BA; All authors discussed the manuscript and reviewed and edited the final version.

Supported by NIH UO1 (to Mehal WZ), No. 5U01AA026962-02.

Conflict-of-interest statement: All the authors report no relevant conflicts of interest for this article.

Open-Access: This article is an open-access article that was selected by an in-house editor and fully peer-reviewed by external reviewers. It is distributed in accordance with the Creative Commons Attribution NonCommercial (CC BY-NC 4.0) license, which permits others to distribute, remix, adapt, build upon this work non-commercially, and license their derivative works on different terms, provided the original work is properly cited and the use is non-commercial. See: <https://creativecommons.org/Licenses/by-nc/4.0/>

Country/Territory of origin: United States

ORCID number: Wajahat Z Mehal 0000-0001-8481-3671; Bubu A Banini 0000-0002-2972-9263.

S-Editor: Fan JR

L-Editor: Filopodia

P-Editor: Fan JR

REFERENCES

- 1 Wray S, Eisner DA, Allen DG. Two hundred years of the foxglove. *Med Hist Suppl* 1985; 132-150 [PMID: 3915521 DOI: 10.1017/s0025727300070551]
- 2 Withering W. An Account of the Foxglove and some of its Medical Uses With Practical Remarks on Dropsy and Other Diseases Birmingham, AL: The Classics of Medicine Library, 1785. [cited 10 November 2023]. Available from: https://www.researchgate.net/publication/281191423_An_account_of_the_foxglove_and_some_of_its_medicinal_uses_With_practical_remarks_on_dropsy_and_other_diseases
- 3 Katz AM. Effects of digitalis on cell biochemistry: sodium pump inhibition. *J Am Coll Cardiol* 1985; 5: 16A-21A [PMID: 2580875 DOI: 10.1016/s0735-1097(85)80459-9]
- 4 Doherty JE, de Soya N, Kane JJ, Bissett JK, Murphy ML. Clinical pharmacokinetics of digitalis glycosides. *Prog Cardiovasc Dis* 1978; 21: 141-158 [PMID: 356122 DOI: 10.1016/0033-0620(78)90020-8]
- 5 Ferguson DW, Abboud FM, Mark AL. Selective impairment of baroreflex-mediated vasoconstrictor responses in patients with ventricular dysfunction. *Circulation* 1984; 69: 451-460 [PMID: 6692507 DOI: 10.1161/01.cir.69.3.451]
- 6 Kelly RA. Cardiac glycosides and congestive heart failure. *Am J Cardiol* 1990; 65: 10E-16E; discussion 22E [PMID: 2178374 DOI: 10.1016/0002-9149(90)90245-v]
- 7 Khand AU, Rankin AC, Martin W, Taylor J, Gemmell I, Cleland JG. Carvedilol alone or in combination with digoxin for the management of atrial fibrillation in patients with heart failure? *J Am Coll Cardiol* 2003; 42: 1944-1951 [PMID: 14662257 DOI: 10.1016/j.jacc.2003.07.020]
- 8 January CT, Wann LS, Alpert JS, Calkins H, Cigarroa JE, Cleveland JC Jr, Conti JB, Ellinor PT, Ezekowitz MD, Field ME, Murray KT, Sacco RL, Stevenson WG, Tchou PJ, Tracy CM, Yancy CW; ACC/AHA Task Force Members. 2014 AHA/ACC/HRS guideline for the management of patients with atrial fibrillation: a report of the American College of Cardiology/American Heart Association Task Force on practice guidelines and the Heart Rhythm Society. *Circulation* 2014; 130: e199-e267 [PMID: 24682347 DOI: 10.1161/CIR.0000000000000041]
- 9 Hunt SA, Abraham WT, Chin MH, Feldman AM, Francis GS, Ganiats TG, Jessup M, Konstam MA, Mancini DM, Michl K, Oates JA, Rahko PS, Silver MA, Stevenson LW, Yancy CW. 2009 focused update incorporated into the ACC/AHA 2005 Guidelines for the Diagnosis and Management of Heart Failure in Adults: a report of the American College of Cardiology Foundation/American Heart Association Task Force on Practice Guidelines: developed in collaboration with the International Society for Heart and Lung Transplantation. *Circulation* 2009; 119: e391-e479 [PMID: 19324966 DOI: 10.1161/CIRCULATIONAHA.109.192065]
- 10 Cheng JW, Rybak I. Use of digoxin for heart failure and atrial fibrillation in elderly patients. *Am J Geriatr Pharmacother* 2010; 8: 419-427 [PMID: 21335295 DOI: 10.1016/j.amjopharm.2010.10.001]
- 11 MacLeod-Glover N, Mink M, Yarema M, Chuang R. Digoxin toxicity: Case for retiring its use in elderly patients? *Can Fam Physician* 2016; 62: 223-228 [PMID: 26975913]
- 12 Cheng JW, Charland SL, Shaw LM, Kobrin S, Goldfarb S, Stanek EJ, Spinler SA. Is the volume of distribution of digoxin reduced in patients with renal dysfunction? *Pharmacotherapy* 1997; 17: 584-590 [PMID: 9165563]
- 13 David MNV, Shetty M. Digoxin. StatPearls. Treasure Island (FL), 2022
- 14 Karaś K, Sałkowska A, Dastych J, Bachorz RA, Ratajewski M. Cardiac glycosides with target at direct and indirect interactions with nuclear receptors. *Biomed Pharmacother* 2020; 127: 110106 [PMID: 32248001 DOI: 10.1016/j.biopha.2020.110106]
- 15 Lee J, Baek S, Lee J, Lee DG, Park MK, Cho ML, Park SH, Kwok SK. Digoxin ameliorates autoimmune arthritis via suppression of Th17 differentiation. *Int Immunopharmacol* 2015; 26: 103-111 [PMID: 25819229 DOI: 10.1016/j.intimp.2015.01.020]

10.1016/j.intimp.2015.03.017]

16 **Csaba G**, Inczezi-Gonda A. Fetal digoxin treatment enhances the binding capacity of thymic glucocorticoid receptors in adult female rats. *Gen Pharmacol* 1998; **30**: 647-649 [PMID: 9559313 DOI: 10.1016/s0306-3623(97)00384-4]

17 **Johansson S**, Lindholm P, Gullbo J, Larsson R, Bohlin L, Claeson P. Cytotoxicity of digitoxin and related cardiac glycosides in human tumor cells. *Anticancer Drugs* 2001; **12**: 475-483 [PMID: 11395576 DOI: 10.1097/00001813-200106000-00009]

18 **Patel S**. Plant-derived cardiac glycosides: Role in heart ailments and cancer management. *Biomed Pharmacother* 2016; **84**: 1036-1041 [PMID: 27780131 DOI: 10.1016/j.biopha.2016.10.030]

19 **Canderan G**, Dellabona P. T helper 17 T cells do good for cancer immunotherapy. *Immunotherapy* 2010; **2**: 21-24 [PMID: 20635888 DOI: 10.2217/imt.09.83]

20 **Farrell GC**, Haczeyni F, Chitturi S. Pathogenesis of NASH: How Metabolic Complications of Overnutrition Favour Lipotoxicity and Pro-Inflammatory Fatty Liver Disease. *Adv Exp Med Biol* 2018; **1061**: 19-44 [PMID: 29956204 DOI: 10.1007/978-981-10-8684-7_3]

21 **Mota M**, Banini BA, Cazanave SC, Sanyal AJ. Molecular mechanisms of lipotoxicity and glucotoxicity in nonalcoholic fatty liver disease. *Metabolism* 2016; **65**: 1049-1061 [PMID: 26997538 DOI: 10.1016/j.metabol.2016.02.014]

22 **Banini BA**, Kumar DP, Cazanave S, Seneshaw M, Mirshahi F, Santhekadur PK, Wang L, Guan HP, Oseini AM, Alonso C, Bedossa P, Koduru SV, Min HK, Sanyal AJ. Identification of a Metabolic, Transcriptomic, and Molecular Signature of Patatin-Like Phospholipase Domain Containing 3-Mediated Acceleration of Steatohepatitis. *Hepatology* 2021; **73**: 1290-1306 [PMID: 33131062 DOI: 10.1002/hep.31609]

23 **Cazanave S**, Podtelezhnikov A, Jensen K, Seneshaw M, Kumar DP, Min HK, Santhekadur PK, Banini B, Mauro AG, M Oseini A, Vincent R, Tanis KQ, Webber AL, Wang L, Bedossa P, Mirshahi F, Sanyal AJ. The Transcriptomic Signature Of Disease Development And Progression Of Nonalcoholic Fatty Liver Disease. *Sci Rep* 2017; **7**: 17193 [PMID: 29222421 DOI: 10.1038/s41598-017-17370-6]

24 **Wree A**, Mehal WZ, Feldstein AE. Targeting Cell Death and Sterile Inflammation Loop for the Treatment of Nonalcoholic Steatohepatitis. *Semin Liver Dis* 2016; **36**: 27-36 [PMID: 26870930 DOI: 10.1055/s-0035-1571272]

25 **Ouyang X**, Ghani A, Malik A, Wilder T, Colegio OR, Flavell RA, Cronstein BN, Mehal WZ. Adenosine is required for sustained inflammasome activation via the A_{2A} receptor and the HIF-1 α pathway. *Nat Commun* 2013; **4**: 2909 [PMID: 24352507 DOI: 10.1038/ncomms3909]

26 **Zhang H**, Qian DZ, Tan YS, Lee K, Gao P, Ren YR, Rey S, Hammers H, Chang D, Pili R, Dang CV, Liu JO, Semenza GL. Digoxin and other cardiac glycosides inhibit HIF-1alpha synthesis and block tumor growth. *Proc Natl Acad Sci U S A* 2008; **105**: 19579-19586 [PMID: 19020076 DOI: 10.1073/pnas.0809763105]

27 **Ouyang X**, Han SN, Zhang JY, Dioleitis E, Nemeth BT, Pacher P, Feng D, Bataller R, Cabezas J, Stärkel P, Caballeria J, Pongratz RL, Cai SY, Schnabl B, Hoque R, Chen Y, Yang WH, Garcia-Martinez I, Wang FS, Gao B, Torok NJ, Kibbey RG, Mehal WZ. Digoxin Suppresses Pyruvate Kinase M2-Promoted HIF-1 α Transactivation in Steatohepatitis. *Cell Metab* 2018; **27**: 339-350.e3 [PMID: 29414684 DOI: 10.1016/j.cmet.2018.01.007]

28 **Zhao P**, Han SN, Arumugam S, Yousaf MN, Qin Y, Jiang JX, Torok NJ, Chen Y, Mankash MS, Liu J, Li J, Iwakiri Y, Ouyang X. Digoxin improves steatohepatitis with differential involvement of liver cell subsets in mice through inhibition of PKM2 transactivation. *Am J Physiol Gastrointest Liver Physiol* 2019; **317**: G387-G397 [PMID: 31411894 DOI: 10.1152/ajpgi.00054.2019]

29 **Luo W**, Semenza GL. Emerging roles of PKM2 in cell metabolism and cancer progression. *Trends Endocrinol Metab* 2012; **23**: 560-566 [PMID: 22824010 DOI: 10.1016/j.tem.2012.06.010]

30 **Luo W**, Hu H, Chang R, Zhong J, Knabel M, O'Meally R, Cole RN, Pandey A, Semenza GL. Pyruvate kinase M2 is a PHD3-stimulated coactivator for hypoxia-inducible factor 1. *Cell* 2011; **145**: 732-744 [PMID: 21620138 DOI: 10.1016/j.cell.2011.03.054]

31 **Burris TP**, Solt LA, Wang Y, Crumbley C, Banerjee S, Griffett K, Lundasen T, Hughes T, Kojetin DJ. Nuclear receptors and their selective pharmacologic modulators. *Pharmacol Rev* 2013; **65**: 710-778 [PMID: 23457206 DOI: 10.1124/pr.112.006833]

32 **Wärnmark A**, Treuter E, Wright AP, Gustafsson JA. Activation functions 1 and 2 of nuclear receptors: molecular strategies for transcriptional activation. *Mol Endocrinol* 2003; **17**: 1901-1909 [PMID: 12893880 DOI: 10.1210/me.2002-0384]

33 **Hörlein AJ**, Näär AM, Heinzel T, Torchia J, Gloss B, Kurokawa R, Ryan A, Kamei Y, Söderström M, Glass CK. Ligand-independent repression by the thyroid hormone receptor mediated by a nuclear receptor co-repressor. *Nature* 1995; **377**: 397-404 [PMID: 7566114 DOI: 10.1038/377397a0]

34 **Pissios P**, Tzameli I, Kushner P, Moore DD. Dynamic stabilization of nuclear receptor ligand binding domains by hormone or corepressor binding. *Mol Cell* 2000; **6**: 245-253 [PMID: 10983973 DOI: 10.1016/s1097-2765(00)00026-5]

35 **Haelens A**, Tanner T, Denayer S, Callewaert L, Claessens F. The hinge region regulates DNA binding, nuclear translocation, and transactivation of the androgen receptor. *Cancer Res* 2007; **67**: 4514-4523 [PMID: 17483368 DOI: 10.1158/0008-5472.CAN-06-1701]

36 **Solt LA**, Griffin PR, Burris TP. Ligand regulation of retinoic acid receptor-related orphan receptors: implications for development of novel therapeutics. *Curr Opin Lipidol* 2010; **21**: 204-211 [PMID: 20463469 DOI: 10.1097/MOL.0b013e328338ca18]

37 **Jetten AM**. Retinoid-related orphan receptors (RORs): critical roles in development, immunity, circadian rhythm, and cellular metabolism. *Nucl Recept Signal* 2009; **7**: e003 [PMID: 19381306 DOI: 10.1621/nrs.07003]

38 **He YW**, Deftos ML, Ojala EW, Bevan MJ. ROR γ t, a novel isoform of an orphan receptor, negatively regulates Fas ligand expression and IL-2 production in T cells. *Immunity* 1998; **9**: 797-806 [PMID: 9881970 DOI: 10.1016/s1074-7613(00)80645-7]

39 **Kang HS**, Angers M, Beak JY, Wu X, Gimble JM, Wada T, Xie W, Collins JB, Grissom SF, Jetten AM. Gene expression profiling reveals a regulatory role for ROR alpha and ROR gamma in phase I and phase II metabolism. *Physiol Genomics* 2007; **31**: 281-294 [PMID: 17666523 DOI: 10.1152/physiolgenomics.00098.2007]

40 **Takeda Y**, Jothi R, Birault V, Jetten AM. ROR γ directly regulates the circadian expression of clock genes and downstream targets in vivo. *Nucleic Acids Res* 2012; **40**: 8519-8535 [PMID: 22753030 DOI: 10.1093/nar/gks630]

41 **Ivanov II**, McKenzie BS, Zhou L, Tadokoro CE, Lepelley A, Lafaille JJ, Cua DJ, Littman DR. The orphan nuclear receptor RORgammat directs the differentiation program of proinflammatory IL-17 $+$ T helper cells. *Cell* 2006; **126**: 1121-1133 [PMID: 16990136 DOI: 10.1016/j.cell.2006.07.035]

42 **Crome SQ**, Wang AY, Kang CY, Levings MK. The role of retinoic acid-related orphan receptor variant 2 and IL-17 in the development and function of human CD4 $+$ T cells. *Eur J Immunol* 2009; **39**: 1480-1493 [PMID: 19449310 DOI: 10.1002/eji.200838908]

43 **Hirota K**, Hashimoto M, Yoshitomi H, Tanaka S, Nomura T, Yamaguchi T, Iwakura Y, Sakaguchi N, Sakaguchi S. T cell self-reactivity forms a cytokine milieu for spontaneous development of IL-17 $+$ Th cells that cause autoimmune arthritis. *J Exp Med* 2007; **204**: 41-47 [PMID: 17227914 DOI: 10.1084/jem.20062259]

44 **Zheng L**, Ye P, Liu C. The role of the IL-23/IL-17 axis in the pathogenesis of Graves' disease. *Endocr J* 2013; **60**: 591-597 [PMID: 23327801 DOI: 10.1507/endocrj.ej12-0264]

45 **Kebir H**, Kreymborg K, Ifergan I, Dodelet-Devillers A, Cayrol R, Bernard M, Giuliani F, Arbour N, Becher B, Prat A. Human TH17 lymphocytes promote blood-brain barrier disruption and central nervous system inflammation. *Nat Med* 2007; **13**: 1173-1175 [PMID: 17828272 DOI: 10.1038/nm1651]

46 **Huh JR**, Leung MW, Huang P, Ryan DA, Krout MR, Malapaka RR, Chow J, Manel N, Ciofani M, Kim SV, Cuesta A, Santori FR, Lafaille JJ, Xu HE, Gin DY, Rastinejad F, Littman DR. Digoxin and its derivatives suppress TH17 cell differentiation by antagonizing ROR γ t activity. *Nature* 2011; **472**: 486-490 [PMID: 21441909 DOI: 10.1038/nature09978]

47 **Karaś K**, Sałkowska A, Walczak-Drzewiecka A, Ryba K, Dastych J, Bachorz RA, Ratajewski M. The cardenolides strophanthidin, digoxigenin and dihydrostrophanthidin act as activators of the human ROR γ /ROR γ T receptors. *Toxicol Lett* 2018; **295**: 314-324 [PMID: 29981919 DOI: 10.1016/j.toxlet.2018.07.002]

48 **Karaś K**, Sałkowska A, Sobalska-Kwapis M, Walczak-Drzewiecka A, Strapagiel D, Dastych J, Bachorz RA, Ratajewski M. Digoxin, an Overlooked Agonist of ROR γ /ROR γ T. *Front Pharmacol* 2018; **9**: 1460 [PMID: 30666196 DOI: 10.3389/fphar.2018.01460]

49 **Škubník J**, Pavličková V, Rimpelová S. Cardiac Glycosides as Immune System Modulators. *Biomolecules* 2021; **11** [PMID: 33947098 DOI: 10.3390/biom11050659]

50 **Takeda Y**, Kang HS, Freudenberg J, DeGraff LM, Jothi R, Jetten AM. Retinoic acid-related orphan receptor γ (ROR γ): a novel participant in the diurnal regulation of hepatic gluconeogenesis and insulin sensitivity. *PLoS Genet* 2014; **10**: e1004331 [PMID: 24831725 DOI: 10.1371/journal.pgen.1004331]

51 **Mithieux G**, Rajas F, Gautier-Stein A. A novel role for glucose 6-phosphatase in the small intestine in the control of glucose homeostasis. *J Biol Chem* 2004; **279**: 44231-44234 [PMID: 15302872 DOI: 10.1074/jbc.R400011200]

52 **Soty M**, Gautier-Stein A, Rajas F, Mithieux G. Gut-Brain Glucose Signaling in Energy Homeostasis. *Cell Metab* 2017; **25**: 1231-1242 [PMID: 28591631 DOI: 10.1016/j.cmet.2017.04.032]

53 **Gjorgjieva M**, Calderaro J, Monteillet L, Silva M, Raffin M, Brevet M, Romestaing C, Roussel D, Zucman-Rossi J, Mithieux G, Rajas F. Dietary exacerbation of metabolic stress leads to accelerated hepatic carcinogenesis in glycogen storage disease type Ia. *J Hepatol* 2018; **69**: 1074-1087 [PMID: 30193922 DOI: 10.1016/j.jhep.2018.07.017]

54 **Mutel E**, Abdul-Wahed A, Ramamonjisoa N, Stefanutti A, Houberdon I, Cavassila S, Pilleul F, Beuf O, Gautier-Stein A, Penhoat A, Mithieux G, Rajas F. Targeted deletion of liver glucose-6 phosphatase mimics glycogen storage disease type Ia including development of multiple adenomas. *J Hepatol* 2011; **54**: 529-537 [PMID: 21109326 DOI: 10.1016/j.jhep.2010.08.014]

55 **Abdul-Wahed A**, Gautier-Stein A, Casteras S, Soty M, Roussel D, Romestaing C, Guillou H, Tourette JA, Pleche N, Zitoun C, Gri B, Sardella A, Rajas F, Mithieux G. A link between hepatic glucose production and peripheral energy metabolism via hepatokines. *Mol Metab* 2014; **3**: 531-543 [PMID: 25061558 DOI: 10.1016/j.molmet.2014.05.005]

56 **Rajas F**, Dentin R, Cannella Milano A, Silva M, Raffin M, Levavasseur F, Gautier-Stein A, Postic C, Mithieux G. The absence of hepatic glucose-6 phosphatase/ChREBP couple is incompatible with survival in mice. *Mol Metab* 2021; **43**: 101108 [PMID: 33137488 DOI: 10.1016/j.molmet.2020.101108]

57 **Mehal WZ**. The Gordian Knot of dysbiosis, obesity and NAFLD. *Nat Rev Gastroenterol Hepatol* 2013; **10**: 637-644 [PMID: 23958600 DOI: 10.1038/nrgastro.2013.146]

58 **Bertola A**, Mathews S, Ki SH, Wang H, Gao B. Mouse model of chronic and binge ethanol feeding (the NIAAA model). *Nat Protoc* 2013; **8**: 627-637 [PMID: 23449255 DOI: 10.1038/nprot.2013.032]

59 **Teijeiro A**, Garrido A, Ferre A, Perna C, Djouder N. Inhibition of the IL-17A axis in adipocytes suppresses diet-induced obesity and metabolic disorders in mice. *Nat Metab* 2021; **3**: 496-512 [PMID: 33859430 DOI: 10.1038/s42255-021-00371-1]

60 **Eckel RH**, Grundy SM, Zimmet PZ. The metabolic syndrome. *Lancet* 2005; **365**: 1415-1428 [PMID: 15836891 DOI: 10.1016/S0140-6736(05)66378-7]

61 **Chouchani ET**, Kazak L, Spiegelman BM. New Advances in Adaptive Thermogenesis: UCP1 and Beyond. *Cell Metab* 2019; **29**: 27-37 [PMID: 30503034 DOI: 10.1016/j.cmet.2018.11.002]

62 **Wang C**, Niederstrasser H, Douglas PM, Lin R, Jaramillo J, Li Y, Oswald NW, Zhou A, McMillan EA, Mendiratta S, Wang Z, Zhao T, Lin Z, Luo M, Huang G, Brekken RA, Posner BA, MacMillan JB, Gao J, White MA. Small-molecule TFEB pathway agonists that ameliorate metabolic syndrome in mice and extend *C. elegans* lifespan. *Nat Commun* 2017; **8**: 2270 [PMID: 29273768 DOI: 10.1038/s41467-017-02322-3]

63 **Clapham DE**. Calcium signaling. *Cell* 2007; **131**: 1047-1058 [PMID: 18083096 DOI: 10.1016/j.cell.2007.11.028]

64 **Rader DJ**, Cohen J, Hobbs HH. Monogenic hypercholesterolemia: new insights in pathogenesis and treatment. *J Clin Invest* 2003; **111**: 1795-1803 [PMID: 12813012 DOI: 10.1172/JCI18925]

65 **Cayo MA**, Mallanna SK, Di Furio F, Jing R, Tolliver LB, Bures M, Urick A, Noto FK, Pashos EE, Greseth MD, Czarnecki M, Traktman P, Yang W, Morrissey EE, Grompe M, Rader DJ, Duncan SA. A Drug Screen using Human iPSC-Derived Hepatocyte-like Cells Reveals Cardiac Glycosides as a Potential Treatment for Hypercholesterolemia. *Cell Stem Cell* 2017; **20**: 478-489.e5 [PMID: 28388428 DOI: 10.1016/j.stem.2017.01.011]

66 **Peters A**, Lee Y, Kuchroo VK. The many faces of Th17 cells. *Curr Opin Immunol* 2011; **23**: 702-706 [PMID: 21899997 DOI: 10.1016/j.coi.2011.08.007]

67 **Saeed H**, Mateen S, Moin S, Khan AQ, Owais M. Cardiac glycoside digoxin ameliorates pro-inflammatory cytokines in PBMCs of rheumatoid arthritis patients in vitro. *Int Immunopharmacol* 2020; **82**: 106331 [PMID: 32106058 DOI: 10.1016/j.intimp.2020.106331]

68 **Madsen M**, Pedersen TX, Nielsen LB, Johansen C, Hansen PR. Differential Effects of Digoxin on Imiquimod-Induced Psoriasis-Like Skin Inflammation on the Ear and Back. *Ann Dermatol* 2018; **30**: 485-488 [PMID: 30065596 DOI: 10.5021/ad.2018.30.4.485]

69 **Patel S**, Gururani R, Jain S, Tripathi N, Paliwal S, Sharma S. Repurposing of digoxin in pain and inflammation: An evidence-based study. *Drug Dev Res* 2022; **83**: 1097-1110 [PMID: 35315525 DOI: 10.1002/ddr.21935]

70 **Imig JD**, Hammock BD. Soluble epoxide hydrolase as a therapeutic target for cardiovascular diseases. *Nat Rev Drug Discov* 2009; **8**: 794-805 [PMID: 19794443 DOI: 10.1038/nrd2875]

71 **Platz EA**, Yegnasubramanian S, Liu JO, Chong CR, Shim JS, Kenfield SA, Stampfer MJ, Willett WC, Giovannucci E, Nelson WG. A novel two-stage, transdisciplinary study identifies digoxin as a possible drug for prostate cancer treatment. *Cancer Discov* 2011; **1**: 68-77 [PMID: 22140654 DOI: 10.1158/2159-8274.CD-10-0020]

72 **Wang Z**, Zheng M, Li Z, Li R, Jia L, Xiong X, Southall N, Wang S, Xia M, Austin CP, Zheng W, Xie Z, Sun Y. Cardiac glycosides inhibit p53 synthesis by a mechanism relieved by Src or MAPK inhibition. *Cancer Res* 2009; **69**: 6556-6564 [PMID: 19679550 DOI: 10.1158/0008-5472.CAN-09-0891]

73 **Beheshti Zavareh R**, Lau KS, Hurren R, Datti A, Ashline DJ, Gronda M, Cheung P, Simpson CD, Liu W, Wasylshen AR, Boutros PC, Shi H, Vengopal A, Jurisica I, Penn LZ, Reinhold VN, Ezzat S, Wrana J, Rose DR, Schachter H, Dennis JW, Schimmer AD. Inhibition of the sodium/potassium ATPase impairs N-glycan expression and function. *Cancer Res* 2008; **68**: 6688-6697 [PMID: 18701493 DOI: 10.1158/0008-5472.CAN-07-6833]

74 **Raynal NJ**, Lee JT, Wang Y, Beaudry A, Madireddi P, Garriga J, Malouf GG, Dumont S, Dettman EJ, Gharibyan V, Ahmed S, Chung W, Chilvers WE, Abou-Gharbia M, Henry RA, Andrews AJ, Jelinek J, Cui Y, Baylin SB, Gill DL, Issa JP. Targeting Calcium Signaling Induces Epigenetic Reactivation of Tumor Suppressor Genes in Cancer. *Cancer Res* 2016; **76**: 1494-1505 [PMID: 26719529 DOI: 10.1158/0008-5472.CAN-14-2391]

75 **Lin SY**, Chang HH, Lai YH, Lin CH, Chen MH, Chang GC, Tsai MF, Chen JJ. Digoxin Suppresses Tumor Malignancy through Inhibiting Multiple Src-Related Signaling Pathways in Non-Small Cell Lung Cancer. *PLoS One* 2015; **10**: e0123305 [PMID: 25955608 DOI: 10.1371/journal.pone.0123305]

76 **Lee DH**, Lee CS, Kim DW, Ae JE, Lee TH. Digitoxin sensitizes glioma cells to TRAIL-mediated apoptosis by upregulation of death receptor 5 and downregulation of survivin. *Anticancer Drugs* 2014; **25**: 44-52 [PMID: 24045365 DOI: 10.1097/CAD.0000000000000015]

77 **Eskiocak U**, Ramesh V, Gill JG, Zhao Z, Yuan SW, Wang M, Vandergriff T, Shackleton M, Quintana E, Frankel AE, Johnson TM, DeBerardinis RJ, Morrison SJ. Erratum: Synergistic effects of ion transporter and MAP kinase pathway inhibitors in melanoma. *Nat Commun* 2016; **7**: 13080 [PMID: 27681157 DOI: 10.1038/ncomms13080]

78 **Muranski P**, Boni A, Antony PA, Cassard L, Irvine KR, Kaiser A, Paulos CM, Palmer DC, Touloudian CE, Ptak K, Gattinoni L, Wrzesinski C, Hinrichs CS, Kerstann KW, Feigenbaum L, Chan CC, Restifo NP. Tumor-specific Th17-polarized cells eradicate large established melanoma. *Blood* 2008; **112**: 362-373 [PMID: 18354038 DOI: 10.1182/blood-2007-11-120998]

79 **Eskiocak U**, Ramesh V, Gill JG, Zhao Z, Yuan SW, Wang M, Vandergriff T, Shackleton M, Quintana E, Johnson TM, DeBerardinis RJ, Morrison SJ. Synergistic effects of ion transporter and MAP kinase pathway inhibitors in melanoma. *Nat Commun* 2016; **7**: 12336 [PMID: 27545456 DOI: 10.1038/ncomms12336]

80 **Amarelle L**, Lecuona E. The Antiviral Effects of Na,K-ATPase Inhibition: A Minireview. *Int J Mol Sci* 2018; **19** [PMID: 30042322 DOI: 10.3390/ijms19082154]

81 **Cho J**, Lee YJ, Kim JH, Kim SI, Kim SS, Choi BS, Choi JH. Antiviral activity of digoxin and ouabain against SARS-CoV-2 infection and its implication for COVID-19. *Sci Rep* 2020; **10**: 16200 [PMID: 33004837 DOI: 10.1038/s41598-020-72879-7]

82 **Norris MJ**, Malhi M, Duan W, Ouyang H, Granados A, Cen Y, Tseng YC, Gubbay J, Maynes J, Moraes TJ. Targeting Intracellular Ion Homeostasis for the Control of Respiratory Syncytial Virus. *Am J Respir Cell Mol Biol* 2018; **59**: 733-744 [PMID: 30095982 DOI: 10.1165/rccm.2017-0345OC]

83 **Bailey ES**, Fieldhouse JK, Choi JY, Gray GC. A Mini Review of the Zoonotic Threat Potential of Influenza Viruses, Coronaviruses, Adenoviruses, and Enteroviruses. *Front Public Health* 2018; **6**: 104 [PMID: 29686984 DOI: 10.3389/fpubh.2018.00104]

84 **Pollard BS**, BLANCOI JC, Pollard JR. Classical Drug Digitoxin Inhibits Influenza Cytokine Storm, With Implications for Covid-19 Therapy. *In Vivo* 2020; **34**: 3723-3730 [PMID: 33144490 DOI: 10.21873/invivo.12221]

85 **Kapoor A**, Cai H, Forman M, He R, Shamay M, Arav-Boger R. Human cytomegalovirus inhibition by cardiac glycosides: evidence for involvement of the HERG gene. *Antimicrob Agents Chemother* 2012; **56**: 4891-4899 [PMID: 2277050 DOI: 10.1128/AAC.00898-12]

86 **Hartley C**, Hartley M, Pardoe I, Knight A. Ionic Contra-Viral Therapy (ICVT); a new approach to the treatment of DNA virus infections. *Arch Virol* 2006; **151**: 2495-2501 [PMID: 16932984 DOI: 10.1007/s00705-006-0824-x]

87 **Rijsbergen M**, Niemeyer-van der Kolk T, Hogendoorn G, Kouwenhoven S, Lemoine C, Klaassen ES, de Koning M, Beck S, Bouwes Bavinck JN, Feiss G, Burggraaf J, Rissmann R. A randomized controlled proof-of-concept trial of digoxin and furosemide in adults with cutaneous warts. *Br J Dermatol* 2019; **180**: 1058-1068 [PMID: 30580460 DOI: 10.1111/bjd.17583]

88 **Bruggink SC**, de Koning MN, Gussekloo J, Egberts PF, Ter Schegget J, Feltkamp MC, Bavinck JN, Quint WG, Assendelft WJ, Eekhof JA. Cutaneous wart-associated HPV types: prevalence and relation with patient characteristics. *J Clin Virol* 2012; **55**: 250-255 [PMID: 22884670 DOI: 10.1016/j.jcv.2012.07.014]

89 **van der Kolk T**, Dillingh MR, Rijneveld R, Klaassen ES, de Koning MNC, Kouwenhoven STP, Genders RE, Bouwes Bavinck JN, Feiss G, Rissmann R, Burggraaf J. Topical ionic contra-viral therapy comprised of digoxin and furosemide as

a potential novel treatment approach for common warts. *J Eur Acad Dermatol Venereol* 2017; **31**: 2088-2090 [PMID: 28833595 DOI: 10.1111/jdv.14527]

90 **Laird GM**, Eisele EE, Rabi SA, Nikolaeva D, Siliciano RF. A novel cell-based high-throughput screen for inhibitors of HIV-1 gene expression and budding identifies the cardiac glycosides. *J Antimicrob Chemother* 2014; **69**: 988-994 [PMID: 24275119 DOI: 10.1093/jac/dkt471]

91 **Wong RW**, Balachandran A, Ostrowski MA, Cochrane A. Digoxin suppresses HIV-1 replication by altering viral RNA processing. *PLoS Pathog* 2013; **9**: e1003241 [PMID: 23555254 DOI: 10.1371/journal.ppat.1003241]

92 **Holbrook JA**, Neu-Yilik G, Hentze MW, Kulozik AE. Nonsense-mediated decay approaches the clinic. *Nat Genet* 2004; **36**: 801-808 [PMID: 15284851 DOI: 10.1038/ng1403]

93 **Kuzmiak HA**, Maquat LE. Applying nonsense-mediated mRNA decay research to the clinic: progress and challenges. *Trends Mol Med* 2006; **12**: 306-316 [PMID: 16782405 DOI: 10.1016/j.molmed.2006.05.005]

94 **Nickless A**, Jackson E, Marasa J, Nugent P, Mercer RW, Piwnica-Worms D, You Z. Intracellular calcium regulates nonsense-mediated mRNA decay. *Nat Med* 2014; **20**: 961-966 [PMID: 25064126 DOI: 10.1038/nm.3620]

95 **Prassas I**, Diamandis EP. Novel therapeutic applications of cardiac glycosides. *Nat Rev Drug Discov* 2008; **7**: 926-935 [PMID: 18948999 DOI: 10.1038/nrd2682]

96 **Bejček J**, Spiwok V, Kmoníčková E, Rimpelová S. Na(+)/K(+) ATPase Revisited: On Its Mechanism of Action, Role in Cancer, and Activity Modulation. *Molecules* 2021; **26** [PMID: 33800655 DOI: 10.3390/molecules26071905]

Autoimmune liver diseases and SARS-CoV-2

Costantino Sgamato, Alba Rocco, Debora Compare, Stefano Minieri, Stefano Andrea Marchitto, Simone Maurea, Gerardo Nardone

Specialty type: Gastroenterology and hepatology

Provenance and peer review:
Invited article; Externally peer reviewed.

Peer-review model: Single blind

Peer-review report's scientific quality classification

Grade A (Excellent): A

Grade B (Very good): B

Grade C (Good): 0

Grade D (Fair): 0

Grade E (Poor): 0

P-Reviewer: Chen S, China;
Popovic DD, Serbia

Received: November 20, 2022

Peer-review started: November 20, 2022

First decision: January 2, 2023

Revised: January 12, 2023

Accepted: March 14, 2023

Article in press: March 14, 2023

Published online: March 28, 2023



Costantino Sgamato, Alba Rocco, Debora Compare, Stefano Minieri, Stefano Andrea Marchitto, Gerardo Nardone, Department of Clinical Medicine and Surgery, University of Naples Federico II, Naples 80131, Italy

Simone Maurea, Department of Advanced Biomedical Sciences, University of Naples Federico II, Naples 80131, Italy

Corresponding author: Alba Rocco, PhD, Doctor, Department of Clinical Medicine and Surgery, University of Naples Federico II, Via S. Pansini, 5, Naples 80131, Italy.
a.rocco@unina.it

Abstract

Severe acute respiratory syndrome coronavirus 2 (SARS-CoV-2), causing coronavirus disease 2019 (COVID-19), can trigger autoimmunity in genetically predisposed individuals through hyperstimulation of immune response and molecular mimicry. Here we summarise the current knowledge about autoimmune liver diseases (AILDs) and SARS-CoV-2, focusing on: (1) The risk of SARS-CoV-2 infection and the course of COVID-19 in patients affected by AILDs; (2) the role of SARS-CoV-2 in inducing liver damage and triggering AILDs; and (3) the ability of vaccines against SARS-CoV-2 to induce autoimmune responses in the liver. Data derived from the literature suggest that patients with AILDs do not carry an increased risk of SARS-CoV-2 infection but may develop a more severe course of COVID-19 if on treatment with steroids or thiopurine. Although SARS-CoV-2 infection can lead to the development of several autoimmune diseases, few reports correlate it to the appearance of *de novo* manifestation of immune-mediated liver diseases such as autoimmune hepatitis (AIH), primary biliary cholangitis (PBC) or AIH/PBC overlap syndrome. Different case series of an AIH-like syndrome with a good prognosis after SARS-CoV-2 vaccination have been described. Although the causal link between SARS-CoV-2 vaccines and AIH cannot be definitively established, these reports suggest that this association could be more than coincidental.

Key Words: Autoimmune liver disease; SARS-CoV-2; COVID-19; COVID-19 vaccine; Autoimmune hepatitis

©The Author(s) 2023. Published by Baishideng Publishing Group Inc. All rights reserved.

Core Tip: Severe acute respiratory syndrome coronavirus 2 (SARS-CoV-2) has emerged as a possible trigger of autoimmunity. Patients with autoimmune liver diseases (AILDs) were considered at higher risk of SARS-CoV-2 infection and more susceptible to severe coronavirus disease 2019 (COVID-19) due to genetic background and immunosuppressive treatments. Case reports documenting autoimmune hepatitis-like syndromes after the COVID vaccine started to emerge, raising worries about a possible risk of unwanted immunological side effects, especially in individuals predisposed to autoimmune disorders. We herein discuss the consequences of SARS-CoV-2 infection in patients with AILDs and the role of the vaccines in inducing liver autoimmunity.

Citation: Sgamato C, Rocco A, Compare D, Minieri S, Marchitto SA, Maurea S, Nardone G. Autoimmune liver diseases and SARS-CoV-2. *World J Gastroenterol* 2023; 29(12): 1838-1851

URL: <https://www.wjgnet.com/1007-9327/full/v29/i12/1838.htm>

DOI: <https://dx.doi.org/10.3748/wjg.v29.i12.1838>

INTRODUCTION

The severe acute respiratory syndrome coronavirus 2 (SARS-CoV-2) is a single-stranded RNA, enveloped, beta coronavirus causing coronavirus disease 2019 (COVID-19), which has developed into a pandemic infection in a short time since its first appearance in Wuhan, China, in December 2019[1,2]. Since then, SARS-CoV-2 has caused more than 620 million infections, with a death toll exceeding 6.5 million as of October 31, 2022, according to the World Health Organization. Although the most common presentation of COVID-19 includes respiratory symptoms such as dry cough and shortness of breath[3], gastrointestinal symptoms, including diarrhoea, anorexia, nausea and or vomiting, and abdominal pain, have been variably reported in up to half of the cases[4,5]. Furthermore, elevated aspartate aminotransferase (AST) and alanine aminotransferase (ALT), hallmarks of liver injury, have been widely recognised as major components of COVID-19[6]. Tissue injury is almost certainly multifactorial and related to several mechanisms, such as direct hepatocellular lesions, immune-mediated liver damage due to the severe inflammatory response, or development of endotheliopathy with hypoxic or ischaemic injury[7-9].

Furthermore, SARS-CoV-2 has also been identified as an instrumental trigger of autoimmunity. Hyper-stimulation of the immune system or molecular mimicry of the virus with human self-components may lead to the synthesis of multiple autoantibodies that could initiate autoimmune diseases in genetically predisposed individuals[10,11].

In this review, we summarised the current knowledge regarding the risk of SARS-CoV-2 infection and the course of COVID-19 in patients with autoimmune liver diseases (AILDs), as well as the role of SARS-CoV-2 in inducing *de novo* AILDs. Finally, since various case reports documenting autoimmune hepatitis (AIH)-like syndromes after receiving the COVID-19 vaccine started to emerge, we reviewed the literature to analyse the role of vaccines in inducing autoimmune responses in the liver.

SARS-COV-2 AND PRE-EXISTING AILDs

AILDs are a heterogeneous group of inflammatory liver disorders mediated by autoimmunity, including AIH, primary biliary cholangitis (PBC), primary sclerosing cholangitis (PSC), and overlapping syndromes. Patients with AILDs could theoretically present an increased risk of SARS-CoV-2 infections and poor outcomes due to lifelong immunosuppressive treatments taken to delay the progression to cirrhosis and liver failure.

However, the clinical impact of SARS-CoV-2 infection on the population with AILDs remains unclear. Preliminary data derived from regional observational studies driven by referral centres suggested that patients with AILDs did not carry a specific risk of becoming infected by SARS-CoV-2. In the earliest reports from Northern Italy, an area particularly affected by the virus's spread, the observed incidence of the infection in a cohort of 148 AILDs patients (133 AIH, 11 autoimmune sclerosing cholangitis, 2 PSC/AIH and 2 PBC/AIH) did not significantly differ from that estimated in the general population (43 vs 38 cases, respectively)[12]. Similarly, Verhelst *et al*[13] found a very limited SARS-CoV-2 infection ratio (1.2%) in a Belgian cohort of 110 patients with AIH[13]. More recently, a survey involving 1779 AILDs patients from 20 European countries detected a rate of COVID-19 (2.2%) equivalent to the period prevalence of the general population, thus indicating that patients with AILDs are not at elevated risk of developing COVID disease[14]. Interestingly, people suffering from autoimmune diseases do not have a higher risk of being positive for COVID-19, as indicated by a study performed in Milan that applied both a test-negative [odds ratio (OR): 0.86, 95% confidence interval (CI): 0.76–0.96] and population (OR: 0.98, 95%CI: 0.90–1.08) case-control design[15].

Regarding the impact of AILDs on the COVID-19 course, early phone-based surveys including patients with AIH ($n = 73$) and PBC ($n = 68$) found a rate of infection of 3.6% with a favourable outcome of COVID-19 in most cases[16]. Likewise, patients under immunosuppressive treatment for AIH show a disease course probably comparable to that reported in the non-immunosuppressed population[17]. Data combined from 3 large-scale international reporting registries, namely the European Association for the Study of the Liver supported COVID-Hep registry, the European Reference Network on Hepatological Diseases (ERN RARE-LIVER) and the American Association for the Study of Liver Diseases supported SECURE-cirrhosis registry, showed that patients with AIH, despite immunosuppressive treatment, did not present an increased risk of adverse outcomes including hospitalisation (76% vs 85%; $P = 0.06$), admission in an intensive care unit (29% vs 23%; $P = 0.240$), or death (23% vs 20%; $P = 0.643$) when compared to other causes of chronic liver disease and matched cases without the liver disease [18]. Another retrospective study collecting data on 110 patients with AIH and COVID-19 from 34 centres in Europe and the Americas confirmed that AIH was not a risk factor for severe COVID-19 (15.5% vs 20.2%, $P = 0.231$) and all-cause mortality (10% vs 11.5%, $P = 0.852$) than other causes of chronic liver disease. Still, continued immunosuppression during COVID-19 was associated with a lower rate of liver injury ($P = 0.009$; OR: 0.26; 95%CI: 0.09-0.71)[19]. However, in another study including 254 AIH patients, the same author observed that the use of systemic glucocorticoids (adjusted OR: 4.73, 95%CI: 1.12-25.89) and thiopurine (adjusted OR: 4.78, 95%CI: 1.33-23.50) was associated with worse COVID-19 outcome compared to patients who were not on immunosuppressive therapy[20].

These results might aid medical decisions when dealing with SARS-CoV-2 infection in immunocompromised patients. Although current expert recommendations advocate against changes in immunosuppressive treatments in patients with AIH before and after SARS-CoV-2 infection[21], data derived from larger case series support the notion of maintaining remission with the lowest effective glucocorticoid dose in AIH patients during the COVID-19 pandemic.

Nonetheless, it should be considered that cirrhotic patients, irrespective of the cirrhosis aetiology, once infected with SARS-CoV-2, are more vulnerable than the general population or patients without cirrhosis. Indeed, they have a higher risk of decompensation of liver disease and developing a more severe COVID-19 with a mortality rate of up to 30%[22,23].

SARS-COV-2 AS A TRIGGER OF AILDs

Increasing evidence indicates that SARS-CoV-2 may have a trigger effect of, possibly pre-existing, autoimmune disease, including Guillain-Barré syndrome, systemic lupus erythematosus, myasthenia gravis, large vessel vasculitis and thrombosis, Graves' disease, sarcoidosis and inflammatory arthritis [24].

It is well-known that SARS-CoV-2 infection can result in hyperstimulation of the immune system, with increased serum concentration of pro-inflammatory cytokines, particularly monocyte chemoattractant protein 1, interferon-inducible protein-10, interleukin (IL)-6, IL-1 β , IL-8, IL-10, IL-17, tumour necrosis factor, granulocyte-macrophage colony-stimulating factor, also referred to as "cytokine storm" or "cytokine release syndrome"[25]. In addition, due to structural homology between some components of SARS-CoV-2 and human proteins[11], the immune responses raised against the virus can cross-react with self-proteins, a concept commonly termed molecular mimicry[26]. These factors may contribute to the development of multiple autoantibodies with a trigger effect on autoimmunity (Figure 1).

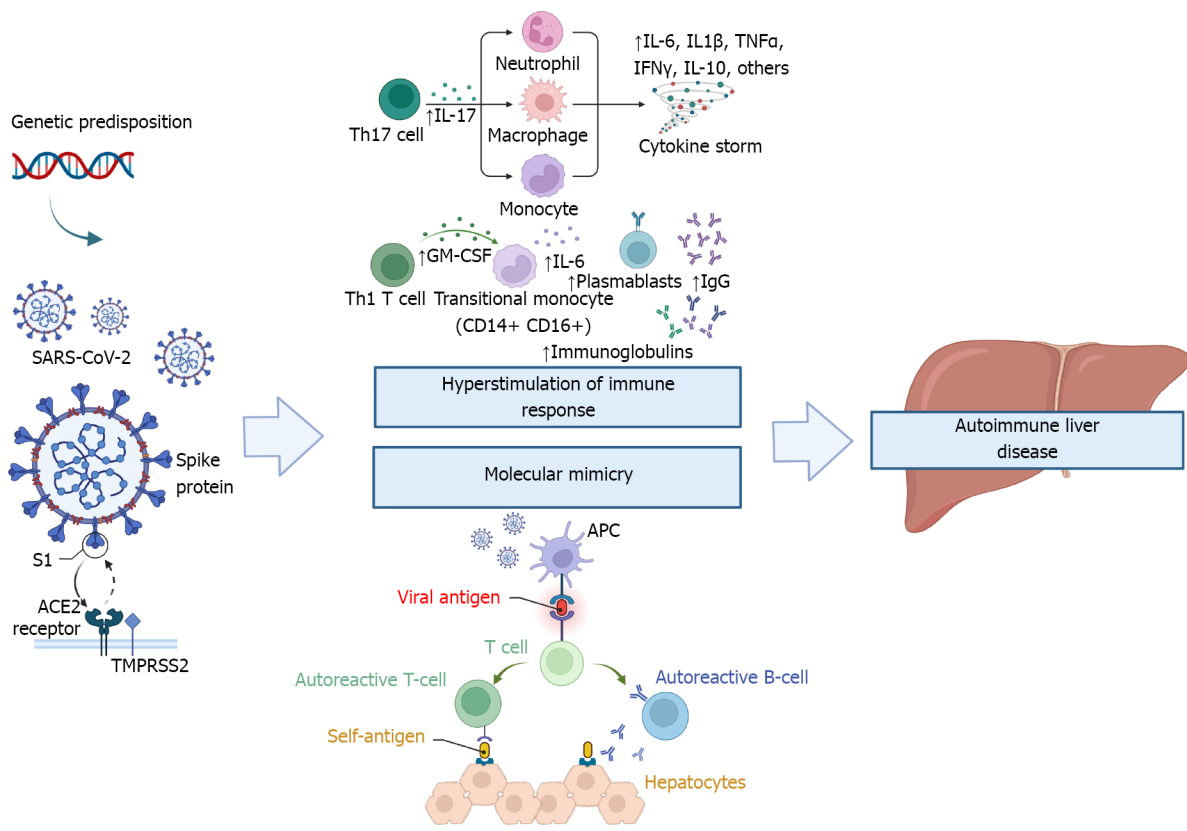
In patients with SARS-CoV-2 infection and especially severely ill patients compared with those with mild or moderate disease, numerous autoantibodies, including antinuclear antibodies (ANA), anti-neutrophil cytoplasmic antibodies, antiphospholipid antibodies, have been detected[27,28]. Since systemic autoimmunity is known to initiate from generalised polyclonal B cell activation, the presence of autoantibodies in such kinds of patients may indicate a pre-AID[29].

However, interestingly, there have been very few reports suggesting that SARS-CoV-2 infection might reflect 'a final hit' leading to de novo manifestation of immune-mediated liver diseases such as PBC[30] or AIH/PBC overlap syndrome[31].

PBC developed concomitantly with Guillain-Barré syndrome following SARS-CoV-2 infection in a 44-year-old obese and hypertensive woman already suffering from Hashimoto's thyroiditis. During her hospitalisation for severe bilateral interstitial pneumonia, she developed an important rise in serum gamma-glutamyl-transferase (GGT) with initially normal alkaline phosphatase (ALP) levels that progressively increased later.

As a result of the ALP increase combined with high-titre anti-mitochondrial (AMA) positivity (1:640), the patient underwent a liver biopsy showing histological findings consistent with an initial phase (stage I in Scheuer and Ludwig classifications) of PBC.

A case of AIH/PBC overlap syndrome has been described in a 57-year-old man suffering from hypertension, beta-thalassemia minor, and diabetes. He developed arthralgias, elevated liver enzymes and hyper hyperferritinemia one month after recovering from moderate COVID-19 disease. Although a liver biopsy was not performed, the patient presented a concomitant seropositivity for AMA and anti-double-stranded DNA antibodies (anti-ds DNA) that can be considered the serological profile of AIH/



DOI: 10.3748/wjg.v29.i12.1838 Copyright ©The Author(s) 2023.

Figure 1 The severe acute respiratory syndrome coronavirus 2 infection may lead to autoimmune liver disease through hyperstimulation of the immune system and molecular mimicry with human self-components. S1: Spike protein subunit 1; ACE2: Angiotensin-converting enzyme 2; TMPRSS2: Transmembrane Serine Protease 2; TH: T helper cells; IL: Interleukin; TNF- α : Tumour necrosis factor alfa; IFN γ : Interferon-gamma; APC: Antigen-presenting cell; GM-CSF: Granulocyte-macrophage colony-stimulating factor; IgG: Immunoglobulin G; SARS-CoV-2: Severe acute respiratory syndrome coronavirus 2.

PBC[32].

On the other hand, liver involvement has been frequently reported in COVID-19. Abnormal liver function test, mainly elevated ALT, hypoalbuminemia, and elevated GGT, has been described in 14.8-53% of SARS-CoV-2 infected patients and up to 78% of those with severe manifestations of COVID-19 disease[8] being independent risk factors for adverse clinical outcomes such as intensive care unit admission, use of invasive mechanical ventilation or longer hospital stay[33].

The pathogenic mechanisms of liver injury during COVID-19 are not fully understood. SARS-CoV-2 cell entry is mediated by the interaction of the virus's spike (S) protein with the host angiotensin-converting enzyme 2 receptor (ACE2). S protein is then cleaved by the transmembrane serine protease 2, allowing the internalisation by endocytosis and the release of the viral genome from the endosome[10]. The liver is a possible target for SARS-CoV-2 due to a high expression, almost in the same percentage of type 2 pneumocytes, of ACE2 receptors in cholangiocytes and, to a lesser extent, hepatocytes[34].

However, rather than direct cytotoxicity derived from active viral replication of SARS-CoV-2 in the liver, current data suggest that tissue injury is likely due to immune dysregulation or cytokine storm and development of endotheliopathy and microthromboses with hypoxic or ischaemic injury[35,36]. Exacerbation of underlying liver disease or drug-induced liver injury can also contribute[37,38].

AILDS FOLLOWING SARS-COV-2 VACCINES

Given the dramatic socio-economical effect of the pandemic, vaccines against SARS-CoV-2 have been rapidly developed. In December 2020, two mRNA vaccines (BNT 162b2 Pfizer-BioNTech[39] and mRNA-1273 Moderna[40]) and one adenovirus (ADV) vector-based vaccine (ChAdOx1 nCOV-19 Oxford University/Astra Zeneca)[41] obtained approval under Emergency Use Listing from the most important drug regulatory agencies. As of October 31, 2022, approximately 68% of the global population has received at least one dose of the anti-SARS-CoV-2 vaccine, with 12.9 billion doses being administered worldwide[42].

Both the mRNA and ADV vaccines encode the intracellular production of the SARS-CoV-2 spike protein, the primary target for neutralising antibodies generated from natural infection and triggering both innate and adaptive responses. *Via* their recognition by innate intracellular sensors, including toll-like receptors 3, 7, 9 and inflammasome components, vaccines stimulate innate immunity through cellular activation and consequent release of interferon I or other pro-inflammatory cytokines, thus promoting differentiation of CD4+ and CD8+ T cells into effector and memory subsets[43].

Although the safety profiles of all vaccines have been extensively studied in large placebo-controlled trials, after their widespread diffusion, case reports and case series describing a range of liver diseases following COVID-19 vaccination started to emerge[44].

In the summer of 2021, Bril *et al*[45] first described an AIH-like syndrome developed after vaccination against SARS-CoV-2[45]. AIH is an inflammatory disease of the liver characterised by circulating autoantibodies, mainly ANA, elevated serum globulin levels, specific histological alterations and response to immunosuppressive therapy. The clinical picture is non-specific and varies among patients, ranging from asymptomatic liver enzyme elevation to acute liver failure[46]. SARS-CoV-2 vaccination has also been linked to other forms of immune-mediated liver injury, such as AIH-PBC overlap syndrome[47] or a specific CD8+ T-cell-dominant hepatitis[48].

Cases of *de novo* AIH or vaccine-induced AIH relapse after vaccination against SARS-CoV-2 are reported in Table 1[45,49-78]. A summary of patient information and disease presentation is shown in Table 2. Laboratory data, treatment, and outcome are reported in Table 3.

Most patients (83%) were female, with a mean age of 58.7 years (range 27-82). In 25 patients, race and ethnicity were not specified, whereas, among the remaining cases, 11 patients were Caucasian, three were Asian, and 1 was Arabic. Seventeen patients (42.5%) had a history of either liver (6) or autoimmune disease (11). One patient was three months postpartum[45].

Although five patients were taking potentially hepatotoxic medication, including substitutive hormonal therapy[62], statin[49,58,76,77], azathioprine[51,76], pegylated interferon for polycythaemia vera[53] and nitrofurantoin[73], each patient had been taking their medications for a long time without recent regimens changes. The patient who reported nitrofurantoin completed a three-day course nearly 90 d before the vaccine, and thus nitrofurantoin-induced liver injury was considered highly improbable. Two patients[63,73] took acetaminophen soon after receiving the first dose, whereas one patient[78] was on chronic treatment. The trigger vaccine was Pfizer-BioNTech in 17 cases (43%), Moderna in 11 (28%), Oxford AstraZeneca in 10 (20%), while CoronaVac, an inactivated whole-virion vaccine, was the trigger of AIH in two cases (5%).

Symptomatic AIH was observed in most cases (78%), with a latency time after receiving the COVID-19 vaccine of about two weeks (16.6 ± 12.8 d, range 2-60). The most common symptoms were jaundice (60%), asthenia/fatigue (33%), chouria (25%) and pruritus (20%), whereas other symptoms such as fever, abdominal pain, nausea, and vomiting were variably reported. Interestingly, two patients presented worsening symptoms after receiving the second dose[62,68]. At the laboratory, most cases showed a hepatocellular pattern of liver injury, with markedly elevated transaminases (mean values of AST and ALT of 936 ± 521 U/L and 1060 ± 567 U/L, respectively). Mean GGT, ALP, and bilirubin were 312 ± 220 U/L, 209 ± 95 U/L, and 9.8 ± 8.5 mg/dL, respectively. Immunoglobulin G was > 20 g/L in 13 patients (46.5%) with a mean value of 21.7 g/L. Thirty-seven patients (93%) had at least one positive autoantibody, and ANA was positive in 33 (83%). The scoring systems, such as the Simplified AIH score [79] and the Revised Original Score[80], guided the diagnosis of AIH in 18 cases. A liver biopsy was performed in almost all cases (98%). Findings were typical with AIH in 3 patients and compatible with AIH in 31 cases.

Steroids were used as a first-line treatment in 38 patients (95%), and azathioprine was used as a second agent in 8 patients. The mean time to the first improvement and disease resolution were 4.6 and 45.9 d, respectively. Improvement in laboratory data or complete resolution was seen in 37 out of 40 patients (93%). Three patients died of AIH triggered by viral vector vaccine (AstraZeneca), one after refusing liver transplantation[66], while the other two died of liver failure and sepsis[52,76].

Notably, vaccine-induced AIH has been previously described following other vaccinations than that against SARS-CoV-2, such as hepatitis A[81,82] or influenza virus[83,84].

Although the precise mechanisms have not been elucidated, molecular mimicry is one of the major explanations of autoimmunity after vaccination. Significant homology of amino acid sequences between determinants of vaccines and self-antigen may result in the synthesis of anti-spike antibodies that cross-react with structurally similar host peptide proteins[85]. Other proposed mechanisms include bystander activation (defined as an intense stimulation of innate immunity after administration of adjuvants) and epitope spreading (immune responses to endogenous epitopes resulting from the release of self-antigens during chronic autoimmune/inflammatory processes)[86].

Cases of AIH reactivation after vaccines underline the necessity for close follow-up in individuals with a pre-existing diagnosis of AILDs.

Current knowledge does not allow us to clearly define whether these cases represent a true AIH triggered by vaccine or transient vaccine-induced liver injury, which could have similar clinical, laboratory and histological characteristics.

Table 1 Cases of autoimmune hepatitis-like syndromes after the coronavirus disease 2019 vaccine

Ref.	Sex, age	Comorbidity	Vaccine	Time onset after vaccination	Symptoms	Antibodies	Histology	Treatment	Outcome
Bril et al[45]	F, 35	None	Pfizer-BioNTech	7 d after dose I	Jaundice, pruritus, cholangitis	ANA, anti-Ds-DNA	Compatible with AIH	Prednisone	Remission
Ghielmetti et al[49]	M, 63	Type II diabetes, ischemic heart disease	Moderna	7 d after dose I	Jaundice, fatigue, anorexia	ANA	Typical for AIH	Prednisone	Remission
Avci and Abasiyanik [50]	F, 61	Hashimoto thyroiditis, hypertension	Pfizer-BioNTech	30 d after dose I	Jaundice, malaise, fatigue, anorexia	ANA, ASMA	Compatible with AIH	Prednisone + AZA	Remission
Mahalingham et al[51]	F, 32	OLT post-AIH, hypertension	Pfizer-BioNTech	21 d after dose III	/	SLA/LP	Compatible with AIH	Methylprednisolone	Remission
Erard et al[52]	F, 80		Pfizer-BioNTech	10 d after dose II	All asthenia, pruritus, jaundice	ANA	Compatible with AIH	Steroids	Remission
	F, 73		Moderna	21 d after dose I		ANA		Steroids	Remission
	F, 68		AstraZeneca	20 d after dose I		ANA, ASMA		Listing for liver transplantation	Death after 3 d
Garrido et al [53]	F, 65	Polycythaemia Vera	Moderna	14 d after dose I	Abdominal pain, jaundice, pruritus, acholia, cholangitis	ANA	Compatible with AIH	Prednisolone	Remission
Goulas et al [54]	F, 52	/	Moderna	14 d after dose I	Malaise, jaundice	ANA, ASMA		Prednisolone + AZA	Remission
Cao et al[55]	F, 57	AIH	CoronaVac	14 d after dose I	Cholangitis, acholia, jaundice	ANA	Compatible with AIH	Methylprednisolone + AZA + UDCA	Remission
Vuille-Lessard et al [56]	F, 76	Hashimoto thyroiditis, urothelial ca.	Moderna	3 d after dose I	Cholangitis, fatigue, jaundice	ANA, ASMA, ANCA	Typical for AIH	Prednisolone + AZA	Remission
Suzuki et al [57]	F, 80	GERD	Pfizer-BioNTech	10 d after dose II	Jaundice	ANA	Compatible with AIH	Prednisone	Remission
	F, 75	Dyslipidemia	Pfizer-BioNTech	4 d after dose II	Cholangitis	ANA, AMA		Prednisone	Remission
	F, 78	Primary biliary cholangitis	Pfizer-BioNTech	7 d after dose I	Fever, malaise	ANA, AMA		Prednisone	Remission
Tan et al[58]	F, 56	/	Moderna	42 d after dose I	Jaundice, malaise, anorexia	ANA, AMA	Compatible with AIH	Budenoside	Remission
Zhou et al[59]	F, 36	Primary sclerosing cholangitis, ulcerative colitis	Moderna	11 d after dose I	/	ANA, Ds-DNA	Compatible with AIH	Prednisone + Azathioprine	Remission
Kang et al[60]	F, 27	/	Pfizer-BioNTech	8 d after dose II	Nausea, vomiting, headache, fever, dark urine	ANA	Compatible with AIH	Prednisolone	Remission
Rocco et al [61]	F, 80	Hashimoto thyroiditis Glomerulonephritis	Pfizer-BioNTech	7 d after dose II	Jaundice	ANA	Typical for AIH	Prednisone	Remission
Londoño et al [62]	F, 41	Premature ovarian failure	Moderna	7 d after dose II	Cholangitis, jaundice, epigastric pain, nausea, and vomiting	ANA, AMA, SLA/LP	Typical for AIH	Prednisone	Remission
McShane et al	F, 71	/	Moderna	4 d after	Jaundice	ASMA	Compatible	Prednisolone	Remission

[63]	dose I					with AIH			
Clayton-Chubb et al [64]	M, 36	Hypertension	AstraZeneca	26 d after dose I	Fever	ANA	Compatible with AIH	Prednisolone	Remission
Palla et al [65]	F, 40	Sarcoidosis	Pfizer-BioNTech	30 d after dose II	/	ANA	Compatible with AIH	Prednisolone	Remission
Rela et al [66]	F, 38	Hypothyroidism	AstraZeneca	20 d after dose I	Jaundice, fever, fatigue	ANA	Compatible with AIH	Prednisolone	Remission
	M, 62	Diabetes	AstraZeneca	16 d after dose I	Anorexia, fever, / jaundice			Prednisolone	Death after 3 wk
Camacho-Domínguez et al [67]	M, 79	/	AstraZeneca	15 d after dose I	Abdominal pain, pruritus, acholia, choluria	ANA, ASMA	Compatible with AIH	Hydrocortisone; Prednisone; Prednisolone	Remission
Zin Tun et al [68]	M, 47	/	Moderna	3 d after dose I and 3 d after dose II	Malaise, jaundice	ANA	Compatible with AIH	Prednisolone	Remission
Torrente et al [69]	F, 46	Hypothyroidism	AstraZeneca	21 d after dose I	/	ANA	Compatible with AIH	Prednisone + AZA	Remission
Fimiano et al [70]	F, 63	Hypothyroidism	Pfizer-BioNTech	54 d after dose III	Abdominal pain, nausea, jaundice, choluria	-	Compatible with AIH	Methylprednisolone + AZA	Remission
Izagirre et al [71]	M, 72	Ischemic heart disease, 30 gr/day alcohol consumption	Pfizer-BioNTech	46 d after dose II	/	ANA	Compatible with AIH	Prednisone+ Azathioprine	Remission
	F, 62	Celiac disease	AstraZeneca	4 d after dose II	/	ANA		Prednisone+ AZA	Remission
	F, 72	/	Pfizer-BioNTech	14 d after dose II	/	ANA		Prednisone	Remission
	F, 59	Hypothyroidism	Pfizer-BioNTech	9 d after dose I	/	ANA	Not performed	No treatment received	Spontaneous improvement
Hasegawa et al [72]	F, 82	Hepatitis C virus	Pfizer-BioNTech	7 d after dose I	Malaise	ANA	Compatible with AIH	Prednisone	Remission
Shroff et al [73]	F, 59	/	Moderna	31 d after dose I	/	ANA	Compatible with AIH	Steroids	Remission
Efe et al [74]	M, 53	/	Pfizer-BioNTech	30 d after dose II	Abdominal pain, pruritus, erythematous skin eruption	/	Compatible with AIH	Prednisolone	Developed HE and liver transplantation
Shahrani et al [75]	F, 59	Dyslipidemia	AstraZeneca	12 d after dose II	Jaundice	/	Compatible with AIH	Prednisolone	Remission
	F, 72	/	Pfizer-BioNTech	10 d after booster	Jaundice	AMA	Compatible with AIH	Prednisolone	Remission
Nik et al [76]	F, 63	Primary sclerosing cholangitis, ulcerative colitis	AstraZeneca	14 d after dose I	Jaundice, pruritus	ANA	Compatible with AIH	Prednisolone	Death after 2 wk for sepsis
Mekrithikrai et al [77]	F, 52	Dyslipidemia, hypertension	Coronavac	After dose II	Jaundice	ANA, ASMA	Compatible with AIH	Prednisolone + AZA	Remission
Mathew et al [78]	F, late 20s	Headache	AstraZeneca	10 d after dose I	Jaundice	ANA	Compatible with AIH	Prednisolone	Remission

ANA: Antinuclear antibody; anti-Ds-DNA: Anti-double stranded DNA; AIH: Autoimmune hepatitis; ASMA: Anti-smooth muscle antibody; AZA: Azathioprine; OLT: Orthotopic liver transplantation; SLA/LP: Anti-soluble liver antigen/liver-pancreas; UDCA: Ursodeoxycholic acid; ANCA: Anti-neutrophil cytoplasmic antibodies; GERD: Gastroesophageal reflux disease; AMA: Anti-mitochondrial antibodies; HE: Hepatic encephalopathy.

Table 2 Cases of autoimmune hepatitis-like syndromes after coronavirus disease 2019 vaccine: Demographics, patient information, and disease presentation

Classification	
Number of patients	40
Females, n (%)	32 (83)
Age (years, mean \pm SD)	58.7 \pm 16
Race/ethnicity, n (%)	
Caucasian	11 (27)
Asian	3 (8)
Arabic	1 (3)
Unspecified	25 (62)
Predisposing conditions, n (%)	
History of liver disease	6 (15)
History of autoimmune disease	11 (28)
Medications, n (%)	
Acetaminophen	3 (8)
Other hepatotoxic drugs (statins, peg-IFN, AZT)	5 (13)
Vaccine, n (%)	
Pfizer-BioNTech	17 (43)
Moderna	11 (28)
AstraZeneca	10 (25)
Coronavac	2 (5)
Symptom onset (days after a dose, mean \pm SD)	16.6 \pm 12.8
Symptoms, n (%)	
Jaundice	24 (60)
Asthenia/Malaise/Fatigue	13 (33)
Choluria	10 (25)
Pruritus	8 (20)
Abdominal pain	4 (10)
Fever	5 (13)
Loss of appetite	4 (10)
Nausea/vomiting	5 (13)

Peg-IFN: Pegylated interferon; AZT: Azathioprine.

A longer follow-up could be helpful to rule out vaccine-induced liver injury since biochemical and histological resolution can spontaneously occur, and immunosuppressive treatment can be withdrawn without the risk of relapse.

In summary, although a causative link between AIH and SARS-CoV-2 vaccination cannot be confirmed, emerging case reports suggest this association could be more than coincidental.

CONCLUSION

Since the initial stage of the COVID-19 pandemic, concerns about the risk of poorer outcomes following SARS-CoV-2 infection have been raised in patients with pre-existing chronic liver disease. We found that people with AILDs are not at increased risk of being infected by SARS-CoV-2, despite immunosuppressive treatment that, however, may predispose them to develop a more severe course of the disease.

Table 3 Cases of autoimmune hepatitis-like syndromes after coronavirus disease 2019 vaccine: Diagnostics, treatment, and clinical outcomes

Diagnostics	
Peak laboratory values (mean ± SD)	
AST (IU/l)	936 ± 523
ALT (IU/l)	1060 ± 567
GGT (IU/l)	312 ± 220
ALP (IU/l)	209 ± 95
Bilirubin (mg/dL)	9.8 ± 8.5
IgG (g/L)	21.7 ± 6.7
Antibodies, n (%)	
ANA	33 (83)
ASMA	7 (18)
SLA/LP	2 (5)
AMA	5 (13)
Others (ANCA, DS-DNA)	3 (8)
Liver biopsy	
Performed	39
Not performed	1
Morphologic characteristics, n (%)	
Interface hepatitis	31 (78)
Lymphoplasmacellular infiltrates	36 (90)
Rosette formation	5 (13)
Treatment	
First agent	
Budesonide	1
Prednisone	15
Prednisolone	17
Methylprednisolone	3
Hydrocortisone	1
Steroids	3
No treatment	2
Second agent	
Azathioprine	8
Prednisolone	2
Clinical outcomes	
Time to the first improvement, days (mean ± SD)	4.6 ± 2.9
Time to resolution, days (mean ± SD)	44.6 ± 37
Alive	37
Dead	3

AST: Aspartate aminotransferase; ALT: Alanine aminotransferase; GGT: Gamma-glutamyl transferase; ALP: Alkaline phosphatase; IgG: Immunoglobulin G; ANA: Antinuclear antibody; ASMA: Anti-smooth muscle antibody; SLA/LP: Anti-soluble liver antigen/liver-pancreas; AMA: Anti-mitochondrial antibodies; ANCA: Anti-neutrophil cytoplasmic antibodies; Ds-DNA: Anti-double stranded DNA.

Furthermore, increasing evidence highlighted the intrinsic capability of the virus to hyper-stimulate immune response leading to the development of autoimmune disease. However, only two reports identify SARS-CoV-2 as a trigger instrument for developing AILDs, making any correlation not feasible.

Post-vaccine AIH-like syndrome raises worries about a risk of unprecedented immunological side effects, especially in individuals predisposed to autoinflammatory disorders. However, COVID-19 vaccine-induced AIH is extremely uncommon and has an exceptional prognosis. Hepatologists should consider AIH in patients with jaundice or elevated liver enzymes following COVID-19 vaccination to readily initiate further work-up and treatment with steroids.

FOOTNOTES

Author contributions: Sgamato C and Rocco A drafted the manuscript; Compare D, Minieri S, and Marchitto SA participated in the acquisition, analysis, and interpretation of the literature; Maurea S and Nardone G revised the manuscript for important intellectual content; All authors have read and approved the final manuscript.

Conflict-of-interest statement: Gerardo Nardone has served as a speaker and advisory board member for AG Pharma, Reckitt Benckiser, and has received research funding from SOFAR Spa and Alfasigma. No relevant conflicts of interest exist for the other authors.

Open-Access: This article is an open-access article that was selected by an in-house editor and fully peer-reviewed by external reviewers. It is distributed in accordance with the Creative Commons Attribution NonCommercial (CC BY-NC 4.0) license, which permits others to distribute, remix, adapt, build upon this work non-commercially, and license their derivative works on different terms, provided the original work is properly cited and the use is non-commercial. See: <https://creativecommons.org/Licenses/by-nc/4.0/>

Country/Territory of origin: Italy

ORCID number: Costantino Sgamato [0000-0001-7188-5174](#); Alba Rocco [0000-0003-0959-1807](#); Debora Compare [0000-0002-6092-4921](#); Stefano Minieri [0000-0002-6381-2132](#); Stefano Andrea Marchitto [0000-0003-1006-7236](#); Simone Maurea [0000-0002-8269-3765](#); Gerardo Nardone [0000-0001-8344-6523](#).

S-Editor: Fan JR

L-Editor: A

P-Editor: Fan JR

REFERENCES

- 1 Zhou P, Yang XL, Wang XG, Hu B, Zhang L, Zhang W, Si HR, Zhu Y, Li B, Huang CL, Chen HD, Chen J, Luo Y, Guo H, Jiang RD, Liu MQ, Chen Y, Shen XR, Wang X, Zheng XS, Zhao K, Chen QJ, Deng F, Liu LL, Yan B, Zhan FX, Wang YY, Xiao GF, Shi ZL. A pneumonia outbreak associated with a new coronavirus of probable bat origin. *Nature* 2020; **579**: 270-273 [PMID: [32015507](#) DOI: [10.1038/s41586-020-2012-7](#)]
- 2 WHO. WHO Director-General's opening remarks at the media briefing on COVID-19-11 March 2020-World Health Organization. World Heal Organ 2020. [cited 10 November 2022]. Available from: <https://www.who.int/>
- 3 Guan WJ, Ni ZY, Hu Y, Liang WH, Ou CQ, He JX, Liu L, Shan H, Lei CL, Hui DSC, Du B, Li LJ, Zeng G, Yuen KY, Chen RC, Tang CL, Wang T, Chen PY, Xiang J, Li SY, Wang JL, Liang ZJ, Peng YX, Wei L, Liu Y, Hu YH, Peng P, Wang JM, Liu JY, Chen Z, Li G, Zheng ZJ, Qiu SQ, Luo J, Ye CJ, Zhu SY, Zhong NS; China Medical Treatment Expert Group for Covid-19. Clinical Characteristics of Coronavirus Disease 2019 in China. *N Engl J Med* 2020; **382**: 1708-1720 [PMID: [32109013](#) DOI: [10.1056/NEJMoa2002032](#)]
- 4 Galanopoulos M, Gkeros F, Doukatas A, Karianakis G, Pontas C, Tsoukalas N, Viazis N, Liatsos C, Mantzaris GJ. COVID-19 pandemic: Pathophysiology and manifestations from the gastrointestinal tract. *World J Gastroenterol* 2020; **26**: 4579-4588 [PMID: [32884218](#) DOI: [10.3748/wjg.v26.i31.4579](#)]
- 5 Tian Y, Rong L, Nian W, He Y. Review article: gastrointestinal features in COVID-19 and the possibility of faecal transmission. *Aliment Pharmacol Ther* 2020; **51**: 843-851 [PMID: [32222988](#) DOI: [10.1111/apt.15731](#)]
- 6 Zhang C, Shi L, Wang FS. Liver injury in COVID-19: management and challenges. *Lancet Gastroenterol Hepatol* 2020; **5**: 428-430 [PMID: [32145190](#) DOI: [10.1016/S2468-1253\(20\)30057-1](#)]
- 7 Wu C, Chen X, Cai Y, Xia J, Zhou X, Xu S, Huang H, Zhang L, Du C, Zhang Y, Song J, Wang S, Chao Y, Yang Z, Xu J, Chen D, Xiong W, Xu L, Zhou F, Jiang J, Bai C, Zheng J, Song Y. Risk Factors Associated With Acute Respiratory Distress Syndrome and Death in Patients With Coronavirus Disease 2019 Pneumonia in Wuhan, China. *JAMA Intern Med* 2020; **180**: 934-943 [PMID: [32167524](#) DOI: [10.1001/jamainternmed.2020.0994](#)]
- 8 Qi X, Liu C, Jiang Z, Gu Y, Zhang G, Shao C, Yue H, Chen Z, Ma B, Liu D, Zhang L, Wang J, Xu D, Lei J, Li X, Huang H, Wang Y, Liu H, Yang J, Pan H, Liu W, Wang W, Li F, Zou S, Zhang H, Dong J. Multicenter analysis of clinical characteristics and outcomes in patients with COVID-19 who develop liver injury. *J Hepatol* 2020; **73**: 455-458 [PMID: [32305291](#) DOI: [10.1016/j.jhep.2020.04.010](#)]
- 9 Fan Z, Chen L, Li J, Cheng X, Yang J, Tian C, Zhang Y, Huang S, Liu Z, Cheng J. Clinical Features of COVID-19-

Related Liver Functional Abnormality. *Clin Gastroenterol Hepatol* 2020; **18**: 1561-1566 [PMID: 32283325 DOI: 10.1016/j.cgh.2020.04.002]

10 **Hoffmann M**, Kleine-Weber H, Schroeder S, Krüger N, Herrler T, Erichsen S, Schiergens TS, Herrler G, Wu NH, Nitsche A, Müller MA, Drosten C, Pöhlmann S. SARS-CoV-2 Cell Entry Depends on ACE2 and TMPRSS2 and Is Blocked by a Clinically Proven Protease Inhibitor. *Cell* 2020; **181**: 271-280.e8 [PMID: 32142651 DOI: 10.1016/j.cell.2020.02.052]

11 **Kanduc D**, Shoenfeld Y. Molecular mimicry between SARS-CoV-2 spike glycoprotein and mammalian proteomes: implications for the vaccine. *Immunol Res* 2020; **68**: 310-313 [PMID: 32946016 DOI: 10.1007/s12026-020-09152-6]

12 **Di Giorgio A**, Nicastro E, Speziani C, De Giorgio M, Pasulo L, Magro B, Fagioli S, D' Antiga L. Health status of patients with autoimmune liver disease during SARS-CoV-2 outbreak in northern Italy. *J Hepatol* 2020; **73**: 702-705 [PMID: 32413378 DOI: 10.1016/j.jhep.2020.05.008]

13 **Verhelst X**, Somers N, Geerts A, Degroote H, Van Vlierberghe H. Health status of patients with autoimmune hepatitis is not affected by the SARS-CoV-2 outbreak in Flanders, Belgium. *J Hepatol* 2021; **74**: 240-241 [PMID: 32918954 DOI: 10.1016/j.jhep.2020.08.035]

14 **Zecher BF**, Buescher G, Willemse J, Walmsley M, Taylor A, Leburgue A, Schramm C, Lohse AW, Sebode M. Prevalence of COVID-19 in patients with autoimmune liver disease in Europe: A patient-oriented online survey. *United European Gastroenterol J* 2021; **9**: 797-808 [PMID: 34105883 DOI: 10.1002/ueg2.12100]

15 **Murtas R**, Andreano A, Gervasi F, Guido D, Consolazio D, Tunesi S, Andreoni L, Greco MT, Gattoni ME, Sandrini M, Riussi A, Russo AG. Association between autoimmune diseases and COVID-19 as assessed in both a test-negative case-control and population case-control design. *Auto Immun Highlights* 2020; **11**: 15 [PMID: 33023649 DOI: 10.1186/s13317-020-00141-1]

16 **Rigamonti C**, Cittone MG, De Benedittis C, Rizzi E, Casciaro GF, Bellan M, Sainaghi PP, Pirisi M. Rates of Symptomatic SARS-CoV-2 Infection in Patients With Autoimmune Liver Diseases in Northern Italy: A Telemedicine Study. *Clin Gastroenterol Hepatol* 2020; **18**: 2369-2371.e1 [PMID: 32480009 DOI: 10.1016/j.cgh.2020.05.047]

17 **Gerussi A**, Rigamonti C, Elia C, Cazzagon N, Floreani A, Pozzi R, Pozzoni P, Claar E, Pasulo L, Fagioli S, Cristoferi L, Carbone M, Invernizzi P. Coronavirus Disease 2019 in Autoimmune Hepatitis: A Lesson From Immunosuppressed Patients. *Hepatol Commun* 2020; **4**: 1257-1262 [PMID: 32838102 DOI: 10.1002/hep4.1557]

18 **Marjot T**, Buescher G, Sebode M, Barnes E, Barratt AS 4th, Armstrong MJ, Baldelli L, Kennedy J, Mercer C, Ozga AK, Casar C, Schramm C; contributing Members and Collaborators of ERN RARE-LIVER/COVID-Hep/SECURE-Cirrhosis, Moon AM, Webb GJ, Lohse AW. SARS-CoV-2 infection in patients with autoimmune hepatitis. *J Hepatol* 2021; **74**: 1335-1343 [PMID: 33508378 DOI: 10.1016/j.jhep.2021.01.021]

19 **Efe C**, Dhanasekaran R, Lammert C, Ebik B, Higuera-de la Tijera F, Aloman C, Riza Çalışkan A, Peralta M, Gerussi A, Massoumi H, Catana AM, Torgutalp M, Purnak T, Rigamonti C, Gomez Aldana AJ, Khakoo N, Kacmaz H, Nazal L, Frager S, Demir N, Irak K, Ellik ZM, Balaban Y, Atay K, Eren F, Cristoferi L, Batıbay E, Urzua Á, Snijders R, Kiyıcı M, Akyıldız M, Ekin N, Carr RM, Harputluoğlu M, Hatemi I, Mendizabal M, Silva M, Idilman R, Silveira M, Drenth JPH, Assis DN, Björnsson E, Boyer JL, Invernizzi P, Levy C, Schiano TD, Ridruejo E, Wahlin S. Outcome of COVID-19 in Patients With Autoimmune Hepatitis: An International Multicenter Study. *Hepatology* 2021; **73**: 2099-2109 [PMID: 33713486 DOI: 10.1002/hep.31797]

20 **Efe C**, Lammert C, Taşçılar K, Dhanasekaran R, Ebik B, Higuera-de la Tijera F, Çalışkan AR, Peralta M, Gerussi A, Massoumi H, Catana AM, Purnak T, Rigamonti C, Aldana AJG, Khakoo N, Nazal L, Frager S, Demir N, Irak K, Melekoğlu-Ellik Z, Kacmaz H, Balaban Y, Atay K, Eren F, Alvares-da-Silva MR, Cristoferi L, Urzua Á, Eşkazan T, Magro B, Snijders R, Barutçu S, Lytyvak E, Zazueta GM, Demirezer-Bolat A, Aydin M, Heurgue-Berlot A, De Martin E, Ekin N, Yıldırım S, Yavuz A, Büyükköy M, Narro GC, Kiyıcı M, Akyıldız M, Kahramanoğlu-Aksoy E, Vincent M, Carr RM, Günşar F, Reyes EC, Harputluoğlu M, Aloman C, Gatselis NK, Üstündağ Y, Brahm J, Vargas NCE, Güzelbulut F, Garcia SR, Aguirre J, Anders M, Ratusnu N, Hatemi I, Mendizabal M, Floreani A, Fagioli S, Silva M, Idilman R, Satapathy SK, Silveira M, Drenth JPH, Dalekos GN, N Assis D, Björnsson E, Boyer JL, Yoshida EM, Invernizzi P, Levy C, Montano-Loza AJ, Schiano TD, Ridruejo E, Wahlin S. Effects of immunosuppressive drugs on COVID-19 severity in patients with autoimmune hepatitis. *Liver Int* 2022; **42**: 607-614 [PMID: 34846800 DOI: 10.1111/liv.15121]

21 **Boettler T**, Marjot T, Newsome PN, Mondelli MU, Maticic M, Cordero E, Jalan R, Moreau R, Cornberg M, Berg T. Impact of COVID-19 on the care of patients with liver disease: EASL-ESCMID position paper after 6 months of the pandemic. *JHEP Rep* 2020; **2**: 100169 [PMID: 32835190 DOI: 10.1016/j.jhepr.2020.100169]

22 **Bajaj JS**, Garcia-Tsao G, Biggins SW, Kamath PS, Wong F, McGeorge S, Shaw J, Pearson M, Chew M, Fagan A, de la Rosa Rodriguez R, Worthington J, Olofson A, Weir V, Trisolini C, Dwyer S, Reddy KR. Comparison of mortality risk in patients with cirrhosis and COVID-19 compared with patients with cirrhosis alone and COVID-19 alone: multicentre matched cohort. *Gut* 2021; **70**: 531-536 [PMID: 32660964 DOI: 10.1136/gutjnl-2020-322118]

23 **Marjot T**, Moon AM, Cook JA, Abd-Elsalam S, Aloman C, Armstrong MJ, Pose E, Brenner EJ, Cargill T, Catana MA, Dhanasekaran R, Eshraghian A, García-Juárez I, Gill US, Jones PD, Kennedy J, Marshall A, Matthews C, Mells G, Mercer C, Perumalswami PV, Avitabile E, Qi X, Su F, Ufere NN, Wong YJ, Zheng MH, Barnes E, Barratt AS 4th, Webb GJ. Outcomes following SARS-CoV-2 infection in patients with chronic liver disease: An international registry study. *J Hepatol* 2021; **74**: 567-577 [PMID: 33035628 DOI: 10.1016/j.jhep.2020.09.024]

24 **Halpert G**, Shoenfeld Y. SARS-CoV-2, the autoimmune virus. *Autoimmun Rev* 2020; **19**: 102695 [PMID: 33130000 DOI: 10.1016/j.autrev.2020.102695]

25 **Qin C**, Zhou L, Hu Z, Zhang S, Yang S, Tao Y, Xie C, Ma K, Shang K, Wang W, Tian DS. Dysregulation of Immune Response in Patients With Coronavirus 2019 (COVID-19) in Wuhan, China. *Clin Infect Dis* 2020; **71**: 762-768 [PMID: 32161940 DOI: 10.1093/cid/ciaa248]

26 **Vojdani A**, Kharazian D. Potential antigenic cross-reactivity between SARS-CoV-2 and human tissue with a possible link to an increase in autoimmune diseases. *Clin Immunol* 2020; **217**: 108480 [PMID: 32461193 DOI: 10.1016/j.clim.2020.108480]

27 **Zuo Y**, Estes SK, Ali RA, Gandhi AA, Yalavarthi S, Shi H, Sule G, Gockman K, Madison JA, Zuo M, Yadav V, Wang J, Woodard W, Lezak SP, Lugogo NL, Smith SA, Morrissey JH, Kanthi Y, Knight JS. Prothrombotic autoantibodies in serum

from patients hospitalized with COVID-19. *Sci Transl Med* 2020; **12** [PMID: 33139519 DOI: 10.1126/scitranslmed.abd3876]

28 **Vlachoyiannopoulos PG**, Magira E, Alexopoulos H, Jahaj E, Theophilopoulou K, Kotanidou A, Tzioufas AG. Autoantibodies related to systemic autoimmune rheumatic diseases in severely ill patients with COVID-19. *Ann Rheum Dis* 2020; **79**: 1661-1663 [PMID: 32581086 DOI: 10.1136/annrheumdis-2020-218009]

29 **Klinman DM**, Steinberg AD. Systemic autoimmune disease arises from polyclonal B cell activation. *J Exp Med* 1987; **165**: 1755-1760 [PMID: 3495631 DOI: 10.1084/jem.165.6.1755]

30 **Bartoli A**, Gitto S, Sighinolfi P, Cursaro C, Andreone P. Primary biliary cholangitis associated with SARS-CoV-2 infection. *J Hepatol* 2021; **74**: 1245-1246 [PMID: 33610679 DOI: 10.1016/j.jhep.2021.02.006]

31 **Singh B**, Kaur P, Maroules M. Autoimmune Hepatitis-Primary Biliary Cholangitis Overlap Syndrome Triggered by COVID-19. *Eur J Case Rep Intern Med* 2021; **8**: 002264 [PMID: 33768072 DOI: 10.12890/2021_002264]

32 **Muratori P**, Granito A, Pappas G, Pendino GM, Quarneri C, Cicola R, Menichella R, Ferri S, Cassani F, Bianchi FB, Lenzi M, Muratori L. The serological profile of the autoimmune hepatitis/primary biliary cirrhosis overlap syndrome. *Am J Gastroenterol* 2009; **104**: 1420-1425 [PMID: 19491855 DOI: 10.1038/ajg.2009.126]

33 **Yip TC**, Lui GC, Wong VW, Chow VC, Ho TH, Li TC, Tse YK, Hui DS, Chan HL, Wong GL. Liver injury is independently associated with adverse clinical outcomes in patients with COVID-19. *Gut* 2021; **70**: 733-742 [PMID: 32641471 DOI: 10.1136/gutjnl-2020-321726]

34 **Chai XQ**, Hu LF, Zhang Y, Han WY, Lu Z, Ke AW, Zhou J, Shi GM, Fang N, Fan J, Cai JB, Lan F. Specific ACE2 expression in cholangiocytes may cause liver damage after 2019-nCoV infection. 2020 Preprint. Available from: bioRxiv:2020.02.03.931766 [DOI: 10.1101/2020.02.03.931766]

35 **Weber S**, Mayerle J, Irlbeck M, Gerbes AL. Severe liver failure during SARS-CoV-2 infection. *Gut* 2020; **69**: 1365-1367 [PMID: 32327526 DOI: 10.1136/gutjnl-2020-321350]

36 **Li J**, Fan JG. Characteristics and Mechanism of Liver Injury in 2019 Coronavirus Disease. *J Clin Transl Hepatol* 2020; **8**: 13-17 [PMID: 32274341 DOI: 10.14218/JCTH.2020.00019]

37 **Li Y**, Xie Z, Lin W, Cai W, Wen C, Guan Y, Mo X, Wang J, Wang Y, Peng P, Chen X, Hong W, Xiao G, Liu J, Zhang L, Hu F, Li F, Zhang F, Deng X, Li L. Efficacy and Safety of Lopinavir/Ritonavir or Arbidol in Adult Patients with Mild/Moderate COVID-19: An Exploratory Randomized Controlled Trial. *Med (N Y)* 2020; **1**: 105-113.e4 [PMID: 32838353 DOI: 10.1016/j.medj.2020.04.001]

38 **Boeckmans J**, Rodrigues RM, Demuyser T, Piérard D, Vanhaecke T, Rogiers V. COVID-19 and drug-induced liver injury: a problem of plenty or a petty point? *Arch Toxicol* 2020; **94**: 1367-1369 [PMID: 32266419 DOI: 10.1007/s00204-020-02734-1]

39 **Polack FP**, Thomas SJ, Kitchin N, Absalon J, Gurtman A, Lockhart S, Perez JL, Pérez Marc G, Moreira ED, Zerbini C, Bailey R, Swanson KA, Roychoudhury S, Koury K, Li P, Kalina WV, Cooper D, Frenck RW Jr, Hammitt LL, Türeci Ö, Nell H, Schaefer A, Ünal S, Tresnan DB, Mather S, Dormitzer PR, Şahin U, Jansen KU, Gruber WC; C4591001 Clinical Trial Group. Safety and Efficacy of the BNT162b2 mRNA Covid-19 Vaccine. *N Engl J Med* 2020; **383**: 2603-2615 [PMID: 33301246 DOI: 10.1056/NEJMoa2034577]

40 **Baden LR**, El Sahly HM, Essink B, Kotloff K, Frey S, Novak R, Diemert D, Spector SA, Roushafel N, Creech CB, McGettigan J, Khetan S, Segall N, Solis J, Brosz A, Fierro C, Schwartz H, Neuzil K, Corey L, Gilbert P, Janes H, Follmann D, Marovich M, Mascola J, Polakowski L, Ledgerwood J, Graham BS, Bennett H, Pajon R, Knightly C, Leav B, Deng W, Zhou H, Han S, Ivarsson M, Miller J, Zaks T; COVE Study Group. Efficacy and Safety of the mRNA-1273 SARS-CoV-2 Vaccine. *N Engl J Med* 2021; **384**: 403-416 [PMID: 33378609 DOI: 10.1056/NEJMoa2035389]

41 **Falsey AR**, Sobieszczyk ME, Hirsch I, Sproule S, Robb ML, Corey L, Neuzil KM, Hahn W, Hunt J, Mulligan MJ, McEvoy C, DeJesus E, Hassman M, Little SJ, Pahud BA, Durbin A, Pickrell P, Daar ES, Bush L, Solis J, Carr QO, Oyedele T, Buchbinder S, Cowden J, Vargas SL, Guerreros Benavides A, Call R, Keefer MC, Kirkpatrick BD, Pullman J, Tong T, Brewinski Isaacs M, Benkeser D, Janes HE, Nason MC, Green JA, Kelly EJ, Maaske J, Mueller N, Shoemaker K, Takas T, Marshall RP, Pangalos MN, Villafana T, Gonzalez-Lopez A; AstraZeneca AZD1222 Clinical Study Group. Phase 3 Safety and Efficacy of AZD1222 (ChAdOx1 nCoV-19) Covid-19 Vaccine. *N Engl J Med* 2021; **385**: 2348-2360 [PMID: 34587382 DOI: 10.1056/NEJMoa2105290]

42 **Our World in Data**. Coronavirus (COVID-19) Vaccinations [cited 10 November 2022]. Available from: <https://ourworldindata.org/covid-vaccinations>

43 **Teijaro JR**, Farber DL. COVID-19 vaccines: modes of immune activation and future challenges. *Nat Rev Immunol* 2021; **21**: 195-197 [PMID: 33674759 DOI: 10.1038/s41577-021-00526-x]

44 **Akinosoglou K**, Tzivaki I, Marangos M. Covid-19 vaccine and autoimmunity: Awakening the sleeping dragon. *Clin Immunol* 2021; **226**: 108721 [PMID: 33823270 DOI: 10.1016/j.clim.2021.108721]

45 **Bril F**, Al Diffalha S, Dean M, Fettig DM. Autoimmune hepatitis developing after coronavirus disease 2019 (COVID-19) vaccine: Causality or casualty? *J Hepatol* 2021; **75**: 222-224 [PMID: 33862041 DOI: 10.1016/j.jhep.2021.04.003]

46 **European Association for the Study of the Liver**. EASL Clinical Practice Guidelines: Autoimmune hepatitis. *J Hepatol* 2015; **63**: 971-1004 [PMID: 26341719 DOI: 10.1016/j.jhep.2015.06.030]

47 **Lee SK**, Kwon JH, Yoon N, Lee SH, Sung PS. Immune-mediated liver injury represented as overlap syndrome after SARS-CoV-2 vaccination. *J Hepatol* 2022; **77**: 1209-1211 [PMID: 35817223 DOI: 10.1016/j.jhep.2022.06.029]

48 **Boettler T**, Csernalabics B, Salié H, Luxenburger H, Wischer L, Salimi Alizei E, Zoldan K, Krimmel L, Bronsert P, Schwabenland M, Prinz M, Mogler C, Neumann-Haefelin C, Thimme R, Hofmann M, Bengsch B. SARS-CoV-2 vaccination can elicit a CD8 T-cell dominant hepatitis. *J Hepatol* 2022; **77**: 653-659 [PMID: 35461912 DOI: 10.1016/j.jhep.2022.03.040]

49 **Ghielmetti M**, Schaufelberger HD, Mieli-Vergani G, Cerny A, Dayer E, Vergani D, Terzioli Beretta-Piccoli B. Acute autoimmune-like hepatitis with atypical anti-mitochondrial antibody after mRNA COVID-19 vaccination: A novel clinical entity? *J Autoimmun* 2021; **123**: 102706 [PMID: 34293683 DOI: 10.1016/j.jaut.2021.102706]

50 **Avcı E**, Abasiyanik F. Autoimmune hepatitis after SARS-CoV-2 vaccine: New-onset or flare-up? *J Autoimmun* 2021; **125**: 102745 [PMID: 34781161 DOI: 10.1016/j.jaut.2021.102745]

51 **Mahalingham A**, Duckworth A, Griffiths WJH. First report of post-transplant autoimmune hepatitis recurrence following SARS-CoV-2 mRNA vaccination. *Transpl Immunol* 2022; **72**: 101600 [PMID: 35390478 DOI: 10.1016/j.trim.2022.101600]

52 **Erard D**, Villeret F, Lavrut PM, Dumortier J. Autoimmune hepatitis developing after COVID 19 vaccine: Presumed guilty? *Clin Res Hepatol Gastroenterol* 2022; **46**: 101841 [PMID: 34920137 DOI: 10.1016/j.clinre.2021.101841]

53 **Garrido I**, Lopes S, Simões MS, Liberal R, Lopes J, Carneiro F, Macedo G. Autoimmune hepatitis after COVID-19 vaccine - more than a coincidence. *J Autoimmun* 2021; **125**: 102741 [PMID: 34717185 DOI: 10.1016/j.jaut.2021.102741]

54 **Goulas A**, Kafiri G, Kranidioti H, Manolakopoulos S. A typical autoimmune hepatitis (AIH) case following Covid-19 mRNA vaccination. More than a coincidence? *Liver Int* 2022; **42**: 254-255 [PMID: 34724315 DOI: 10.1111/liv.15092]

55 **Cao Z**, Gui H, Sheng Z, Xin H, Xie Q. Letter to the editor: Exacerbation of autoimmune hepatitis after COVID-19 vaccination. *Hepatology* 2022; **75**: 757-759 [PMID: 34862637 DOI: 10.1002/hep.32269]

56 **Vuille-Lessard É**, Montani M, Bosch J, Semmo N. Autoimmune hepatitis triggered by SARS-CoV-2 vaccination. *J Autoimmun* 2021; **123**: 102710 [PMID: 34332438 DOI: 10.1016/j.jaut.2021.102710]

57 **Suzuki Y**, Kakisaka K, Takikawa Y. Letter to the editor: Autoimmune hepatitis after COVID-19 vaccination: Need for population-based epidemiological study. *Hepatology* 2022; **75**: 759-760 [PMID: 34904265 DOI: 10.1002/hep.32280]

58 **Tan CK**, Wong YJ, Wang LM, Ang TL, Kumar R. Autoimmune hepatitis following COVID-19 vaccination: True causality or mere association? *J Hepatol* 2021; **75**: 1250-1252 [PMID: 34153398 DOI: 10.1016/j.jhep.2021.06.009]

59 **Zhou T**, Fronhoffs F, Dold L, Strassburg CP, Weismüller TJ. New-onset autoimmune hepatitis following mRNA COVID-19 vaccination in a 36-year-old woman with primary sclerosing cholangitis - should we be more vigilant? *J Hepatol* 2022; **76**: 218-220 [PMID: 34450237 DOI: 10.1016/j.jhep.2021.08.006]

60 **Kang SH**, Kim MY, Cho MY, Baik SK. Autoimmune Hepatitis Following Vaccination for SARS-CoV-2 in Korea: Coincidence or Autoimmunity? *J Korean Med Sci* 2022; **37**: e116 [PMID: 35437965 DOI: 10.3346/jkms.2022.37.e116]

61 **Rocco A**, Sgamato C, Compare D, Nardone G. Autoimmune hepatitis following SARS-CoV-2 vaccine: May not be a casualty. *J Hepatol* 2021; **75**: 728-729 [PMID: 34116081 DOI: 10.1016/j.jhep.2021.05.038]

62 **Londoño MC**, Gratacós-Ginès J, Sáez-Peñataro J. Another case of autoimmune hepatitis after SARS-CoV-2 vaccination - still casualty? *J Hepatol* 2021; **75**: 1248-1249 [PMID: 34129886 DOI: 10.1016/j.jhep.2021.06.004]

63 **McShane C**, Kiat C, Rigby J, Crosbie Ó. The mRNA COVID-19 vaccine - A rare trigger of autoimmune hepatitis? *J Hepatol* 2021; **75**: 1252-1254 [PMID: 34245804 DOI: 10.1016/j.jhep.2021.06.044]

64 **Clayton-Chubb D**, Schneider D, Freeman E, Kemp W, Roberts SK. Autoimmune hepatitis developing after the ChAdOx1 nCoV-19 (Oxford-AstraZeneca) vaccine. *J Hepatol* 2021; **75**: 1249-1250 [PMID: 34171435 DOI: 10.1016/j.jhep.2021.06.014]

65 **Palla P**, Vergadis C, Sakellariou S, Androutsakos T. Letter to the editor: Autoimmune hepatitis after COVID-19 vaccination: A rare adverse effect? *Hepatology* 2022; **75**: 489-490 [PMID: 34528278 DOI: 10.1002/hep.32156]

66 **Rela M**, Jothimani D, Vij M, Rajakumar A, Rammohan A. Auto-immune hepatitis following COVID vaccination. *J Autoimmun* 2021; **123**: 102688 [PMID: 34225251 DOI: 10.1016/j.jaut.2021.102688]

67 **Camacho-Domínguez L**, Rodríguez Y, Polo F, Restrepo Gutierrez JC, Zapata E, Rojas M, Anaya JM. COVID-19 vaccine and autoimmunity. A new case of autoimmune hepatitis and review of the literature. *J Transl Autoimmun* 2022; **5**: 100140 [PMID: 35013724 DOI: 10.1016/j.jtauto.2022.100140]

68 **Zin Tun GS**, Gleeson D, Al-Joudeh A, Dube A. Immune-mediated hepatitis with the Moderna vaccine, no longer a coincidence but confirmed. *J Hepatol* 2022; **76**: 747-749 [PMID: 34619252 DOI: 10.1016/j.jhep.2021.09.031]

69 **Torrente S**, Castiella A, Garmendia M, Zapata E. Probable autoimmune hepatitis reactivated after COVID-19 vaccination. *Gastroenterol Hepatol* 2022; **45** Suppl 1: 115-116 [PMID: 34756976 DOI: 10.1016/j.gastrohep.2021.10.002]

70 **Fimiano F**, D'Amato D, Gambella A, Marzano A, Saracco GM, Morgando A. Autoimmune hepatitis or drug-induced autoimmune hepatitis following Covid-19 vaccination? *Liver Int* 2022; **42**: 1204-1205 [PMID: 35230737 DOI: 10.1111/liv.15224]

71 **Izagirre A**, Arzallus T, Garmendia M, Torrente S, Castiella A, Zapata EM. Autoimmune hepatitis following COVID-19 vaccination. *J Autoimmun* 2022; **132**: 102874 [PMID: 35985054 DOI: 10.1016/j.jaut.2022.102874]

72 **Hasegawa N**, Matsuoka R, Ishikawa N, Endo M, Terasaki M, Seo E, Tsuchiya K. Autoimmune hepatitis with history of HCV treatment triggered by COVID-19 vaccination: case report and literature review. *Clin J Gastroenterol* 2022; **15**: 791-795 [PMID: 35716255 DOI: 10.1007/s12328-022-01654-0]

73 **Shroff H**, Satapathy SK, Crawford JM, Todd NJ, VanWagner LB. Liver injury following SARS-CoV-2 vaccination: A multicenter case series. *J Hepatol* 2022; **76**: 211-214 [PMID: 34339763 DOI: 10.1016/j.jhep.2021.07.024]

74 **Efe C**, Harputluoglu M, Soylu NK, Yilmaz S. Letter to the editor: Liver transplantation following severe acute respiratory syndrome-coronavirus-2 vaccination-induced liver failure. *Hepatology* 2022; **75**: 1669-1671 [PMID: 35175635 DOI: 10.1002/hep.32409]

75 **Shahrani S**, Sooi CY, Hilmi IN, Mahadeva S. Autoimmune hepatitis (AIH) following coronavirus (COVID-19) vaccine- No longer exclusive to mRNA vaccine? *Liver Int* 2022; **42**: 2344-2345 [PMID: 35762286 DOI: 10.1111/liv.15350]

76 **Nik Muhamad Affendi NA**, Ravindran S, Siam TS, Leow AH, Hilmi I. Jaundice in a Primary Sclerosing Cholangitis Patient: A New Cause in a New Era. *Inflamm Bowel Dis* 2022; **28**: e29-e30 [PMID: 34652425 DOI: 10.1093/ibd/izab250]

77 **Mekritthikrai K**, Jaru-Ampornpan P, Komolmit P, Thanapirom K. Autoimmune Hepatitis Triggered by COVID-19 Vaccine: The First Case From Inactivated Vaccine. *ACG Case Rep J* 2022; **9**: e00811 [PMID: 35784513 DOI: 10.14309/crj.00000000000000811]

78 **Mathew M**, John SB, Sebastian J, Ravi MD. COVID-19 vaccine triggered autoimmune hepatitis: case report. *Eur J Hosp Pharm* 2022 [PMID: 36207131 DOI: 10.1136/ejhp pharm-2022-003485]

79 **Hennes EM**, Zeniya M, Czaja AJ, Parés A, Dalekos GN, Krawitt EL, Bittencourt PL, Porta G, Boberg KM, Hofer H, Bianchi FB, Shibata M, Schramm C, Eisenmann de Torres B, Galle PR, McFarlane I, Dienes HP, Lohse AW; International Autoimmune Hepatitis Group. Simplified criteria for the diagnosis of autoimmune hepatitis. *Hepatology* 2008; **48**: 169-176 [PMID: 18537184 DOI: 10.1002/hep.22322]

80 **Alvarez F**, Berg PA, Bianchi FB, Bianchi L, Burroughs AK, Cancado EL, Chapman RW, Cooksley WG, Czaja AJ, Desmet VJ, Donaldson PT, Eddleston AL, Fainboim L, Heathcote J, Homberg JC, Hoofnagle JH, Kakumu S, Krawitt EL, Mackay IR, MacSween RN, Maddrey WC, Manns MP, McFarlane IG, Meyer zum Büschenfelde KH, Zeniya M. International Autoimmune Hepatitis Group Report: review of criteria for diagnosis of autoimmune hepatitis. *J Hepatol* 1999; **31**: 929-938 [PMID: 10580593 DOI: 10.1016/S0168-8278(99)80297-9]

81 **Berry PA**, Smith-Laing G. Hepatitis A vaccine associated with autoimmune hepatitis. *World J Gastroenterol* 2007; **13**: 2238-2239 [PMID: 17465509 DOI: 10.3748/wjg.v13.i15.2238]

82 **van Gemeren MA**, van Wijngaarden P, Doukas M, de Man RA. Vaccine-related autoimmune hepatitis: the same disease as idiopathic autoimmune hepatitis? *Scand J Gastroenterol* 2017; **52**: 18-22 [PMID: 27565372 DOI: 10.1080/00365521.2016.1224379]

83 **Muratori P**, Serio I, Lalanne C, Lenzi M. Development of autoimmune hepatitis after influenza vaccination: trigger or killer? *Clin Res Hepatol Gastroenterol* 2019; **43**: e95-e96 [PMID: 30926201 DOI: 10.1016/j.clinre.2019.02.007]

84 **Sasaki T**, Suzuki Y, Ishida K, Kakisaka K, Abe H, Sugai T, Takikawa Y. Autoimmune hepatitis following influenza virus vaccination: Two case reports. *Medicine (Baltimore)* 2018; **97**: e11621 [PMID: 30045302 DOI: 10.1097/MD.00000000000011621]

85 **Talotta R**. Do COVID-19 RNA-based vaccines put at risk of immune-mediated diseases? *Clin Immunol* 2021; **224**: 108665 [PMID: 33429060 DOI: 10.1016/j.clim.2021.108665]

86 **Caso F**, Costa L, Ruscitti P, Navarini L, Del Puente A, Giacomelli R, Scarpa R. Could Sars-coronavirus-2 trigger autoimmune and/or autoinflammatory mechanisms in genetically predisposed subjects? *Autoimmun Rev* 2020; **19**: 102524 [PMID: 32220633 DOI: 10.1016/j.autrev.2020.102524]

Submit a Manuscript: <https://www.f6publishing.com>

World J Gastroenterol 2023 March 28; 29(12): 1852-1862

DOI: [10.3748/wjg.v29.i12.1852](https://doi.org/10.3748/wjg.v29.i12.1852)

ISSN 1007-9327 (print) ISSN 2219-2840 (online)

MINIREVIEWS

Review of lymphoma in the duodenum: An update of diagnosis and management

Masaya Iwamuro, Takehiro Tanaka, Hiroyuki Okada

Specialty type: Gastroenterology and hepatology**Provenance and peer review:**

Invited article; Externally peer reviewed.

Peer-review model: Single blind**Peer-review report's scientific quality classification**

Grade A (Excellent): 0

Grade B (Very good): B

Grade C (Good): C

Grade D (Fair): 0

Grade E (Poor): 0

P-Reviewer: Di Meglio L, Italy;
Yamada T, United States**Received:** December 5, 2022**Peer-review started:** December 5, 2022**First decision:** February 8, 2023**Revised:** February 11, 2023**Accepted:** March 14, 2023**Article in press:** March 14, 2023**Published online:** March 28, 2023**Masaya Iwamuro, Hiroyuki Okada**, Department of Gastroenterology and Hepatology, Okayama University Graduate School of Medicine, Dentistry, and Pharmaceutical Sciences, Okayama 700-8558, Japan**Takehiro Tanaka**, Department of Pathology, Okayama University Hospital, Okayama 700-8558, Japan**Corresponding author:** Masaya Iwamuro, MD, PhD, Assistant Professor, Doctor, Department of Gastroenterology and Hepatology, Okayama University Graduate School of Medicine, Dentistry, and Pharmaceutical Sciences, 2-5-1 Shikata-cho, Kita-ku, Okayama 700-8558, Japan. pr145h2k@okayama-u.ac.jp

Abstract

The presentation, subtype, and macroscopic images of lymphoma vary depending on the site of the tumor within the gastrointestinal tract. We searched PubMed for publications between January 1, 2012 and October 10, 2022, and retrieved 130 articles relating to duodenal lymphoma. A further 22 articles were added based on the manual screening of relevant articles, yielding 152 articles for full-text review. The most predominant primary duodenal lymphoma was follicular lymphoma. In this review, we provide an update of the diagnosis and management of representative lymphoma subtypes occurring in the duodenum: Follicular lymphoma, diffuse large B-cell lymphoma, extranodal marginal zone lymphoma of mucosa-associated lymphoid tissue, mantle cell lymphoma, and T-cell lymphomas.

Key Words: Diagnosis; Diffuse large B-cell lymphoma; Duodenal neoplasms; Esophagogastroduodenoscopy; Follicular lymphoma; Gastrointestinal lymphoma**©The Author(s) 2023.** Published by Baishideng Publishing Group Inc. All rights reserved.

Core Tip: Among cases of primary duodenal lymphoma, follicular lymphoma was the most predominant, followed by diffuse large B-cell lymphoma, extranodal marginal zone lymphoma of mucosa associated lymphoid tissue (MALT lymphoma), mantle cell lymphoma, and T-cell lymphomas. A watch and wait policy is acceptable for follicular lymphoma. Observation without treatment is also an option for MALT lymphoma. However, it should be noted that duodenal MALT lymphoma has a higher rate of transformation to diffuse large B-cell lymphoma than gastric MALT lymphoma. Diffuse large B-cell lymphoma, mantle cell lymphoma, and T-cell lymphomas generally require systemic treatment.

Citation: Iwamuro M, Tanaka T, Okada H. Review of lymphoma in the duodenum: An update of diagnosis and management. *World J Gastroenterol* 2023; 29(12): 1852-1862

URL: <https://www.wjgnet.com/1007-9327/full/v29/i12/1852.htm>

DOI: <https://dx.doi.org/10.3748/wjg.v29.i12.1852>

INTRODUCTION

Gastrointestinal lymphoma is a relatively rare tumor, accounting for 1%–8% of malignant neoplasms of the gastrointestinal tract[1-3]. However, detection and management of gastrointestinal lymphoma lesions is important, as 30%–40% of extranodal lymphomas occur in the gastrointestinal tract[4]. The lymphoma subtype, presentation, and macroscopic images vary depending on the site of the tumor in the gastrointestinal tract. Thus, understanding of the specific features is essential for gastroenterologists to ensure prompt diagnosis and appropriate management. The stomach is the most commonly involved site of lymphomas in the gastrointestinal tract, with the duodenum being less common. Analysis of the United States population based on the Surveillance, Epidemiology, and End Results (SEER) program revealed that the prevalence of primary gastric, small intestinal, and duodenal lymphomas is approximately in the ratio of 10:3:1[5]. Recent studies have found that some subtypes of lymphoma that develop in the duodenum are distinct from those that develop in other parts of the gastrointestinal tract. Here, we review articles describing duodenal lymphoma published within the last 10 years and provide a summary update of contemporary diagnosis and management of the disease.

SEARCH STRATEGY

We searched PubMed for all peer-reviewed articles from January 1, 2012 to October 10, 2022. No study design filters were used. Manual screening of additional relevant articles was performed using a reference list of selected articles meeting eligibility criteria. The search strategy used the keywords 'lymphoma' and 'duodenum'. The search was performed by the lead author (Iwamuro M). Criteria for article inclusion were: (1) Peer-reviewed articles describing cases of duodenal lymphoma; and (2) review articles, original articles, case series, and case reports. Exclusion criteria were: (1) Articles written in languages other than English; (2) animal and cell studies; and (3) the primary topic of study was not duodenal lymphoma. Eligible articles were evaluated in full.

SEARCH RESULTS

Figure 1 shows a flow diagram summarizing the identification, screening, eligibility, and exclusion processes of the literature search. The initial search returned 288 articles. Among these, lymphoma was not the subject in 42 articles. Meanwhile, in 36 articles, case(s) of lymphoma was described but the duodenum was not involved. Articles on animal and cell studies ($n = 31$), articles in which the primary topic was not duodenal lymphoma ($n = 26$), and articles written in language other than English ($n = 23$) were also excluded. After application of the exclusion criteria, 130 articles were retrieved from the initial PubMed search. A further 22 articles were added based on the manual screening of relevant articles. In total, 152 articles were used for full-text review.

Table 1 shows the results of the PubMed database literature search according to the lymphoma subtype. Follicular lymphoma was reported most frequently (48 articles), followed by diffuse large B-cell lymphoma (17 articles), extranodal marginal zone lymphoma of mucosa associated lymphoid tissue (MALT lymphoma) (9 articles), enteropathy-associated T-cell lymphoma (9 articles), mantle cell lymphoma (5 articles), plasmablastic lymphoma (4 articles), monomorphic epitheliotrophic intestinal T-cell lymphoma (4 articles), Burkitt lymphoma (4 articles), and anaplastic large cell lymphoma (4 articles). Other rare subtypes of lymphoma occurring in the duodenum reported within the last 10 years were also included.

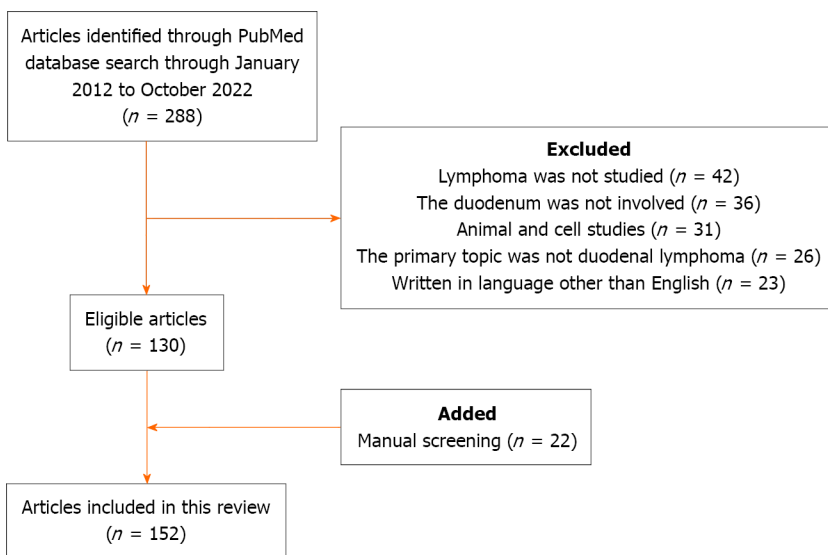
Table 1 Literature search results

Lymphoma subtype	Number of articles
Follicular lymphoma	48 ¹
Diffuse large B-cell lymphoma	17 ¹
MALT lymphoma	9 ¹
Enteropathy-associated T-cell lymphoma	9
Mantle cell lymphoma	5
Plasmablastic lymphoma	4
Monomorphic epitheliotropic intestinal T-cell lymphoma	4
Burkitt lymphoma	4
Anaplastic large cell lymphoma	4
Refractory celiac disease type II	2
Peripheral T-cell lymphoma	2
Marginal zone lymphoma	2
Intravascular Lymphoma	2
NK/T-cell lymphoma	2
Post-transplant lymphoproliferative disease	1
Mycosis fungoides	1
Methotrexate-associated lymphoproliferative disorder	1
Intestinal T-cell lymphoma	1
Immunoproliferative small intestinal disease	1
Extracavitary primary effusion lymphoma	1
Cutaneous large B cell lymphoma	1
Cutaneous aggressive T-cell lymphoma	1
B-lymphoblastic lymphoma	1
Non-Hodgkin lymphoma	1
T cell lymphoma	1
B cell lymphoma	1
Aggressive B-cell lymphoma	1
General review of lymphoma	3
Subtype unspecified	2

¹One article described follicular lymphoma and MALT lymphoma and another article described follicular lymphoma and diffuse large B-cell lymphoma.
MALT lymphoma: Extranodal marginal zone lymphoma of mucosa associated lymphoid tissue.

PREVALENCE OF LYMPHOMA SUBTYPES IN THE DUODENUM

Analysis of the United States population based on the SEER program revealed a total of 1060 cases of primary duodenal lymphoma identified between 1998 and 2015[5]. Among the primary duodenal lymphoma, the most frequent was follicular lymphoma (41.1%), followed by diffuse large B-cell lymphoma (32.8%), MALT lymphoma (13.8%), mantle cell lymphoma (2.7%), and T-cell lymphoma (2.6%). Meanwhile, diffuse large B-cell lymphoma was the most predominant subtype in the stomach (48.9%) and small intestine (jejunum and ileum, 54.9%), while follicular lymphoma was less frequent in the stomach (2.2%) and small intestine (23.0%). A population-based study in a Japanese prefecture included 350 cases of lymphoma involving the gastrointestinal tract, whether primarily or secondarily [6]. The affected sites were the stomach (62.6%), large intestine (15.4%), small intestine (14.3%), duodenum (6.0%), esophagus (0.3%), and appendix (0.3%). The subtypes of duodenal lymphoma ($n = 21$) were follicular lymphoma (61.9%), followed by diffuse large B-cell lymphoma (14.3%), MALT lymphoma (14.3%), peripheral T-cell lymphoma (4.8%), and adult T-cell leukemia/lymphoma (4.8%).



DOI: 10.3748/wjg.v29.i12.1852 Copyright ©The Author(s) 2023.

Figure 1 Flow diagram summarizing the identification, screening, eligibility, and exclusion processes of the literature search.

In the following sections, we review recent advances and basic knowledge relating to the diagnosis and management of representative lymphoma subtypes occurring in the duodenum.

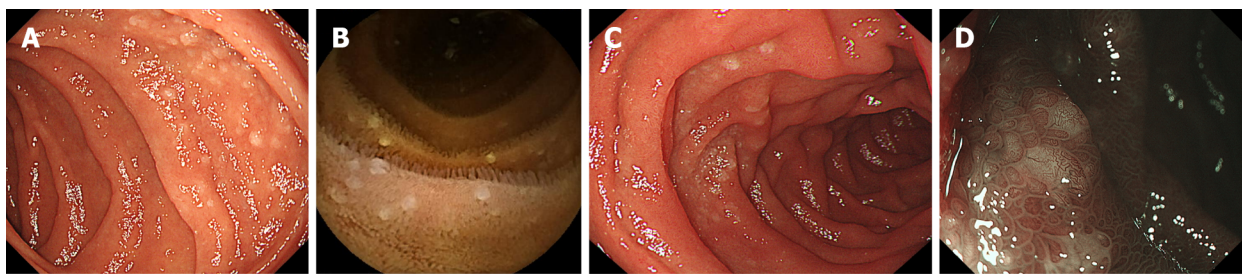
FOLLICULAR LYMPHOMA

As described above, follicular lymphoma is the most common subtype of lymphoma occurring in the duodenum. The majority of cases are asymptomatic and are identified serendipitously during esophagogastroduodenoscopy examinations[7,8]. Follicular lymphomas most frequently occur in the descending part of the duodenum. The typical macroscopic feature is multiple white granules[9] (Figure 2). Magnified observation is useful when it is difficult to distinguish between minute lesions of this and other diseases. Follicular lymphoma is suspected if nodular white submucosal deposits or white villus enlargement are observed by magnified observation[10] (Figure 3). Biopsy reveals small to medium-sized tumor cells that form follicular structures and diffusely invade into the villi. Immunostaining is essential for definitive diagnosis, and CD10, BCL6 and BCL2 are usually positive in follicular lymphoma[7]. In addition, the t(14;18)(q32;q21) translocation of the immunoglobulin heavy chain gene and the BCL2 gene is characteristic of follicular lymphoma. Thus, fluorescence *in situ* hybridization analysis of chromosomal translocation provides complementary information for diagnosis.

Follicular lymphoma is an indolent lymphoma that grows slowly over years. A watch and wait policy is acceptable, provided that appropriate chemotherapy is initiated when the disease progresses and symptoms develop. Comparative study between patients with intestinal follicular lymphoma treated with rituximab-combined chemotherapy (n = 14) and those with watch and wait policy (n = 15) showed comparable outcomes[11-13]. In addition, one prospective study of 31 patients with primary gastrointestinal follicular lymphoma revealed that spontaneous shrinkage or complete disappearance was observed in nine patients[14]. These results confirm the suitability of follicular lymphoma management using the watch and wait policy. Radiation therapy is one option for duodenal lymphomas if the lesion is localized to the field of irradiation[15]. However, duodenal lymphomas are often accompanied by jejunal and/or ileum lesions. Since the gastrointestinal lesions are sometimes negative by positron emission tomography or computed tomography scans[16], evaluation of the whole intestines with colonoscopy and small-intestinal endoscopy is essential when radiotherapy is considered [8]. Recent research has revealed that circumferential location of follicular lesions (more than half of the circumference of the intestinal lumen) and fusion of follicular lesions (dense granular elevations with indistinct boundaries) are significant predictive factors for progression of clinical stage, extension of intestinal lesions, or transformation to diffuse large B-cell lymphoma[17]. Patients with these endoscopic features may require surveillance in the short term.

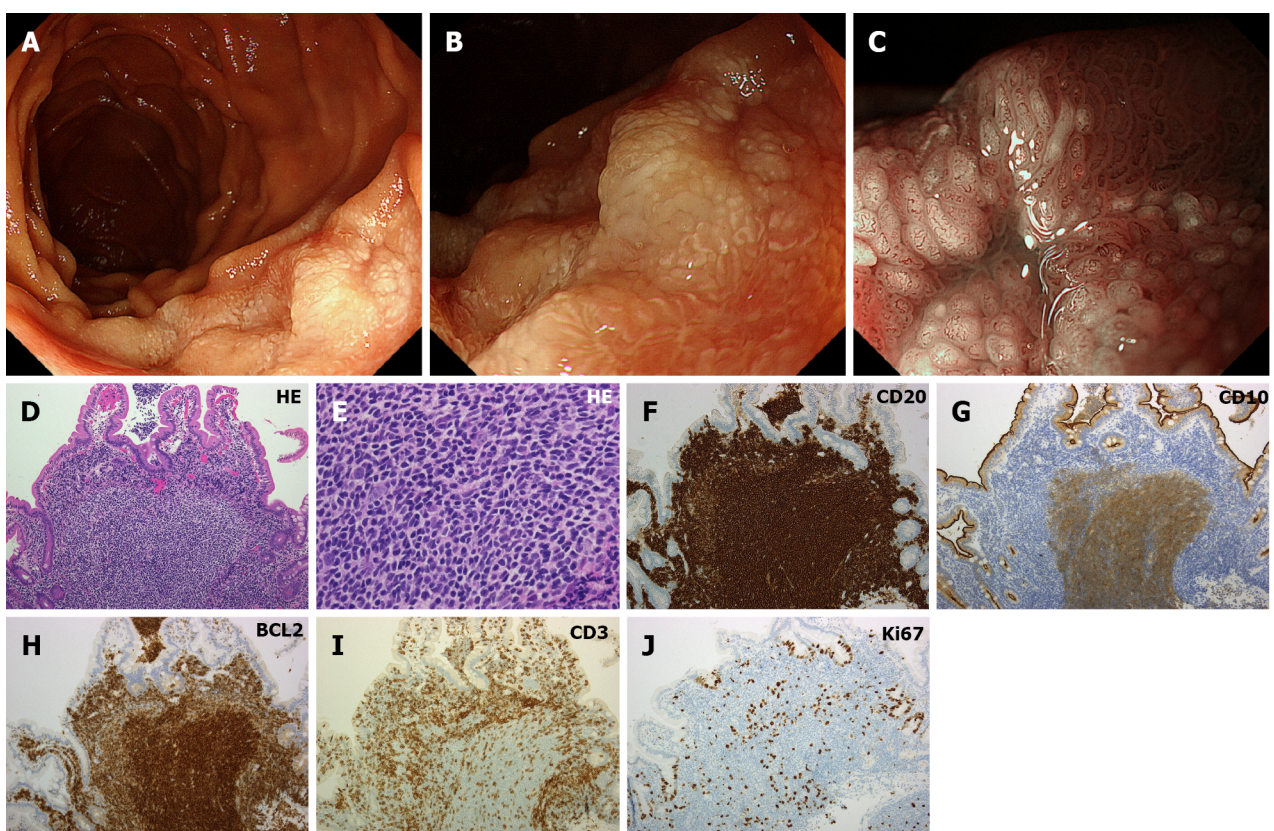
DIFFUSE LARGE B-CELL LYMPHOMA

Diffuse large B-cell lymphoma can occur in any part of the gastrointestinal tract, but it is often seen in



DOI: 10.3748/wjg.v29.i12.1852 Copyright ©The Author(s) 2023.

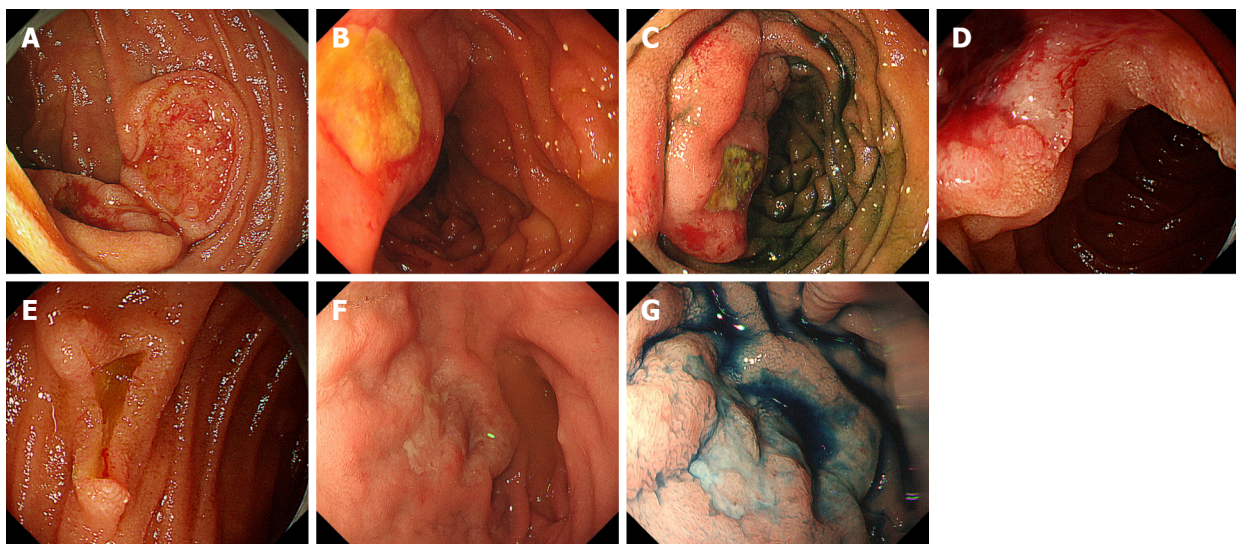
Figure 2 Representative endoscopic images of duodenal follicular lymphoma (Cases 1 and 2). A: Case 1. Esophagogastroduodenoscopy reveals typical feature of follicular lymphoma showing multiple whitish granules in the descending portion of the duodenum; B: Case 1. Video capsule enteroscopy shows follicular lymphoma lesions in the jejunum; C: Case 2. Another case of duodenal follicular lymphoma; D: Case 2. Magnifying observation with narrow band imaging shows white deposits.



DOI: 10.3748/wjg.v29.i12.1852 Copyright ©The Author(s) 2023.

Figure 3 Representative endoscopic and pathological images of duodenal follicular lymphoma (Case 3). A: Esophagogastroduodenoscopy shows thick, white mucosa in the descending portion of the duodenum; B: Magnifying observation reveals enlarged whitish villi; C: Magnifying observation with narrow band imaging emphasizes enlarged villi with elongated vasculature on the surface; D–J: Pathological images of the biopsied specimen. Hematoxylin and eosin stain shows medium-sized tumor cells that form follicular structures and diffusely invade into the villi (D: × 10, E: × 40). Lymphoma cells are positive for CD20, CD10, and BCL2, while negative for CD3. Tumor cells are sparsely positive for Ki67. HE: Hematoxylin and eosin.

the stomach and ileocecal region, and duodenal involvement is rare[18]. Retrospective analysis of 126 patients with intestinal diffuse large B-cell lymphomas revealed that the ileocecal region was the most commonly involved (50.0%), followed by the small intestine (*i.e.*, jejunum and/or ileum, 23.0%), duodenum (18.3%), colon (11.1%), and rectum (5.6%)[19]. Diffuse large B-cell lymphoma lesions in the duodenum and large intestine tend to be secondarily involved, while those in the ileocecal region and small intestine are *de novo* neoplasms found in limited-stage disease[19]. It has also been reported that in approximately 30% of cases, duodenal diffuse large B-cell lymphoma are accompanied by gastric lesions [19]. On esophagogastroduodenoscopy, ulcerative and protruded lesions are typical morphology of duodenal diffuse large B-cell lymphoma[20]. Particularly, an auriculate ulcer mound is characteristic of diffuse large B-cell lymphoma[21] (Figure 4), although it is rarely seen in other lymphomas and cancers. Biopsies tend to consist of a diffuse proliferation of large B cells, with Ki-67 positivity generally greater



DOI: 10.3748/wjg.v29.i12.1852 Copyright ©The Author(s) 2023.

Figure 4 Representative endoscopic images of diffuse large B-cell lymphoma (Cases 4–7). A: Case 4. Esophagogastrroduodenoscopy reveals duodenal lesions showing auriculate ulcer mounds; B and C: Case 5. A protruded, ulcerative lesion is seen in the duodenum; C: After indigo carmine spraying; D and E: Case 6. Multiple ulcerative lesions in the duodenum; F and G: Case 7. Irregular-shaped, shallow ulcers in the duodenum.

than 40%.

Diffuse large B-cell lymphoma is an aggressive (intermediate-grade) lymphoma that progresses on a monthly basis. However, this disease often responds well to treatment and long-term remission can be expected. Neoplastic cells of diffuse large B-cell lymphoma often exist through the entire thickness of the gastrointestinal tract[18]. Thus, patients should be counseled on the risk of intestinal perforation, bleeding, and stricture after the initiation of chemotherapy[22].

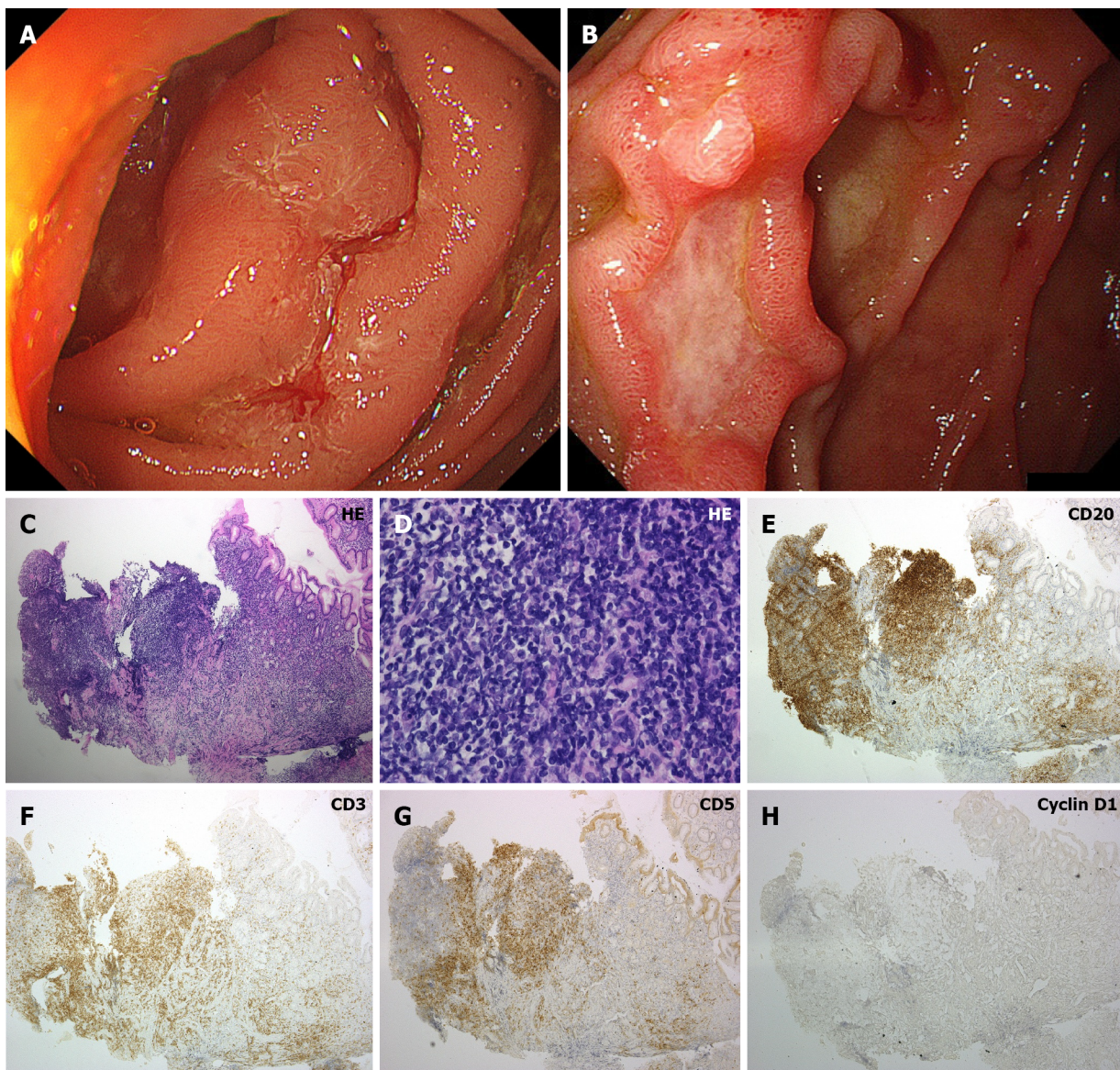
MALT LYMPHOMA

MALT lymphoma is common in the stomach and occurs less frequently in the duodenum. Duodenal MALT lymphoma presents various macroscopic features (Figure 5). According to reports describing 13 cases of duodenal MALT lymphoma, nodular lesions were the predominant feature (58.3%), followed by ulcer (16.7%), flat depression (16.7%), and subepithelial tumor (8.3%)[23]. Elevated lesions have also been described in case reports[24,25]. Among these, nodular lesions showing white granular protrusions must be differentiated from follicular lymphoma[23,26]. Endoscopic biopsy specimen predominantly shows small to medium-sized lymphoma cells, mixed with varying proportions of large cells. Lymphoepithelial lesions are infrequently observed in the duodenal MALT lymphoma[27]. Immunostaining is essential for definitive diagnosis and differentiation from other B-cell lymphomas.

Although some of the duodenal MALT lymphoma lesions reportedly regress with *H. pylori* eradication therapy, the response rate is lower than that for gastric MALT lymphoma[23]. Radiation therapy is indicated for limited-stage disease in which the disease is confined to the duodenum or limited to the regional lymph nodes[28,29]. Systemic chemotherapy is administered for non-limited-stage disease. Observation without treatment is an option because MALT lymphoma generally spreads slowly, but it should be noted that duodenal MALT lymphoma has a higher rate of transformation to diffuse large B-cell lymphoma than gastric MALT lymphoma[23].

MANTLE CELL LYMPHOMA

Mantle cell lymphoma forms multiple polypoid elevations throughout the gastrointestinal tract including the duodenum, and has been termed multiple lymphomatous polyposis[30–32] (Figure 6). Multiple lymphomatous polyposis is a typical intestinal lesion of mantle cell lymphoma. However, although infrequently, other lymphomas can also present with this feature. We reviewed 35 cases of mantle cell lymphoma with gastrointestinal involvement and the involved sites were the stomach (74.3%), colon (57.1%), ileum (47.6%), rectum (47.6%), duodenum (34.3%), cecum (14.3%), and esophagus (5.7%)[33]. Mantle cell lymphoma lesions in the intestines (from duodenum to rectum, $n = 22$) predominantly showed multiple lymphomatous polyposis (10 or more elevated lesions, 77.3%), followed by protruded (1–9 elevated lesions, 18.2%) and superficial lesions (4.5%). The duodenal lesions



DOI: 10.3748/wjg.v29.i12.1852 Copyright ©The Author(s) 2023.

Figure 5 Representative endoscopic and pathological images of duodenal MALT lymphoma (Cases 8 and 9). A: Case 8. A protruded lesion mimicking hypertrophic folds is observed in the duodenum; B: Case 9. Esophagogastroduodenoscopy shows ulcerative tumor in the duodenum; C-H: Pathological images of Case 9. On hematoxylin and eosin stain, small to medium-sized lymphoma cells are predominant (C: $\times 10$, D: $\times 40$). Neoplastic cells are positive for CD20, while negative for CD3, CD5, and Cyclin D1. HE: Hematoxylin and eosin.

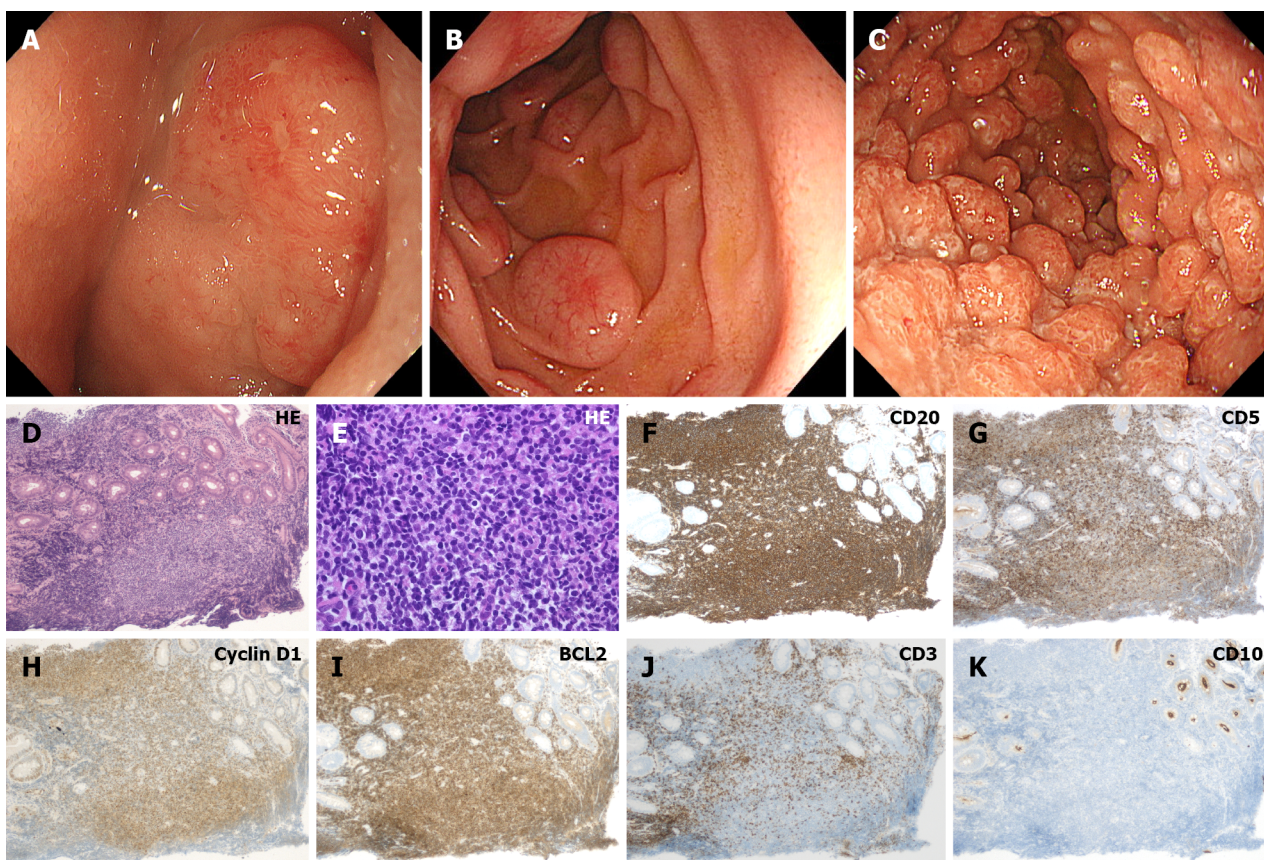
of mantle cell lymphoma often accompany erosion of the tumorous nodules[30,34]. Endoscopic biopsy specimens consist of a homogeneous growth of small to medium-sized lymphoma cells with loose nodular structures in a diffuse pattern. As for other lymphomas, immunostaining is essential for definitive diagnosis. CD5, Cyclin D1, and SOX11 are often positive in mantle cell lymphoma[35].

Despite intensive chemotherapy regimens, mantle cell lymphoma generally remains incurable and is treatment-resistant with multiple relapses. Thus, prompt consultation with hematologists is required after the diagnosis[36].

T-CELL LYMPHOMAS

In the latest version of WHO classification of hematolymphoid tumors of the digestive system, T-cell lymphomas have been classified under four major types: Enteropathy-associated T-cell lymphoma, monomorphic epitheliotropic intestinal T-cell lymphoma, intestinal T-cell lymphoma not otherwise specified (NOS), and indolent T-cell lymphoproliferative disorder of the gastrointestinal tract[36].

Enteropathy-associated T-cell lymphoma, formerly known as type I enteropathy-associated T-cell lymphoma, is the most prevalent among primary intestinal T-cell neoplasms. Lymphoma cells derive



DOI: 10.3748/wjg.v29.i12.1852 Copyright ©The Author(s) 2023.

Figure 6 Representative endoscopic and pathological images of duodenal mantle cell lymphoma (Cases 10–12). A: Case 10. Elevated lesion with erosions on the surface in the duodenum; B: Case 11. Typical morphology of mantle cell lymphoma showing multiple lymphomatous polyposis in the duodenum. Subepithelial lesion-like protruded lesions accompanying dilated vasculature on the surface are seen; C: Case 12. Numerous, diffuse polypoid lesions in the duodenum; D–K: Pathological images of Case 12. Lymphoma cells retain a homogeneous pattern of cell size on hematoxylin and eosin stain (D: $\times 10$, E: $\times 40$). Cells are positive for CD20, CD5, Cyclin D1, BCL2, while negative for CD3 and CD10. HE: Hematoxylin and eosin.

from intraepithelial lymphocytes in celiac disease patients[37,38]. In particular, 30%–52% of refractory celiac disease type II transforms into an enteropathy-associated T-cell lymphoma within five years[39]. Monomorphic epitheliotrophic intestinal T-cell lymphoma, formerly known as type II enteropathy-associated T-cell lymphoma, derives from intraepithelial T lymphocytes and is typically not linked to celiac disease[40–44]. Aggressive T-cell lymphoma that lacks the clinical and pathological features of enteropathy-associated T-cell lymphoma, monomorphic epitheliotrophic intestinal T-cell lymphoma, anaplastic large cell lymphoma, or extranodal NK/T-cell lymphoma is now categorized as intestinal T-cell lymphoma NOS[45]. Indolent T-cell lymphoproliferative disorder of the gastrointestinal tract represents clonal proliferation of T lymphocytes within the lamina propria, most commonly in the small intestine and colon[46]. The prognosis of T-cell lymphomas is generally poor, except for indolent T-cell lymphoproliferative disorder that shows prolonged survival with persistent, chronic relapsing disease.

CONCLUSION

We reviewed relevant articles mainly published within the last 10 years associated with duodenal lymphomas and summarized updates of representative lymphoma subtypes. Though there is no doubt that endoscopic examinations play a major role in the diagnosis of duodenal lymphoma, understanding of each pathological subtype will improve the diagnosis and initial treatment response to the disease. We believe this review will be helpful for gastroenterologists and endoscopists who diagnose and treat patients with duodenal lymphoma.

FOOTNOTES

Author contributions: Iwamuro M designed the research study and wrote the paper; Tanaka T critically reviewed the

manuscript for important intellectual content; Okada H approved the manuscript.

Conflict-of-interest statement: All the authors report no relevant conflicts of interest for this article.

Open-Access: This article is an open-access article that was selected by an in-house editor and fully peer-reviewed by external reviewers. It is distributed in accordance with the Creative Commons Attribution NonCommercial (CC BY-NC 4.0) license, which permits others to distribute, remix, adapt, build upon this work non-commercially, and license their derivative works on different terms, provided the original work is properly cited and the use is non-commercial. See: <https://creativecommons.org/Licenses/by-nc/4.0/>

Country/Territory of origin: Japan

ORCID number: Masaya Iwamuro 0000-0002-1757-5754; Takehiro Tanaka 0000-0002-1509-5706; Hiroyuki Okada 0000-0003-2814-7146.

S-Editor: Fan JR

L-Editor: A

P-Editor: Fan JR

REFERENCES

- 1 Nakamura S, Matsumoto T. Gastrointestinal lymphoma: recent advances in diagnosis and treatment. *Digestion* 2013; **87**: 182-188 [PMID: 23635497 DOI: 10.1159/000350051]
- 2 Freeman C, Berg JW, Cutler SJ. Occurrence and prognosis of extranodal lymphomas. *Cancer* 1972; **29**: 252-260 [PMID: 5007387 DOI: 10.1002/1097-0142(197201)29:1<252::aid-cncr280290138>3.0.co;2-#]
- 3 Ghimire P, Wu GY, Zhu L. Primary gastrointestinal lymphoma. *World J Gastroenterol* 2011; **17**: 697-707 [PMID: 21390139 DOI: 10.3748/wjg.v17.i6.697]
- 4 Bautista-Quach MA, Ake CD, Chen M, Wang J. Gastrointestinal lymphomas: Morphology, immunophenotype and molecular features. *J Gastrointest Oncol* 2012; **3**: 209-225 [PMID: 22943012 DOI: 10.3978/j.issn.2078-6891.2012.024]
- 5 Zheng G, Wang Y, Zhao Y, Zheng Z. Clinicopathological Features, Treatment Strategy, and Prognosis of Primary Non-Hodgkin's Lymphoma of the Duodenum: A SEER Database Analysis. *Can J Gastroenterol Hepatol* 2020; **2020**: 9327868 [PMID: 32399459 DOI: 10.1155/2020/9327868]
- 6 Fujishima F, Katsushima H, Fukuhara N, Konosu-Fukaya S, Nakamura Y, Sasano H, Ichinohasama R. Incidence Rate, Subtype Frequency, and Occurrence Site of Malignant Lymphoma in the Gastrointestinal Tract: Population-Based Analysis in Miyagi, Japan. *Tohoku J Exp Med* 2018; **245**: 159-165 [PMID: 29998914 DOI: 10.1620/tjem.245.159]
- 7 Yoshino T, Chott A. Duodenal-type follicular lymphoma. The WHO classification of tumours editorial board, eds. WHO classification of tumours, digestive system tumours. Lyon: IARC, 2019: 383-385
- 8 Iwamuro M, Kondo E, Takata K, Yoshino T, Okada H. Diagnosis of follicular lymphoma of the gastrointestinal tract: A better initial diagnostic workup. *World J Gastroenterol* 2016; **22**: 1674-1683 [PMID: 26819532 DOI: 10.3748/wjg.v22.i4.1674]
- 9 Iwamuro M, Okada H, Takata K, Nose S, Miyatani K, Yoshino T, Yamamoto K. Diagnostic accuracy of endoscopic biopsies for the diagnosis of gastrointestinal follicular lymphoma: a clinicopathologic study of 48 patients. *Ann Diagn Pathol* 2014; **18**: 99-103 [PMID: 24513028 DOI: 10.1016/j.anndiagpath.2013.12.006]
- 10 Iwamuro M, Okada H, Takata K, Kawai Y, Kawano S, Nasu J, Kawahara Y, Tanaka T, Yoshino T, Yamamoto K. Magnified endoscopic features of duodenal follicular lymphoma and other whitish lesions. *Acta Med Okayama* 2015; **69**: 37-44 [PMID: 25703169 DOI: 10.1892/AMO/53120]
- 11 Kamiyo K, Shimomura Y, Yoshioka S, Yamashita D, Hara S, Ishikawa T. Clinical features and outcomes of duodenal-type follicular lymphoma: A single-center retrospective study. *EJHaem* 2022; **3**: 379-384 [PMID: 35846028 DOI: 10.1002/jha.2.384]
- 12 Tari A, Asaoku H, Takata K, Fujimori S, Tanaka S, Fujihara M, Koga T, Yoshino T. The role of "watch and wait" in intestinal follicular lymphoma in rituximab era. *Scand J Gastroenterol* 2016; **51**: 321-328 [PMID: 26382560 DOI: 10.3109/00365521.2015.1087589]
- 13 Marks E, Shi Y. Duodenal-Type Follicular Lymphoma: A Clinicopathologic Review. *Arch Pathol Lab Med* 2018; **142**: 542-547 [PMID: 29565210 DOI: 10.5858/arpa.2016-0519-RS]
- 14 Matysiak-Budnik T, Jamet P, Chapelle N, Fabiani B, Coppo P, Ruskoné-Fournestraux A. Primary Gastrointestinal Follicular Lymphomas: A Prospective Study of 31 Patients with Long-term Follow-up Registered in the French Gastrointestinal Lymphoma Study Group (GELD) of the French Federation of Digestive Oncology (FFCD). *Gut Liver* 2022; **16**: 207-215 [PMID: 35249892 DOI: 10.5009/gnl210300]
- 15 Schmatz AI, Streubel B, Kretschmer-Chott E, Püspök A, Jäger U, Mannhalter C, Tiemann M, Ott G, Fischbach W, Herzog P, Seitz G, Stolte M, Raderer M, Chott A. Primary follicular lymphoma of the duodenum is a distinct mucosal/submucosal variant of follicular lymphoma: a retrospective study of 63 cases. *J Clin Oncol* 2011; **29**: 1445-1451 [PMID: 21383289 DOI: 10.1200/JCO.2010.32.9193]
- 16 Iwamuro M, Okada H, Takata K, Shinagawa K, Fujiki S, Shiode J, Imagawa A, Araki M, Morito T, Nishimura M, Mizuno M, Inaba T, Suzuki S, Kawai Y, Yoshino T, Kawahara Y, Takaki A, Yamamoto K. Diagnostic role of 18F-fluorodeoxyglucose positron emission tomography for follicular lymphoma with gastrointestinal involvement. *World J Gastroenterol* 2012; **18**: 6427-36; discussion p.6434 [PMID: 23197888 DOI: 10.3748/wjg.v18.i44.6427]

17 **Sumioka A**, Oka S, Hirata I, Iio S, Tsuboi A, Takigawa H, Yuge R, Urabe Y, Boda K, Kohno T, Okanobu H, Kitadai Y, Arihiro K, Tanaka S. Predictive factors for the progression of primary localized stage small-bowel follicular lymphoma. *J Gastroenterol* 2022; **57**: 667-675 [PMID: 35831477 DOI: 10.1007/s00535-022-01897-1]

18 **Chan WC**, Lai J, Nakamura S, Rosenwald A: Diffuse large B-cell lymphoma. The WHO classification of tumours editorial board, eds. WHO classification of tumours, digestive system tumours. Lyon: IARC, 2019: 402-405

19 **Maeshima AM**, Taniguchi H, Ito Y, Hatta S, Suzuki T, Yuda S, Makita S, Fukuhara S, Munakata W, Maruyama D, Izutsu K. Clinicopathological characteristics of diffuse large B-cell lymphoma involving small and large intestines: an analysis of 126 patients. *Int J Hematol* 2019; **110**: 340-346 [PMID: 31187439 DOI: 10.1007/s12185-019-02687-x]

20 **Vetro C**, Romano A, Amico I, Conticello C, Motta G, Figueira A, Chiarenza A, Di Raimondo C, Giulietti G, Bonanno G, Palumbo GA, Di Raimondo F. Endoscopic features of gastro-intestinal lymphomas: from diagnosis to follow-up. *World J Gastroenterol* 2014; **20**: 12993-13005 [PMID: 25278693 DOI: 10.3748/wjg.v20.i36.12993]

21 **Murakami D**, Harada H, Amano Y. Auriculate Ulcers in Gastrointestinal Tract. *Clin Gastroenterol Hepatol* 2022; **20**: A19 [PMID: 32911065 DOI: 10.1016/j.cgh.2020.09.013]

22 **Vaidya R**, Habermann TM, Donohue JH, Ristow KM, Maurer MJ, Macon WR, Colgan JP, Inwards DJ, Ansell SM, Porrata LF, Micallef IN, Johnston PB, Markovic SN, Thompson CA, Nowakowski GS, Witzig TE. Bowel perforation in intestinal lymphoma: incidence and clinical features. *Ann Oncol* 2013; **24**: 2439-2443 [PMID: 23704194 DOI: 10.1093/annonc/mdt188]

23 **Na HK**, Won SH, Ahn JY, Kim GH, Jung KW, Lee JH, Kim DH, Choi KD, Song HJ, Lee GH, Jung HY, Kim HJ. Clinical course of duodenal mucosa-associated lymphoid tissue lymphoma: Comparison with gastric mucosa-associated lymphoid tissue lymphoma. *J Gastroenterol Hepatol* 2021; **36**: 406-412 [PMID: 32573049 DOI: 10.1111/jgh.15157]

24 **Yokota K**, Namikawa T, Maeda M, Tanioka N, Iwabu J, Uemura S, Munekage M, Maeda H, Kitagawa H, Kobayashi M, Hanazaki K. Synchronous duodenal mucosa-associated lymphoid tissue lymphoma and gastric cancer. *Clin J Gastroenterol* 2021; **14**: 109-114 [PMID: 32959165 DOI: 10.1007/s12328-020-01241-1]

25 **Yokoyama T**, Tanaka T, Harada S, Ueda T, Ejiri G, Sasaki S, Takeda M, Yoshimura A. A case of gastric and duodenal mucosa-associated lymphoid tissue lymphoma with multiple gastric cancers: a case report. *Surg Case Rep* 2021; **7**: 30 [PMID: 33492581 DOI: 10.1186/s40792-020-01081-8]

26 **Kim SJ**, Kim HW, Choi CW, Ha JK, Hong YM, Park JH, Park SB, Kang DH. Duodenal mucosa-associated lymphoid tissue lymphomas: two cases and the evaluation of endoscopic ultrasonography. *Clin Endosc* 2013; **46**: 563-567 [PMID: 24143321 DOI: 10.5946/ce.2013.46.5.563]

27 **Nakamura S**, Delabie J: Extranodal marginal zone lymphoma of mucosa-associated lymphoid tissue (MALT lymphoma) involving the digestive tract. The WHO classification of tumours editorial board, eds. WHO classification of tumours, digestive system tumours. Lyon: IARC, 2019: 378-382

28 **Smith CD**, Gupta S, Sinn Chin Y, Thompson SR. Long term outcomes of gastric mucosa-associated lymphoid tissue lymphoma treated with radiotherapy: A multi-center retrospective cohort study. *Hematol Oncol* 2023; **41**: 71-77 [PMID: 36150219 DOI: 10.1002/hon.3078]

29 **Kaddu-Mulindwa D**, Thurner L, Christofyllakis K, Bewarder M, Kos IA. Management of Extranodal Marginal Zone Lymphoma: Present and Upcoming Perspectives. *Cancers (Basel)* 2022; **14** [PMID: 35740684 DOI: 10.3390/cancers14123019]

30 **Yanai S**, Nakamura S, Yamaguchi S, Kawasaki K, Ishida K, Sugai T, Umeno J, Esaki M, Matsumoto T. Gastrointestinal mantle cell lymphoma with isolated mass and multiple lymphomatous polyposis: report of two cases. *Clin J Gastroenterol* 2017; **10**: 327-330 [PMID: 28451951 DOI: 10.1007/s12328-017-0740-5]

31 **Fujita N**, Ono Y, Sano A, Tanaka Y. Mantle Cell Lymphoma with Multiple Lymphomatous Polyposis. *Intern Med* 2022; **61**: 591-592 [PMID: 34565780 DOI: 10.2169/internalmedicine.8287-21]

32 **Gallivan C**, Akbar A. Multiple lymphomatous polyposis: A presentation for mantle cell lymphoma. *Clin Case Rep* 2020; **8**: 3038-3042 [PMID: 33363875 DOI: 10.1002/ccr3.3291]

33 **Iwamuro M**, Okada H, Kawahara Y, Shinagawa K, Morito T, Yoshino T, Yamamoto K. Endoscopic features and prognoses of mantle cell lymphoma with gastrointestinal involvement. *World J Gastroenterol* 2010; **16**: 4661-4669 [PMID: 20872966 DOI: 10.3748/wjg.v16.i37.4661]

34 **Zheng QF**, Li JY, Qin L, Wei HM, Cai LY, Nong B. Gastrointestinal involvement by mantle cell lymphoma identified by biopsy performed during endoscopy: A case report. *Medicine (Baltimore)* 2018; **97**: e9799 [PMID: 29419676 DOI: 10.1097/MD.00000000000009799]

35 **Campo E**, Seto M: Mantle cell lymphoma. The WHO classification of tumours editorial board, eds. WHO classification of tumours, digestive system tumours. Lyon: IARC, 2019: 408-410

36 **Foukas PG**, Bisig B, de Leval L. Recent advances upper gastrointestinal lymphomas: molecular updates and diagnostic implications. *Histopathology* 2021; **78**: 187-214 [PMID: 33382495 DOI: 10.1111/his.14289]

37 **Bhagat G**, Chott A: Enteropathy-associated T-cell lymphoma. The WHO classification of tumours editorial board, eds. WHO classification of tumours, digestive system tumours. Lyon: IARC, 2019: 386-389

38 **Hiraga H**, Sakuraba H, Tanaka N, Watanabe R, Akemoto Y, Ota S, Kikuchi H, Sawaya M, Hiraga N, Chinda D, Hanabata N, Mikami T, Shimoyama T, Takahata T, Tanaka M, Fukuda S. A case of celiac disease with type I enteropathy-associated T-cell lymphoma in a Japanese male patient. *Immunol Med* 2019; **42**: 142-147 [PMID: 31603739 DOI: 10.1080/25785826.2019.1673031]

39 **Dieckman T**, Schreurs M, Mahfouz A, Kooy-Winkelaar Y, Neefjes-Borst A, Bouma G, Koning F. Single-Cell Analysis of Refractory Celiac Disease Demonstrates Inter- and Intra-Patient Aberrant Cell Heterogeneity. *Cell Mol Gastroenterol Hepatol* 2022; **14**: 173-192 [PMID: 35338007 DOI: 10.1016/j.jcmgh.2022.03.005]

40 **Tan SY**, de Leval L: Monomorphic epitheliotropic intestinal T-cell lymphoma. The WHO classification of tumours editorial board, eds. WHO classification of tumours, digestive system tumours. Lyon: IARC, 2019: 390-392

41 **Olecki EJ**, Rakrzawski KL, Peng JS. Pancreatoduodenectomy for monomorphic epitheliotropic intestinal T-cell lymphoma with duodenal obstruction. *BMJ Case Rep* 2022; **15** [PMID: 35318206 DOI: 10.1136/bcr-2022-248948]

42 **Ozaka S**, Inoue K, Okajima T, Tasaki T, Ariki S, Ono H, Ando T, Daa T, Murakami K. Monomorphic epitheliotropic

intestinal T-cell lymphoma presenting as melena with long-term survival: A case report and review of literature. *World J Gastroenterol* 2021; **27**: 6501-6510 [PMID: 34720538 DOI: 10.3748/wjg.v27.i38.6501]

43 **Kasinathan G.** Monomorphic epitheliotropic intestinal T-cell lymphoma of the duodenum: an aggressive disease. *Hematol Transfus Cell Ther* 2021; **43**: 518-520 [PMID: 32536535 DOI: 10.1016/j.htct.2020.04.005]

44 **Fukushima M**, Honda T, Komatsu N, Sasaki R, Ozawa E, Miuma S, Miyaaki H, Irie J, Okano S, Nakao K. Initial and advanced endoscopic findings of monomorphic epitheliotropic intestinal T-cell lymphoma in the duodenum: A case report. *DEN Open* 2022; **2**: e118 [PMID: 35873525 DOI: 10.1002/deo2.118]

45 **Bhagat G**, Tan SY: Intestinal T-cell lymphoma NOS. The WHO classification of tumours editorial board, eds. WHO classification of tumours, digestive system tumours. Lyon: IARC, 2019: 393-394

46 **Jaffe ES**, Chan WC: Indolent T-cell lymphoproliferative disorder of the GI tract. The WHO classification of tumours editorial board, eds. WHO classification of tumours, digestive system tumours. Lyon: IARC, 2019: 395-396

Comprehensive review on endoscopic ultrasound-guided tissue acquisition techniques for solid pancreatic tumor

Sakue Masuda, Kazuya Koizumi, Kento Shionoya, Ryuhei Jinushi, Makomo Makazu, Takashi Nishino, Karen Kimura, Chihiro Sumida, Jun Kubota, Chikamasa Ichita, Akiko Sasaki, Masahiro Kobayashi, Makoto Kako, Uojima Haruki

Specialty type: Gastroenterology and hepatology

Provenance and peer review:

Invited article; Externally peer reviewed.

Peer-review model: Single blind

Peer-review report's scientific quality classification

Grade A (Excellent): 0

Grade B (Very good): 0

Grade C (Good): C, C, C

Grade D (Fair): 0

Grade E (Poor): 0

P-Reviewer: Kaneko J, Japan; Tan B, China

Received: December 27, 2022

Peer-review started: December 27, 2022

First decision: January 22, 2023

Revised: February 2, 2023

Accepted: March 15, 2023

Article in press: March 15, 2023

Published online: March 28, 2023



Sakue Masuda, Kazuya Koizumi, Kento Shionoya, Ryuhei Jinushi, Makomo Makazu, Takashi Nishino, Karen Kimura, Chihiro Sumida, Jun Kubota, Chikamasa Ichita, Akiko Sasaki, Masahiro Kobayashi, Makoto Kako, Uojima Haruki, Department of Gastroenterology, Shonan Kamakura General Hospital, Kanagawa 247-8533, Japan

Uojima Haruki, Department of Gastroenterology, Internal Medicine, Kitasato University School of Medicine, Kanagawa 252-0375, Japan

Corresponding author: Sakue Masuda, MD, Chief Doctor, Department of Gastroenterology, Shonan Kamakura General Hospital, 1370-1 Okamoto, Kamakura, Kanagawa 247-8533, Japan. sakue.masuda@tokushukai.jp

Abstract

Pancreatic ductal adenocarcinoma is speculated to become the second leading cause of cancer-related mortality by 2030, a high mortality rate considering the number of cases. Surgery and chemotherapy are the main treatment options, but they are burdensome for patients. A clear histological diagnosis is needed to determine a treatment plan, and endoscopic ultrasound (EUS)-guided tissue acquisition (TA) is a suitable technique that does not worsen the cancer-specific prognosis even for lesions at risk of needle tract seeding. With the development of personalized medicine and precision treatment, there has been an increasing demand to increase cell counts and collect specimens while preserving tissue structure, leading to the development of the fine-needle biopsy (FNB) needle. EUS-FNB is rapidly replacing EUS-guided fine-needle aspiration (FNA) as the procedure of choice for EUS-TA of pancreatic cancer. However, EUS-FNA is sometimes necessary where the FNB needle cannot penetrate small hard lesions, so it is important clinicians are familiar with both. Given these recent developments, we present an up-to-date review of the role of EUS-TA in pancreatic cancer. Particularly, technical aspects, such as needle caliber, negative pressure, and puncture methods, for obtaining an adequate specimen in EUS-TA are discussed.

Key Words: Endoscopic ultrasound-guided fine needle biopsy; Endoscopic ultrasound-guided tissue acquisition; Personalized medicine; Genomic profiling test; Pancreatic cancer; Puncture procedure

Core Tip: Endoscopic ultrasound (EUS)-guided tissue acquisition (TA) began in 1992 as EUS-guided fine-needle aspiration (FNA). Recently, with the development of personalized medicine and precision treatment, the fine-needle biopsy (FNB) needle was developed. EUS-FNB is rapidly replacing EUS-FNA for pancreatic cancer. The EUS-TA strategy with three or more punctures, the stylet retraction method, the torque or fanning technique, and a 22-G or thicker FNB needle may be effective in patients with solid pancreatic tumors scheduled for treatment, including personalized medicine. It is also important clinicians are familiar with both procedures, as EUS-FNA is occasionally necessary when FNB is unsuccessful.

Citation: Masuda S, Koizumi K, Shionoya K, Jinushi R, Makazu M, Nishino T, Kimura K, Sumida C, Kubota J, Ichita C, Sasaki A, Kobayashi M, Kako M, Haruki U. Comprehensive review on endoscopic ultrasound-guided tissue acquisition techniques for solid pancreatic tumor. *World J Gastroenterol* 2023; 29(12): 1863-1874

URL: <https://www.wjgnet.com/1007-9327/full/v29/i12/1863.htm>

DOI: <https://dx.doi.org/10.3748/wjg.v29.i12.1863>

INTRODUCTION

Approximately 80%-85% of patients with pancreatic cancer are borderline-resectable (BR) requiring neoadjuvant treatment and unresectable with metastases. International guidelines for pancreatic neoplasms recommend pathological diagnosis of pancreatic adenocarcinoma prior to chemotherapy. Therefore, endoscopic ultrasound (EUS)-guided tissue acquisition (TA) is usually performed in patients with BR requiring neoadjuvant therapy, or in metastatic disease requiring palliative therapy[1]. The remaining 15%-20% of patients may benefit from EUS-TA prior to surgery; this can confirm pancreatic neoplasms, and reduce the number of unnecessary operations for other similar conditions (e.g., autoimmune pancreatitis, local chronic pancreatitis, and lymphomas). Before the development of EUS-TA, 5%-10% of patients were misdiagnosed with pancreatic cancer and underwent surgery for pancreatic lesions[2-4].

EUS-TA can be divided into EUS-fine-needle aspiration (FNA) using Menghini needles, and EUS-fine-needle biopsy (FNB) using Franseen or fork-tip needles. FNB has equal or better diagnostic accuracy than FNA, with increased tissue volume and decreased number of punctures for diagnosis[5-8]. Moreover, EUS-FNB may provide higher diagnostic yield for peri-hepatic lymph nodes[9]. FNB increases the number of cases for which ancillary tests such as immunohistochemistry and tumor molecular profiling can be performed[9,10]. Therefore, with the advent of personalized medicine and precision therapy, EUS-FNB is rapidly becoming the procedure of choice for EUS-TA of pancreatic cancer. However, EUS-FNA may be used where the FNB needle cannot penetrate small hard lesions; therefore, there is a need for familiarity with both procedures. Conti *et al*[11] also recommend EUS-FNA and FNB in difficult cases of puncture and sampling. Needle size, the negative pressure applied to the needle, and puncture techniques are important for obtaining an adequate specimen in EUS-TA.

Considering recent developments, we present an up-to-date review of the role of EUS-TA in pancreatic cancer. In particular, technical aspects and novel applications for obtaining appropriate specimens during EUS-TA are discussed.

EUS-FNA

EUS-FNA has 87%-92% sensitivity and 96%-98% specificity for the pathological diagnosis of solid pancreatic malignancy[12-15]. FNA needles with calibers ranging from 19-gauge (G)-25G are available, with many studies comparing the different calibers and technical aspects of the EUS-FNA technique. We present a table summarizing the respective characteristics of FNA and FNB, focusing on key points (Table 1).

FNA needle caliber

The small 25G FNA needle may have a technical advantage over larger bore needles when sampling very fibrous, solid lesions. Moreover, its superior flexibility improves operability, especially when sampling pancreatic head and apex masses from the duodenum[1]. Three meta-analyses compared 25G FNA needles with 22G FNA needles. One of them showed increased diagnostic sensitivity (with similar specificity), while the other two showed no significant differences. Therefore, both calibers (25G and 22G needles) can be used when sampling solid pancreatic lesions[16]. Compared with thinner needles, 19G FNA needles are stiffer and harder to manipulate, increasing technical failure when sampling

Table 1 The respective characteristics of fine-needle aspiration and fine-needle biopsy

	EUS-FNA	EUS-FNB
Recommended needle caliber	22-25G	22G or thicker
Recommended negative pressure	Suction or wet suction	Stylet retraction
Recommended puncture technique	Fanning or DKM	Fanning or torque
Recommended number of needle passes	1-3 times for histological diagnosis, depending on site and size	Three times for NGS
Diagnostic accuracy		FNB ≥ FNA
Tissue volume		FNB ≥ FNA
Suitability for NGS		FNB ≥ FNA
MOSE	Recommended for use in combination	Recommended for use in combination
Complications	Rare	Rare
Cost-effectiveness		FNB ≥ FNA

DKM: Door knocking method; G: Gauge; EUS: Endoscopic ultrasound; FNA: Fine-needle aspiration; FNB: Fine-needle biopsy; MOSE: Macroscopic on-site evaluation; NGS: Next-generation sequencing.

pancreatic head lesions[17].

Negative pressure during EUS-FNA

The conventional aspiration method, where 10 mL of negative pressure is applied using a syringe attached to a needle, is recommended because of its higher sensitivity and diagnostic rate[18,19]. In addition, EUS-FNA with 50 mL negative pressure is superior to 10 mL during tissue collection[20]. The wet aspiration method involves precleaning the needle with saline solution, replacing the air column with liquid, and applying negative pressure. Theoretically, this method improves the cell count and sample quality compared with the conventional aspiration and suction methods, as the negative pressure applied from the syringe is better transmitted to the needle tip[21]. In the stylet-throw-pull method, the stylet is slowly and gradually removed (without using a syringe) while the needle is moved within the lesion to create minimal negative pressure. The diagnostic results for solid pancreatic lesions sampled using stylet-throw-pull method are comparable to the conventional aspiration method[22,23].

EUS-FNA puncture technique

The fanning technique is used to collect specimens from multiple sites with a single puncture by fanning the needle back and forth using the elevator of the endoscope and the up/down dial control. The fanning technique improves diagnostic yield, especially in cancerous tumors with necrotic centers. In a study of pancreatic masses, fanning reduced the number of passes required for diagnosis and resulted in a high first-pass diagnostic rate[24]. The door knocking method (DKM), in which the needle is moved forward within the mass so quickly and powerfully that a sound is emitted when a part of the handle hits the needle stopper, did not improve the accuracy of histological diagnosis. However, it enabled the acquisition of a larger amount of tissue specimen compared with the conventional puncture[25]. Thus, DKM may be advantageous for genomic profiling tests; however, to our knowledge, no study has verified this.

Uehara *et al*[26] reported the optimal number of needle passes for accuracy of histological diagnosis: 3 where the head was < 15 mm; 2 where the head was ≥ 15 mm; 2 where the body and tail were ≤ 15 mm; and 1 where the body and tail were ≥ 15 mm. In total, 93% of pancreatic lesions were correctly diagnosed using these numbers of passes. In addition, size of ≤ 15 mm, head location, and neuroendocrine tumors independently required 2 or more needle passes[26].

EUS-FNB FOR HISTOLOGICAL DIAGNOSIS

The desire to collect samples with increased cell counts and preserved tissue structures led to the development of a new type of needle, the FNB needle. This needle is specifically designed to collect core tissue samples. To date, three generations of FNB needles exist. The first generation, the Tru-Cut 19G needle (QuickCore, Cook Endoscopy, Limerick, Ireland), became rapidly outdated due to inflexibility and technical problems[27]. In a randomized controlled trial (RCT) comparing a 19G Tru-Cut needle with a conventional 22G FNA needle in transduodenal EUS-TA of pancreatic head lesions, Sakamoto *et*

al[28] reported that the 22G FNA needle group had significantly higher diagnostic accuracy for malignancy and technical success rate than the 19G Tru-Cut needle group. The second generation of FNB needles, Procore needles (Cook Endoscopy, Limerick, Ireland), were created with a reverse bevel design. More than 10 years after the Tru-Cut needle was introduced, the third generation EUS-FNB needles for core biopsy were developed. They could collect more tissue than the conventional FNA needle, thus improving diagnostic results. Various types of needles have been developed, including the fork type (SharkCore; Medtronic, Minneapolis, MN, United States), flanged type (Acquire; Boston Scientific, Marlborough, MA, United States) (Top-gain; Medi-Globe, Achenmühle, Germany), and 20G FNB needles with forward-facing core traps (ProCore 20G; Cook Medical)[27] (Figure 1). A meta-analysis demonstrated the diagnostic performance of the new generation FNB needles, namely the crown and fork tip needles. They showed a remarkable diagnostic accuracy of 96% for solid pancreatic lesions, with no significant difference between the crown and fork-tip needles (97% and 95%, respectively, $P = 0.8$)[29]. Renelus *et al*[7] conducted a meta-analysis of RCTs published between 2012 and 2019; they found that FNA demonstrated significantly reduced diagnostic accuracy compared with FNB (81% and 87%, respectively, $P = 0.005$). In addition, FNA required an increased number of mean passes compared with FNB (2.3 and 1.6, respectively, $P < 0.0001$). Furthermore, there was no significant difference in the rate of adverse events between FNA and FNB needles (1.8% and 2.3%, respectively, $P = 0.64$)[7].

An RCT analysing cost-effectiveness found that pancreatic mass EUS-FNB (two passes without on-site cytopathology evaluation) was more cost-effective than EUS-FNA (number of passes dictated by on-site cytopathology evaluation). Variables with the largest impact were EUS procedure and sedation cost, specimen adequacy, and diagnostic yield associated with EUS-FNB[30].

THE ERA OF PERSONALIZED AND PRECISION MEDICINE

Several studies have reported increased tissue volume with EUS-FNB samples compared with EUS-FNA. One study reported a 20-fold increase in tissue volume[9,31,32]. Elhanafi *et al*[10] reported that FNB resulted in a higher proportion of sufficient samples for targeted next-generation sequencing (NGS) than FNA (90.9% vs 66.9%; $P = 0.02$). In multivariable modeling, only FNB [odds ratio = 4.95, 95% confidence interval (CI): 1.11-22.05, and $P = 0.04$] was associated with sufficient sampling capacity for genomic testing[10].

Pancreatic ductal adenocarcinoma is anticipated to become the second leading cause of cancer-related mortality by 2030, with high mortality considering the incidence. Given the low median survival time of 12 mo for patients with advanced metastatic pancreatic cancer (ductal adenocarcinoma in particular)[33, 34], urgent new treatments are warranted. Molecular profiling data has recently revealed that up to 25% of pancreatic cancers have actionable molecular changes[35-42], defined as changes with strong clinical or preclinical evidence suggesting specific treatment efficacy[34]. Actionable molecular changes were found in 5.5%-21.7% of EUS-FNA/B specimens from pancreatic ductal adenocarcinoma patients [39,43]. Pishvaian *et al*[34] reported that patients with actionable molecular alterations treated with matched therapy ($n = 46$) had significantly longer median overall survival times than those treated with unmatched therapies [$n = 143$; 2.58 years vs 1.51 years; hazard ratio (HR) 0.42 (95%CI: 0.26-0.68), $P < 0.001$][34]. Therefore, EUS-TA can improve diagnostic accuracy and help ensure successful personalized medicine, with EUS-FNB expected to be particularly useful.

Advances have been made in both tissue collection methods and devices, and genetic analysis technology. The most common genomic alterations noted in metastatic pancreatic cancer specimens are in the KRAS, TP53, CDKN2A, and SMAD4 genes. The first genetic analysis reported using EUS-FNA samples was KRAS mutation analysis. This driver mutation is found in more than 90% of pancreatic cancers, and drugs targeting KRAS mutations, such as Sotrasib, may be effective for pancreatic cancer [27,44]. The DNA mismatch repair (MMR) pathway is an important function that identifies and corrects base pair mismatches in DNA. Loss of MMR function leads to elevated microsatellite instability (MSI)-high, making the MSI test useful for evaluating pembrolizumab response. Sugimoto *et al*[45] reported that in unresectable pancreatic ductal adenocarcinoma, EUS-FNB with the Franseen 22G needle had a higher success rate in MSI analysis than EUS-FNA [FNB, 88.9% (8/9) vs FNA, 35.7% (5/14); $P = 0.03$].

Targeted genome sequencing (TGS) applies polymerase chain reaction technology to construct and sequence a library of specific regions. Currently available multigene NGS systems, such as MSK-IMPACT (Memorial Sloan Kettering Cancer Center, New York, NY, United States) and FoundationOne CDx (F1CDx; Foundation Medicine, Cambridge, MA, United States), screen several hundred cancer-related genes simultaneously as companion diagnostic tests[46,47]. Whole genome sequencing (WGS) can detect various genomic structural alterations (translocations, inversions, duplications, chromosomal aberrations, chromosomal breaks) by obtaining sequence information of the entire genome, including non-coding regions. WGS may be more useful than TGS, but it is significantly more costly, requires more samples, and its superiority in therapeutic selection has not yet been proven[48]. RNA sequencing is a newly developed technology that can identify fusion genes faster, with greater sensitivity, and more efficiently than DNA panels. It can also detect new genes and genetic mutations.



DOI: 10.3748/wjg.v29.i12.1863 Copyright ©The Author(s) 2023.

Figure 1 Examples of needle designs. A: Menghini needle (EZ shot 3, Olympus medical systems, Tokyo, Japan); B: Reverse-beveled needle (ProCore, Cook Medical, Bloomington, IN, United States); C: Franseen needle (AcquireTM, Boston Scientific, Marlborough, MA, United States); D: Fork-tip needle (SharkCore, Medtronic, Minneapolis, MN, United States).

Agents for actionable molecular changes are still being investigated. For example, evidence suggests trametinib in GNAS alterations[49], sotorasib in KRAS G12C alterations[44], olaparib in germline *BRCA1/2* mutation[50], entrectinib in *NTRK* gene fusion[51], pembrolizumab in MSI-high[52,53], and afatinib in NRG1 fusions[54,55] may be effective treatment options. In malignancies such as pancreatic cancer, it is likely that multiple genomic drivers may be present. A combination of compatible drugs with targeting multiple genomic alterations at once may overcome this; however, evidence is lacking, and further studies are needed[56,57]. The application of precision medicine for treating pancreatic ductal adenocarcinoma has just begun, and further development of genetic testing equipment, drugs, and tissue collection devices is required[27].

EUS-FNB FOR THE ERA OF PERSONALIZED AND PRECISION MEDICINE

FNB needle type and caliber

Since EUS-FNB is more suitable than EUS-FNA for personalized medicine, further investigation into needle size and type has been conducted. The abovementioned meta-analysis evaluating crown and fork-tip needles, showed equivalent sample adequacy, diagnostic accuracy, optimal histological core procurement, mean number of needle passes, pooled specificity, and sensitivity of these two FNB needles[29]. Oh *et al*[58] compared 22G with 25G Franseen needles in the three needle passes technique, with suction using 10 mL syringe, and movement within the target lesion at least 10 times using the fanning technique. They reported no diagnostic accuracy difference between the two needles; however, the 22G Franseen needle was superior to the 25G needle in histologic core facilitated easier collection of appropriate specimens for the OncoGuide NCC Oncopanel System [70.0% (49/70) vs 28.6% (20/70), respectively; $P < 0.001$]. The 19G FNB needle was reported to have the potential for easier collection of appropriate specimens for the OncoGuide NCC Oncopanel System compared with the 22G FNB needle, however, concerns were expressed about risks such as bleeding and pancreatic juice leakage[59,60]. For successful personalized medicine, 22G FNB needles are better than 25G ones. However, usage of 19G FNB needles raises concerns regarding accidental injury and harder to manipulate compared with 22G ones.

Negative pressure during EUS-FNB

A randomized controlled trial of tissue samples from patients with pancreatic masses on imaging compared collection techniques using Menghini-tip, reverse-bevel, Franseen, and fork-tip needles. A second randomized control, patient-by-patient analysis, compared the use of suction, no suction, and stylet retraction during biopsies. The biopsy samples collected by fork-tip or Franseen needles had significantly higher cellularity than those collected by Menghini-tip needles or reverse-bevels ($P < 0.001$). The predictors of high cellularity for pancreatic masses showed that Franseen needles, fork-tip needles, not applying suction, stylet retraction, and pancreatic mass size of > 3 cm were associated with high cellularity. Therefore, they recommended using a negative pressure technique with every EUS-TA needle for an optimal outcome, as shown in Table 2[61]. Stylet retraction and standard suction technique may be equivalent when using the 20G reverse-beveled needle[62]; however, the stylet retraction technique is considered equally or more useful than the standard suction technique when performing EUS-FNB.

EUS-FNB puncture technique

Sample quality scores were significantly higher when obtained by the torque and fanning techniques rather than the standard one ($P < 0.001$)[63]. The new torque technique consists of turning the echoendoscope counterclockwise or clockwise while repeated to-and-fro movements are performed to reach multiple areas within the lesion; this is obtained by maneuvering the "up-down" articulating dial of the echoendoscope. Conversely, in the standard technique, the mass is pierced by the tip of the needle in a unidirectional movement. Studies on FNA needles suggest that the DKM may be useful for increasing cell volume[25]; however, there are no specific studies on DKM in FNB.

The European Society of Gastrointestinal Endoscopy recommends that 2-3 needle passes are sufficient to ensure a sensitivity of at least 90% for the diagnosis of malignancy[16]. However, evidence on the number of needle passes required for successful personalized medicine is lacking. In a few recent retrospective studies, a median number of 3 FNB needle passes (interquartile range 3-4) yielded sufficient tissue for targeted NGS in 91% of patients[10].

Based on these findings, we believe that the EUS-TA strategy with three or more punctures, the stylet retraction method, the torque or fanning technique, and a 22-G or thicker FNB needle may be effective in patients with solid pancreatic tumors scheduled for treatment, including personalized medicine.

RAPID ON-SITE PATHOLOGIST EVALUATION AND MACROSCOPIC ON-SITE QUALITY EVALUATION

It is unclear whether an on-site pathologist improves the diagnostic accuracy of EUS-FNA for solid pancreatic lesions; however, Rapid On-Site Pathologist Evaluation (ROSE) can reduce the number of needle passes required to obtain a pathological diagnosis[64,65]. The subsequent introduction of the FNB needle has made it possible to collect large quantities of macroscopic white samples. A recent global, randomized trial showed that ROSE did not affect the diagnostic accuracy of EUS-FNB (96.4% with ROSE vs 97.4% without ROSE, $P = 0.396$)[66]. In addition, the application of ROSE is limited by the availability and additional cost of trained cytopathologists at each facility; therefore, ROSE is unlikely to be recommended for future diagnostic practice[67].

Direct observation of specimens obtained by FNA/B, macroscopic on-site evaluation (MOSE), is more feasible and readily available alternative to ROSE[68,69]. Kaneko *et al*[70] showed that the macroscopic visible core (MVC) length and histological sample quantity were positively correlated in EUS-FNB using a 22G Franseen needle. Multivariate analysis showed that MVC length ≥ 30 mm on MOSE was a significant factor affecting suitability for NGS (odds ratio 6.19; 95%CI: 2.72-14.10).

NEEDLE TRACT SEEDING

Theoretically, cancer seeding through the needle tract may occur more frequently in the body or tail of the lesion when using the transgastric approach, than in the head of the lesion using the transduodenal approach[71]. This is because the EUS-FNA tract of pancreatic head cancers is later resected in a blocked fashion along with the pancreatic head in curative surgery. In contrast, the EUS-FNA tract of lesions in the body or tail lies beyond the surgical resection margin[72,73].

Ngamruengphong *et al*[73] reported that EUS-FNA for pancreatic head, body, and tail cancers was marginally associated with improved overall survival (HR 0.84, 95%CI: 0.72-0.99) but did not affect cancer-specific survival (HR 0.87, 95%CI: 0.74-1.03). Park *et al*[74] reported 528 patients with distal pancreatic cancer who underwent distal pancreatectomy. Among these, 193 were treated using EUS-FNA, and 335 were not. The between-group recurrence rates were comparable (EUS-FNA, 72.7%; non-EUS-FNA, 75%; $P = 0.58$) at follow-up (median, 21.7 mo), with similar cancer-free survival ($P = 0.58$), showing that preoperative EUS-FNA does not reduce cancer-specific or overall survival[74]. However,

Table 2 Recommended negative pressure procedural technique for each endoscopic ultrasound-guided tissue acquisition needle to achieve optimal outcomes[61]

Needle type	Best cellularity	Best diagnostic accuracy	Best overall outcome (specimen)
Menghini	Stylet retraction = suction = no suction	Suction	Suction
Reverse-bevel	Stylet retraction = suction	Suction	Suction
Franseen	Stylet retraction	Stylet retraction = suction	Stylet retraction
Fork-tip	Stylet retraction = no suction	Stylet retraction = suction	Stylet retraction

as gastric wall recurrence only occurred in patients treated using EUS-FNA ($n = 2$), clinicians must consider the potential risks of needle tract seeding, and patients should be carefully selected[74]. Yane *et al*[75] also reported that the 5-year cumulative needle tract seeding rate, estimated using Fine and Gray's method, was 3.8% (95%CI: 1.6%-7.8%). They concluded that, although preoperative EUS-FNA for pancreatic body and tail cancers has no negative effect on recurrence-free survival or overall survival, needle tract seeding after EUS-FNA was observed to have a non-negligible rate[75]. Sakamoto reported that among the six cases with needle tract seeding occurred, it was revealed by upper gastrointestinal endoscopy in four. They suggested upper gastrointestinal endoscopy follow-up, as well as computed tomography, in patients who undergo gastric EUS-FNA before distal pancreatectomy to identify needle tract seeding at soon as possible[76].

CONCLUSION

Since pancreatic cancer treatment is highly invasive and EUS-TA does not worsen cancer-specific prognosis, histological diagnosis should be made to establish effective treatment options. Furthermore, with genomic profiling, a large volume of tissue are needed from each biopsy; Franseen and Fork-tip needles should be the first choice for this purpose. EUS-TA involving three or more punctures using the stylet retraction method and the torque or fanning technique with a 22-G FNB or thicker needle is the most effective tissue-sampling method for patients with solid pancreatic tumors scheduled for treatment, including those receiving personalized medicine. The prediction of MOSE histological specimen volume by measuring MVC length may have clinical significance, especially when submitting specimens for NGS. The application of precision medicine for treating pancreatic ductal adenocarcinoma has just begun, and further development of genetic testing equipment, drugs, tissue collection devices, and puncture technique is required.

ACKNOWLEDGEMENTS

Table 2 in this paper is adapted from Figure 5 of a report titled “Comparing Needles and Methods of Endoscopic Ultrasound-Guided Fine-Needle Biopsy to Optimize Specimen Quality and Diagnostic Accuracy for Patients With Pancreatic Masses in a Randomized Trial”. We thank Young Bang *et al* and “Clinical Gastroenterology and Hepatology” for granting us permission to use it on December 26, 2022.

FOOTNOTES

Author contributions: Masuda S and Koizumi K were major contributors to writing the manuscript; Shionoya K, Jinushi R, Makazu M, Nishino T, and Kimura K designed the outline and coordinated the writing of the manuscript; Sumida C, Kubota J, Ichita C, Sasaki A, Kobayashi M, Kako M, and Haruki U provided input for writing the paper.

Conflict-of-interest statement: The authors declare that they have no conflicts of interest.

Open-Access: This article is an open-access article that was selected by an in-house editor and fully peer-reviewed by external reviewers. It is distributed in accordance with the Creative Commons Attribution NonCommercial (CC BY-NC 4.0) license, which permits others to distribute, remix, adapt, build upon this work non-commercially, and license their derivative works on different terms, provided the original work is properly cited and the use is non-commercial. See: <https://creativecommons.org/Licenses/by-nc/4.0/>

Country/Territory of origin: Japan

ORCID number: Sakue Masuda 0000-0002-8127-0154; Kazuya Koizumi 0000-0002-3677-5030; Kento Shionoya 0000-0002-

8399-4797; Takashi Nishino 0000-0002-6717-1096; Karen Kimura 0000-0001-8165-1777; Chihiro Sumida 0000-0002-4616-6407; Chikamasa Ichita 0000-0001-9210-7371; Akiko Sasaki 0000-0003-4219-554X; Makoto Kako 0000-0002-6447-8471; Uojima Haruki 0000-0003-1719-1352.

Corresponding Author's Membership in Professional Societies: The Japanese Society of Gastroenterology; Japan Biliary Association; Japan Gastroenterological Endoscopy Society; Japan Pancreas Society; The Japan Society of Hepatology; The Japanese Society of Internal Medicine.

S-Editor: Yan JP

L-Editor: A

P-Editor: Yan JP

REFERENCES

- 1 **Marques S**, Bispo M, Rio-Tinto R, Fidalgo P, Devière J. The Impact of Recent Advances in Endoscopic Ultrasound-Guided Tissue Acquisition on the Management of Pancreatic Cancer. *GE Port J Gastroenterol* 2021; **28**: 185-192 [PMID: 34056041 DOI: 10.1159/000510730]
- 2 **Smith CD**, Behrns KE, van Heerden JA, Sarr MG. Radical pancreateoduodenectomy for misdiagnosed pancreatic mass. *Br J Surg* 1994; **81**: 585-589 [PMID: 7911387 DOI: 10.1002/bjs.1800810435]
- 3 **Thompson JS**, Murayama KM, Edney JA, Rikkers LF. Pancreaticoduodenectomy for suspected but unproven malignancy. *Am J Surg* 1994; **168**: 571-3; discussion 573 [PMID: 7977998 DOI: 10.1016/s0002-9610(05)80124-2]
- 4 **Abraham SC**, Wilentz RE, Yeo CJ, Sohn TA, Cameron JL, Boitnott JK, Hruban RH. Pancreaticoduodenectomy (Whipple resections) in patients without malignancy: are they all 'chronic pancreatitis'? *Am J Surg Pathol* 2003; **27**: 110-120 [PMID: 12502933 DOI: 10.1097/00000478-200301000-00012]
- 5 **van Riet PA**, Larghi A, Attili F, Rindi G, Nguyen NQ, Ruszkiewicz A, Kitano M, Chikugo T, Aslanian H, Farrell J, Robert M, Adeniran A, Van Der Merwe S, Roskams T, Chang K, Lin F, Lee JG, Arcidiacono PG, Petrone M, Doglioni C, Iglesias-Garcia J, Abdulkader I, Giovannini M, Bories E, Poizat F, Santo E, Scapa E, Marmor S, Bucobo JC, Buscaglia JM, Heimann A, Wu M, Baldaque-Silva F, Moro CF, Erler NS, Biermann K, Poley JW, Cahen DL, Bruno MJ. A multicenter randomized trial comparing a 25-gauge EUS fine-needle aspiration device with a 20-gauge EUS fine-needle biopsy device. *Gastrointest Endosc* 2019; **89**: 329-339 [PMID: 30367877 DOI: 10.1016/j.gie.2018.10.026]
- 6 **Bang JY**, Kirtane S, Krall K, Navaneethan U, Hasan M, Hawes R, Varadarajulu S. In memoriam: Fine-needle aspiration, birth: Fine-needle biopsy: The changing trend in endoscopic ultrasound-guided tissue acquisition. *Dig Endosc* 2019; **31**: 197-202 [PMID: 30256458 DOI: 10.1111/den.13280]
- 7 **Renelus BD**, Jamorabo DS, Boston I, Briggs WM, Poneros JM. Endoscopic Ultrasound-Guided Fine Needle Biopsy Needles Provide Higher Diagnostic Yield Compared to Endoscopic Ultrasound-Guided Fine Needle Aspiration Needles When Sampling Solid Pancreatic Lesions: A Meta-Analysis. *Clin Endosc* 2021; **54**: 261-268 [PMID: 32892519 DOI: 10.5946/ce.2020.101]
- 8 **Facciorusso A**, Bajwa HS, Menon K, Buccino VR, Muscatiello N. Comparison between 22G aspiration and 22G biopsy needles for EUS-guided sampling of pancreatic lesions: A meta-analysis. *Endosc Ultrasound* 2020; **9**: 167-174 [PMID: 31031330 DOI: 10.4103/eus.eus_4_19]
- 9 **Levine I**, Trindade AJ. Endoscopic ultrasound fine needle aspiration vs fine needle biopsy for pancreatic masses, subepithelial lesions, and lymph nodes. *World J Gastroenterol* 2021; **27**: 4194-4207 [PMID: 34326619 DOI: 10.3748/wjg.v27.i26.4194]
- 10 **Elhanafi S**, Mahmud N, Vergara N, Kochman ML, Das KK, Ginsberg GG, Rajala M, Chandrasekhara V. Comparison of endoscopic ultrasound tissue acquisition methods for genomic analysis of pancreatic cancer. *J Gastroenterol Hepatol* 2019; **34**: 907-913 [PMID: 30422342 DOI: 10.1111/jgh.14540]
- 11 **Conti CB**, Cereatti F, Grassia R. Endoscopic ultrasound-guided sampling of solid pancreatic masses: the fine needle aspiration or fine needle biopsy dilemma. Is the best needle yet to come? *World J Gastrointest Endosc* 2019; **11**: 454-471 [PMID: 31523377 DOI: 10.4253/wjge.v11.i8.454]
- 12 **Banafea O**, Mghanga FP, Zhao J, Zhao R, Zhu L. Endoscopic ultrasonography with fine-needle aspiration for histological diagnosis of solid pancreatic masses: a meta-analysis of diagnostic accuracy studies. *BMC Gastroenterol* 2016; **16**: 108 [PMID: 27580856 DOI: 10.1186/s12876-016-0519-z]
- 13 **Hewitt MJ**, McPhail MJ, Possamai L, Dhar A, Vlavianos P, Monahan KJ. EUS-guided FNA for diagnosis of solid pancreatic neoplasms: a meta-analysis. *Gastrointest Endosc* 2012; **75**: 319-331 [PMID: 22248600 DOI: 10.1016/j.gie.2011.08.049]
- 14 **Puli SR**, Bechtold ML, Buxbaum JL, Eloubeidi MA. How good is endoscopic ultrasound-guided fine-needle aspiration in diagnosing the correct etiology for a solid pancreatic mass? *Pancreas* 2013; **42**: 20-26 [PMID: 23254913 DOI: 10.1097/MPA.0b013e3182546e79]
- 15 **Chen J**, Yang R, Lu Y, Xia Y, Zhou H. Diagnostic accuracy of endoscopic ultrasound-guided fine-needle aspiration for solid pancreatic lesion: a systematic review. *J Cancer Res Clin Oncol* 2012; **138**: 1433-1441 [PMID: 22752601 DOI: 10.1007/s00432-012-1268-1]
- 16 **Polkowski M**, Jenssen C, Kaye P, Carrara S, Deprez P, Gines A, Fernández-Esparrach G, Eisendrath P, Aithal GP, Arcidiacono P, Barthet M, Bastos P, Fornelli A, Napoleon B, Iglesias-Garcia J, Seicean A, Larghi A, Hassan C, van Hooft JE, Dumonceau JM. Technical aspects of endoscopic ultrasound (EUS)-guided sampling in gastroenterology: European Society of Gastrointestinal Endoscopy (ESGE) Technical Guideline - March 2017. *Endoscopy* 2017; **49**: 989-1006 [PMID: 28898917 DOI: 10.1055/s-0043-119219]

17 **Song TJ**, Kim JH, Lee SS, Eum JB, Moon SH, Park DY, Seo DW, Lee SK, Jang SJ, Yun SC, Kim MH. The prospective randomized, controlled trial of endoscopic ultrasound-guided fine-needle aspiration using 22G and 19G aspiration needles for solid pancreatic or peripancreatic masses. *Am J Gastroenterol* 2010; **105**: 1739-1745 [PMID: 20216532 DOI: 10.1038/ajg.2010.108]

18 **Tarantino I**, Di Mitri R, Fabbri C, Pagano N, Barresi L, Granata A, Liotta R, Moccia F, Maimone A, Baccarini P, Fabio T, Curcio G, Repici A, Traina M. Is diagnostic accuracy of fine needle aspiration on solid pancreatic lesions aspiration-related? *Dig Liver Dis* 2014; **46**: 523-526 [PMID: 24704290 DOI: 10.1016/j.dld.2014.02.023]

19 **Lee JK**, Choi JH, Lee KH, Kim KM, Shin JU, Lee JK, Lee KT, Jang KT. A prospective, comparative trial to optimize sampling techniques in EUS-guided FNA of solid pancreatic masses. *Gastrointest Endosc* 2013; **77**: 745-751 [PMID: 23433878 DOI: 10.1016/j.gie.2012.12.009]

20 **Kudo T**, Kawakami H, Hayashi T, Yasuda I, Mukai T, Inoue H, Katanuma A, Kawakubo K, Ishiwatari H, Doi S, Yamada R, Maguchi H, Isayama H, Mitsuhashi T, Sakamoto N; Japan EUS-FNA Negative Pressure Suction Study Group. High and low negative pressure suction techniques in EUS-guided fine-needle tissue acquisition by using 25-gauge needles: a multicenter, prospective, randomized, controlled trial. *Gastrointest Endosc* 2014; **80**: 1030-7.e1 [PMID: 24890422 DOI: 10.1016/j.gie.2014.04.012]

21 **Attam R**, Arain MA, Bloechl SJ, Trikudanathan G, Munigala S, Bakman Y, Singh M, Wallace T, Henderson JB, Catalano MF, Guda NM. "Wet suction technique (WEST)": a novel way to enhance the quality of EUS-FNA aspirate. Results of a prospective, single-blind, randomized, controlled trial using a 22-gauge needle for EUS-FNA of solid lesions. *Gastrointest Endosc* 2015; **81**: 1401-1407 [PMID: 25733127 DOI: 10.1016/j.gie.2014.11.023]

22 **Kin T**, Katanuma A, Yane K, Takahashi K, Osanai M, Takaki R, Matsumoto K, Gon K, Matsumori T, Tomonari A, Maguchi H, Shinohara T, Nojima M. Diagnostic ability of EUS-FNA for pancreatic solid lesions with conventional 22-gauge needle using the slow pull technique: a prospective study. *Scand J Gastroenterol* 2015; **50**: 900-907 [PMID: 25732902 DOI: 10.3109/00365521.2014.983155]

23 **Saxena P**, El Zein M, Stevens T, Abdelgelil A, Besharati S, Messallam A, Kumbhari V, Azola A, Brainard J, Shin EJ, Lennon AM, Canto MI, Singh VK, Khashab MA. Stylet slow-pull *versus* standard suction for endoscopic ultrasound-guided fine-needle aspiration of solid pancreatic lesions: a multicenter randomized trial. *Endoscopy* 2018; **50**: 497-504 [PMID: 29272906 DOI: 10.1055/s-0043-122381]

24 **Bang JY**, Magee SH, Ramesh J, Trevino JM, Varadarajulu S. Randomized trial comparing fanning with standard technique for endoscopic ultrasound-guided fine-needle aspiration of solid pancreatic mass lesions. *Endoscopy* 2013; **45**: 445-450 [PMID: 23504490 DOI: 10.1055/s-0032-1326268]

25 **Mukai S**, Itoi T, Ashida R, Tsuchiya T, Ikeuchi N, Kamada K, Tanaka R, Umeda J, Tonozuka R, Fukutake N, Hoshi K, Moriyasu F, Gotoda T, Irisawa A. Multicenter, prospective, crossover trial comparing the door-knocking method with the conventional method for EUS-FNA of solid pancreatic masses (with videos). *Gastrointest Endosc* 2016; **83**: 1210-1217 [PMID: 26522372 DOI: 10.1016/j.gie.2015.10.025]

26 **Uehara H**, Sueyoshi H, Takada R, Fukutake N, Katayama K, Ashida R, Ioka T, Takenaka A, Nagata S, Tomita Y. Optimal number of needle passes in endoscopic ultrasound-guided fine needle aspiration for pancreatic lesions. *Pancreatology* 2015; **15**: 392-396 [PMID: 25979252 DOI: 10.1016/j.pan.2015.04.005]

27 **Ashida R**, Kitano M. Endoscopic ultrasound-guided tissue acquisition for pancreatic ductal adenocarcinoma in the era of precision medicine. *Dig Endosc* 2022; **34**: 1329-1339 [PMID: 35488448 DOI: 10.1111/den.14344]

28 **Sakamoto H**, Kitano M, Komaki T, Noda K, Chikugo T, Dote K, Takeyama Y, Das K, Yamao K, Kudo M. Prospective comparative study of the EUS guided 25-gauge FNA needle with the 19-gauge Trucut needle and 22-gauge FNA needle in patients with solid pancreatic masses. *J Gastroenterol Hepatol* 2009; **24**: 384-390 [PMID: 19032453 DOI: 10.1111/j.1440-1746.2008.05636.x]

29 **Facciorusso A**, Del Prete V, Buccino VR, Purohit P, Setia P, Muscatiello N. Diagnostic yield of Franseen and Fork-Tip biopsy needles for endoscopic ultrasound-guided tissue acquisition: a meta-analysis. *Endosc Int Open* 2019; **7**: E1221-E1230 [PMID: 31579703 DOI: 10.1055/a-0982-2997]

30 **Aadam AA**, Wani S, Amick A, Shah JN, Bhat YM, Hamerski CM, Klapman JB, Muthusamy VR, Watson RR, Rademaker AW, Keswani RN, Keefer L, Das A, Komanduri S. A randomized controlled cross-over trial and cost analysis comparing endoscopic ultrasound fine needle aspiration and fine needle biopsy. *Endosc Int Open* 2016; **4**: E497-E505 [PMID: 27227104 DOI: 10.1055/s-0042-106958]

31 **Bang JY**, Hebert-Magee S, Navaneethan U, Hasan MK, Hawes R, Varadarajulu S. EUS-guided fine needle biopsy of pancreatic masses can yield true histology. *Gut* 2018; **67**: 2081-2084 [PMID: 28988195 DOI: 10.1136/gutjnl-2017-315154]

32 **Mukai S**, Itoi T, Yamaguchi H, Sofuni A, Tsuchiya T, Tanaka R, Tonozuka R, Honjo M, Fujita M, Yamamoto K, Matsunami Y, Asai Y, Kurosawa T, Nagakawa Y. A retrospective histological comparison of EUS-guided fine-needle biopsy using a novel franseen needle and a conventional end-cut type needle. *Endosc Ultrasound* 2019; **8**: 50-57 [PMID: 29786033 DOI: 10.4103/eus.eus_11_18]

33 **Rahib L**, Smith BD, Aizenberg R, Rosenzweig AB, Fleshman JM, Matrisian LM. Projecting cancer incidence and deaths to 2030: the unexpected burden of thyroid, liver, and pancreas cancers in the United States. *Cancer Res* 2014; **74**: 2913-2921 [PMID: 24840647 DOI: 10.1158/0008-5472.CAN-14-0155]

34 **Pishvaian MJ**, Blais EM, Brody JR, Lyons E, DeArbeloa P, Hendifar A, Mikhail S, Chung V, Sahai V, Sohal DPS, Bellakbira S, Thach D, Rahib L, Madhavan S, Matrisian LM, Petricoin EF 3rd. Overall survival in patients with pancreatic cancer receiving matched therapies following molecular profiling: a retrospective analysis of the Know Your Tumor registry trial. *Lancet Oncol* 2020; **21**: 508-518 [PMID: 32135080 DOI: 10.1016/S1470-2045(20)30074-7]

35 **Aguirre AJ**, Nowak JA, Camarda ND, Moffitt RA, Ghazani AA, Hazar-Rethinam M, Raghavan S, Kim J, Brais LK, Ragon D, Welch MW, Reilly E, McCabe D, Marini L, Anderka K, Helvie K, Oliver N, Babic A, Da Silva A, Nadres B, Van Sevenster EE, Shahzade HA, St Pierre JP, Burke KP, Clancy T, Cleary JM, Doyle LA, Jajoo K, McCleary NJ, Meyerhardt JA, Murphy JE, Ng K, Patel AK, Perez K, Rosenthal MH, Robinson DA, Ryou M, Shapiro GI, Sicinska E, Silverman SG, Nagy RJ, Lanman RB, Knoerzer D, Welsch DJ, Yurgelun MB, Fuchs CS, Garraway LA, Getz G, Hornick JL, Johnson BE, Kulke MH, Mayer RJ, Miller JW, Shyn PB, Tuveson DA, Wagle N, Yeh JJ, Hahn WC, Corcoran RB,

Carter SL, Wolpin BM. Real-time Genomic Characterization of Advanced Pancreatic Cancer to Enable Precision Medicine. *Cancer Discov* 2018; **8**: 1096-1111 [PMID: 29903880 DOI: 10.1158/2159-8290.CD-18-0275]

36 **Bailey P**, Chang DK, Nones K, Johns AL, Patch AM, Gingras MC, Miller DK, Christ AN, Bruxner TJ, Quinn MC, Nourse C, Murtaugh LC, Harliwong I, Idrisoglu S, Manning S, Nourbakhsh E, Wani S, Fink L, Holmes O, Chin V, Anderson MJ, Kazakoff S, Leonard C, Newell F, Waddell N, Wood S, Xu Q, Wilson PJ, Cloonan N, Kassahn KS, Taylor D, Quek K, Robertson A, Pantano L, Mincarelli L, Sanchez LN, Evers L, Wu J, Pines M, Cowley MJ, Jones MD, Colvin EK, Nagrial AM, Humphrey ES, Chantrill LA, Mawson A, Humphris J, Chou A, Pajic M, Scarlett CJ, Pinho AV, Giry-Laterriere M, Rooman I, Samra JS, Kench JG, Lovell JA, Merrett ND, Toon CW, Epari K, Nguyen NQ, Barbour A, Zeps N, Moran-Jones K, Jamieson NB, Graham JS, Duthie F, Oien K, Hair J, Grützmann R, Maitra A, Iacobuzio-Donahue CA, Wolfgang CL, Morgan RA, Lawlor RT, Corbo V, Bassi C, Rusev B, Capelli P, Salvia R, Tortora G, Mukhopadhyay D, Petersen GM; Australian Pancreatic Cancer Genome Initiative, Munzny DM, Fisher WE, Karim SA, Eshleman JR, Hruban RH, Pilarsky C, Morton JP, Sansom OJ, Scarpa A, Musgrove EA, Bailey UM, Hofmann O, Sutherland RL, Wheeler DA, Gill AJ, Gibbs RA, Pearson JV, Waddell N, Biankin AV, Grimmond SM. Genomic analyses identify molecular subtypes of pancreatic cancer. *Nature* 2016; **531**: 47-52 [PMID: 26909576 DOI: 10.1038/nature16965]

37 **Biankin AV**, Waddell N, Kassahn KS, Gingras MC, Muthuswamy LB, Johns AL, Miller DK, Wilson PJ, Patch AM, Wu J, Chang DK, Cowley MJ, Gardiner BB, Song S, Harliwong I, Idrisoglu S, Nourse C, Nourbakhsh E, Manning S, Wani S, Gongora M, Pajic M, Scarlett CJ, Gill AJ, Pinho AV, Rooman I, Anderson M, Holmes O, Leonard C, Taylor D, Wood S, Xu Q, Nones K, Fink JL, Christ A, Bruxner T, Cloonan N, Newell F, Pines M, Mead RS, Humphris JL, Kaplan W, Jones MD, Colvin EK, Nagrial AM, Humphrey ES, Chou A, Chin VT, Chantrill LA, Mawson A, Samra JS, Kench JG, Lovell JA, Daly RJ, Merrett ND, Toon C, Epari K, Nguyen NQ, Barbour A, Zeps N; Australian Pancreatic Cancer Genome Initiative, Kakkar N, Zhao F, Wu YQ, Wang M, Muzny DM, Fisher WE, Brunicardi FC, Hodges SE, Reid JG, Drummond J, Chang K, Han Y, Lewis LR, Dinh H, Buhay CJ, Beck T, Timms L, Sam M, Begley K, Brown A, Pai D, Panchal A, Buchner N, De Borja R, Denroche RE, Yung CK, Serra S, Onetto N, Mukhopadhyay D, Tsao MS, Shaw PA, Petersen GM, Gallinger S, Hruban RH, Maitra A, Iacobuzio-Donahue CA, Schulick RD, Wolfgang CL, Morgan RA, Lawlor RT, Capelli P, Corbo V, Scardoni M, Tortora G, Tempero MA, Mann KM, Jenkins NA, Perez-Mancera PA, Adams DJ, Largaespada DA, Wessels LF, Rust AG, Stein LD, Tuveson DA, Copeland NG, Musgrove EA, Scarpa A, Eshleman JR, Hudson TJ, Sutherland RL, Wheeler DA, Pearson JV, McPherson JD, Gibbs RA, Grimmond SM. Pancreatic cancer genomes reveal aberrations in axon guidance pathway genes. *Nature* 2012; **491**: 399-405 [PMID: 23103869 DOI: 10.1038/nature11547]

38 **Collisson EA**, Sadanandam A, Olson P, Gibb WJ, Truitt M, Gu S, Cooc J, Weinkle J, Kim GE, Jakkula L, Feiler HS, Ko AH, Olshen AB, Danenberg KL, Tempero MA, Spellman PT, Hanahan D, Gray JW. Subtypes of pancreatic ductal adenocarcinoma and their differing responses to therapy. *Nat Med* 2011; **17**: 500-503 [PMID: 21460848 DOI: 10.1038/nm.2344]

39 **Lowery MA**, Jordan EJ, Basturk O, Ptashkin RN, Zehir A, Berger MF, Leach T, Herbst B, Askan G, Maynard H, Glassman D, Covington C, Schultz N, Abou-Alfa GK, Harding JJ, Klimstra DS, Hechtman JF, Hyman DM, Allen PJ, Jarnagin WR, Balachandran VP, Varghese AM, Schattner MA, Yu KH, Saltz LB, Solit DB, Iacobuzio-Donahue CA, Leach SD, O'Reilly EM. Real-Time Genomic Profiling of Pancreatic Ductal Adenocarcinoma: Potential Actionability and Correlation with Clinical Phenotype. *Clin Cancer Res* 2017; **23**: 6094-6100 [PMID: 28754816 DOI: 10.1158/1078-0432.CCR-17-0899]

40 **Moffitt RA**, Marayati R, Flate EL, Volmar KE, Loeza SG, Hoadley KA, Rashid NU, Williams LA, Eaton SC, Chung AH, Smyla JK, Anderson JM, Kim HJ, Bentrem DJ, Talamonti MS, Iacobuzio-Donahue CA, Hollingsworth MA, Yeh JJ. Virtual microdissection identifies distinct tumor- and stroma-specific subtypes of pancreatic ductal adenocarcinoma. *Nat Genet* 2015; **47**: 1168-1178 [PMID: 26343385 DOI: 10.1038/ng.3398]

41 **Waddell N**, Pajic M, Patch AM, Chang DK, Kassahn KS, Bailey P, Johns AL, Miller D, Nones K, Quek K, Quinn MC, Robertson AJ, Fadlullah MZ, Bruxner TJ, Christ AN, Harliwong I, Idrisoglu S, Manning S, Nourse C, Nourbakhsh E, Wani S, Wilson PJ, Markham E, Cloonan N, Anderson MJ, Fink JL, Holmes O, Kazakoff SH, Leonard C, Newell F, Poudel B, Song S, Taylor D, Waddell N, Wood S, Xu Q, Wu J, Pines M, Cowley MJ, Lee HC, Jones MD, Nagrial AM, Humphris J, Chantrill LA, Chin V, Steinmann AM, Mawson A, Humphrey ES, Colvin EK, Chou A, Scarlett CJ, Pinho AV, Giry-Laterriere M, Rooman I, Samra JS, Kench JG, Pettitt JA, Merrett ND, Toon C, Epari K, Nguyen NQ, Barbour A, Zeps N, Jamieson NB, Graham JS, Niclou SP, Bjerkvig R, Grützmann R, Aust D, Hruban RH, Maitra A, Iacobuzio-Donahue CA, Wolfgang CL, Morgan RA, Lawlor RT, Corbo V, Bassi C, Falconi M, Zamboni G, Tortora G, Tempero MA; Australian Pancreatic Cancer Genome Initiative, Gill AJ, Eshleman JR, Pilarsky C, Scarpa A, Musgrove EA, Pearson JV, Biankin AV, Grimmond SM. Whole genomes redefine the mutational landscape of pancreatic cancer. *Nature* 2015; **518**: 495-501 [PMID: 25719666 DOI: 10.1038/nature14169]

42 **Witkiewicz AK**, McMillan EA, Balaji U, Baek G, Lin WC, Mansour J, Mollaee M, Wagner KU, Koduru P, Yopp A, Choti MA, Yeo CJ, McCue P, White MA, Knudsen ES. Whole-exome sequencing of pancreatic cancer defines genetic diversity and therapeutic targets. *Nat Commun* 2015; **6**: 6744 [PMID: 25855536 DOI: 10.1038/ncomms7744]

43 **Semaan A**, Bernard V, Lee JJ, Wong JW, Huang J, Swartzlander DB, Stephens BM, Monberg ME, Weston BR, Bhutani MS, Chang K, Scheet PA, Maitra A, Jakubek YA, Guerrero PA. Defining the Comprehensive Genomic Landscapes of Pancreatic Ductal Adenocarcinoma Using Real-World Endoscopic Aspiration Samples. *Clin Cancer Res* 2021; **27**: 1082-1093 [PMID: 33188144 DOI: 10.1158/1078-0432.CCR-20-2667]

44 **Hong DS**, Kuo J, Sacher AG, Barlesi F, Besse B, Kuboki Y, Dy GK, Dembla V, Krauss JC, Burns TF, Kim J, Henary H, Ngarmchananrith G, Li BT. CodeBreak 100: Phase I study of AMG 510, a novel KRASG12C inhibitor, in patients (pts) with advanced solid tumors other than non-small cell lung cancer (NSCLC) and colorectal cancer (CRC). *J Clin Orthod* 2020; **38**: 3511-3511 [DOI: 10.1200/jco.2020.38.15_suppl.3511]

45 **Sugimoto M**, Irie H, Takagi T, Suzuki R, Konno N, Asama H, Sato Y, Nakamura J, Takasumi M, Hashimoto M, Kato T, Kobashi R, Kobayashi Y, Hashimoto Y, Hikichi T, Ohira H. Efficacy of EUS-guided FNB using a Franseen needle for tissue acquisition and microsatellite instability evaluation in unresectable pancreatic lesions. *BMC Cancer* 2020; **20**: 1094 [PMID: 33176750 DOI: 10.1186/s12885-020-07588-5]

46 **Cheng DT**, Mitchell TN, Zehir A, Shah RH, Benayed R, Syed A, Chandramohan R, Liu ZY, Won HH, Scott SN, Brannon

AR, O'Reilly C, Sadowska J, Casanova J, Yannes A, Hechtman JF, Yao J, Song W, Ross DS, Oultache A, Dogan S, Borsu L, Hameed M, Nafa K, Arcila ME, Ladanyi M, Berger MF. Memorial Sloan Kettering-Integrated Mutation Profiling of Actionable Cancer Targets (MSK-IMPACT): A Hybridization Capture-Based Next-Generation Sequencing Clinical Assay for Solid Tumor Molecular Oncology. *J Mol Diagn* 2015; **17**: 251-264 [PMID: 25801821 DOI: 10.1016/j.jmoldx.2014.12.006]

47 **Allegretti M**, Fabi A, Buglioni S, Martayan A, Conti L, Pescarmona E, Ciliberto G, Giacomini P. Tearing down the walls: FDA approves next generation sequencing (NGS) assays for actionable cancer genomic aberrations. *J Exp Clin Cancer Res* 2018; **37**: 47 [PMID: 29506529 DOI: 10.1186/s13046-018-0702-x]

48 **Golan T**, O'Kane GM, Denroche RE, Raitses-Gurevich M, Grant RC, Holter S, Wang Y, Zhang A, Jang GH, Stossel C, Atias D, Halperin S, Berger R, Glick Y, Park JP, Cuggia A, Williamson L, Wong HL, Schaeffer DF, Renouf DJ, Borgida A, Dodd A, Wilson JM, Fischer SE, Notta F, Knox JJ, Zogopoulos G, Gallinger S. Genomic Features and Classification of Homologous Recombination Deficient Pancreatic Ductal Adenocarcinoma. *Gastroenterology* 2021; **160**: 2119-2132.e9 [PMID: 33524400 DOI: 10.1053/j.gastro.2021.01.220]

49 **Parish AJ**, Nguyen V, Goodman AM, Murugesan K, Frampton GM, Kurzrock R. GNAS, GNAQ, and GNA11 alterations in patients with diverse cancers. *Cancer* 2018; **124**: 4080-4089 [PMID: 30204251 DOI: 10.1002/cncr.31724]

50 **Golan T**, Hammel P, Reni M, Van Cutsem E, Macarulla T, Hall MJ, Park JO, Hochhauser D, Arnold D, Oh DY, Reinacher-Schick A, Tortora G, Algül H, O'Reilly EM, McGuinness D, Cui KY, Schlienger K, Locker GY, Kindler HL. Maintenance Olaparib for Germline BRCA-Mutated Metastatic Pancreatic Cancer. *N Engl J Med* 2019; **381**: 317-327 [PMID: 31157963 DOI: 10.1056/NEJMoa1903387]

51 **Pishvaian MJ**, Garrido-Laguna I, Liu SV, Multani PS, Chow-Manevel E, Rolfo C. Entrectinib in TRK and ROS1 Fusion-Positive Metastatic Pancreatic Cancer. *JCO Precis Oncol* 2018; **2**: 1-7 [PMID: 35135135 DOI: 10.1200/PO.18.00039]

52 **Zhao L**, Singh V, Ricca A, Lee P. Survival Benefit of Pembrolizumab for Patients With Pancreatic Adenocarcinoma: A Case Series. *J Med Cases* 2022; **13**: 240-243 [PMID: 35655630 DOI: 10.14740/jmc3918]

53 **Mizrahi JD**, Surana R, Valle JW, Shroff RT. Pancreatic cancer. *Lancet* 2020; **395**: 2008-2020 [PMID: 32593337 DOI: 10.1016/S0140-6736(20)30974-0]

54 **Jones MR**, Williamson LM, Topham JT, Lee MKC, Goytai A, Ho J, Denroche RE, Jang G, Pleasance E, Shen Y, Karasinska JM, McGhie JP, Gill S, Lim HJ, Moore MJ, Wong HL, Ng T, Yip S, Zhang W, Sadeghi S, Reisle C, Mungall AJ, Mungall KL, Moore RA, Ma Y, Knox JJ, Gallinger S, Laskin J, Marra MA, Schaeffer DF, Jones SJM, Renouf DJ. NRG1 Gene Fusions Are Recurrent, Clinically Actionable Gene Rearrangements in KRAS Wild-Type Pancreatic Ductal Adenocarcinoma. *Clin Cancer Res* 2019; **25**: 4674-4681 [PMID: 31068372 DOI: 10.1158/1078-0432.CCR-19-0191]

55 **Laskin JJ**, Cadanel J, Renouf DJ, Weinberg BA, Goto Y, Duruisseaux M, Tolba K, Branden E, Doebele RC, Heining C, Schlenk RF, Cheema PK, Jones MR, Trombetta D, Muscarella LA, Cseh A, Solca F, Liu SV. Afatinib as a novel potential treatment option for NRG1 fusion-positive tumors. *J Glob Oncol* 2019; **5**: 110-110 [DOI: 10.1200/JGO.2019.5.suppl.110]

56 **Sicklick JK**, Kato S, Okamura R, Schwaederle M, Hahn ME, Williams CB, De P, Krie A, Piccioni DE, Miller VA, Ross JS, Benson A, Webster J, Stephens PJ, Lee JJ, Fanta PT, Lippman SM, Leyland-Jones B, Kurzrock R. Molecular profiling of cancer patients enables personalized combination therapy: the I-PREDICT study. *Nat Med* 2019; **25**: 744-750 [PMID: 31011206 DOI: 10.1038/s41591-019-0407-5]

57 **Shaya J**, Kato S, Adashek JJ, Patel H, Fanta PT, Botta GP, Sicklick JK, Kurzrock R. Personalized matched targeted therapy in advanced pancreatic cancer: a pilot cohort analysis. *NPJ Genom Med* 2023; **8**: 1 [PMID: 36670111 DOI: 10.1038/s41525-022-00346-5]

58 **Oh D**, Kong J, Ko SW, Hong SM, So H, Hwang JS, Song TJ, Lee SK, Kim MH, Lee SS. A comparison between 25-gauge and 22-gauge Franseen needles for endoscopic ultrasound-guided sampling of pancreatic and peripancreatic masses: a randomized non-inferiority study. *Endoscopy* 2021; **53**: 1122-1129 [PMID: 33652495 DOI: 10.1055/a-1369-8610]

59 **Ikeda G**, Hijioka S, Nagashio Y, Maruki Y, Ohba A, Hisada Y, Yoshinari M, Harai S, Kitamura H, Koga T, Murashima Y, Maehara K, Okada M, Yamashige D, Okamoto K, Hara H, Hagiwara Y, Agarie D, Takasaki T, Takeshita K, Kawasaki Y, Kondo S, Morizane C, Ueno H, Hiraoka N, Yatabe Y, Saito Y, Iwakiri K, Okusaka T. Fine-needle biopsy with 19G needle is effective in combination with endoscopic ultrasound-guided tissue acquisition for genomic profiling of unresectable pancreatic cancer. *Dig Endosc* 2023; **35**: 124-133 [PMID: 35993898 DOI: 10.1111/den.14423]

60 **Hisada Y**, Hijioka S, Ikeda G, Maehara K, Hashimoto T, Kitamura H, Harai S, Yoshinari M, Kawasaki Y, Murashima Y, Koga T, Takeshita K, Maruki Y, Ohba A, Nagashio Y, Kondo S, Morizane C, Ueno H, Saito Y, Yatabe Y, Okusaka T. Proportion of unresectable pancreatic cancer specimens obtained by endoscopic ultrasound-guided tissue acquisition meeting the OncoGuide™ NCC Oncopanel System analysis suitability criteria: a single-arm, phase II clinical trial. *J Gastroenterol* 2022; **57**: 990-998 [PMID: 36190682 DOI: 10.1007/s00535-022-01926-z]

61 **Young Bang J**, Krall K, Jhala N, Singh C, Tejani M, Arnoletti JP, Navaneethan U, Hawes R, Varadarajulu S. Comparing Needles and Methods of Endoscopic Ultrasound-Guided Fine-Needle Biopsy to Optimize Specimen Quality and Diagnostic Accuracy for Patients With Pancreatic Masses in a Randomized Trial. *Clin Gastroenterol Hepatol* 2021; **19**: 825-835.e7 [PMID: 32652307 DOI: 10.1016/j.cgh.2020.06.042]

62 **Di Mitri R**, Moccia F, Antonini F, Scimeca D, Conte E, Bonaccorso A, Scibetta N, Unti E, Fornelli A, Giorgini S, Bindu C, Macarri G, Larghi A, Fabbri C. Stylet slow-pull vs. standard suction technique for endoscopic ultrasound-guided fine needle biopsy in pancreatic solid lesions using 20 Gauge Procore™ needle: A multicenter randomized trial. *Dig Liver Dis* 2020; **52**: 178-184 [PMID: 31601535 DOI: 10.1016/j.dld.2019.08.023]

63 **Yang MJ**, Park SW, Lee KJ, Koh DH, Lee J, Lee YN, Park CH, Shin E, Kim S. EUS-guided tissue acquisition using a novel torque technique is comparable with that of the fanning technique for solid pancreatic lesions: A multicenter randomized trial. *J Hepatobiliary Pancreat Sci* 2022 [PMID: 36271512 DOI: 10.1002/jhbp.1255]

64 **Wani S**, Mullady D, Early DS, Rastogi A, Collins B, Wang JF, Marshall C, Sams SB, Yen R, Rizeq M, Romanas M, Ulusarac O, Brauer B, Attwell A, Gaddam S, Hollander TG, Hosford L, Johnson S, Kushnir V, Amateau SK, Kohlmeier C, Azar RR, Vargo J, Fukami N, Shah RJ, Das A, Edmundowicz SA. The clinical impact of immediate on-site cytopathology evaluation during endoscopic ultrasound-guided fine needle aspiration of pancreatic masses: a prospective multicenter randomized controlled trial. *Am J Gastroenterol* 2015; **110**: 1429-1439 [PMID: 26346868 DOI: 10.1038/ajg.2015.262]

65 **Lee LS**, Nieto J, Watson RR, Hwang AL, Muthusamy VR, Walter L, Jajoo K, Ryoo MK, Saltzman JR, Saunders MD, Suleiman S, Kadiyala V. Randomized Noninferiority Trial Comparing Diagnostic Yield of Cytopathologist-guided *versus* 7 passes for EUS-FNA of Pancreatic Masses. *Dig Endosc* 2016; **28**: 469-475 [PMID: 26694852 DOI: 10.1111/den.12594]

66 **Crinò SF**, Di Miti R, Nguyen NQ, Tarantino I, de Nucci G, Deprez PH, Carrara S, Kitano M, Shami VM, Fernández-Esparrach G, Poley JW, Baldaque-Silva F, Itoi T, Manfrin E, Bernardoni L, Gabbrilli A, Conte E, Unti E, Naidu J, Ruszkiewicz A, Amata M, Liotta R, Manes G, Di Nuovo F, Borbath I, Komuta M, Lamonaca L, Rahal D, Hatamaru K, Itonaga M, Rizzatti G, Costamagna G, Inzani F, Curatolo M, Strand DS, Wang AY, Ginès À, Sendino O, Signoretti M, van Driel LMJW, Dolapcsiev K, Matsunami Y, van der Merwe S, van Malenstein H, Locatelli F, Correale L, Scarpa A, Larghi A. Endoscopic Ultrasound-guided Fine-needle Biopsy With or Without Rapid On-site Evaluation for Diagnosis of Solid Pancreatic Lesions: A Randomized Controlled Non-Inferiority Trial. *Gastroenterology* 2021; **161**: 899-909.e5 [PMID: 34116031 DOI: 10.1053/j.gastro.2021.06.005]

67 **Pausawasdi N**, Cheirsilpa K, Chalermwai W, Asokan I, Sriprayoon T, Charatcharoenwitthaya P. Endoscopic Ultrasound-Guided Fine-Needle Biopsy Using 22G Franseen Needles without Rapid On-Site Evaluation for Diagnosis of Intraabdominal Masses. *J Clin Med* 2022; **11** [PMID: 35207324 DOI: 10.3390/jcm11041051]

68 **Iwashita T**, Yasuda I, Mukai T, Doi S, Nakashima M, Uemura S, Mabuchi M, Shimizu M, Hatano Y, Hara A, Moriwaki H. Macroscopic on-site quality evaluation of biopsy specimens to improve the diagnostic accuracy during EUS-guided FNA using a 19-gauge needle for solid lesions: a single-center prospective pilot study (MOSE study). *Gastrointest Endosc* 2015; **81**: 177-185 [PMID: 25440688 DOI: 10.1016/j.gie.2014.08.040]

69 **Ishiwatari H**, Sato J, Fujie S, Sasaki K, Kaneko J, Satoh T, Matsubayashi H, Kishida Y, Yoshida M, Ito S, Kawata N, Imai K, Kakushima N, Takizawa K, Hotta K, Ono H. Gross visual inspection by endosonographers during endoscopic ultrasound-guided fine needle aspiration. *Pancreatology* 2019; **19**: 191-195 [PMID: 30528644 DOI: 10.1016/j.pan.2018.12.001]

70 **Kaneko J**, Ishiwatari H, Sasaki K, Yasuda I, Takahashi K, Imura J, Iwashita T, Uemura S, Hatano Y, Miyazaki T, Satoh T, Sato J, Ishikawa K. Macroscopic visible core length can predict the histological sample quantity in endoscopic ultrasound-guided tissue acquisition: Multicenter prospective study. *Dig Endosc* 2022; **34**: 622-631 [PMID: 34437732 DOI: 10.1111/den.14116]

71 **Beane JD**, House MG, Coté GA, DeWitt JM, Al-Haddad M, LeBlanc JK, McHenry L, Sherman S, Schmidt CM, Zyromski NJ, Nakeeb A, Pitt HA, Lillemoe KD. Outcomes after preoperative endoscopic ultrasonography and biopsy in patients undergoing distal pancreatectomy. *Surgery* 2011; **150**: 844-853 [PMID: 22000199 DOI: 10.1016/j.surg.2011.07.068]

72 **Cosgrove ND**, Yan L, Siddiqui A. Preoperative endoscopic ultrasound-guided fine needle aspiration for diagnosis of pancreatic cancer in potentially resectable patients: Is this safe? *Endosc Ultrasound* 2015; **4**: 81-84 [PMID: 26020040 DOI: 10.4103/2303-9027.156708]

73 **Ngamruengphong S**, Swanson KM, Shah ND, Wallace MB. Preoperative endoscopic ultrasound-guided fine needle aspiration does not impair survival of patients with resected pancreatic cancer. *Gut* 2015; **64**: 1105-1110 [PMID: 25575893 DOI: 10.1136/gutjnl-2014-307475]

74 **Park JS**, Lee JH, Song TJ, Lee JS, Jo SJ, Oh DW, Song KB, Hwang DW, Park DH, Lee SS, Kim SC, Seo DW, Lee SK, Kim MH. The impact of preoperative EUS-FNA for distal resectable pancreatic cancer: Is it really effective enough to take risks? *Surg Endosc* 2022; **36**: 3192-3199 [PMID: 34254183 DOI: 10.1007/s00464-021-08627-3]

75 **Yane K**, Kuwatani M, Yoshida M, Goto T, Matsumoto R, Ihara H, Okuda T, Taya Y, Ehira N, Kudo T, Adachi T, Eto K, Onodera M, Sano I, Nojima M, Katanuma A. Non-negligible rate of needle tract seeding after endoscopic ultrasound-guided fine-needle aspiration for patients undergoing distal pancreatectomy for pancreatic cancer. *Dig Endosc* 2020; **32**: 801-811 [PMID: 31876309 DOI: 10.1111/den.13615]

76 **Sakamoto U**, Fukuba N, Ishihara S, Sumi S, Okada M, Sonoyama H, Ohshima N, Moriyama I, Kawashima K, Kinoshita Y. Postoperative recurrence from tract seeding after use of EUS-FNA for preoperative diagnosis of cancer in pancreatic tail. *Clin J Gastroenterol* 2018; **11**: 200-205 [PMID: 29392646 DOI: 10.1007/s12328-018-0822-z]

Basic Study

Antihepatoma peptide, scolopentide, derived from the centipede *scolopendra subspinipes mutilans*

Yu-Xing Hu, Zhuo Liu, Zhen Zhang, Zhe Deng, Zhen Huang, Ting Feng, Qing-Hong Zhou, Si Mei, Chun Yi, Qing Zhou, Pu-Hua Zeng, Gang Pei, Sha Tian, Xue-Fei Tian

Specialty type: Integrative and complementary medicine

Provenance and peer review:

Unsolicited article; Externally peer reviewed.

Peer-review model: Single blind

Peer-review report's scientific quality classification

Grade A (Excellent): 0

Grade B (Very good): B

Grade C (Good): C

Grade D (Fair): 0

Grade E (Poor): 0

P-Reviewer: Lekshmi.R Nath India; Portugal RV, Portugal

Received: December 18, 2022

Peer-review started: December 18, 2022

First decision: January 22, 2023

Revised: February 2, 2023

Accepted: March 15, 2023

Article in press: March 15, 2023

Published online: March 28, 2023



Yu-Xing Hu, Zhen Zhang, Zhe Deng, Zhen Huang, Ting Feng, Sha Tian, Xue-Fei Tian, College of Integrated Chinese and Western Medicine, Hunan University of Chinese Medicine, Changsha 410208, Hunan Province, China

Yu-Xing Hu, Xue-Fei Tian, Hunan Key Laboratory of Translational Research in Formulas and Zheng of Traditional Chinese Medicine, Hunan University of Chinese Medicine, Changsha 410208, Hunan Province, China

Zhuo Liu, Zhen Zhang, Department of Scientific Research, Hunan Academy of Traditional Chinese Medicine Affiliated Hospital, Changsha 410208, Hunan Province, China

Zhe Deng, Hunan Province University Key Laboratory of Oncology of Traditional Chinese Medicine, Hunan University of Chinese Medicine, Changsha 410208, Hunan Province, China

Qing-Hong Zhou, Department of Pediatric, Shenzhen Hospital of Beijing University of Chinese Medicine, Shenzhen 518000, Guangdong Province, China

Si Mei, Department of Physiology, Hunan University of Chinese Medicine, Changsha 410208, Hunan Province, China

Chun Yi, Department of Pathology, Hunan University of Chinese Medicine, Changsha 410208, Hunan Province, China

Qing Zhou, Department of Andrology, First Hospital of Hunan University of Chinese Medicine, Changsha 410007, Hunan Province, China

Pu-Hua Zeng, Department of Oncology, Hunan Academy of Traditional Chinese Medicine Affiliated Hospital, Changsha 410208, Hunan Province, China

Gang Pei, College of Pharmacy, Hunan University of Chinese Medicine, Changsha 410208, Hunan Province, China

Sha Tian, Dr Neher's Biophysics Laboratory for Innovative Drug Discovery, Macau University of Science and Technology, Macau 999078, China

Corresponding author: Xue-Fei Tian, PhD, Professor, College of Integrated Chinese and Western Medicine, Hunan University of Chinese Medicine, No. 300 Xueshi Road, Changsha 410208, Hunan Province, China. 003640@hnucm.edu.cn

Abstract

BACKGROUND

Centipedes have been used to treat tumors for hundreds of years in China. However, current studies focus on antimicrobial and anticoagulation agents rather than tumors. The molecular identities of antihepatoma bioactive components in centipedes have not yet been extensively investigated. It is a challenge to isolate and characterize the effective components of centipedes due to limited peptide purification technologies for animal-derived medicines.

AIM

To purify, characterize, and synthesize the bioactive components with the strongest antihepatoma activity from centipedes and determine the antihepatoma mechanism.

METHODS

An antihepatoma peptide (scolopentide) was isolated and identified from the centipede *scolopendra subspinipes mutilans* using a combination of enzymatic hydrolysis, a Sephadex G-25 column, and two steps of high-performance liquid chromatography (HPLC). Additionally, the CCK8 assay was used to select the extracted fraction with the strongest antihepatoma activity. The molecular weight of the extracted scolopentide was characterized by quadrupole time of flight mass spectrometry (QTOF MS), and the sequence was matched by using the Mascot search engine. Based on the sequence and molecular weight, scolopentide was synthesized using solid-phase peptide synthesis methods. The synthetic scolopentide was confirmed by MS and HPLC. The antineoplastic effect of extracted scolopentide was confirmed by CCK8 assay and morphological changes again *in vitro*. The antihepatoma effect of synthetic scolopentide was assessed by the CCK8 assay and Hoechst staining *in vitro* and tumor volume and tumor weight *in vivo*. In the tumor xenograft experiments, qualified model mice (male 5-week-old BALB/c nude mice) were randomly divided into 2 groups ($n = 6$): The scolopentide group (0.15 mL/d, *via* intraperitoneal injection of synthetic scolopentide, 500 mg/kg/d) and the vehicle group (0.15 mL/d, *via* intraperitoneal injection of normal saline). The mice were euthanized by cervical dislocation after 14 d of continuous treatment. Mechanistically, flow cytometry was conducted to evaluate the apoptosis rate of HepG2 cells after treatment with extracted scolopentide *in vitro*. A Hoechst staining assay was also used to observe apoptosis in HepG2 cells after treatment with synthetic scolopentide *in vitro*. CCK8 assays and morphological changes were used to compare the cytotoxicity of synthetic scolopentide to liver cancer cells and normal liver cells *in vitro*. Molecular docking was performed to clarify whether scolopentide tightly bound to death receptor 4 (DR4) and DR5. qRT-PCR was used to measure the mRNA expression of DR4, DR5, fas-associated death domain protein (FADD), Caspase-8, Caspase-3, cytochrome c (Cyto-C), B-cell lymphoma-2 (Bcl-2), Bcl-2-associated X protein (Bax), x-chromosome linked inhibitor-of-apoptosis protein and Cellular fas-associated death domain-like interleukin-1 β converting enzyme inhibitory protein in hepatocarcinoma subcutaneous xenograft tumors from mice. Western blot assays were used to measure the protein expression of DR4, DR5, FADD, Caspase-8, Caspase-3, and Cyto-C in the tumor tissues. The reactive oxygen species (ROS) of tumor tissues were tested.

RESULTS

In the process of purification, characterization and synthesis of scolopentide, the optimal enzymatic hydrolysis conditions (extract ratio: 5.86%, IC_{50} : 0.310 mg/mL) were as follows: Trypsin at 0.1 g (300 U/g, centipede-trypsin ratio of 20:1), enzymolysis temperature of 46 °C, and enzymolysis time of 4 h, which was superior to freeze-thawing with liquid nitrogen (IC_{50} : 3.07 mg/mL). A peptide with the strongest antihepatoma activity (scolopentide) was further purified through a Sephadex G-25 column (obtained A2) and two steps of HPLC (obtained B5 and C3). The molecular weight of the extracted scolopentide was 1018.997 Da, and the peptide sequence was RAQNHYCK, as characterized by QTOF MS and Mascot. Scolopentide was synthesized *in vitro* with a qualified molecular weight (1018.8 Da) and purity (98.014%), which was characterized by MS and HPLC. Extracted scolopentide still had an antineoplastic effect *in vitro*, which inhibited the proliferation of Eca-109 (IC_{50} : 76.27 µg/mL), HepG2 (IC_{50} : 22.06 µg/mL), and A549 (IC_{50} : 35.13 µg/mL) cells, especially HepG2 cells. Synthetic scolopentide inhibited the proliferation of HepG2 cells (treated 6, 12, and 24 h) in a concentration-dependent manner *in vitro*, and the inhibitory effects were the strongest at 12 h (IC_{50} : 208.11 µg/mL). Synthetic scolopentide also inhibited the tumor volume (Vehicle *vs* Scolopentide, $P = 0.0003$) and weight (Vehicle *vs* Scolopentide, $P = 0.0022$) in the tumor xenograft experiment. Mechanistically, flow cytometry suggested that the apoptosis ratios of HepG2 cells after treatment with extracted scolopentide were 5.01% (0 µg/mL), 12.13% (10 µg/mL), 16.52% (20 µg/mL), and 23.20% (40 µg/mL). Hoechst staining revealed apoptosis in HepG2 cells after treatment with synthetic scolopentide *in vitro*. The CCK8 assay and

morphological changes indicated that synthetic scolopentide was cytotoxic and was significantly stronger in HepG2 cells than in L02 cells. Molecular docking suggested that scolopentide tightly bound to DR4 and DR5, and the binding free energies were -10.4 kcal/mol and -7.1 kcal/mol, respectively. In subcutaneous xenograft tumors from mice, quantitative real-time polymerase chain reaction and western blotting suggested that scolopentide activated DR4 and DR5 and induced apoptosis in SMMC-7721 Liver cancer cells by promoting the expression of FADD, caspase-8 and caspase-3 through a mitochondria-independent pathway.

CONCLUSION

Scolopentide, an antihepatoma peptide purified from centipedes, may inspire new antihepatoma agents. Scolopentide activates DR4 and DR5 and induces apoptosis in liver cancer cells through a mitochondria-independent pathway.

Key Words: Scolopendra; Centipede; Antihepatoma peptide; Hepatocellular carcinoma; Death receptor 4; Death receptor 5

©The Author(s) 2023. Published by Baishideng Publishing Group Inc. All rights reserved.

Core Tip: Centipedes have been used to treat tumors for hundreds of years in China. However, the molecular identities of their bioactive components have not yet been extensively investigated. We have modified the centipede extraction method and found a polypeptide (scolopentide) with the strongest antihepatoma activity. Mechanistically, scolopentide activated death receptor 4 and death receptor 5 to induce apoptosis through a mitochondria-independent pathway. Scolopentide may be an inspiration for the development of antihepatoma agents. We also aim to provide a reference for the purification and characterization of effective components in animal-derived medicines.

Citation: Hu YX, Liu Z, Zhang Z, Deng Z, Huang Z, Feng T, Zhou QH, Mei S, Yi C, Zhou Q, Zeng PH, Pei G, Tian S, Tian XF. Antihepatoma peptide, scolopentide, derived from the centipede scolopendra subspinipes mutilans. *World J Gastroenterol* 2023; 29(12): 1875-1898

URL: <https://www.wjgnet.com/1007-9327/full/v29/i12/1875.htm>

DOI: <https://dx.doi.org/10.3748/wjg.v29.i12.1875>

INTRODUCTION

Centipedes have been widely used in traditional Chinese medicine to treat many diseases, including convulsions, strokes, rheumatic joint diseases, snake bites and tumors [1]. It is a major challenge to isolate and characterize the effective components of centipedes due to limited peptide purification technologies for animal-derived medicines. Currently, the main extraction technologies are as follows: Aqueous extraction [2], organic solvent extraction [2-5], enzymatic hydrolysis [6], ultrasonic extraction [2], and freeze-thaw extraction [2]. To obtain low-weight peptides, extracted proteins require further purification. At present, the main purification technologies of animal proteins are as follows: Sephadex column gel chromatography (GC) [3,7,8], HPLC/RP-HPLC [3,5-8], ion exchange chromatography [7,9], and graded ultrafiltration [7]. SDS-polyacrylamide gel electrophoresis (SDS-PAGE) is a traditional separation and identification technique [10], and mass spectrometry (MS) is the most widely used technique for identifying peptides for use in animal-derived medicines [5-7]. To date, there is no single method that can extract a single peptide from complex mixtures (Table 1). Compound extraction plans are mostly used, which are costly and complicated. Consequently, animal-derived medicines have not been developed as herbal medicines. Currently, the main extracts are still crude peptides, and they have some disadvantages, such as a low extraction ratio, undefined composition, unstable properties and susceptibility [11,12]. These disadvantages may be prevented by identifying and characterizing the effective compositions of animal-derived medicines and synthesizing them *in vitro*.

Some ancient Chinese medical studies have reported that centipedes can be used to treat tumors. "Compendium of Materia Medica" [13], a famous ancient Chinese pharmaceutical work, recorded that centipedes can be used to treat tumors in the chest and abdomen. It is also recorded in the modern Chinese medical literature "Integrating Chinese and Western Medicine" [14] that centipede liquor can be used to treat esophageal cancer with excellent clinical effects. Moreover, the Shendan Sanjie capsule, a medicine containing centipedes, has already been applied to treat cancers and has been proven to inhibit colitis-associated cancer [15]. Although the antitumor theory and clinical efficacy of centipedes have been verified for hundreds of years in China, current experimental studies still focus on antimi-

Table 1 Small molecular extracts of centipede

Name	Extract methods	Function	Ref.
Scolopendrin I	Cation-exchange chromatography and two steps RP-HPLC	Antimicrobial (G ⁺ , G ⁻ , and fungi)	[53]
Scolopin 1	(1) Sephadex Gel Chromatography; (2) RP-HPLC; and (3) characterized by MALDI-TOF MS	Antimicrobial (G ⁺ , G ⁻ , fungi, drug-resistant bacteria)	[37]
Scolopin 2, Scolopin 2-NH2	(1) Sephadex Gel Chromatography; (2) RP-HPLC; and (3) Scolopin2-NH2 was amidation modification from scolopin 2	(1) Antimicrobial (G ⁺ , G ⁻ , fungi, and drug-resistant bacteria); and (2) inhibit proliferation of cervical cancer HeLa cells	[16, 37,45]
LBLP	Transcriptomic data analysis, peptide synthesis	Anti-fungi	[54]
Scolopendrasin II, V, III, X	Next-generation sequencing	(1) Antimicrobial (G ⁺ , G ⁻ , drug-resistant bacteria, fungi); and (2) regulating immune system to antimicrobial indirectly	[40, 55-57]
Scolopendrasin IX	Next-generation sequencing	(1) Regulating immune system to antimicrobial indirectly; and (2) treating autoimmune arthritis	[58]
Scolopendrasin VII	Next-generation sequencing	(1) Antimicrobial (G ⁺ , G ⁻ , drug-resistant bacteria, and fungi); (2) regulating immune system to antimicrobial indirectly; and (3) inhibiting leukemia U937 and jurkat cells	[17, 59,60]
Scolopedin, 1, 2	RNA sequencing	Antimicrobial (G ⁺ , G ⁻ , drug-resistant bacteria, and fungi)	[41-44]
SerGln-Leu (SQL)	(1) Ultrafiltration, Sephadex G-50 column, Source 15Q anion exchange Column; (2) RP-HPLC C18 column; and (3) characterized by ESI-MS	Anticoagulation and antithrombotic	[7]
Thr-Asn-Gly-Tyr-Thr, (TNGYT)	(1) Sephadex G-50 column; (2) RP-HPLC C18 column; and (3) Characterized by ESI-MS	Anticoagulation and antithrombotic	[38]
SsTx-R12A	Red-headed centipede's venom cDNA arsenal	Treating autoimmune diseases mediated by T cells	[61]
SsmTX-I	Red-headed centipede's venom cDNA arsenal	Analgesic	[62]
SsTx	Sephadex G-50 Gel Chromatography and RP-HPLC	Blocking KCNQ potassium channels leads to cardiovascular, respiratory, muscular and nervous system damage	[8]
Ssm6a	Sephadex Gel Chromatography and RP-HPLC	Analgesic	[39]
Haemolymph and tissue extracts	(1) Enzymatic hydrolysis; (2) HPLC; and (3) characterized by MS	Antimicrobial (G ⁺ , G ⁻ , fungi, viruses, and parasites)	[6]
Lacrain	RP-HPLC and characterized by MS	Antibacterial (G ⁻)	[63]
Pinipesin	(1) Organic solvent extraction; (2) HPLC Jupiter [®] C18 column; and (3) characterized by MS	Antimicrobial	[5]
AECS	Organic solvent extraction (ethanol)	Inducing apoptosis of human epidermal carcinoma A431 cells and human melanoma HEK293/EGFR, A375 cells	[4,18]
Two isoquinoline alkaloids	(1) Organic solvent extraction (ethanol); (2) sephadex G-25 Gel chromatography; and (3) HPLC	Inducing apoptosis of brain glioma U87 cells	[3]
Centipede water extract, alcohol extract	(1) Water extraction; (2) freeze-thawing with liquid nitrogen, ultrasonic extraction; and (3) organic solvent extraction (ethanol)	No tumour inhibition in S180 and H22 Transplanted tumour mice	[2]
CE, CA	Organic solvent extraction	Inhibiting cervical tumours <i>in vivo</i>	[64]
Centipede chloroform extract	Organic solvent extraction (hexane, chloroform, ethanol)	Reducing central nervous system symptoms of Alzheimer's disease	[65]
Scom 5	(1) Superdex 75 gel filtration; (2) RESOURCE S ion chromatography; and (3) characterized by LC-MS/MS, MALDI-TOF/TOF and protein sequencing techniques	Human allergens	[11]

HPLC: High performance liquid chromatography; RP-HPLC: Reversed-phase high-performance liquid chromatography; MS: Mass spectrum.

crobial and anticoagulation agents. Only a few studies have observed the antitumor effects of centipedes (Table 1). The potential mechanism is also poorly understood. The tumor types focused on have been gliomas[3], cervical cancer[16], leukemia[17], epidermal cancer[4], and melanoma[18], rather than tumors in the chest and abdomen. Purified centipede peptides can suppress tumor cells by inducing caspase-related apoptosis through a mitochondria-dependent pathway[3,4,16,18], inducing cell cycle arrest[3,18] and necrosis through a specific interaction with phosphatidylserine (Table 1)[17]. Additionally, our previous studies showed that crude centipede peptides could induce apoptosis in

HepG2 cells and lung cancer A549 cells by arresting cells at the G2/M phase[19,20].

Apoptosis has been widely used as a target in cancer treatment[21]. There are two main apoptosis signaling pathways: Mitochondria-dependent and mitochondria-independent pathways. The mitochondria-dependent pathway is controlled by Bcl-2 family proteins and is activated by DNA damage caused by chemotherapy and radiotherapy through activation of the tumor suppressor gene p53[22]. However, the loss of p53 is common in the clinic, contributing to the resistance of conventional chemotherapy and the development of most cancers[23,24]. Thus, the mitochondria-independent pathway, which is independent of p53, has become a promising target[25]. Tumor necrosis factor-related apoptosis-inducing ligand (TRAIL) is part of the mitochondria-independent pathway. TRAIL can selectively initiate apoptosis of cancer cells but has no obvious toxic effect on normal cells[26-28], which makes it a promising chemotherapy drug for many cancers. Nonetheless, recent studies have shown that some cancers, including liver cancer and esophageal cancer, are resistant to TRAIL-mediated apoptosis, which greatly reduces its clinical efficacy[29,30]. Current research focuses on finding suitable TRAIL sensitizers and developing TRAIL receptor agonists to maximize the cell-killing effect. However, current studies mainly focus on sensitizers rather than receptor agonists, and the clinical and laboratory results are not ideal[26,28]. Therefore, for research and clinical applications, it would be useful to find stable and efficient TRAIL receptor agonists. Recently, the regulatory effect of Chinese herbal extracts on the TRAIL apoptosis pathway was gradually discovered. Chinese herbal extracts such as luteolin and artemisinin derivatives can induce apoptosis of liver cancer cells by upregulating the expression of death receptor 4 (DR4) or DR5, which are TRAIL receptors on the cell surface[31,32].

In this study, we isolated a novel low-molecular-weight antihepatoma peptide, designated scolopentide, from *Scolopendra subspinipes mutilans L. Koch* and synthesized it *in vitro*. We observed that synthetic scolopentide inhibited tumor proliferation and was more toxic to HepG2 human liver cancer cells than to L02 human embryonic hepatocytes. Mechanistically, scolopentide activated TRAIL receptors (DR4 and DR5), upregulated the expression of fas-associated death domain protein (FADD), caspase-8 and caspase-3 through a mitochondria-independent pathway and finally induced tumor cell apoptosis.

MATERIALS AND METHODS

Chemicals and reagents

Dulbecco's modified Eagle medium (DMEM) was purchased from Gibco (Thermo Fisher Scientific Inc., United States) and HyClone (Logan, United States). Fetal bovine serum (FBS) was purchased from Gibco and Invitrogen (Thermo Fisher Scientific Inc., United States). DMSO was purchased from Amresco (Solon, United States). PBS was purchased from Boster (Wuhan, Hubei Province, China) and WellBio (Shanghai, China). Trypsin was purchased from Invitrogen. Penicillin-streptomycin was purchased from Beyotime (Shanghai, China). Hoechst was purchased from SolarBio (Beijing, China).

Cell culture

The Bel-7402 Liver cancer cell line, Eca-109 esophageal cancer cell line and A549 Lung cancer cell line were purchased from the Cell Resource Center of Shanghai University of Biology. The HepG2 Liver cancer cell line and L02 human embryonic hepatocyte cell line were purchased from The Cell Center of Xiangya Medical College, Central South University. The SMMC-7721 liver cancer cell line was purchased from the BeNa Culture Collection (Suzhou, Jiangsu Province, China). Cells were placed in culture flasks (Corning Inc., United States) and cultured in a constant temperature incubator (SHEL-LAB, Hitachi, United States) at 37 °C and 5% CO₂ with saturated humidity. The medium comprised 10% FBS, low-glucose DMEM and penicillin-streptomycin (100 U/mL). Cells were observed under an inverted microscope (Olympus, Japan).

Cell viability assay

The viability of HepG2, A549, Eca-109 and Bel7402 cells treated with different centipede extracts was determined by a Cell Counting Kit-8 (Dojindo, Japan). The viability of HepG2 and L02 cells treated with synthetic scolopentide was also determined. Groups and treatments were as follows: (1) Vehicle group: 100 μL cell suspension + 100 μL complete medium; (2) zero group: 200 μL of complete medium; and (3) scolopentide group: Cells were treated with different centipede extracts/synthetic scolopentide. Three replicate wells were used for each group.

Cells at the logarithmic growth stage were collected, and the density was adjusted to 1 × 10⁴ cells/mL. The cell suspension (100 μL) was plated into a 96-well plate (Corning Inc., United States). Four hours later, drugs were added after the cells had adhered to the well. Twelve hours later, 100 μL culture solution containing 10% CCK8 was added to each well. Cells were incubated for 2 h at 37 °C with 5% CO₂. Then, the absorbance (OD) at 450 nm was analyzed by a microplate reader, and the mean was calculated. Cell viability (%) = scolopentide group OD/vehicle group OD × 100%. The cell suppression ratio (IR) was determined with the following formula: IR (%) = (vehicle group OD-scolopentide group OD)/vehicle group OD × 100%. The zero group OD was subtracted from the OD of all groups for

correction. The 50% maximum inhibitory concentration (IC_{50}) was determined by constructing dose-response curves.

Extraction of Crude Peptides from *Scolopendra subspinipes mutilans*

Crude centipede peptides were obtained by enzymolysis combined with acetone precipitation. The "Pharmacopoeia of the People's Republic of China (2020)" references the use of the whole dried body of *Scolopendra subspinipes mutilans*[1]. Centipedes were purchased from the pharmacy department of the First Affiliated Hospital of Hunan University of Chinese Medicine. They were identified as *Scolopendra subspinipes mutilans L. Koch* by Chinese herbal experts. Then, the whole bodies of the centipedes were ground into ultrafine powder by low-temperature ultrafine grinding in the Superfine Powder Engineering Research Center of the Ministry of Education of China. First, 100 g of centipede was dried at 50-60 °C. The superfine powder (particle size 1-75 μ m) was crushed by a BFM-6 Bailey superfine powder machine (amplitude 100 Hz, grinding temperature 0-10 °C, grinding time 10-15 min). Microscopic image analysis and laser light scattering were used in combination to assess the particle size, and the particle size of more than 95% of the powder was smaller than 75 μ m. Finally, the powder was stored at room temperature until subsequent experiments.

We chose an optimized enzymatic hydrolysis method. The extraction process was as follows: 2 g of centipede superfine powder was added to 10 mL of double distilled water, mixed with trypsin, and incubated in water at 55 °C for 4 h. The trypsin was inactivated in a 99 °C water bath for 10 min. Then, the samples were centrifuged at 3500 r/min for 5 min (low temperature ultracentrifuge, Pharmacia Inc., Sweden), and the supernatant was collected. The samples were centrifuged at 5000 r/min at 4 °C for 10 min. The supernatant was collected again. Two volumes of precooled acetone were added to precipitate the former supernatant, which was centrifuged at 5000 r/min at 4 °C for 10 min. The precipitate was dissolved in double steaming water, and the process was repeated twice. Finally, 2 volumes of precooled acetone and petroleum ether (1:1) were added to precipitate again, which was centrifuged at 5000 r/min at 4 °C for 10 min, and the precipitate was collected. Finally, the precipitate was freeze-dried (FD-1 Freeze Dryer, Rikakika Co., Ltd., Tokyo, Japan), weighed, and stored at -20 °C, and the protein content was determined for subsequent experiments.

Optimization of enzymolysis extraction methods

In the process of preparing crude centipede peptides, we tested the influence of single factors on the extraction rate of the crude extract. The five factors included protease type (trypsin, pepsin), water-centipede ratio, protease dose, enzymolysis temperature and enzymolysis time. Then, an $L_9(3^4)$ orthogonal design was adopted to investigate the effects of enzymolysis time, enzymolysis temperature and trypsin dose on crude extracts, which were the three most influential factors in single-factor experiments (Table 2). In addition to the extraction ratio, a CCK8 assay was used to detect the suppression effect of different crude extracts on HepG2 cell viability to determine the optimal technological conditions. We also compared the cytotoxicity of the crude extracts obtained from two methods, freeze-thawing with liquid nitrogen and enzymolysis with acetone precipitation, under optimal technological conditions to determine the significance of this improvement.

Purification and identification of an antihepatoma peptide from crude centipede peptides

Gel chromatography: For the first step, a Sephadex G-25 column was used to isolate the component with the strongest antitumor effect. With 0.1% trifluoroacetic acid-acetonitrile as the mobile phase, gradient elution was performed using an AKTA protein purification system (Amersham Bioscience, United States). In detail, a crude centipede peptide solution (50 mg/mL) was slowly added to a Sephadex G-25 column. Chromatographic columns were eluted with 0.1% trifluoroacetic acid-acetonitrile (flow rate 0.5 mL/min). The resulting columns (3 mL/tube) were collected by an automatic collector. After isolation, tubes with the same peak are collected together, according to the peaks displayed on the computer ultraviolet spectrum. The protein contents of different peaks were determined by a fluorescence microplate reader (TECAN, Austria). The CCK8 assay was used to assess the antitumor activity of different peaks and to select the strongest peak for subsequent experiments.

High-performance liquid chromatography: For further purification, high-performance liquid chromatography (HPLC) was used as the next step. Initially, we used a conventional C18 column, but the results showed that the sample was hydrophilic. Thus, a hydrophilic XAmide column (5 μ m, 100 A, 4.6 mm \times 250.0 mm) was chosen. The sample solution (1 mg/mL) was filtered through a 0.45 μ m microporous membrane and eluted with acetonitrile-water-100 mmol/L ammonium formate (pH 3.5) (flow rate 4 mL/min, detection wavelength 260 nm, injection volume 20 μ L). Different fractions were collected according to the HPLC chromatogram peaks. The CCK8 assay was used to select the fraction with the strongest antitumor activity. Then, the above HPLC and CCK8 assays were repeated. The final centipede peptide was concentrated, purified, freeze dried and designated scolopentide.

Determination of the molecular weight and peptide sequence of scolopentide

Quadrupole time of flight mass spectrometry (UPLC-QTOF MS 6530, SHIMADZU, Japan) was used to

Table 2 L₉(3⁴) levels of orthogonal experimental design

Level	Trypsin (g)	Time (h)	Temperature (°C)
1	0.1	3	37
2	0.2	4	46
3	0.3	5	55

measure molecular weight. The ion source parameters were as follows: Electrospray ion source, positive ion mode, temperature 300 °C, gas flow 11 L/min, and spray pressure 15 psi. Scolopentide did not pass through the liquid column but went directly through the mobile phase to the QTOF system. The Mascot search engine from Matrix Science was used to match peptide sequences. Based on the protein sequence library of Mascot, the molecular weight of scolopentide was compared with that of known centipede proteins. The amino acid sequence that best matched the molecular weight was selected.

Solid-phase peptide synthesis

Scolopentides that were characterized by QTOF MS and Mascot were synthesized using solid-phase peptide synthesis methods. Peptide synthesis was performed by Genscript (Nanjing, China) as follows: (1) A total of 400 mg chloromethyl resin was selected to synthesize the polypeptides, 20% piperidine/N, n-dimethylformamide was added to the reactor, and the reactor was shaken for 20 min; (2) the solvent was removed by filtration, N, n-dimethylformamide was added to the system, and the reactor was shaken for 1 min, followed by filtering to remove the liquid, which was carried out three times; (3) a total of 150 µL ninhydrin and a small amount of resin were added to the detection tube, which was placed at 100 °C for 20 s, after which the resin's color was checked for change, which indicated that Fmoc was removed successfully; (4) the prepared amino acid solution was added to the reactor, 1 mL of N,N'-diisopropyl carbon diimine/1-hydroxybenzotriazole was added, and the reactor was shaken for 1 h; (5) step 3 was repeated, and if the color did not change, the coupling was considered successful; (6) step 2 was repeated to wash the resin; and (7) the above operation was repeated, and the corresponding amino acids were added until polypeptide synthesis was completed. Then, HPLC was used to test the purity of the synthetic scolopentide, and MS was used to test the molecular weight. Finally, the peptides were freeze-dried and stored at -20 °C until they were used.

Flow cytometry

The apoptosis of HepG2 cells treated with extracted scolopentide was determined by Annexin V-Alexa Fluor660/7-AAD (BB20121, BestBio, China). The cells were digested and collected by trypsin. Approximately 5×10^5 cells were collected after washing with PBS twice and centrifuged at 2000 rpm for 5 min. Then, 100 µL of Annexin V binding buffer was added to resuspend the cells, and the concentration was adjusted to 3×10^6 cells/mL. Five microliters of annexin V-FITC and 5 µL of propidium iodide were added to the cell suspension, mixed and incubated for 10 min at 4 °C in the dark. Then, 400 µL of PBS was added to the cell suspension and mixed. Within 1 h, flow CytoFlex (A00-1-1102, Beckman, United States) was utilized to detect cell apoptosis.

Molecular docking

To investigate the antihepatoma mechanism of scolopentide, Discovery Studio 2020 Client and AutoDock-Vina 1.1.2 were used to predict the binding affinity between scolopentide and DR4 and DR5. BIOVIA Discovery Studio 2020 was applied to process and visualize the results. To obtain molecular structure files, scolopentide structures were constructed with Discovery Studio (Small Molecules) according to the sequence RAQNHYCK. Molecular structure files of DR4 (PDB code 5CIR) and DR5 (PDB code 419X) were retrieved from the RCSB PDB database (<https://www.rcsb.org/>). The DR4 and DR5 structures were modified by Discovery Studio for water deletion, binding pocket prediction, hydrogenation, and conformation optimization. Then, AutoDock-Vina was used to perform molecular docking and calculate the affinity potential energy of the protein molecule potential binding modes between scolopentide and DR4 and DR5.

Hoechst staining assay

HepG2 cells were inoculated into 6-well plates (1×10^6 cells per well), and 100 µg/mL synthetic scolopentide was added. The cell slides were removed and washed with PBS 2 or 3 times after incubation at 37 °C and 5% CO₂ with saturated humidity for different durations (6 h, 12 h, and 24 h). Then, the slides were fixed with 4% paraformaldehyde for 30 min and rinsed with PBS 3 times. Hoechst (working concentration: 25 µM) was added to the slides, which were incubated for 3 min and rinsed with PBS 3 times. Finally, the slides were sealed with glycerin buffer, stored away from light and observed under a fluorescence microscope (Zeiss, Germany).

Animal and tumor xenograft experiments

Male 5-wk-old BALB/c nude mice (Shanghai SLAC Laboratory Animal Co., Ltd., Shanghai, China) were chosen for the formation of subcutaneous xenograft tumors. SMMC-7721 cells (0.2 mL/mouse, 1×10^7 cells/mL) were subcutaneously injected into the right back. The tumor diameter reached 1 cm at 3 wk. Qualified model mice were randomly divided into 2 groups ($n = 6$ per group): The scolopentide group (intraperitoneal injection of synthetic scolopentide, 500 mg/kg/d) and the vehicle group (same volume of normal saline). The length and width of tumors were measured every 2 d, and volume was calculated as the maximum tumor length \times width $^2 \times 0.5$. After 14 d of treatment, all mice were euthanized by cervical dislocation, and tumor weights were measured. All operations followed the United Kingdom Animals (Scientific Procedures) Act, 1986. All laboratory animals were carefully handled, and the study was reviewed and approved by the Ethical Review Committee of Experimental Animal Welfare at Hunan University of Chinese Medicine (Approval No. LL2021040705).

Quantitative real-time polymerase chain reaction

Total RNA was extracted from tumor tissues based on the instructions of the RNA Simple Total RNA Kit (Novoprotein Scientific Inc., Suzhou, Jiangsu Province, China), and the RNA concentration was measured by a microplate reader. Then, NovoScript[®]Plus (Novoprotein Scientific Inc., Suzhou, China) was utilized to reverse-transcribe the RNA into cDNA, which was stored at -20 °C until subsequent use. According to the instructions of NovoStart[®]SYBR (Novoprotein Scientific Inc., Suzhou, Jiangsu Province, China), 10 μ L SuperMix Plus, 7 μ L RNase Freewater, 2 μ L cDNA, 0.5 μ L forward primers and 0.5 reverse primers (Genecreate Inc., Wuhan, Hubei Province, China) were mixed. GAPDH was used as the internal reference. A LightCycler[®]96 (Roche, Switzerland) was used for quantitative real-time polymerase chain reaction (qRT-PCR). The primer sequences are shown in Table 3. The qRT-PCR conditions were as follows: Predenaturation for 60 s at 95 °C; 45 cycles of denaturation for 20 s at 95 °C, 20 s at 60 °C, and 30 s at 72 °C; 1 cycle of melting for 10 s at 95 °C, 60 s at 65 °C, and 1 s at 97 °C; and cooling for 30 s at 37 °C. Data were individually normalized to the mean of the relative expression of GAPDH. The fold change was calculated using the $2^{-\Delta\Delta CT}$ method. The experiment was repeated at least three times, and the results that were the most representative are shown.

Western blotting

Tumor tissue specimens were prepared and suspended in ice-cold RIPA lysis buffer (CWBIO Co., Ltd, Beijing, China) and incubated for 20 min. The supernatant was removed after centrifugation. The protein levels of tumor tissues were determined by the BCA assay using a BCA Protein Assay Kit (CWBIO Co., Ltd, Beijing, China). Proteins (50 μ g) were mixed with pure water and SDS loading buffer and denatured at 100 °C for 10 min. Proteins were resolved by sodium dodecyl sulfate-polyacrylamide gel electrophoresis and transferred to PVDF membranes (Merck Millipore Ltd., Germany). Then, PVDF membranes were blocked for 1 h in blocking buffer (5% milk in TBST). The membranes were removed and washed with PBST (PBS + 0.1% Tween 20) 3 times, incubated with primary antibodies overnight at 4 °C, washed with TBST 3 times, incubated with Proteintech HRP Goat Anti-Rabbit IgG (H + L) (SA00001-2, diluted 1:6000) for 90 min at room temperature and washed with TBST 3 times. Protein signals were visualized by enhanced chemiluminescence using an eECL western blot kit (CWBIO Co., Ltd, Beijing, China). Membrane images were collected by an Amersham Imager 600 (GE Healthcare, United States) and qualified by Quantity One software. All experiments were repeated three times. Primary antibodies against DR5 (ab199357, diluted 1:1000), FADD (ab108601, diluted 1:1000), cleaved caspase-3 (ab32042, diluted 1:1000), and cytochrome c (Cyto-C) (ab133504, diluted 1:5000) were obtained from Abcam (Cambridge, England). Antibodies against GAPDH (10494-1-AP, diluted 1:5000) and DR4 (24063-1-AP, diluted 1:2000) were obtained from Proteintech Group, Inc. (Chicago, United States). The antibody against cleaved caspase-8 (AF5267, diluted 1:1000) was obtained from Affinity Biosciences, Inc. (Jiangsu, China).

Analysis of intracellular reactive oxygen species accumulation

Reactive oxygen species (ROS) were measured using a ROS Assay Kit (E004-1-1 Jiancheng, Nanjing, China) according to the manufacturer's instructions. Briefly, the tumor tissue was prepared into a single cell suspension by enzymatic hydrolysis. Three groups of tubes were set up as follows: (1) Negative vehicle tube: cells without any treatment were resuspended in 0.01 M PBS; (2) positive vehicle tube: cells were resuspended in diluted 2,7-dichlorofluorescin diacetate (DCFH-DA), and an ROS hydrogen donor (concentration: 30 μ M) was added to induce the cells; and (3) sample tube: cells were resuspended in diluted DCFH-DA (cell density: 1×10^6 - 2×10^7 /mL). Then, all cells were incubated for 50 min at 37 °C. After labeling with the probe, the single-cell suspensions were subsequently collected and centrifuged for 5-10 min. The precipitates were collected and washed with 0.01 M PBS 1-2 times. The precipitates were centrifuged and collected again. Finally, the cell precipitates were resuspended in PBS and measured on a fluorescence microplate reader (optimum excitation wavelength 500 nm, optimum emission wavelength 525 nm). All results are expressed as fluorescence values.

Table 3 Primer sequences used for quantitative real-time polymerase chain reaction

Gene	Sequence (5' to 3')	
GAPDH	F: AGAAGGCTGGGCTCATTG	R: AGGGCCATCCACAGTCTTC
DR4	F: CCAGGCAGCATTGAAGTCAG	R: GTTCCAGCATCACCAGGGT
DR5	F: CCCTGGAGTGACATCGAATG	R: CAGCCACAATCAAGACTACGG
FADD	F: TGCGGGAGTCACTGAGAATC	R: GGAGGTAGATGCGTCTGAGTTTC
Caspase-8	F: GAGAACGAGCAGCCTGAAG	R: GACAGTATCCCCGAGGTTTG
Caspase-3	F: CCCTCCTCAGCATCTTATCC	R: TGGTACAGTCAGAGCCAACCT
Cyto-C	F: CACAAGACTGGGCCAAATCTC	R: CCAGGGATGTACTTCTGGGA
XIAP	F: CTATGCTCACCTAACCCAAAG	R: TTCTGACCAGGCACGATCAC
c-FLIP	F: GGAACCCCTCACCTTGTTCG	R: CTCCTTGCTTATCTGCCTCG
Bcl-2	F: CCTTCTTGAGTTGGTGGG	R: CGGTTCAAGGTACTCAGTCATCC
Bax	F: CACCAGCTCTGAGCAGATCA	R: TGTACTGTCCAGTCGTCCC

DR4: Death receptor 4; DR5: Death receptor 5; FADD: Fas-associated death domain protein; Cyto-C: Cytochrome C; XIAP: X-chromosome linked inhibitor-of-apoptosis protein; c-FLIP: Cellular Fas associated death domain-like interleukin-1 β converting enzyme inhibitory protein; Bcl-2: B-cell lymphoma-2; Bax: Bcl-2-associated X protein.

Statistical analysis

SPSS 25.0 and GraphPad Prism 8.3 software were used for all statistical analyses. Unless otherwise stated, $P < 0.05$ was considered statistically significant. All data are expressed as the mean \pm SD. For the cell viability assay, ANOVA was used to compare the means of multiple groups, Student's t test was used for pairwise comparisons, and Fisher's exact test was used for ratio comparisons. For tumor weight, qRT-PCR and WB, Student's t test was used when normality and ANOVA were satisfied. For ROS assessment, the Mann-Whitney rank-sum test was used due to unsatisfactory normality. Two-way ANOVA was used for tumor volume analysis.

RESULTS

Crude centipede peptides extracted by optimal enzymolysis hydrolysis extraction ratio of crude peptides under different conditions

Based on the extract ratio and protein content, we carried out five single-factor experiments and finally obtained the optimum conditions: the protease was trypsin, the water-centipede ratio was 5:1, the protease dose was 0.1 g (300 U/g, with a centipede-trypsin ratio of 20:1), the enzymolysis temperature was 46 °C, and the enzymolysis time was 4 h. The three most influential factors were enzymolysis time, enzymolysis temperature and trypsin dose. Therefore, an $L_9(3^4)$ orthogonal design was adopted to further investigate the optimal group of three factors on the extract ratio, as shown in Table 4. In conclusion, Group 4 (A2B1C2), Group 2 (A1B2C2), and Group 9 (A3B3C2) had higher extract ratios.

Cytotoxicity of crude peptides under different conditions

The $L_9(3^4)$ orthogonal design was adopted to further investigate the optimal group of the three factors for cytotoxicity in HepG2 cells, as shown in Table 5. A CCK8 assay was used to evaluate HepG2 cell viability. The results indicated that the 9 extracts induced cell death in a concentration-dependent manner ($P < 0.05$). Extracts from Groups 4, 2, and 9 showed stronger cytotoxicity, and Groups 1, 3, 5, 6, 7, and 8 showed moderate cytotoxicity. In the $L_9(3^4)$ orthogonal experiment, Group 2 (5.86%, 0.310 mg/mL), which used the optimal process of the single-factor experiment, showed little difference from the nonoptimal process of Group 9 (5.94% and 0.278 mg/mL). Indeed, Group 2 required less time and a lower trypsin dose. Based on the IC_{50} , extract ratio and suppression ratio shown in Table 5, Group 2 was ultimately determined to have the optimal extraction process. The optimal extraction conditions were as follows: Trypsin at 0.1 g (300 U/g, centipede-trypsin ratio of 20:1), enzymolysis temperature of 46 °C, and enzymolysis time of 4 h.

Table 4 Extract ratio analysis of L₉(3⁴) orthogonal experimental design

Run	A (mg, trypsin)	B (min, time)	C (°C) (temperature)	D (blank)	Extract ratio (%)
1	1	1	1	1	4.55
2	1	2	2	2	5.86
3	1	3	3	3	4.32
4	2	1	2	3	5.63
5	2	2	3	1	4.21
6	2	3	1	2	3.98
7	3	1	3	2	3.34
8	3	2	1	3	3.68
9	3	3	2	1	5.94
K1	14.73	13.52	12.21	14.70	-
K2	13.82	16.01	14.83	13.18	-
K3	12.96	11.64	11.87	13.63	-
R	1.77	4.37	2.96	1.52	-

K_{ij} parameters in a first level of the first i-j-average quality index; I = 1, 2, 3, representative of 3 levels; j = 1, 2, 3; representing three factors.

Table 5 Inhibitory effects of crude centipede peptides on HepG2 cells in different conditions

Concentration (mg/mL)	Suppression ratio (%)								
	Group 1	Group 2	Group 3	Group 4	Group 5	Group 6	Group 7	Group 8	Group 9
0.039	12.510	6.880	12.070	5.394	3.389	3.213	0.570	1.641	7.094
0.078	22.270	11.240	13.060	16.430	12.890	4.709	2.280	4.540	9.883
0.156	45.770	36.430	45.680	52.290	18.610	16.620	26.110	11.540	33.170
0.3125	85.510	85.040	88.540	94.360	68.110	63.660	58.500	64.170	76.610
0.625	89.090	86.060	92.440	94.520	94.170	94.96	83.200	95.180	94.570
1.250	91.840	87.490	93.050	94.770	96.780	95.730	94.660	95.300	96.000
2.500	92.070	89.470	93.430	94.690	96.940	96.670	95.540	95.670	96.920
5.000	92.750	92.000	95.800	96.680	97.720	97.780	95.880	95.790	97.650
IC ₅₀ (mg/mL)	0.457	0.310	0.480	0.360	0.584	0.681	0.812	0.757	0.278
Extract ratio (%)	4.550	5.860	4.320	5.630	4.210	3.980	3.340	3.680	5.940

Cytotoxicity of crude peptides from the optimal enzymolysis hydrolysis and freeze-thawing with liquid nitrogen

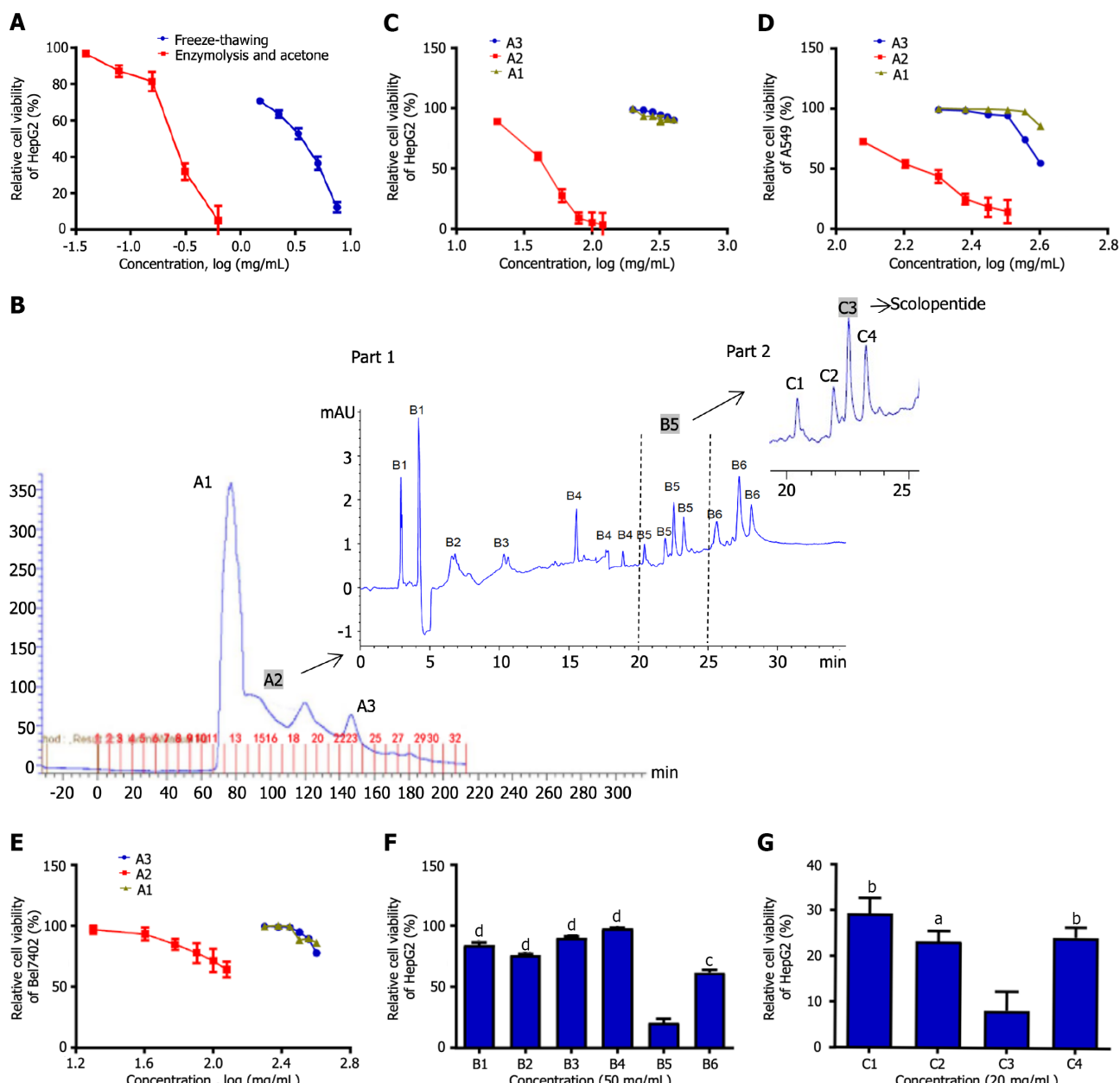
HepG2 cells were treated with crude peptides extracted using two extraction methods. The results showed that extracts obtained from the two methods significantly inhibited HepG2 cells in a concentration-dependent manner. Optimal enzymatic hydrolysis (IC₅₀: 0.31 mg/mL) was superior to freeze-thawing with liquid nitrogen (IC₅₀: 3.07 mg/mL), and the cytotoxicity of extracts increased nearly 10 times (Figure 1A).

Purification of scolopentide from crude centipede peptides

We purified and screened crude centipede peptides three times and obtained a low-molecular-weight peptide with the strongest antihepatoma effect, which was designated scolopentide.

The first purification step (Part A): Separation by a sephadex g-25 column

Sephadex G-25 gel chromatography was used, and the chromatogram obtained showed 3 peaks (Figure 1B). Part A samples (sample ID nos. A1 to A3) were then collected based on 3 peaks and assessed by a microplate reader. The protein and polypeptide contents of A1, A2 and A3 were 55, 40



DOI: 10.3748/wjg.v29.i12.1875 Copyright ©The Author(s) 2023.

Figure 1 Purification of scolopentide from crude centipede peptides. A: The CCK8 assay showed the cytotoxicity of extracts from two methods, and optimal enzymatic hydrolysis was superior to freeze-thawing with liquid nitrogen; B: After the first purification, the Sephadex G-25 chromatogram showed 3 peaks, and A2 was chosen for further isolation; after the second purification, the high-performance liquid chromatography (HPLC) chromatogram showed 6 parts, and B5 was chosen for further purification (part 1); after the third purification, the HPLC chromatogram showed 4 parts, and C3 was chosen for further purification (part 2); C-E: Relative cell viability of HepG2 (C), A549 (D), and Bel7402 (E) cells treated with A1-3 at different concentrations (mg/mL). A2 showed stronger suppression than A1 and A3; F: The CCK8 assay showed that B5 (50 µg/mL) had the strongest suppression of HepG2 cells among B1-6; G: The CCK8 assay showed that C3 (20 µg/mL) had the strongest suppression of HepG2 cells among C1-4. ^aP < 0.05, ^bP < 0.01, ^cP < 0.001, and ^dP < 0.0001.

and 20 µg/mL, indicating that samples A1-3 were mainly composed of protein. Since the separation range of the Sephadex G-25 column was 1-5 kDa, we speculated that A1 contained proteins > 5 kDa and that A2 and A3 were composed of low-molecular-weight polypeptides (1-5 kDa). Subsequently, a CCK8 assay was used to detect the suppressive effects of A1, A2 and A3 on HepG2, Bel-7402 and A549 cells (Figure 1C-E). The CCK8 assay showed the following: (1) A2 showed the most significant inhibition of proliferation of the three tumor cell lines among samples A1-3 ($P < 0.05$); (2) A2 showed the strongest inhibitory effect on HepG2 cells: The IC_{50} values of A2 against the three tumor cell lines were 50.1 mg/mL (HepG2), 132.8 mg/mL (Bel-7402) and 154.5 mg/mL (A549); and (3) A1-3 showed an inhibitory effect on the three tumor cell lines in a concentration-dependent manner.

The second purification step (Part B): Purification by HPLC

In Part B, A2, which had the best antineoplastic effect *in vitro* among samples A1-3, was used. HepG2

cells, which were the most strongly inhibited among the three tumor cell lines, were used. First, tricine-SDS-PAGE[10] was performed to further purify this sample in Part B, but the peptide separation was not obvious, and the band patterns were light and diffuse. The reason may be that the molecular weight of the sample was too low for separation by tricine-SDS-PAGE. However, satisfactory results were obtained from HPLC. Therefore, HPLC was adopted for further purification. The chromatogram indicated that the sample from Part B was composed of a variety of peptides with very similar and low molecular weights in 6 peaks (Figure 1B; part 1). Subsequently, the Part B sample was collected in 6 parts (sample ID nos. B1 to B6) based on 6 peaks. A CCK8 assay was used to assess the suppressive effect of B1-6 on HepG2 cells cultured for 48 h, which were the tumor cells that were most sensitive to the centipede extracts. The CCK8 assay showed that B1-4 hardly inhibited the proliferation of HepG2 cells, while B5 and B6 inhibited proliferation ($P < 0.05$), with B5 having the strongest effect (Figure 1F).

The third purification step (Part C): Purification by HPLC

In Part C, the B5 sample, which had the best antihepatoma effect *in vitro* among B1-6, was used. HPLC was adopted for purification, and the chromatogram showed 4 peaks (Figure 1B; part 2). Then, the sample from Part C was collected in 4 parts (C1-4) based on the 4 peaks. The CCK8 assay showed that C3 had the strongest inhibitory effect on HepG2 cells cultured for 48 h, while C1, C2, and C4 showed relatively weak inhibition of proliferation (Figure 1G). Finally, we concentrated and purified C3 and designated it scolopentide.

Characterization of scolopentide

The peptide sequence of the extracted scolopentide is RAQNHYCK, and the mass spectrum (Figure 2A) showed that its molecular weight was 1018.997 Da (the highest peak). Mascot was used to determine the specific peptide sequence of scolopentide, and the final matched sequence was RAQNHYCK, which conformed to the restriction site of the protease. The molecular structure of scolopentide ($C_{42}H_{66}N_{16}O_{12}S$) is shown in Figure 2A (the asterisk).

Synthesis and detection of scolopentide

Scolopentide was synthesized *in vitro* according to the peptide sequence RAQNHYCK, the length of which is 8 AA. Then, MS was used to detect the molecular weight. The observed molecular weight of synthetic scolopentide was 1018.8 Da (Figure 2B), which was similar to that of the extract (1018.997 Da). HPLC was used to assess the purity. The chromatogram is shown in Figure 2C, and the peak proportion is shown in Figure 2D. The synthetic scolopentide corresponds to peak 3; thus, its purity was inferred to be 98.014% according to the area fraction of peak 3. Consequently, the purity and molecular weight of synthetic scolopentide met the requirements.

Antineoplastic effect of extract scolopentide *in vitro*

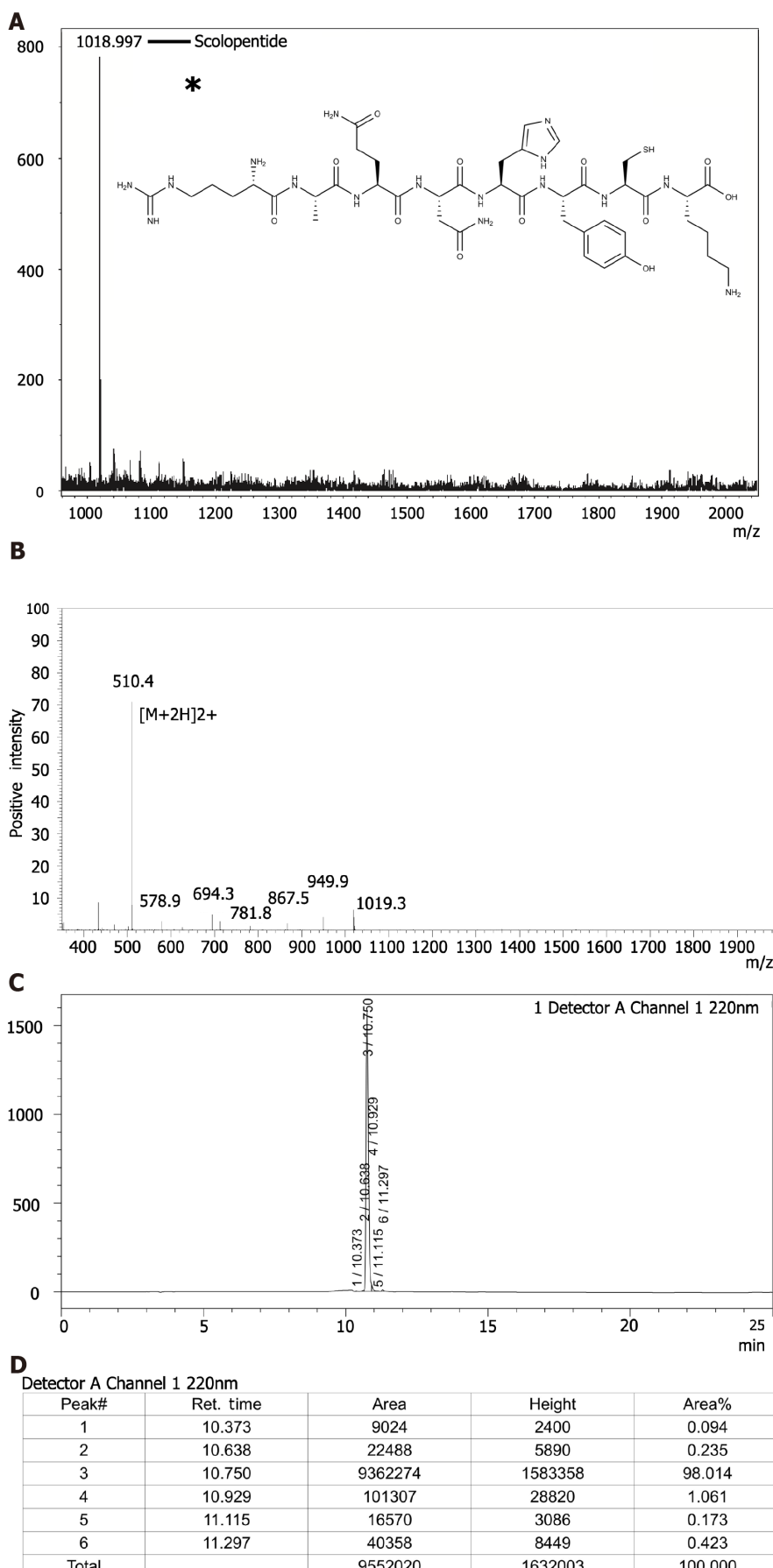
Eca-109, HepG2, and A549 cells were treated with the extracted scolopentide. A CCK8 assay showed that the IC_{50} values in the three cell types were 76.27 μ g/mL (Eca-109), 22.06 μ g/mL (HepG2), and 35.13 μ g/mL (A549) (Figure 3A). Morphological changes in the three cell lines showed that the A549 and HepG2 cells changed considerably (Figure 3B). Based on the CCK8 assay and morphological changes, the following conclusions were drawn: extracted scolopentide still has antineoplastic effects *in vitro*, which inhibited the proliferation of three tumor cell lines, especially HepG2 cells.

Antihepatoma effect of synthetic scolopentide *in vitro* and *in vivo*

We wanted to determine whether synthetic scolopentide can exert an antihepatoma effect. Our experiments suggested that synthetic scolopentide had antihepatoma effects *in vitro* and *in vivo*, which may be related to apoptosis induction. *In vitro*, the CCK8 assay suggested that synthetic scolopentide inhibited the proliferation of HepG2 cells in a concentration-dependent manner. The inhibitory effects were the strongest at 12 h, and there was no significant difference between 24 h and 48 h (Figure 3C). Moreover, a Hoechst staining assay was used to observe the morphological changes in HepG2 cells treated with scolopentide (100 μ g/mL) (6 h, 12 h, and 24 h). The results showed that cytoplasmic staining and nuclear pyknosis occurred after treatment for 12 h and 24 h, which indicated apoptosis. Apoptosis was most clearly observed at 12 h (IC_{50} : 208.11 μ g/mL), consistent with the CCK8 assay (Figure 3D). *In vivo*, the tumor xenograft experiment suggested that the mean tumor volume of the two groups increased gradually, but that of the scolopentide group grew slower. The tumor weight of the scolopentide group was lower than that of the vehicle group (Figure 3E-G).

Cytotoxicity of synthetic scolopentide to L02 cells and HepG2 cells

CCK8 assays and morphological changes were used to compare the cytotoxicity of synthetic scolopentide to liver cancer cells and normal liver cells. After treatment with synthetic scolopentide for 12 h, the CCK8 assay suggested that the cytotoxicity in L02 cells was significantly lower than that in HepG2 cells (100, 150, and 200 μ g/mL) (Figure 4A). Morphological changes in the scolopentide group (100 μ g/mL) and vehicle group (0 μ g/mL) are shown in Figure 4B. Compared to the vehicle group, most HepG2 cells in the scolopentide group died, while some L02 cells survived. The CCK8 assay and



DOI: 10.3748/wjg.v29.i12.1875 Copyright ©The Author(s) 2023.

Figure 2 Characterization of extracted scolopentide and detection of synthetic scolopentide. A: Mass spectrum of extracted scolopentide; the

highest peak indicates the active peptide (scolopentide). The observed molecular weight was 1018.997 Da; the asterisk “*” means molecular structure of scolopentide; B: Mass spectrum of synthetic scolopentide. The observed molecular weight was 1018.8 Da; C and D: HPLC chromatogram of synthetic scolopentide (C); the highest peak (peak 3) indicates the active peptide, and the area % of peak 3 indicates the purity of synthetic scolopentide (98.014%) (D).

morphological changes indicated that synthetic scolopentide was cytotoxic and was significantly stronger in HepG2 cells than in L02 cells.

Molecular docking of scolopentide with DR4 and DR5

Scolopentide was more cytotoxic in HepG2 cells than in L02 cells (Figure 4), which is similar to the activity of TRAIL, which selectively initiates apoptosis in cancer cells without significant toxicity to normal cells. Among the known TRAIL receptors, only DR4 and DR5 are able to induce apoptosis[33]. In addition, Hoechst staining indicated that HepG2 cells underwent apoptosis after treatment with synthetic scolopentide (Figure 3D). Therefore, we hypothesized that scolopentide could induce apoptosis by activating DR4/DR5. The binding free energies of scolopentide to DR4 and DR5 were -10.4 kcal/mol and -7.1 kcal/mol, respectively. Molecular docking suggested that scolopentide tightly bound to DR4 (Figure 5A) and DR5 (Figure 5B), which supported our hypothesis.

Apoptosis of HepG2 cells treated with extracted scolopentide

Flow cytometry suggested that apoptosis occurred in HepG2 cells after treatment with extracted scolopentide *in vitro*. The apoptosis ratios were 5.01% (0 µg/mL), 12.13% (10 µg/mL), 16.52% (20 µg/mL), and 23.2% (40 µg/mL), which indicates concentration-dependence (Figure 6A).

The antihepatoma mechanism of scolopentide was determined to be induction of apoptosis by activating the TRAIL pathway

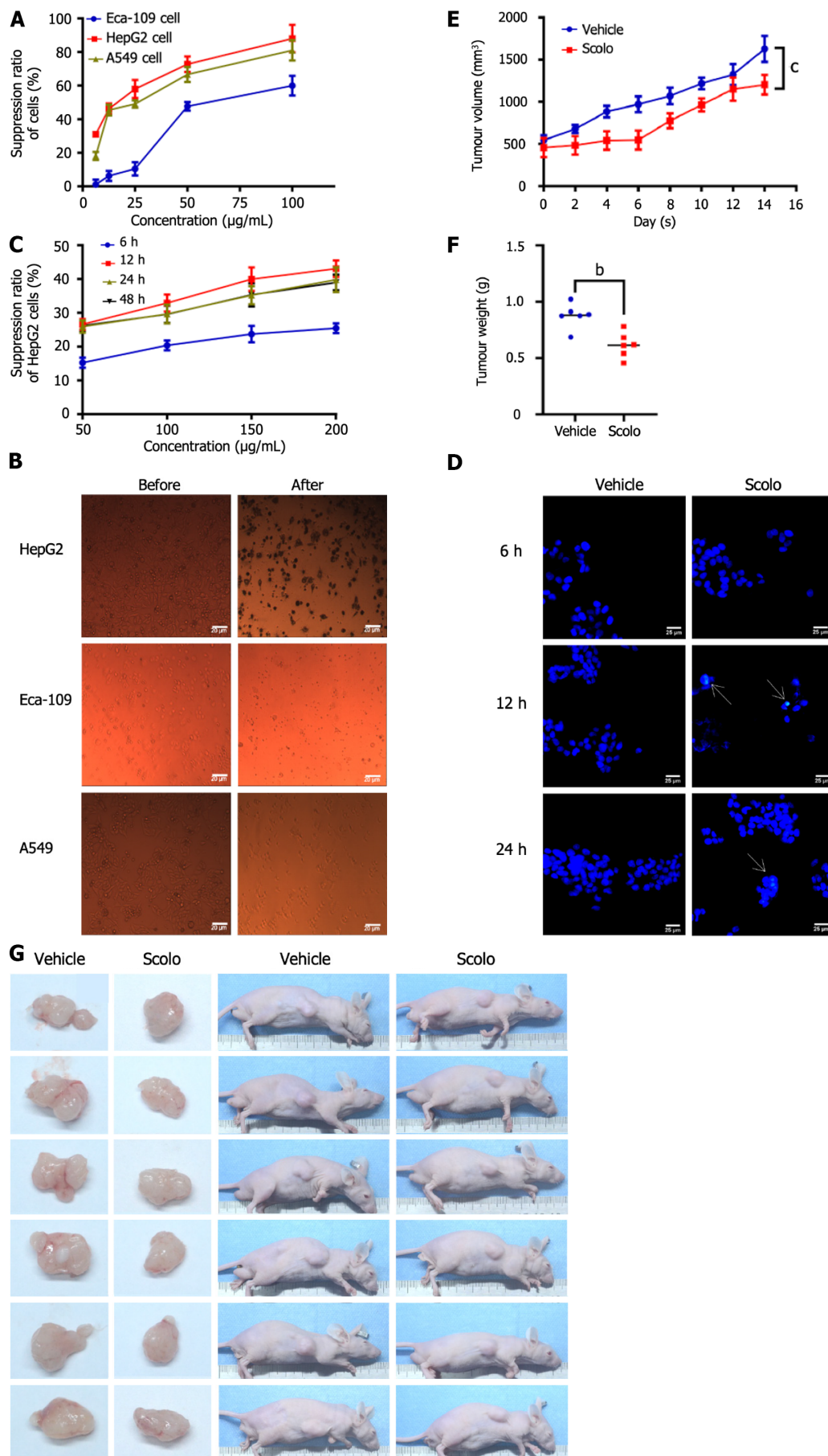
Animal experiments were used to further verify our hypothesis that scolopentide can stimulate the TRAIL pathway to induce apoptosis. The results of qRT-PCR and western blotting suggested that scolopentide activated DR4 (Figure 6B and C) and DR5 (Figure 6H and I), which promoted the expression of FADD (Figure 6E and F), activated the apoptosis promoter caspase-8 (Figure 6F and G) and the executor caspase-3 (Figure 6C and D), and finally induced apoptosis in SMMC-7721 Liver cancer cells. This form of apoptosis appears to be more related to the mitochondria-independent pathway, as Cyto-C and Bcl-2-associated X protein/B-cell lymphoma-2 (Bax/Bcl-2), which are key indicators in the mitochondria-dependent pathway, showed only slight upregulation and insignificant differences (Figure 6I-K). In addition, ROS levels were upregulated (Figure 6L). Cellular fas-associated death domain-like interleukin-1β converting enzyme inhibitory protein (c-FLIP), an inhibitory protein of caspase-8, was downregulated (Figure 6M), and x-chromosome linked inhibitor-of-apoptosis protein (XIAP), an inhibitory protein of caspase-3, was insignificantly upregulated (Figure 6N).

DISCUSSION

Peptides from centipedes have potential antitumor activity that should not be ignored. We isolated and purified crude centipede peptides 3 times and finally obtained a low molecular weight peptide (scolopentide) with the strongest antihepatoma effect. We further demonstrated that mechanistically, scolopentide induced apoptosis in liver cancer cells by activating DR4 and DR5 and promoting the upregulation of FADD, caspase-8 and caspase-3.

Centipedes, an important part of animal Chinese medicine, have played an important role in clinical treatment[1]. The remarkable activities and novel structure also give bioactive components of centipedes enormous potential to be exploited and modified as biological drugs[34]. However, pharmacological studies of centipedes are far behind those of other animals, such as snakes and scorpions[34,35]. Similar to animal-derived medicines, most centipede extracts are still crude. These crude extracts may contain a large number of histamines, polypeptide toxins and other biologically active substances[34], leading to allergic reactions such as itching or serious adverse reactions such as acute myocardial infarction, arrhythmia, tissue necrosis, respiratory depression and hemolysis, which hinder the clinical use of centipedes[11,36]. Small molecular substances from centipedes may not cause adverse reactions and may play a critical role with precise effects.

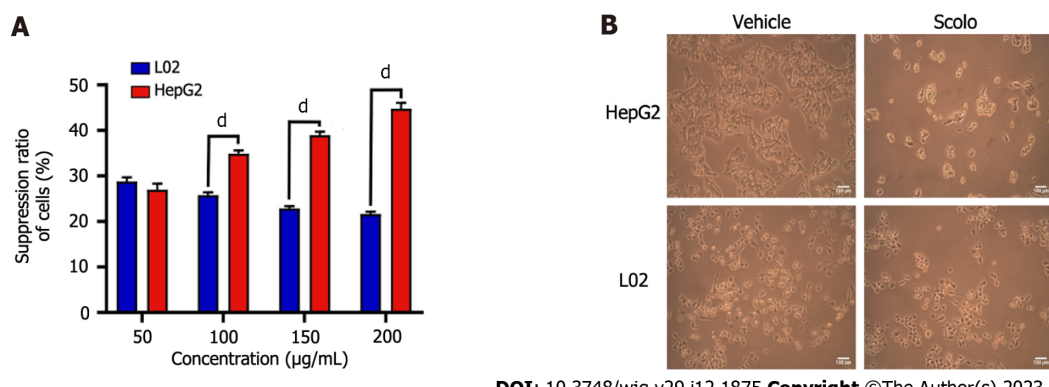
We tried a variety of ways to obtain a higher extraction rate and more accurate activity. For protein extraction, the optimal conditions were determined: 0.1 g trypsin (300 U/g, centipede-trypsin ratio of 20:1), enzymolysis temperature of 46 °C and enzymolysis time of 4 h. For peptide purification, GC[37-39] and HPLC[3,5,6], widely used techniques, were adopted to further purify crude centipede peptides. Mass spectrometry[5-7], the most widely used technique for peptide characterization, was used to identify scolopentide. The object of extraction and method used here are also noteworthy. The whole body of the centipede was chosen for extraction as recorded in Chinese works[14], even though most



DOI: 10.3748/wjg.v29.i12.1875 Copyright ©The Author(s) 2023.

Figure 3 Antihepatoma effect of scolopentide. A: The CCK8 assay showed the suppression ratio of Eca-109, HepG2, and A549 cells treated with extracted

scolopentide at different concentrations; B: Morphological changes in Eca-109, HepG2, and A549 cells under a light microscope ($\times 40$); after treatment with extracted scolopentide, three cells were morphologically changed, especially HepG2 cells; C: The CCK8 assay showed the suppression ratio of HepG2 cells treated with synthetic scolopentide at different times (6 h, 12 h, 24 h, and 48 h) and different concentrations (50 $\mu\text{g/mL}$, 100 $\mu\text{g/mL}$, 150 $\mu\text{g/mL}$, and 200 $\mu\text{g/mL}$); D: Hoechst 33342 staining ($\times 400$) of HepG2 cells. After treatment with synthetic scolopentide for 12 h and 24 h, cytoplasmic highlight staining and nuclear pyknosis occurred; E-G: Tumor volume and weight of the scolopentide group (synthetic scolopentide 500 mg/kg/d) and vehicle group (constant volume of normal saline). $n = 6$, $^bP < 0.01$, $^cP < 0.001$.



DOI: 10.3748/wjg.v29.i12.1875 Copyright ©The Author(s) 2023.

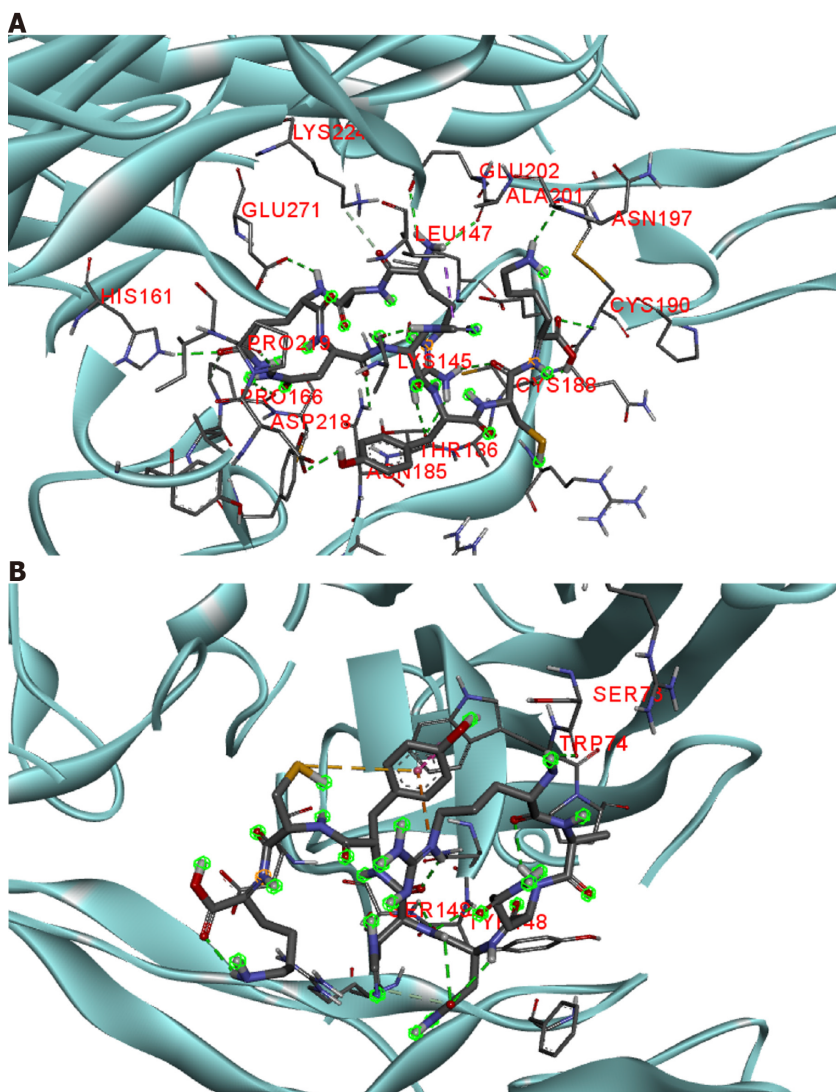
Figure 4 Cytotoxicity of synthetic scolopentide to L02 cells and HepG2 cells. A: The CCK8 assay showed that cytotoxicity to L02 cells was significantly lower than that to HepG2 cells after treatment with synthetic scolopentide for 12 h (100 $\mu\text{g/mL}$, 150 $\mu\text{g/mL}$, and 200 $\mu\text{g/mL}$); B: Morphological changes in HepG2 and L02 cells under a light microscope after treatment with synthetic scolopentide for 12 h ($\times 100$). Compared to cells in the vehicle group (0 $\mu\text{g/mL}$), most HepG2 cells in the scolopentide group (100 $\mu\text{g/mL}$) died, while some L02 cells survived. $^dP < 0.0001$.

current studies focus on the venom[12,34]. In addition, enzymatic hydrolysis[6], a special extract technique, was chosen for the initial extraction to obtain crude centipede peptides. We aimed to simulate the environment of Chinese medicine being digested by various proteinases in the stomach after oral administration.

Currently, studies on the antihepatoma components of centipedes are rare (Table 1). Thus, we isolated, purified, and screened the crude centipede peptides three times. Finally, we obtained scolopentide (1018.997 Da), which had the strongest antihepatoma activity. Moreover, the peptide sequence RAQNHYCK of scolopentide was matched with the Mascot search engine, which helped to achieve scolopentide synthesis *in vitro*. Mascot also revealed that scolopentide was supposed to be a polypeptide from centipede venom proteins located in Kappa-scoloptoxin (07)-Ssm^a OS. It is worth noting that the tumor types used for screening were tumors in the chest and abdomen, such as liver cancer and esophageal cancer, as recorded in ancient Chinese works[13]. Liver cancer cells were more sensitive than other tumor cells and were chosen for subsequent mechanistic exploration (Figure 3A).

Antimicrobial activity is the most common pharmacological characteristic known among isolated centipede peptides at present (Table 1). Centipede peptides mainly destroy the integrity of cell membranes, which leads to the death of microbes[40-42]. Inducing apoptosis is the second major mechanism by which centipede peptides induce resistance to microorganisms (Table 1). Two antimicrobial centipede peptides, scolopendin and scolopendin 1, were obtained by RNA sequencing[41,43]. They have been shown to cause ROS accumulation in *Candida albicans*, which leads to mitochondrial depolarization, thus releasing Cyto-C into the cytoplasm from mitochondria and resulting in an increase in Ca^{2+} in the cytoplasm and mitochondria, ultimately inducing caspase-related apoptosis[43,44]. Some centipede peptides can also block the cell cycle and affect the expression of genes related to DNA replication and repair[45]. Additionally, some scholars have shown that a few antimicrobial centipede peptides also have antitumor activity[17,26]. Distinct from the antimicrobial mechanism, the antitumor activities are mainly related to apoptosis, especially the mitochondrial-dependent pathway[3,4,18]. To date, there have been no studies related to the mitochondrial-independent pathway of centipede effects (Table 1).

DR4 and DR5 are involved in the mitochondria-independent apoptosis pathway, which can receive extracellular death signals and induce intracellular apoptosis[46]. FADD receives apoptosis signals transmitted from DR4/DR5 and forms the death-inducing signaling complex TRAIL-DR4/DR5-FADD-procaspase. Then, caspase-8 is activated to initiate two apoptotic pathways: (1) The mitochondria-independent pathway, in which caspase-8 directly activates caspase-3; and (2) the mitochondria-dependent pathway, in which caspase-8 cleaves Bid, resulting in tBID that triggers the release of Cyto-C. Then, Cyto-C successively activates the promoter caspase-9 and the executor caspase-3. ROS accumulation can cause mitochondrial permeability transition pore opening, also leading to Cyto-C release. Apoptosis is the common end of these two pathways (Figure 7)[28,47-49].

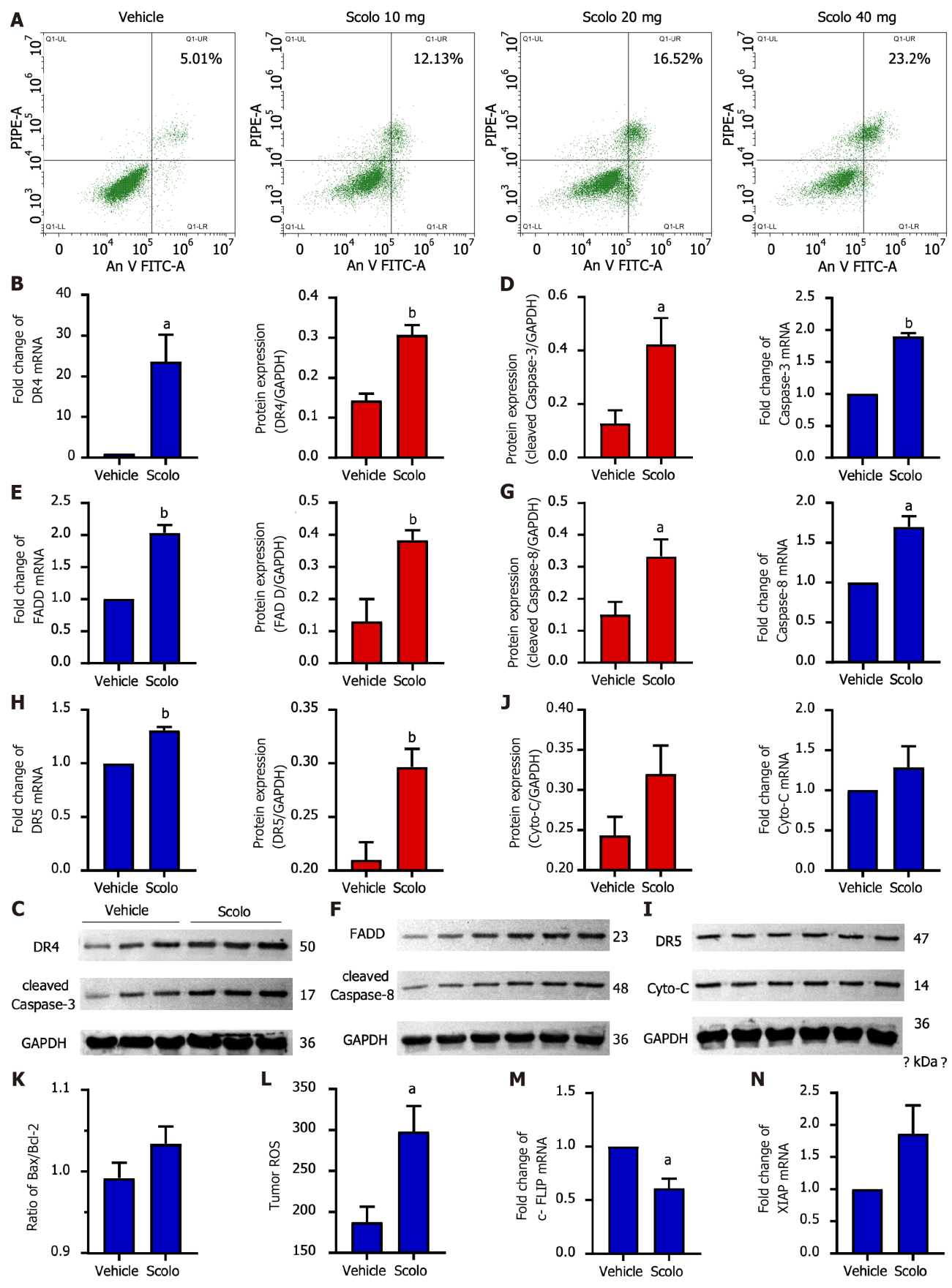


DOI: 10.3748/wjg.v29.i12.1875 Copyright ©The Author(s) 2023.

Figure 5 Molecular docking of scolopentide and death receptor 4 and death receptor 5. A: Stereograms of the molecular docking of scolopentide and death receptor 4. Hydrogen bonds formed with amino acid residues of the receptor include LYS145, ALA201, PRO219, and CYS190; B: Stereograms of molecular docking of scolopentide and death receptor 5. Hydrogen bonds formed with amino acid residues of the receptor are TRP74, SER73, ER149, and TYR148.

We found that scolopentide may activate DR4 and DR5 and induce apoptosis. Flow cytometry suggested that apoptosis occurred in HepG2 cells after treatment with extracted scolopentide *in vitro* (Figure 6A). Hoechst staining showed the occurrence of apoptosis in HepG2 cells after treatment with synthetic scolopentide (Figure 3D). The CCK8 assay showed that scolopentide was significantly more cytotoxic in HepG2 cells than in L02 cells (Figure 4), which was similar to the effect of TRAIL, which selectively induced tumor cell apoptosis. Molecular docking also indicated that scolopentide binds well to TRAIL receptors (DR4 and DR5) (Figure 5). In our previous study, crude centipede peptides were also found to inhibit STAT3 protein phosphorylation[19], while some studies have suggested that dovitinib and sorafenib could overcome TRAIL resistance in HCC by inhibiting STAT3[50,51]. Consequently, animal experiments were used to further verify our hypothesis that scolopentide can stimulate the TRAIL pathway to induce apoptosis. In animal experiments, after treatment with synthetic scolopentide, the expression of DR4 and DR5, which are upstream of the TRAIL pathway, was clearly upregulated, especially the expression of DR4. The expression of FADD, caspase-8, and caspase-3, which are downstream of the TRAIL pathway, was also upregulated (Figure 6B-I). The animal experiments further confirmed the viewpoint that scolopentide induces apoptosis by activating DR4 and DR5.

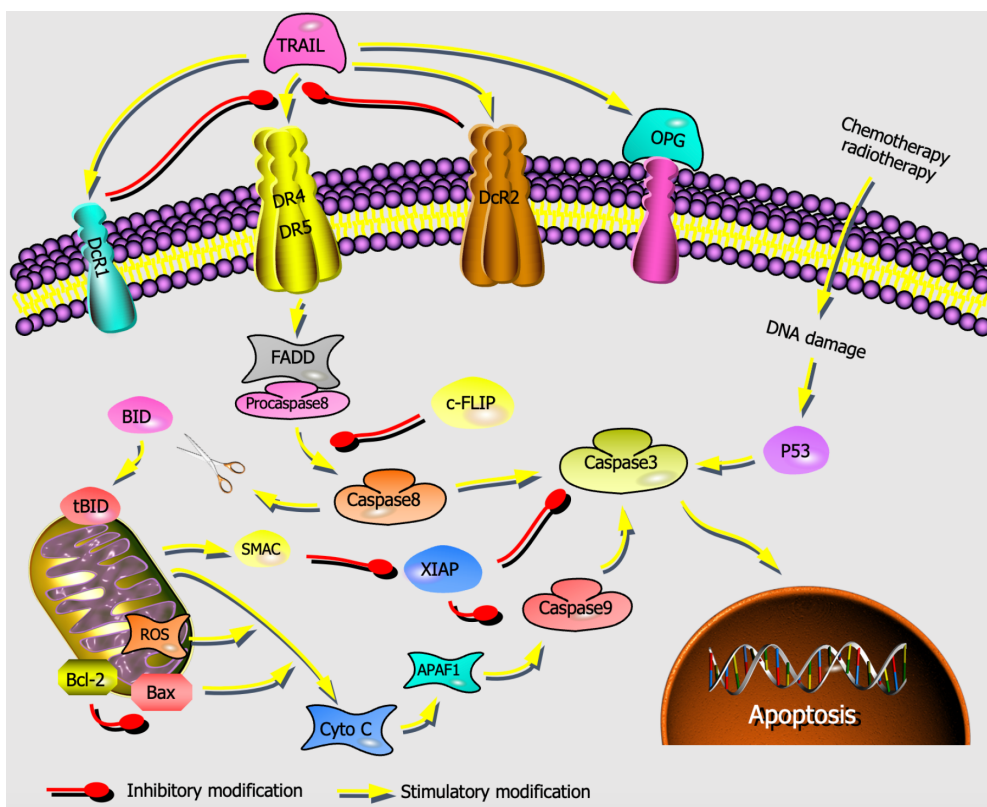
This process may be more related to the mitochondria-independent pathway, as Cyto-C and Bax/Bcl-2 showed only slight upregulation and insignificant differences (Figure 6I-K), which are key indicators in the mitochondria-dependent pathway[52]. ROS were significantly upregulated but could not cause Cyto-C release (Figure 6I, J and L). Thus, we hypothesized that ROS mainly acted as signal transduction factors of the TRAIL pathway rather than the mitochondrial-dependent pathway[49]. Additionally, c-FLIP was inhibited, but XIAP was slightly upregulated (Figure 6M and N). A negative feedback



DOI: 10.3748/wjg.v29.i12.1875 Copyright ©The Author(s) 2023.

Figure 6 Antihepatoma mechanism of scolopentide. A: Flow cytometry suggested that apoptosis occurred in HepG2 cells after treatment with extracted scolopentide *in vitro*. B-I: Quantitative real-time polymerase chain reaction (qRT-PCR) and western blotting showed that the expression of DR4 (B and C), DR5 (H and I), FADD (E and F), caspase-8 (F and G), and caspase-3 (C and D) was significantly upregulated in the scolopentide group. DR4 was the most considerably

upregulated; I-K: qRT-PCR and western blotting showed that the expression of Cyto-C (I and J) and Bax/Bcl-2 (K) was not upregulated, which are key indicators of mitochondria dependence; L: Tumor ROS levels in the scolopentide group were higher than those in the vehicle group; M: c-FLIP, an inhibitory protein of caspase-8, was significantly downregulated in qRT-PCR; N: XIAP, an inhibitory protein of caspase-3, was insignificantly upregulated in qRT-PCR. DR4: Death receptor 4; DR5: Death receptor 5; FADD: Fas-associated death domain protein. $n = 4$ per group in qRT-PCR, $n = 3$ per group in Western blotting, $n = 4$ per group in ROS; $^aP < 0.05$, $^bP < 0.01$.



DOI: 10.3748/wjg.v29.i12.1875 Copyright ©The Author(s) 2023.

Figure 7 Activation of the mitochondria-independent and mitochondria-dependent apoptosis pathways by tumor necrosis factor-related apoptosis-inducing ligand. The mitochondria-independent pathway (engaged through death receptors, activated caspase family directly) and mitochondria-dependent pathway (triggered through the Bcl-2 gene superfamily) are represented. TRAIL: Tumor necrosis factor-related apoptosis-inducing ligand; DR4: Death receptor 4; DR5: Death receptor 5; FADD: Fas-associated death domain protein; Cyto-C: Cytochrome c; Bax: Bcl-2-associated X protein; Bcl-2: B-cell lymphoma-2; ROS: Reactive oxygen species; c-FLIP: Cellular Fas associated death domain-like interleukin-1 β converting enzyme inhibitory protein; XIAP: X-chromosome linked inhibitor-of-apoptosis protein.

mechanism of apoptosis may contribute to preventing excessive apoptosis in the body. Overall, our findings suggested that scolopentide may induce apoptosis in tumor cells, especially gastrointestinal tumors, by activating DR4 and DR5 and leading to the caspase cascade.

CONCLUSION

In summary, we obtained a small molecule polypeptide from *Scolopendra subspinipes mutilans* L. Koch with the strongest antitumor activity, especially for liver tumors. Mechanistically, scolopentide may induce tumor cell apoptosis by activating DR4 and DR5. Scolopentide is considered to be a promising drug candidate for cancer treatment, especially treatment of gastrointestinal tumors. Our studies are also expected to provide a reference for the extraction, purification and characterization of effective components in animal-derived medicines. Both extracted and synthesized scolopentide had antihepatoma activity. When HepG2 cells were cultured with two scolopentides for 48 h, a CCK8 assay showed that the IC₅₀ values were 22.06 μ g/mL (extracted scolopentide) and 237.726 μ g/mL (synthesized scolopentide), which indicates that the antihepatoma activity of synthesized scolopentide was weaker than that of the extracted scolopentide. This may be due to the lack of dimensional folding configurations in the synthesized peptide during synthesis. Additionally, the TRAIL pathway was activated but decreased incrementally. Key areas of future research include investigating methods of modifying the spatial architecture of synthetic scolopentide, fully activating the TRAIL pathway and improving its

antihepatoma activity.

ARTICLE HIGHLIGHTS

Research background

Centipedes have been used to treat tumors for hundreds of years in China, while current studies rarely focus on hepatoma. The molecular identities of antihepatoma bioactive components in centipedes have not yet been extensively investigated. It is a challenge to isolate and characterize the effective components of centipedes due to limited peptide purification technologies for animal-derived medicines.

Research motivation

The antihepatoma components in centipedes remain unclear. We investigated the centipede components with the strongest antihepatoma activity to develop candidates for antihepatoma drugs.

Research objectives

To purify, characterize, and synthesize the bioactive components with the strongest antihepatoma activity from centipedes and determine the antihepatoma mechanism. To provide a reference for the extraction, purification and characterization of effective components for animal-derived medicines.

Research methods

An antihepatoma peptide (scolopentide) was isolated and identified from the centipede *Scolopendra subspinipes mutilans* using a combination of enzymatic hydrolysis, a Sephadex G-25 column, and two steps of high-performance liquid chromatography. Additionally, the CCK8 assay was used to select the extracted fraction with the strongest antihepatoma activity. The molecular weight of the extracted scolopentide was characterized by quadrupole time-of-flight mass spectrometry, and the sequence was matched by using the Mascot search engine. Scolopentide was then synthesized using solid-phase peptide synthesis methods. The antihepatoma effects of extracted and synthetic scolopentide were confirmed *in vitro* and *in vivo*. Mechanistically, flow cytometry and Hoechst staining were conducted to confirm the occurrence of apoptosis. Molecular docking and CCK8 assays were performed to determine the relationship between scolopentide and the tumor necrosis factor-related apoptosis-inducing ligand (TRAIL) pathway. Reactive oxygen species assessment, quantitative real-time polymerase chain reaction and Western blot were used to further verify the hypothesis that scolopentide can stimulate the TRAIL pathway to induce apoptosis.

Research results

A small molecule polypeptide with the strongest antihepatoma activity was derived from *Scolopendra subspinipes mutilans* L. Koch. The molecular weight was 1018.997 Da, and the peptide sequence was RAQNHYCK. Both extracted and synthesized scolopentide had antihepatoma activity in a concentration-dependent manner. Mechanistically, scolopentide activated death receptor 4 (DR4) and DR5 and induced apoptosis in liver cancer cells by promoting the expression of Fas-associated death domain protein (FADD), caspase-8 and caspase-3 through a mitochondria-independent pathway.

Research conclusions

Scolopentide, an antihepatoma peptide, was isolated and identified from centipedes, which activated DR4 and DR5 and induced apoptosis through a mitochondria-independent pathway.

Research perspectives

Scolopentide is considered to be a promising drug candidate for cancer treatment, especially treatment of liver cancer. Ways in which to modify the spatial architecture of synthetic scolopentide, fully activate the TRAIL pathway and improve its antihepatoma activity will be key areas for future research.

ACKNOWLEDGEMENTS

The authors would like to thank Professor Feng Li (University of California) for providing suggestion on peptide sequence screening, and Professor Yangu Peng (Hunan University of Chinese Medicine) for providing guidance on extraction technology of centipede.

FOOTNOTES

Author contributions: Tian XF and Tian S contributed equally to this work, and they are co-corresponding authors; Tian XF, Tian S, Pei G, and Hu YX designed the study; Hu YX, Liu Z, Deng Z, Mei S, Yi C, Huang Z, and Feng T performed experiments; Pei G helped perform the high performance liquid chromatography and mass spectrum; Zhang Z performed data analyses; Zhou QH processed figures and tables; Hu YX wrote the manuscript; Tian XF, Zhou Q, and Zeng PH reviewed and edited the manuscript; all authors reviewed and approved the final version of the article.

Supported by the National Natural Science Foundation of China, No. U20A20408 and No. 82074450; Natural Science Foundation of Hunan Province, No. 2020JJ4066 and No. 2021JJ40405; Key scientific research project of Hunan Education Department, No. 21A0243; and Key project of academician workstation guidance project, No. 21YSZQ007.

Institutional animal care and use committee statement: All animal experiments were conducted according to a protocol approved by the Ethics Review Committee of Experimental Animal Welfare at the Hunan University of Chinese Medicine (Approval No. LL2021040705).

Conflict-of-interest statement: The authors declare that they have no competing interests.

Data sharing statement: Dataset available from the corresponding author at 003640@hnucm.edu.cn.

ARRIVE guidelines statement: The authors have read the ARRIVE Guidelines, and the manuscript was prepared and revised according to the ARRIVE Guidelines.

Open-Access: This article is an open-access article that was selected by an in-house editor and fully peer-reviewed by external reviewers. It is distributed in accordance with the Creative Commons Attribution NonCommercial (CC BY-NC 4.0) license, which permits others to distribute, remix, adapt, build upon this work non-commercially, and license their derivative works on different terms, provided the original work is properly cited and the use is non-commercial. See: <https://creativecommons.org/Licenses/by-nc/4.0/>

Country/Territory of origin: China

ORCID number: Yu-Xing Hu [0000-0001-7413-1394](https://orcid.org/0000-0001-7413-1394); Zhuo Liu [0000-0001-9235-5244](https://orcid.org/0000-0001-9235-5244); Zhen Zhang [0000-0001-9257-1449](https://orcid.org/0000-0001-9257-1449); Zhe Deng [0000-0002-3283-6289](https://orcid.org/0000-0002-3283-6289); Zhen Huang [0000-0002-8437-7141](https://orcid.org/0000-0002-8437-7141); Ting Feng [0000-0001-5306-3572](https://orcid.org/0000-0001-5306-3572); Qing-Hong Zhou [0000-0003-0510-6915](https://orcid.org/0000-0003-0510-6915); Si Mei [0000-0002-4263-1121](https://orcid.org/0000-0002-4263-1121); Chun Yi [0000-0003-1740-0329](https://orcid.org/0000-0003-1740-0329); Qing Zhou [0000-0002-9633-7542](https://orcid.org/0000-0002-9633-7542); Gang Pei [0000-0002-3389-7868](https://orcid.org/0000-0002-3389-7868); Sha Tian [0000-0002-2557-5674](https://orcid.org/0000-0002-2557-5674); Xue-Fei Tian [0000-0003-4786-0844](https://orcid.org/0000-0003-4786-0844).

S-Editor: Chen YL

L-Editor: A

P-Editor: Zhang XD

REFERENCES

- 1 **Commission NP.** Pharmacopoeia of the People's Republic of China. 2020. [cited 3 September 2022]. Available from: <https://www.semanticscholar.org/paper/Pharmacopoeia-of-the-People%27s-Republic-of-China-Pharmacopoeia/8726ceef0b79ae17b4f2fd7490728945711b717>
- 2 **Xu XL**, Wang CM, Geng D, Zhang L, Hu B. [Effects of centipede extracts on normal mouse and S180, H22 bearing mouse]. *Zhong Yao Cai* 2010; **33**: 499-503 [PMID: [20845773](https://pubmed.ncbi.nlm.nih.gov/20845773/)]
- 3 **Ding D**, Guo YR, Wu RL, Qi WY, Xu HM. Two new isoquinoline alkaloids from Scolopendra subspinipes mutilans induce cell cycle arrest and apoptosis in human glioma cancer U87 cells. *Fitoterapia* 2016; **110**: 103-109 [PMID: [26947248](https://pubmed.ncbi.nlm.nih.gov/26947248/) DOI: [10.1016/j.fitote.2016.03.004](https://doi.org/10.1016/j.fitote.2016.03.004)]
- 4 **Ma W**, Zhang D, Zheng L, Zhan Y, Zhang Y. Potential roles of Centipede Scolopendra extracts as a strategy against EGFR-dependent cancers. *Am J Transl Res* 2015; **7**: 39-52 [PMID: [25755827](https://pubmed.ncbi.nlm.nih.gov/25755827/)]
- 5 **Chaparro-Aguirre E**, Segura-Ramírez PJ, Alves FL, Riske KA, Miranda A, Silva Júnior PI. Antimicrobial activity and mechanism of action of a novel peptide present in the ecdysis process of centipede Scolopendra subspinipes subspinipes. *Sci Rep* 2019; **9**: 13631 [PMID: [31541146](https://pubmed.ncbi.nlm.nih.gov/31541146/) DOI: [10.1038/s41598-019-50061-y](https://doi.org/10.1038/s41598-019-50061-y)]
- 6 **Ali SM**, Khan NA, Sagathevan K, Anwar A, Siddiqui R. Biologically active metabolite(s) from haemolymph of red-headed centipede Scolopendra subspinipes possess broad spectrum antibacterial activity. *AMB Express* 2019; **9**: 95 [PMID: [31254123](https://pubmed.ncbi.nlm.nih.gov/31254123/) DOI: [10.1186/s13568-019-0816-3](https://doi.org/10.1186/s13568-019-0816-3)]
- 7 **Kong Y**, Huang SL, Shao Y, Li S, Wei JF. Purification and characterization of a novel antithrombotic peptide from Scolopendra subspinipes mutilans. *J Ethnopharmacol* 2013; **145**: 182-186 [PMID: [23127646](https://pubmed.ncbi.nlm.nih.gov/23127646/) DOI: [10.1016/j.jep.2012.10.048](https://doi.org/10.1016/j.jep.2012.10.048)]
- 8 **Luo L**, Li B, Wang S, Wu F, Wang X, Liang P, Ombati R, Chen J, Lu X, Cui J, Lu Q, Zhang L, Zhou M, Tian C, Yang S, Lai R. Centipedes subdue giant prey by blocking KCNQ channels. *Proc Natl Acad Sci U S A* 2018; **115**: 1646-1651 [PMID: [29358396](https://pubmed.ncbi.nlm.nih.gov/29358396/) DOI: [10.1073/pnas.1714760115](https://doi.org/10.1073/pnas.1714760115)]
- 9 **Kong Y**, Xu C, He ZL, Zhou QM, Wang JB, Li ZY, Ming X. A novel peptide inhibitor of platelet aggregation from stiff

silkworm, *Bombyx batryticatus*. *Peptides* 2014; **53**: 70-78 [PMID: 24361453 DOI: 10.1016/j.peptides.2013.12.004]

10 **Schägger H**, von Jagow G. Tricine-sodium dodecyl sulfate-polyacrylamide gel electrophoresis for the separation of proteins in the range from 1 to 100 kDa. *Anal Biochem* 1987; **166**: 368-379 [PMID: 2449095 DOI: 10.1016/0003-2697(87)90587-2]

11 **Lan XQ**, Zhao F, Wang QQ, Li JH, Zeng L, Zhang Y, Lee WH. Isolation and characterization of the major centipede allergen Sco m 5 from *Scolopendra subspinipes mutilans*. *Allergol Int* 2021; **70**: 121-128 [PMID: 32680616 DOI: 10.1016/j.alit.2020.06.003]

12 **Han Y**, Kamau PM, Lai R, Luo L. Bioactive Peptides and Proteins from Centipede Venoms. *Molecules* 2022; **27** [PMID: 35889297 DOI: 10.3390/molecules27144423]

13 **Li SZ**. Compendium of Materia Medica. 21st Century Press. Nanchang: National Top 100 Publishing House, 2017: 273-274

14 **Zhang X**. Integrating Chinese and Western Medicine. Shijiazhuang: Hebei Science and Technology Press, 1985: 135-136

15 **Xie LS**, Huan T, Yang JL, Wu J, Zhao P. [The effect of Shendan Sanjie capsule on angiogenesis in mice with colitis associated cancer and mechanism]. *Zhonghua Zhong Liu Za Zhi* 2021; **43**: 1170-1176 [PMID: 34794219 DOI: 10.3760/cma.j.cn112152-20210318-00240]

16 **Yan W**, Lu J, Li G, Wei H, Ren WH. Amidated Scolopin-2 inhibits proliferation and induces apoptosis of Hela cells in vitro and in vivo. *Biotechnol Appl Biochem* 2018; **65**: 672-679 [PMID: 29644748 DOI: 10.1002/bab.1661]

17 **Lee JH**, Kim IW, Kim SH, Kim MA, Yun EY, Nam SH, Ahn MY, Kang D, Hwang JS. Anticancer Activity of the Antimicrobial Peptide Scolopendrasin VII Derived from the Centipede, *Scolopendra subspinipes mutilans*. *J Microbiol Biotechnol* 2015; **25**: 1275-1280 [PMID: 25907065 DOI: 10.4014/jmb.1503.03091]

18 **Ma W**, Liu R, Qi J, Zhang Y. Extracts of centipede *Scolopendra subspinipes mutilans* induce cell cycle arrest and apoptosis in A375 human melanoma cells. *Oncol Lett* 2014; **8**: 414-420 [PMID: 24595287 DOI: 10.3892/ol.2014.2139]

19 **Yong-Jiea T**, Zhuob L, Liuc L, Yuanc C, Xiao-Did H, Xue-Feic T. STAT3 Inhibition by Centipede Scolopendra Extract in Liver Cancer HepG2 Cells and Orthotopic Mouse Models of Hepatocellular Carcinoma. *Dig Chin Med* 2020; **3**: 67-79 [DOI: 10.1016/j.dcm.2020.06.002]

20 **Chen Y**, Ai XJ, Wang ZQ, Tian S, Zhou Q, Pei G, Tian XF. Study on Anti-lung Cancer Efficiency of Centipede Extracts in Vitro and Vivo Experiments. *Zhongguo Zhongyiyo Xinxi Zazhi* 2016; **23**: 61-63 [DOI: 10.3969/j.issn.1005-5304.2016.05.016]

21 **Fesik SW**. Promoting apoptosis as a strategy for cancer drug discovery. *Nat Rev Cancer* 2005; **5**: 876-885 [PMID: 16239906 DOI: 10.1038/nrc1736]

22 **Jin Z**, El-Deiry WS. Overview of cell death signaling pathways. *Cancer Biol Ther* 2005; **4**: 139-163 [PMID: 15725726 DOI: 10.4161/cbt.4.2.1508]

23 **Labuschagne CF**, Zani F, Vousden KH. Control of metabolism by p53 - Cancer and beyond. *Biochim Biophys Acta Rev Cancer* 2018; **1870**: 32-42 [PMID: 29883595 DOI: 10.1016/j.bbcan.2018.06.001]

24 **Marei HE**, Althani A, Afifi N, Hasan A, Caceci T, Pozzoli G, Morrione A, Giordano A, Cenciarelli C. p53 signaling in cancer progression and therapy. *Cancer Cell Int* 2021; **21**: 703 [PMID: 34952583 DOI: 10.1186/s12935-021-02396-8]

25 **Aubrey BJ**, Kelly GL, Janic A, Herold MJ, Strasser A. How does p53 induce apoptosis and how does this relate to p53-mediated tumour suppression? *Cell Death Differ* 2018; **25**: 104-113 [PMID: 29149101 DOI: 10.1038/cdd.2017.169]

26 **Holland PM**. Death receptor agonist therapies for cancer, which is the right TRAIL? *Cytokine Growth Factor Rev* 2014; **25**: 185-193 [PMID: 24418173 DOI: 10.1016/j.cytoogr.2013.12.009]

27 **Yuan X**, Gajan A, Chu Q, Xiong H, Wu K, Wu GS. Developing TRAIL/TRAIL death receptor-based cancer therapies. *Cancer Metastasis Rev* 2018; **37**: 733-748 [PMID: 29541897 DOI: 10.1007/s10555-018-9728-y]

28 **von Karstedt S**, Montinaro A, Walczak H. Exploring the TRAILS less travelled: TRAIL in cancer biology and therapy. *Nat Rev Cancer* 2017; **17**: 352-366 [PMID: 28536452 DOI: 10.1038/nrc.2017.28]

29 **Chen CY**, Yiin SJ, Hsu JL, Wang WC, Lin SC, Chern CL. Isoobtusilactone A sensitizes human hepatoma Hep G2 cells to TRAIL-induced apoptosis via ROS and CHOP-mediated up-regulation of DR5. *J Agric Food Chem* 2012; **60**: 3533-3539 [PMID: 22400995 DOI: 10.1021/jf2051224]

30 **Kondo K**, Yamasaki S, Sugie T, Teratani N, Kan T, Imamura M, Shimada Y. Cisplatin-dependent upregulation of death receptors 4 and 5 augments induction of apoptosis by TNF-related apoptosis-inducing ligand against esophageal squamous cell carcinoma. *Int J Cancer* 2006; **118**: 230-242 [PMID: 16003725 DOI: 10.1002/ijc.21283]

31 **Zhou X**, Zijlstra SN, Soto-Gamez A, Setroikromo R, Quax WJ. Artemisinin Derivatives Stimulate DR5-Specific TRAIL-Induced Apoptosis by Regulating Wildtype P53. *Cancers (Basel)* 2020; **12** [PMID: 32899699 DOI: 10.3390/cancers12092514]

32 **Nazim UM**, Park SY. Luteolin sensitizes human liver cancer cells to TRAIL-induced apoptosis via autophagy and JNKmediated death receptor 5 upregulation. *Int J Oncol* 2019; **54**: 665-672 [PMID: 30431076 DOI: 10.3892/ijo.2018.4633]

33 **Pavet V**, Beyrath J, Pardin C, Morizot A, Lechner MC, Briand JP, Wendland M, Maison W, Fournel S, Micheau O, Guichard G, Gronemeyer H. Multivalent DR5 peptides activate the TRAIL death pathway and exert tumoricidal activity. *Cancer Res* 2010; **70**: 1101-1110 [PMID: 20103630 DOI: 10.1158/0008-5472.CAN-09-2889]

34 **Luo A**, Wang A, Kamau PM, Lai R, Luo L. Centipede Venom: A Potential Source of Ion Channel Modulators. *Int J Mol Sci* 2022; **23** [PMID: 35806107 DOI: 10.3390/ijms23137105]

35 **Undheim EA**, Jenner RA, King GF. Centipede venoms as a source of drug leads. *Expert Opin Drug Discov* 2016; **11**: 1139-1149 [PMID: 27611363 DOI: 10.1080/17460441.2016.1235155]

36 **Ombatti R**, Luo L, Yang S, Lai R. Centipede envenomation: Clinical importance and the underlying molecular mechanisms. *Toxicon* 2018; **154**: 60-68 [PMID: 30273703 DOI: 10.1016/j.toxicon.2018.09.008]

37 **Peng K**, Kong Y, Zhai L, Wu X, Jia P, Liu J, Yu H. Two novel antimicrobial peptides from centipede venoms. *Toxicon* 2010; **55**: 274-279 [PMID: 19716842 DOI: 10.1016/j.toxicon.2009.07.040]

38 **Kong Y**, Shao Y, Chen H, Ming X, Wang JB, Li ZY, Wei JF. A Novel Factor Xa-Inhibiting Peptide from Centipedes Venom. *Int J Pept Res Ther* 2013; **19**: 303-311 [PMID: 24273471 DOI: 10.1007/s10989-013-9353-0]

39 **Yang S**, Xiao Y, Kang D, Liu J, Li Y, Undheim EA, Klint JK, Rong M, Lai R, King GF. Discovery of a selective NaV1.7 inhibitor from centipede venom with analgesic efficacy exceeding morphine in rodent pain models. *Proc Natl Acad Sci U S A* 2013; **110**: 17534-17539 [PMID: 24082113 DOI: 10.1073/pnas.1306285110]

40 **Lee JH**, Kim IW, Kim MA, Ahn MY, Yun EY, Hwang JS. Antimicrobial Activity of the Scolopendrasin V Peptide Identified from the Centipede Scolopendra subspinipes mutilans. *J Microbiol Biotechnol* 2017; **27**: 43-48 [PMID: 27780954 DOI: 10.4014/jmb.1609.09057]

41 **Lee W**, Hwang JS, Lee DG. A novel antimicrobial peptide, scolopendin, from Scolopendra subspinipes mutilans and its microbicidal mechanism. *Biochimie* 2015; **118**: 176-184 [PMID: 26342880 DOI: 10.1016/j.biochi.2015.08.015]

42 **Lee H**, Hwang JS, Lee J, Kim JI, Lee DG. Scolopendin 2, a cationic antimicrobial peptide from centipede, and its membrane-active mechanism. *Biochim Biophys Acta* 2015; **1848**: 634-642 [PMID: 25462167 DOI: 10.1016/j.bbamem.2014.11.016]

43 **Choi H**, Hwang JS, Lee DG. Identification of a novel antimicrobial peptide, scolopendin 1, derived from centipede Scolopendra subspinipes mutilans and its antifungal mechanism. *Insect Mol Biol* 2014; **23**: 788-799 [PMID: 25209888 DOI: 10.1111/im.12124]

44 **Lee H**, Hwang JS, Lee DG. Scolopendin, an antimicrobial peptide from centipede, attenuates mitochondrial functions and triggers apoptosis in *Candida albicans*. *Biochem J* 2017; **474**: 635-645 [PMID: 28008133 DOI: 10.1042/BCJ20161039]

45 **Lu J**, Qiu PD, Wen HR. Mechanism of Antimicrobial Peptide Scolopin 2-NH2 Isolated from Scolopendra subspinipes mutilans. *Biol Bull* 2018; **34**: 179-190 [DOI: 10.13560/j.cnki.biotech.bull.1985.2018-0476]

46 **den Hollander MW**, Gietema JA, de Jong S, Walenkamp AM, Reyners AK, Oldenhuis CN, de Vries EG. Translating TRAIL-receptor targeting agents to the clinic. *Cancer Lett* 2013; **332**: 194-201 [PMID: 22531313 DOI: 10.1016/j.canlet.2012.04.007]

47 **Kelley SK**, Ashkenazi A. Targeting death receptors in cancer with Apo2L/TRAIL. *Curr Opin Pharmacol* 2004; **4**: 333-339 [PMID: 15251125 DOI: 10.1016/j.coph.2004.02.006]

48 **Zorov DB**, Juhaszova M, Sollott SJ. Mitochondrial reactive oxygen species (ROS) and ROS-induced ROS release. *Physiol Rev* 2014; **94**: 909-950 [PMID: 24987008 DOI: 10.1152/physrev.00026.2013]

49 **Eberle J**. Countering TRAIL Resistance in Melanoma. *Cancers (Basel)* 2019; **11** [PMID: 31083589 DOI: 10.3390/cancers11050656]

50 **Chen KF**, Tai WT, Liu TH, Huang HP, Lin YC, Shiao CW, Li PK, Chen PJ, Cheng AL. Sorafenib overcomes TRAIL resistance of hepatocellular carcinoma cells through the inhibition of STAT3. *Clin Cancer Res* 2010; **16**: 5189-5199 [PMID: 20884624 DOI: 10.1158/1078-0432.CCR-09-3389]

51 **Chen KF**, Chen HL, Liu CY, Tai WT, Ichikawa K, Chen PJ, Cheng AL. Dovitinib sensitizes hepatocellular carcinoma cells to TRAIL and tigatuzumab, a novel anti-DR5 antibody, through SHP-1-dependent inhibition of STAT3. *Biochem Pharmacol* 2012; **83**: 769-777 [PMID: 22230479 DOI: 10.1016/j.bcp.2011.12.035]

52 **Yamaguchi R**, Lartigue L, Perkins G. Targeting Mcl-1 and other Bcl-2 family member proteins in cancer therapy. *Pharmacol Ther* 2019; **195**: 13-20 [PMID: 30347215 DOI: 10.1016/j.pharmthera.2018.10.009]

53 **Wenhua R**, Shuangquan Z, Daxiang S, Kaiya Z, Guang Y. Induction, purification and characterization of an antibacterial peptide scolopendrin I from the venom of centipede Scolopendra subspinipes mutilans. *Indian J Biochem Biophys* 2006; **43**: 88-93 [PMID: 16955756]

54 **Choi H**, Hwang JS, Lee DG. Antifungal effect and pore-forming action of lactoferricin B like peptide derived from centipede Scolopendra subspinipes mutilans. *Biochim Biophys Acta* 2013; **1828**: 2745-2750 [PMID: 23896552 DOI: 10.1016/j.bbamem.2013.07.021]

55 **Park YJ**, Kim HS, Lee HY, Hwang JS, Bae YS. A novel antimicrobial peptide isolated from centipede Scolopendra subspinipes mutilans stimulates neutrophil activity through formyl peptide receptor 2. *Biochem Biophys Res Commun* 2017; **494**: 352-357 [PMID: 28988115 DOI: 10.1016/j.bbrc.2017.10.019]

56 **Kwon YN**, Lee JH, Kim IW, Kim SH, Yun EY, Nam SH, Ahn MY, Jeong M, Kang DC, Lee IH, Hwang JS. Antimicrobial activity of the synthetic peptide scolopendrasin ii from the centipede Scolopendra subspinipes mutilans. *J Microbiol Biotechnol* 2013; **23**: 1381-1385 [PMID: 23801249 DOI: 10.4014/jmb.1306.06013]

57 **Park YJ**, Lee SK, Jung YS, Lee M, Lee HY, Kim SD, Park JS, Koo J, Hwang JS, Bae YS. Promotion of formyl peptide receptor 1-mediated neutrophil chemotactic migration by antimicrobial peptides isolated from the centipede Scolopendra subspinipes mutilans. *BMB Rep* 2016; **49**: 520-525 [PMID: 27502013]

58 **Park YJ**, Park B, Lee M, Jeong YS, Lee HY, Sohn DH, Song JJ, Lee JH, Hwang JS, Bae YS. A novel antimicrobial peptide acting via formyl peptide receptor 2 shows therapeutic effects against rheumatoid arthritis. *Sci Rep* 2018; **8**: 14664 [PMID: 30279454 DOI: 10.1038/s41598-018-32963-5]

59 **Yoo WG**, Lee JH, Shin Y, Shim JY, Jung M, Kang BC, Oh J, Seong J, Lee HK, Kong HS, Song KD, Yun EY, Kim IW, Kwon YN, Lee DG, Hwang UW, Park J, Hwang JS. Antimicrobial peptides in the centipede Scolopendra subspinipes mutilans. *Funct Integr Genomics* 2014; **14**: 275-283 [PMID: 24652097 DOI: 10.1007/s10142-014-0366-3]

60 **Park YJ**, Lee HY, Jung YS, Park JS, Hwang JS, Bae YS. Antimicrobial peptide scolopendrasin VII, derived from the centipede Scolopendra subspinipes mutilans, stimulates macrophage chemotaxis via formyl peptide receptor 1. *BMB Rep* 2015; **48**: 479-484 [PMID: 26129676 DOI: 10.5483/bmbr.2015.48.8.115]

61 **Du C**, Li J, Shao Z, Mwangi J, Xu R, Tian H, Mo G, Lai R, Yang S. Centipede KCNQ Inhibitor SsTx Also Targets K(V)1.3. *Toxins (Basel)* 2019; **11** [PMID: 30717088 DOI: 10.3390/toxins11020076]

62 **Wang Y**, Li X, Yang M, Wu C, Zou Z, Tang J, Yang X. Centipede venom peptide SsmTX-I with two intramolecular disulfide bonds shows analgesic activities in animal models. *J Pept Sci* 2017; **23**: 384-391 [PMID: 28247497 DOI: 10.1002/psc.2988]

63 **Chaparro E**, da Silva PI Junior. Lacrain: the first antimicrobial peptide from the body extract of the Brazilian centipede Scolopendra viridicornis. *Int J Antimicrob Agents* 2016; **48**: 277-285 [PMID: 27451089 DOI: 10.1016/j.ijantimicag.2016.05.015]

64 **Zhou YQ**, Han L, Liu ZQ, Du KC, Li KY. [Effect of centipede extract on cervical tumor of mice and its mechanism]. *Zhong Yao Cai* 2011; **34**: 859-864 [PMID: 22017000]

65 **Ren Y**, Houghton P, Hider RC. Relevant activities of extracts and constituents of animals used in traditional Chinese medicine for central nervous system effects associated with Alzheimer's disease. *J Pharm Pharmacol* 2006; **58**: 989-996 [PMID: 16805960 DOI: 10.1211/jpp.58.7.0015]

Submit a Manuscript: <https://www.f6publishing.com>

World J Gastroenterol 2023 March 28; 29(12): 1899-1910

DOI: [10.3748/wjg.v29.i12.1899](https://doi.org/10.3748/wjg.v29.i12.1899)

ISSN 1007-9327 (print) ISSN 2219-2840 (online)

ORIGINAL ARTICLE

Clinical Trials Study

Linked color imaging vs Lugol chromoendoscopy for esophageal squamous cell cancer and precancerous lesion screening: A noninferiority study

Zi-Xin Wang, Long-Song Li, Song Su, Jin-Ping Li, Bo Zhang, Nan-Jun Wang, Sheng-Zhen Liu, Sha-Sha Wang, Shuai Zhang, Ya-Wei Bi, Fei Gao, Qun Shao, Ning Xu, Bo-Zong Shao, Yi Yao, Fang Liu, En-Qiang Linghu, Ning-Li Chai

Specialty type: Gastroenterology and hepatology

Provenance and peer review:

Unsolicited article; Externally peer reviewed.

Peer-review model: Single blind

Peer-review report's scientific quality classification

Grade A (Excellent): 0

Grade B (Very good): B, B, B

Grade C (Good): 0

Grade D (Fair): 0

Grade E (Poor): 0

P-Reviewer: Abe Y, Japan; Tyakht AV, United Kingdom; Woromogo SH, Congo

Received: November 30, 2022

Peer-review started: November 30, 2022

First decision: December 20, 2022

Revised: December 29, 2022

Accepted: March 9, 2023

Article in press: March 9, 2023

Published online: March 28, 2023

Zi-Xin Wang, Long-Song Li, Song Su, Jin-Ping Li, Bo Zhang, Nan-Jun Wang, Sheng-Zhen Liu, Sha-Sha Wang, Shuai Zhang, Ya-Wei Bi, Fei Gao, Qun Shao, Ning Xu, Bo-Zong Shao, Yi Yao, Fang Liu, En-Qiang Linghu, Ning-Li Chai, Department of Gastroenterology, The First Medical Center of Chinese PLA General Hospital, Beijing 100853, China

Corresponding author: Ning-Li Chai, MD, Chief Physician, Professor, Department of Gastroenterology, The First Medical Center of Chinese PLA General Hospital, No. 28 Fuxing Road, Haidian District, Beijing 100853, China. csxlily@163.com

Abstract

BACKGROUND

Lugol chromoendoscopy (LCE) has served as a standard screening technique in high-risk patients with esophageal cancer. Nevertheless, LCE is not suitable for general population screening given its side effects. Linked color imaging (LCI) is a novel image-enhanced endoscopic technique that can distinguish subtle differences in mucosal color.

AIM

To compare the diagnostic performance of LCI with LCE in detecting esophageal squamous cell cancer and precancerous lesions and to evaluate whether LCE can be replaced by LCI in detecting esophageal neoplastic lesions.

METHODS

In this prospective study, we enrolled 543 patients who underwent white light imaging (WLI), LCI and LCE successively. We compared the sensitivity and specificity of LCI and LCE in the detection of esophageal neoplastic lesions. Clinicopathological features and color analysis of lesions were assessed.

RESULTS

In total, 43 patients (45 neoplastic lesions) were analyzed. Among them, 36 patients (38 neoplastic lesions) were diagnosed with LCI, and 39 patients (41 neoplastic lesions) were diagnosed with LCE. The sensitivity of LCI was similar to that of LCE (83.7% vs 90.7%, $P = 0.520$), whereas the specificity of LCI was greater



than that of LCE (92.4% *vs* 87.0%, $P = 0.007$). The LCI procedure time in the esophageal examination was significantly shorter than that of LCE [42 (34, 50) s *vs* 160 (130, 189) s, $P < 0.001$]. The color difference between the lesion and surrounding mucosa in LCI was significantly greater than that observed with WLI. However, the color difference in LCI was similar in different pathological types of esophageal squamous cell cancer.

CONCLUSION

LCI offers greater specificity than LCE in the detection of esophageal squamous cell cancer and precancerous lesions, and LCI represents a promising screening strategy for general populations.

Key Words: Linked color imaging; Lugol chromoendoscopy; Esophageal squamous cell cancer; Precancerous lesions; Color difference

©The Author(s) 2023. Published by Baishideng Publishing Group Inc. All rights reserved.

Core Tip: Lugol chromoendoscopy (LCE) has served as the standard screening technique in high-risk patients with esophageal cancer. Nevertheless, LCE can induce esophageal spasms and chest pain and is associated with the risk of aspiration and iodine allergy. Therefore, LCE is not suitable for general population screening. Linked color imaging (LCI) is a novel image-enhanced endoscopy that can distinguish subtle differences in mucosal color. In this study, we compared the use of LCI and LCE in the screening of esophageal neoplastic lesions. Based on our analysis, we found that LCI is more specific than LCE and represents a promising screening strategy.

Citation: Wang ZX, Li LS, Su S, Li JP, Zhang B, Wang NJ, Liu SZ, Wang SS, Zhang S, Bi YW, Gao F, Shao Q, Xu N, Shao BZ, Yao Y, Liu F, Linghu EQ, Chai NL. Linked color imaging *vs* Lugol chromoendoscopy for esophageal squamous cell cancer and precancerous lesion screening: A noninferiority study. *World J Gastroenterol* 2023; 29(12): 1899-1910

URL: <https://www.wjgnet.com/1007-9327/full/v29/i12/1899.htm>

DOI: <https://dx.doi.org/10.3748/wjg.v29.i12.1899>

INTRODUCTION

Esophageal cancer is the seventh most common cancer and the sixth leading cause of cancer-related deaths worldwide[1]. Most patients with esophageal cancer have progressed to an advanced stage when diagnosed, with poor quality of life and an overall 5-year survival rate of less than 20%[2,3]. Esophageal squamous cell carcinoma (ESCC) is the most common form of esophageal cancer worldwide, representing greater than 85% of all esophageal cancer cases[4,5]. Curative resection using endoscopic mucosal resection or endoscopic submucosal dissection is possible for lesions with high-grade intraepithelial neoplasia and most T1 tumors, offering less trauma, faster recovery and fewer complications[6]. Therefore, early diagnosis is critical for treatment success and prognostic improvement. Early identification and timely intervention of esophageal cancer or precancerous lesions are of great significance to delay the progression of the disease, improve the prognosis and improve the quality of life.

However, under white light imaging (WLI) endoscopy, early neoplastic lesions are easily missed due to the presence of small lesion areas and subtle differences in the surrounding mucosa color[7]. Historically, Lugol chromoendoscopy (LCE) has served as the standard diagnostic technique given its higher detection rate[8-12]. However, its specificity is low due to light staining under conditions of inflammation, which has been demonstrated in previous studies[13-15]. Furthermore, LCE occasionally induces esophageal spasms and chest pain and is associated with the risk of aspiration and iodine allergy[16,17].

With the advent of image-enhanced endoscopy, many studies have confirmed its efficacy in diagnosing upper gastrointestinal neoplasms[13,18]. The LASEREO system (Fujifilm Corporation, Tokyo, Japan), a new linked color imaging (LCI) technology, was recently developed. LCI images are illuminated with white light and short wavelength narrow-band light in an appropriate proportion simultaneously to realize the simultaneous expansion and contraction of colors. This procedure facilitates enhancement of the red and white colors and makes it easier for the operators to identify the subtle differences in mucosal color[18-21]. In our clinical work, it was found that LCI significantly improved the ability to identify lesions. In a large-scale randomized comparative study, Ono *et al*[20] reported the superiority of LCI over WLI in detecting neoplastic lesions in the upper gastrointestinal tract. Previous studies reported the usefulness of LCI for esophageal neoplasm detection and

assessments of invasive depth[20-24]. Although Yi *et al*[25] compared LCI and LCE in the diagnosis of multiple primary esophageal cancers, no prospective study has compared the diagnosability of LCI with LCE in screening esophageal neoplastic lesions to date. Therefore, we conducted a prospective noninferiority study to compare the efficacy of non-magnifying LCI and LCE in detecting and diagnosing ESCC and precancerous lesions. We evaluated whether LCE can be replaced by LCI in detecting esophageal neoplastic lesions for the general population.

MATERIALS AND METHODS

Study design

This was a single-center, prospective, registered clinical study (No. ChiCTR2100045636) conducted at the First Medical Center of Chinese PLA General Hospital that compared the detection of ESCC and precancerous lesions using LCI *vs* LCE after a conventional white light examination. Endoscopic biopsy is considered the gold standard for ESCC detection. The study was approved by the medical ethics committee of the Chinese PLA General Hospital (Beijing, China), and informed consent forms were obtained from all patients.

Patients

The regional screening studies of esophageal cancer in China revealed that endoscopic screening starting at 40 years of age was cost-effective[26,27]. We recommended 40 years as the beginning age for screening in the Chinese consensus[28]. The following inclusion criteria were employed: (1) Age > 40-year-old; and (2) Provision of written consent to participate. The exclusion criteria were as follows: (1) Contraindication for upper gastrointestinal endoscopy or general anesthesia; (2) Iodine allergy or hyperthyroidism; and (3) Previous surgical resection or chemotherapy, radiotherapy or chemoradiotherapy for ESCC (as these procedures may influence the mucosal surface, which is important for detecting these lesions).

Diagnostic strategies

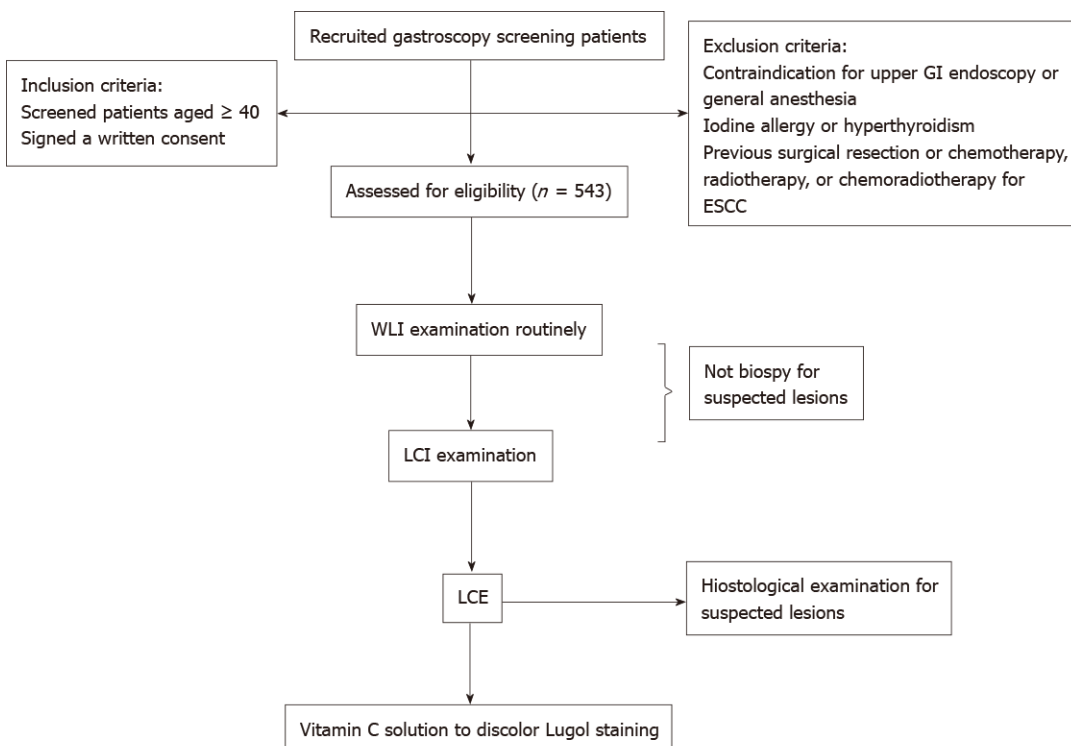
This study used an upper EG-590WR scope (Fujifilm) for gastroscopy. The specific examination procedure was performed as follows. First, WLI examination was performed, and all detected lesions were described. Second, LCI examination was performed, and all lesions detected were recorded in the report (another researcher) but not biopsied immediately to avoid bleeding that could influence the Lugol examination. Third, LCE was performed (2% Lugol dye was spread over the entire esophagus using a spray catheter except near the upper esophageal sphincter given the risk of aspiration), and we biopsied the suspected lesions detected by LCE. Finally, vitamin C solution was used to discolor the Lugol-stained mucosa[29], and lesions suspected only in LCI mode were biopsied based on the recorded location. All suspected lesions were biopsied, and the modality (only LCI, only LCE, or both LCI and LCE) that detected each lesion was indicated in the report. A flow chart of the study is described in Figure 1. All endoscopic operators were experienced and had completed at least 1000 endoscopies. The diagnosis modality (LCI or/and LCE), size, location and macroscopic type (Paris classification[30]) of each detected lesion were recorded and described after examination.

Outcome

The diagnostic criteria for intraepithelial neoplasia and ESCC proposed by the Vienna Classification are as follows: Low-grade intraepithelial neoplasia (LGIN); high-grade intraepithelial neoplasia (HGIN), ESCC and negative for neoplasia, including chronic esophagitis[31]. The primary outcome was the sensitivity and specificity of the diagnostic strategies to detect squamous cell neoplastic lesions (LGIN, HGIN and/or ESCC) according to histology. Endoscopically suspicious ESCC lesions and precancerous lesions were defined as follows: (1) The presence of a reddish color change with a rough mucosal surface in WLI (Figure 2A); (2) The presence of a well-demarcated red or red-orange color region in LCI (Figure 2B)[21,22]; and (3) The presence of a well-demarcated unstained area ≥ 5 mm in diameter or a pink color area after iodine staining given that a Lugol-voiding lesion is more likely to be neoplastic with increasing size (Figure 2C)[32,33].

All suspected lesions were pathologically evaluated by biopsy to determine their neoplastic nature. If the lesion was confirmed to be neoplastic, it was a true positive for the detection modality. Conversely, for non-neoplastic lesions, an unconfirmed suspected lesion was defined as a false positive for the detection modality.

Major outcomes included sensitivity and specificity. The secondary outcome was procedure time. It was possible to determine the length of the imaging operation using a clock linked to the endoscopic equipment. The LCI procedure time was defined as the total examination time from the epiglottis to the dentate line in the image files. The LCE procedure time was defined as the examination time from spraying Lugol dye to complete discoloration.



DOI: 10.3748/wjg.v29.i12.1899 Copyright ©The Author(s) 2023.

Figure 1 Flow chart of study design. ESCC: Esophageal squamous cell carcinoma; GI: Gastrointestinal; LCE: Lugol chromoendoscopy; LCI: Linked color imaging; WLI: White light imaging.

Sample size

In this study, we calculated the required sample size for a noninferiority test using the PASS 15.0.5 sample size software (NCSS, LLC, Kaysville, UT, United States). We regarded LCE as the reference endoscopy technique, and sensitivity was assumed to be 90.0%[13,14]. A sensitivity of 80.0% would be a clinically adequate diagnostic value for screening endoscopy for ESCC. The sample size required was 535 patients using the Z test with pooled variance for a statistical power of 90% with statistical significance defined as $P < 0.05$ ($\alpha = 0.05$ and $\beta = 0.10$).

Color analysis

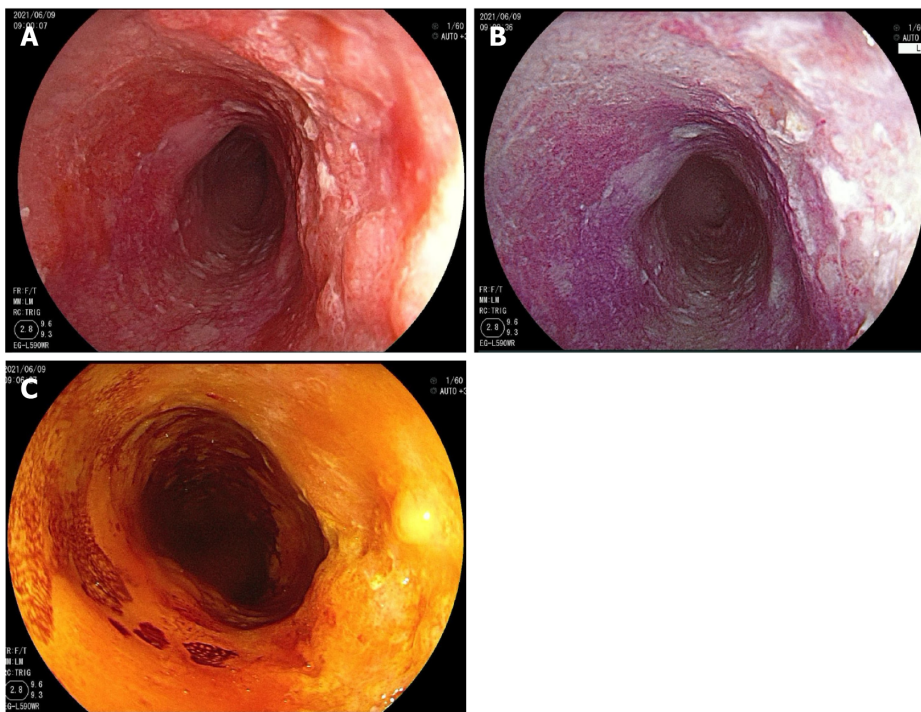
Color analysis was performed using Adobe Photoshop CC2017 (Adobe Systems Inc., San Jose, CA, United States). First, regions of interest of the lesion mucosa and surrounding mucosa were selected in WLI and LCI, separately (Figure 3). Second, the Commission International de l'Eclairage - L*a*b* color space was used to evaluate the mean color value in the regions of interest[34]. The three-dimensional color parameters L* (black to white; range: 0 to + 100), a* (green to red; range: 128 to + 127) and b* (blue to yellow; range: 128 to + 127) were used to define the color value. In Photoshop, L*, a* and b* represent color scores (Lab color unit). Third, the color difference between the lesion and the surrounding mucosa (ΔE) was represented by the distance connecting the two points:

$$\Delta E = \sqrt{(\Delta L^*)^2 + (\Delta a^*)^2 + (\Delta b^*)^2}$$

To reduce the influence of color difference depending on imaging conditions, we chose similar distance and angle images in each mode to calculate color values. We calculated the ΔE of each image in LCI and WLI. In addition, we calculated the ΔE of different neoplastic pathologies in LCI and compared them.

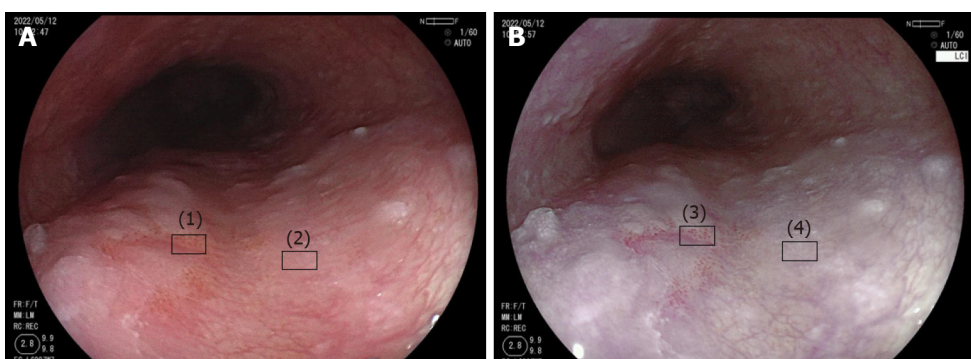
Statistical analysis

All analyses were performed using SPSS 26.0 statistical software (IBM Corp., Armonk, NY, United States). The characteristics and diagnostic yields of patients were presented as percentages (%) or medians (interquartile range), and the color difference variables were expressed as the mean \pm SD. Continuous variables were compared using the student's *t*-test or the Mann-Whitney *U* test, whereas categorical variables were compared using Pearson's χ^2 test or Fisher's exact test. A two-tailed *P* value of < 0.05 was considered statistically significant. The statistical methods of this study were reviewed by the staff of the Department of Epidemiology and Statistics from the First Medical Center of PLA General Hospital (Beijing, China).



DOI: 10.3748/wjg.v29.i12.1899 Copyright ©The Author(s) 2023.

Figure 2 A single esophageal squamous cell carcinoma lesion visualized under the three detection methods. A: Under white light imaging; B: Under linked color imaging; C: Under Lugol chromoendoscopy.



DOI: 10.3748/wjg.v29.i12.1899 Copyright ©The Author(s) 2023.

Figure 3 Method to measure the color difference between neoplastic and non-neoplastic lesions detected by white light imaging and linked color imaging. A: Neoplastic lesion (1) and non-neoplastic lesion (2) detected by white light imaging; B: Neoplastic lesion (3) and non-neoplastic lesion (4) detected by linked color imaging.

RESULTS

Participants

From March 2021 to May 2022, a total of 543 patients were enrolled in our study (Figure 1). Among them, a total of 141 suspected lesions were identified in 115 patients. Of these lesions, 45 neoplastic lesions (17 ESCC, 3 HGIN and 25 LGIN) were histologically confirmed in 43 (7.8%) patients (Table 1). Among the 45 lesions, 38 lesions (17 ESCC, 3 HGIN and 18 LGIN) were endoscopically suspicious during LCI examination; further, 41 lesions (17 ESCC, 3 HGIN and 21 LGIN) were endoscopically suspicious during LCE examination. Regarding the diagnostic modality of the 45 lesions, 34 (75.6%) lesions were identified by LCI and LCE compared to 4 (8.9%) lesions that were detected only by LCI and 7 (15.6%) lesions that were detected only by LCE.

Diagnostic performance of LCI and LCE for neoplastic lesions

In LCI mode, 74 suspected lesions underwent histological examination, and 38 lesions were confirmed histologically in 36 patients. In LCE mode, 104 suspected lesions were detected, and 41 lesions were

Table 1 Clinicopathological features of the patients

Item	n	% (n/n total)
Patients with suspected lesions ¹	115	21.2 (115/543)
Inflammation	72	13.2
LGIN	25	4.6
HGIN	3	0.5
ESCC	15	2.7
Suspected lesions, including non-neoplastic	141	-
Neoplastic lesions ²	45	31.9 (45/141)
LGIN	25	17.7 (25/141)
HGIN	3	2.1 (3/141)
ESCC	17	12.1 (17/141)
Neoplastic lesions detected with LCI		
LGIN	18	72.0 (18/25)
HGIN	3	100 (3/3)
ESCC	17	100 (17/17)
Neoplastic lesions detected with LCE		
LGIN	21	84.0 (21/25)
HGIN	3	100 (3/3)
ESCC	17	100 (17/17)
Neoplastic lesions detected by different diagnosis modality		
Only LCI	4	8.9 (4/45)
Only LCE	7	15.6 (7/45)
Both LCI and LCE	34	75.6 (34/45)
Neoplastic lesions per patient, mean (SD)	0.08 (0.29)	

¹Suspected lesions included neoplastic lesions and false positives (lesions detected but not confirmed to be neoplastic after histological examination).

²Neoplastic lesions confirmed by histological examination.

ESCC: Esophageal squamous cell carcinoma; HGIN: High-grade intraepithelial neoplasia; LCE: Lugol chromoendoscopy; LCI: Linked color imaging; LGIN; Low-grade intraepithelial neoplasia; SD: Standard deviation.

histologically confirmed in 39 patients. In Table 2, the sensitivity, specificity, positive predictive value and negative predictive value for LCI for the diagnosis of ESCC/HGIN/LGIN were 83.7%, 92.4%, 48.6% and 98.5%, respectively. The sensitivity, specificity, positive predictive value and negative predictive value for LCE were 90.7%, 87.0%, 37.5% and 99.1%, respectively. No significant differences in sensitivity, positive predictive value and negative predictive value were noted between LCI and LCE. However, the specificity of LCI was significantly higher than that of LCE (92.4% vs 87.0%, $P = 0.0023$).

Characteristics of the neoplastic lesions detected by LCI and LCE

The characteristics of the neoplastic lesions detected by LCI and LCE of the respective comparison groups are shown in Table 3. No significant differences in lesion location, size, morphologic type or pathology were noted between the two modality groups. However, the procedure time was significantly shorter for the LCI group compared with the LCE group [42 (34, 50) s vs 160 (130, 189) s, $P < 0.001$].

All detected neoplastic lesions were further divided into three subgroups according to the different diagnosis modalities: LCI only group (detected by LCI only, $n = 4$ lesions), LCE only group (detected by LCE only, $n = 7$ lesions), and LCI + LCE group (detected by both LCI and LCE, $n = 34$ lesions). We compared the clinicopathological features of the three groups in Supplementary Table 1. The lesion location, morphologic type and pathology were comparable among the three groups. However, the lesion sizes of the three groups were significantly different: 20 (55.8%) lesions in the LCI + LCE group were > 20 mm; 3 (75%) lesions in the LCI only group were ≤ 10 mm; and 7 (100%) lesions in the LCE only group were ≤ 10 mm ($P = 0.016$). We further compared the lesion size in the LCI only group and

Table 2 Esophageal neoplastic lesions (non-inflammation) detected using linked color imaging and Lugol chromoendoscopy

Parameter	LCI	LCE	P value
Sensitivity	83.7 (36/43)	90.7 (39/43)	0.520
Specificity	92.4 (462/500)	87.0 (435/500)	0.007 ¹
PPV	48.6 (36/74)	37.5 (39/104)	0.166
NPV	98.5 (462/469)	99.1 (435/439)	0.549

¹P < 0.01.

Data are presented as % (n/n total). LCE: Lugol chromoendoscopy; LCI: Linked color imaging; NPV: Negative predictive value; PPV: Positive predictive value.

Table 3 Clinicopathological features of neoplastic lesions (non-inflammation) detected by linked color imaging and Lugol chromoendoscopy, n (%)

Item	Detected by LCI, n = 36 patients/38 lesions	Detected by LCE, n = 39 patients/41 lesions	P value
Lesion location			0.969
Upper	3 (7.9)	3 (7.3)	
Middle	11 (28.9)	11 (26.8)	
Lower	24 (63.2)	27 (65.9)	
Morphologic type			0.902
I	1 (2.6)	1 (2.4)	
IIa	9 (23.7)	8 (19.5)	
IIb	18 (47.4)	24 (58.5)	
IIc	9 (23.7)	7 (17.1)	
III	1 (2.6)	1 (2.4)	
Size in mm			0.814
≤ 10	14 (36.8)	18 (43.9)	
10-20	3 (7.9)	3 (7.3)	
> 20	21 (55.3)	20 (48.8)	
Pathology			0.998
LGIN	18 (47.4)	21 (51.2)	
HGIN	3 (7.9)	3 (7.3)	
ESCC	EP/LPM	3 (7.9)	
	MM/SM1	1 (2.6)	
	≥ SM2	13 (34.2)	
Procedure time (s), median (IQR)	42 (34, 50)	160 (130, 189)	< 0.001 ¹

¹P value < 0.01.

EP: Epithelial; ESCC: Esophageal squamous cell carcinoma; HGIN: High-grade intraepithelial neoplasia; IQR: Interquartile range; LCE: Lugol chromoendoscopy; LCI: Linked color imaging; LGIN: Low-grade intraepithelial neoplasia; LPM: Lamina propria mucosa; MM: Muscularis mucosa; SM1: Submucosa invading ≤ 200 μm below the inferior margin of the muscularis mucosa; SM2: Submucosa invading > 200 μm below the inferior margin of the muscularis mucosa.

LCE only group, and the difference was not statistically significant (P = 0.364).

Color analysis

Of the 45 neoplastic lesions, 30 lesions had endoscopic images with clear visibility. Color analysis was conducted in the 30 lesions. *Supplementary Table 2* compares the color difference between the lesion

and surrounding mucosa in WLI and LCI. We found that the ΔE between the lesions and the surrounding mucosa was significantly higher in LCI compared with WLI (21.20 ± 9.79 vs 15.92 ± 7.50 , respectively, $P = 0.023$). For the three-dimensional color parameters of $L^*a^*b^*$, Δa^* was higher in LCI than in WLI (12.43 ± 10.00 vs 4.97 ± 6.96 , respectively, $P = 0.001$), and ΔL^* and Δb^* were similar in LCI and WLI. We further analyzed the color difference between the lesion and surrounding mucosa in different neoplastic pathologies (LGIN, HGIN and ESCC) in LCI mode, as shown in [Supplementary Table 3](#). However, no significant differences in ΔE , ΔL^* , Δa^* and Δb^* were noted among the three pathological types.

DISCUSSION

In this prospective study, we demonstrated that the sensitivity and specificity of LCI to detect ESCC and/or precancerous lesions (LGIN or/and HGIN) are acceptable. The specificity of LCI is higher than that of LCE, and the differences in sensitivity between the two modes were not obvious.

Previous studies have reported the utility of LCE in the detection of esophageal cancer[7,10-12]. LCE has served as the reference technique in patients at high risk for esophageal cancer[8,9]. Nevertheless, LCE is not suitable for general population screening given its side effects[16,17]. As a type of enhanced endoscopy, some studies have shown that narrow-band imaging is comparable to LCE in detecting esophageal cancer due to its excellent sensitivity and specificity[13-15]. Narrow-band imaging is typically combined with magnifying endoscopy, and the requirements for hospitals and operators are relatively high. LCI is a novel enhanced endoscopic technique, and Ono *et al*[20] reported that the detection rate of LCI in the diagnosis of neoplastic lesions in the upper gastrointestinal tract is 1.67 times higher than that of WLI. Yi *et al*[25] compared LCI and LCE in the detection of multiple primary esophageal cancers in primary ESCC patients and found that both modalities exhibited great value for multiple primary esophageal cancers. However, no study has compared their screening ability. To the best of our knowledge, this was the first prospective study to compare the effectiveness of LCI and LCE in screening esophageal cancer and precancerous lesions.

The present results showed that LCI is significantly more specific than LCE (92.4% vs 87.0%, $P = 0.0023$), and both modes exhibited high sensitivity for detecting neoplastic lesions (LGIN/HGIN/ESCC) (83.7% vs 90.7%, $P = 0.520$). The lesions were all pathologically diagnosed as LGIN (7 lesions in LCI and 4 in LCE). Therefore, our study results were consistent with previously published data reporting that the sensitivity of narrow-band imaging and Lugol for the diagnosis of ESCC and/or HGIN was approximately 100%[13,14]. The LCI only group included a lesion approximately 4 cm in length, and no unstained areas were observed. Based on the endoscopic findings, we thought that it was an erosive mucosal lesion caused by gastric acid reflux. Our results indicate that the capability of LCI to detect neoplastic lesions is acceptable.

The LCI technique is convenient for clinical endoscopists to use with the Fujifilm system because the imaging modes can easily be switched during the examination. Thus, the process is not as time-consuming as iodine staining. In our research, the median LCI procedure time was significantly shorter than for LCE (42 s vs 160 s, $P < 0.001$). In addition, Lugol solution can irritate the mucosa and may cause many side effects (chemical esophagitis, laryngitis, bronchopneumonia, chest pain, esophagospasm, gastritis and hypersensitivity)[16,17]. In clinical practice, the upper end of the Lugol staining site is generally less than 20 cm from the incisor given the high risk of solution aspiration. Therefore, it is difficult to detect cervical esophageal lesions, which reduces the detection of synchronous or metachronous neoplastic lesions. Therefore, the LCI technique is more useful for the diagnosis of ESCC or precancerous lesions given the mild mucosal irritation.

After color analysis, we found that the color difference between the lesion and the surrounding mucosa was greater for LCI compared with WLI. The results demonstrated that the lesion was more visible in LCI mode, which is consistent with previous studies[18,19,21,22]. Kobayashi *et al*[21] investigated the relationship between color information and the invasion depth of ESCC in LCI mode. They found that the color difference was greater in muscularis mucosa/submucosa invading ≤ 200 μm below the inferior margin of the muscularis mucosa or deeper lesions compared with epithelium and lamina propria mucosa lesions using LCI. However, they did not compare the color differences between ESCC and precancerous lesions. In our study, we further compared the color difference of different neoplastic pathologies in LCI mode, and the differences among LGIN, HGIN and ESCC were not significant. Notably, Tsunoda *et al*[35] reported a case using LCI and blue laser imaging with Lugol staining to provide an accurate diagnosis of ESCC and squamous intraepithelial neoplasia. Therefore, whether LCI and blue laser imaging combined with Lugol staining can be used to evaluate esophageal neoplastic lesions before endoscopic treatment deserves further study.

There are some limitations in our study. First, the number of lesions, especially neoplastic lesions, was low. Second, LCI and LCE can be performed sequentially during the same endoscopy procedure, but it is impossible to perform them in the reverse order. Thus, we were unable to perform a random crossover trial. Third, the images obtained in this study included two arbitrary regions of interest in the lesion mucosa and surrounding mucosa, which may have sampling errors and affected the

measurement results. However, for the WLI and LCI modes, we choose similar distance and angle images to calculate color values to reduce the influence of color differences based on various conditions. In the future, we need to conduct a multicenter study and collect more neoplastic lesions to further evaluate the usefulness of LCI. Further evaluation of the validity of LCI in diagnosing the depth of invasion of ESCC is also warranted.

CONCLUSION

Our study confirmed that LCI is efficient and specific for the surveillance of ESCC without causing discomfort. In the future, LCI, as a promising screening strategy, could replace LCE in the screening of esophageal neoplastic lesions in the general population.

ARTICLE HIGHLIGHTS

Research background

Lugol chromoendoscopy (LCE) has served as a standard screening technique in high-risk patients with esophageal cancer. Nevertheless, LCE is not suitable for the general population screening given its side effects. Linked color imaging (LCI) is a novel image-enhanced endoscopic technique that can distinguish subtle differences in mucosal color. It would be beneficial for the general population if LCE can provide similar diagnostic performance to LCI.

Research motivation

We compared the diagnostic performance of LCI with LCE in detecting esophageal squamous cell carcinoma (ESCC) and precancerous lesions. If LCI can replace LCE in detecting esophageal neoplastic lesions, it would be useful for esophageal screening in the general population.

Research objectives

As a novel image-enhanced endoscopic technique, LCI has been confirmed to be superior to white light imaging (WLI) in detecting neoplastic lesions in the upper gastrointestinal tract. We aimed to confirm that the diagnostic performance of LCI is comparable to LCE for the surveillance of ESCC.

Research methods

This was a single-center, prospective, registered clinical study. In this noninferiority study, we prospectively enrolled 543 patients who underwent WLI, LCI and LCE successively. We compared the sensitivity and specificity of LCI and LCE in the detection of esophageal neoplastic lesions. We further used L*a*b* color space to evaluate the color differences of LCI.

Research results

In total, 43 patients were analyzed. The sensitivity of LCI was similar to that of LCE, whereas the specificity of LCI was greater than that of LCE. The LCI procedure time in the esophageal examination was significantly shorter than that of LCE. However, the color difference in LCI was similar in different pathological types.

Research conclusions

Our study showed that LCI is efficient and specific for the surveillance of ESCC without causing discomfort. In the future, LCI, as a promising screening strategy, could replace LCE in the screening of esophageal neoplastic lesions in the general population.

Research perspectives

Because of the low detection rate of esophageal cancer, we were only able to enroll a limited number of neoplastic lesions. In the future, we need to conduct a multicenter study and collect more neoplastic lesions to further evaluate the usefulness of LCI. Further evaluation of the validity of LCI in diagnosing the depth of invasion of ESCC is also warranted.

ACKNOWLEDGEMENTS

We thank our peer reviewers for the insightful and thorough suggestions on this manuscript.

FOOTNOTES

Author contributions: Wang ZX and Li LS contributed equally to this work; Chai NL and Linghu EQ contributed to study conception and design; Wang ZX and Li LS contributed to manuscript drafting; Li LS, Su S, Li JP, Wang NJ, Zhang B, Liu SZ, Zhang S, Wang SS, Bi YW, Gao F, Shao Q, Xu N, Shao BZ, Yao Y, and Liu F contributed to data acquisition; Chai NL, Linghu EQ, Li LS and Su S contributed to critical revision of the article for important intellectual content; and all authors issued final approval for the version to be submitted.

Supported by the National Natural Science Foundation of China, No. 81270564 and 82100697.

Institutional review board statement: The study was reviewed and approved by the ethics committee of the Chinese PLA general hospital (Approval No. of Ethics Committee: S2021-145-01).

Clinical trial registration statement: This study was registered in the Chinese clinical trial database (chictr.org) with the number ChiCTR2100045636.

Informed consent statement: All study participants, or their legal guardian, provided informed written consent prior to study enrollment.

Conflict-of-interest statement: All the authors report no relevant conflicts of interest for this article.

Data sharing statement: No additional data are available.

CONSORT 2010 statement: The authors have read the CONSORT 2010 statement, and the manuscript was prepared and revised according to the CONSORT 2010 statement.

Open-Access: This article is an open-access article that was selected by an in-house editor and fully peer-reviewed by external reviewers. It is distributed in accordance with the Creative Commons Attribution NonCommercial (CC BY-NC 4.0) license, which permits others to distribute, remix, adapt, build upon this work non-commercially, and license their derivative works on different terms, provided the original work is properly cited and the use is non-commercial. See: <https://creativecommons.org/Licenses/by-nc/4.0/>

Country/Territory of origin: China

ORCID number: Zi-Xin Wang 0000-0003-3929-3448; Long-Song Li 0000-0002-4000-7501; Song Su 0000-0002-3199-7865; Jin-Ping Li 0000-0003-4891-922X; Bo Zhang 0000-0002-4333-0750; Nan-Jun Wang 0000-0002-6061-4798; Sheng-Zhen Liu 0000-0001-9206-8173; Sha-Sha Wang 0000-0001-6916-7552; Shuai Zhang 0000-0003-3748-5438; Ya-Wei Bi 0000-0003-3762-5920; Fei Gao 0000-0002-9444-4168; Qun Shao 0000-0001-6503-6133; Ning Xu 0000-0002-7770-8731; Bo-Zong Shao 0000-0002-2621-0669; Yi Yao 0000-0001-6976-3418; Fang Liu 0000-0002-2013-9881; En-Qiang Linghu 0000-0003-4506-7877; Ning-Li Chai 0000-0002-6791-5817.

S-Editor: Wang JJ

L-Editor: A

P-Editor: Wang JJ

REFERENCES

- 1 Erratum: Global cancer statistics 2018: GLOBOCAN estimates of incidence and mortality worldwide for 36 cancers in 185 countries. *CA Cancer J Clin* 2020; **70**: 313 [PMID: 32767693 DOI: 10.3322/caac.21609]
- 2 Ciocirlan M, Lapalus MG, Hervieu V, Souquet JC, Napoléon B, Scoazec JY, Lefort C, Saurin JC, Ponchon T. Endoscopic mucosal resection for squamous premalignant and early malignant lesions of the esophagus. *Endoscopy* 2007; **39**: 24-29 [PMID: 17252456 DOI: 10.1055/s-2006-945182]
- 3 Merkow RP, Bilmoria KY, Keswani RN, Chung J, Sherman KL, Knab LM, Posner MC, Bentrem DJ. Treatment trends, risk of lymph node metastasis, and outcomes for localized esophageal cancer. *J Natl Cancer Inst* 2014; **106** [PMID: 25031273 DOI: 10.1093/jnci/dju133]
- 4 Morgan E, Soerjomataram I, Rungay H, Coleman HG, Thrift AP, Vignat J, Laversanne M, Ferlay J, Arnold M. The Global Landscape of Esophageal Squamous Cell Carcinoma and Esophageal Adenocarcinoma Incidence and Mortality in 2020 and Projections to 2040: New Estimates From GLOBOCAN 2020. *Gastroenterology* 2022; **163**: 649-658.e2 [PMID: 35671803 DOI: 10.1053/j.gastro.2022.05.054]
- 5 Arnold M, Abnet CC, Neale RE, Vignat J, Giovannucci EL, McGlynn KA, Bray F. Global Burden of 5 Major Types of Gastrointestinal Cancer. *Gastroenterology* 2020; **159**: 335-349.e15 [PMID: 32247694 DOI: 10.1053/j.gastro.2020.02.068]
- 6 Obermannová R, Alsina M, Cervantes A, Leong T, Lordick F, Nilsson M, van Grieken NCT, Vogel A, Smyth EC; ESMO Guidelines Committee. Electronic address: clinicalguidelines@esmo.org. Oesophageal cancer: ESMO Clinical Practice Guideline for diagnosis, treatment and follow-up. *Ann Oncol* 2022; **33**: 992-1004 [PMID: 35914638 DOI: 10.1016/j.annonc.2022.07.003]
- 7 Hashimoto CL, Iriya K, Baba ER, Navarro-Rodriguez T, Zerbini MC, Eisig JN, Barbuti R, Chinzon D, Moraes-Filho JP. Lugol's dye spray chromoendoscopy establishes early diagnosis of esophageal cancer in patients with primary head and

neck cancer. *Am J Gastroenterol* 2005; **100**: 275-282 [PMID: 15667482 DOI: 10.1111/j.1572-0241.2005.30189.x]

8 **Bisschops R**, Areia M, Coron E, Dobru D, Kaskas B, Kuvaev R, Pech O, Ragunath K, Weusten B, Familiari P, Domagk D, Valori R, Kaminski MF, Spada C, Brethauer M, Bennett C, Senore C, Dinis-Ribeiro M, Rutter MD. Performance measures for upper gastrointestinal endoscopy: a European Society of Gastrointestinal Endoscopy (ESGE) Quality Improvement Initiative. *Endoscopy* 2016; **48**: 843-864 [PMID: 27548885 DOI: 10.1055/s-0042-113128]

9 **Hirota WK**, Zuckerman MJ, Adler DG, Davila RE, Egan J, Leighton JA, Qureshi WA, Rajan E, Fanelli R, Wheeler-Harbaugh J, Baron TH, Faigel DO; Standards of Practice Committee, American Society for Gastrointestinal Endoscopy. ASGE guideline: the role of endoscopy in the surveillance of premalignant conditions of the upper GI tract. *Gastrointest Endosc* 2006; **63**: 570-580 [PMID: 16564854 DOI: 10.1016/j.gie.2006.02.004]

10 **Shiozaki H**, Tahara H, Kobayashi K, Yano H, Tamura S, Imamoto H, Yano T, Oku K, Miyata M, Nishiyama K. Endoscopic screening of early esophageal cancer with the Lugol dye method in patients with head and neck cancers. *Cancer* 1990; **66**: 2068-2071 [PMID: 1699649 DOI: 10.1002/1097-0142(19901115)66:10<2068::aid-cncr2820661005>3.0.co;2-w]

11 **Muto M**, Hironaka S, Nakane M, Boku N, Ohtsu A, Yoshida S. Association of multiple Lugol-voiding lesions with synchronous and metachronous esophageal squamous cell carcinoma in patients with head and neck cancer. *Gastrointest Endosc* 2002; **56**: 517-521 [PMID: 12297767 DOI: 10.1067/mge.2002.128104]

12 **Shimizu Y**, Tukagoshi H, Fujita M, Hosokawa M, Kato M, Asaka M. Endoscopic screening for early esophageal cancer by iodine staining in patients with other current or prior primary cancers. *Gastrointest Endosc* 2001; **53**: 1-5 [PMID: 11154480 DOI: 10.1067/mge.2001.111387]

13 **Morita FH**, Bernardo WM, Ide E, Rocha RS, Aquino JC, Minata MK, Yamazaki K, Marques SB, Sakai P, de Moura EG. Narrow band imaging versus lugol chromoendoscopy to diagnose squamous cell carcinoma of the esophagus: a systematic review and meta-analysis. *BMC Cancer* 2017; **17**: 54 [PMID: 28086818 DOI: 10.1186/s12885-016-3011-9]

14 **Gruner M**, Denis A, Masliah C, Amil M, Metivier-Cesbron E, Luet D, Kaasis M, Coron E, Le Rhun M, Lecleire S, Antonietti M, Legoux JL, Lefrou L, Renkes P, Tarreirias AL, Balian P, Rey P, Prost B, Cellier C, Rahmi G, Samaha E, Fratte S, Guerrier B, Landel V, Touzet S, Ponchon T, Pioche M. Narrow-band imaging versus Lugol chromoendoscopy for esophageal squamous cell cancer screening in normal endoscopic practice: randomized controlled trial. *Endoscopy* 2021; **53**: 674-682 [PMID: 32698233 DOI: 10.1055/a-1224-6822]

15 **Nagami Y**, Tominaga K, Machida H, Nakatani M, Kameda N, Sugimori S, Okazaki H, Tanigawa T, Yamagami H, Kubo N, Shiba M, Watanabe K, Watanabe T, Iguchi H, Fujiwara Y, Ohira M, Hirakawa K, Arakawa T. Usefulness of non-magnifying narrow-band imaging in screening of early esophageal squamous cell carcinoma: a prospective comparative study using propensity score matching. *Am J Gastroenterol* 2014; **109**: 845-854 [PMID: 24751580 DOI: 10.1038/ajg.2014.94]

16 **Sreedharan A**, Rembacken BJ, Rotimi O. Acute toxic gastric mucosal damage induced by Lugol's iodine spray during chromoendoscopy. *Gut* 2005; **54**: 886-887 [PMID: 15888800 DOI: 10.1136/gut.2004.061739]

17 **Park JM**, Seok Lee I, Young Kang J, Nyol Paik C, Kyung Cho Y, Woo Kim S, Choi MG, Chung IS. Acute esophageal and gastric injury: complication of Lugol's solution. *Scand J Gastroenterol* 2007; **42**: 135-137 [PMID: 17190773 DOI: 10.1080/00365520600825141]

18 **Kanzaki H**, Takenaka R, Kawahara Y, Kawai D, Obayashi Y, Baba Y, Sakae H, Gotoda T, Kono Y, Miura K, Iwamuro M, Kawano S, Tanaka T, Okada H. Linked color imaging (LCI), a novel image-enhanced endoscopy technology, emphasizes the color of early gastric cancer. *Endosc Int Open* 2017; **5**: E1005-E1013 [PMID: 29159276 DOI: 10.1055/s-0043-117881]

19 **Khurelbaatar T**, Miura Y, Osawa H, Nomoto Y, Tokoro S, Tsunoda M, Sekiguchi H, Kobayashi T, Funayama Y, Nagayama M, Takezawa T, Mieno M, Ueno T, Fukuda H, Iwashita C, Takahashi H, Ino Y, Kawarai Lefor A, Yamamoto H. Usefulness of linked color imaging for the detection of obscure early gastric cancer: Multivariate analysis of 508 lesions. *Dig Endosc* 2022; **34**: 1012-1020 [PMID: 34942042 DOI: 10.1111/den.14221]

20 **Ono S**, Kawada K, Dohi O, Kitamura S, Koike T, Hori S, Kanzaki H, Murao T, Yagi N, Sasaki F, Hashiguchi K, Oka S, Katada K, Shimoda R, Mizukami K, Suehiro M, Takeuchi T, Katsuki S, Tsuda M, Naito Y, Kawano T, Haruma K, Ishikawa H, Mori K, Kato M; LCI-FIND Trial Group. Linked Color Imaging Focused on Neoplasm Detection in the Upper Gastrointestinal Tract : A Randomized Trial. *Ann Intern Med* 2021; **174**: 18-24 [PMID: 33076693 DOI: 10.7326/M19-2561]

21 **Kobayashi K**, Miyahara R, Funasaka K, Furukawa K, Sawada T, Maeda K, Yamamura T, Ishikawa T, Ohno E, Nakamura M, Kawashima H, Nakaguro M, Okumura Y, Hirooka Y, Fujishiro M. Color information from linked color imaging is associated with invasion depth and vascular diameter in superficial esophageal squamous cell carcinoma. *Dig Endosc* 2020; **32**: 65-73 [PMID: 31220372 DOI: 10.1111/den.13469]

22 **Nakamura K**, Urabe Y, Oka S, Nagasaki N, Yorita N, Hata K, Masuda K, Kurihara M, Kotachi T, Boda T, Tanaka S, Chayama K. Usefulness of linked color imaging in the early detection of superficial esophageal squamous cell carcinomas. *Esophagus* 2021; **18**: 118-124 [PMID: 32447591 DOI: 10.1007/s10388-020-00749-2]

23 **de Groot AJ**, Fockens KN, Struyvenberg MR, Pouw RE, Weusten BLAM, Schoon EJ, Mostafavi N, Bisschops R, Curvers WL, Bergman JJ. Blue-light imaging and linked-color imaging improve visualization of Barrett's neoplasia by nonexpert endoscopists. *Gastrointest Endosc* 2020; **91**: 1050-1057 [PMID: 31904377 DOI: 10.1016/j.gie.2019.12.037]

24 **Diao W**, Huang X, Shen L, Zeng Z. Diagnostic ability of blue laser imaging combined with magnifying endoscopy for early esophageal cancer. *Dig Liver Dis* 2018; **50**: 1035-1040 [PMID: 29685806 DOI: 10.1016/j.dld.2018.03.027]

25 **Yi N**, Huang P, Zhang W, Jiang C, Liang L. [A comparative study of endoscopic linked color imaging and iodine staining in the diagnosis of multiple primary esophageal carcinoma]. *Chin J Clin Gastroenterol* 2019; **31**: 139-144

26 **Wei WQ**, Chen ZF, He YT, Feng H, Hou J, Lin DM, Li XQ, Guo CL, Li SS, Wang GQ, Dong ZW, Abnet CC, Qiao YL. Long-Term Follow-Up of a Community Assignment, One-Time Endoscopic Screening Study of Esophageal Cancer in China. *J Clin Oncol* 2015; **33**: 1951-1957 [PMID: 25940715 DOI: 10.1200/JCO.2014.58.0423]

27 **Zhang N**, Li Y, Chang X, Lei F, Ma H, Liu J, Yang J, Su M, Sun X, Zhao D, Sun Q, Wei W, Wang G, Wang J. Long-term effectiveness of one-time endoscopic screening for esophageal cancer: A community-based study in rural China. *Cancer* 2020; **126**: 4511-4520 [PMID: 33460056 DOI: 10.1002/cncr.33119]

28 **National Quality Control Center of Digestive Endoscopy NCRCfDDS**, National Early Gastrointestinal-Cancer Prevention & Treatment Center Alliance (GECA); Digestive Endoscopy Professional Committee of Chinese Endoscopist Association, Chinese Society of Digestive Endoscopy, Chinese Society of Health Management; Cancer Endoscopy Professional Committee of China Anti-Cancer. [China experts consensus on the protocol of early esophageal cancer and pre-cancerous lesion screening (2019, Xinxiang)]. *Chin J Dig Endosc* 2019; **36**: 793-801

29 **Jin D**, Wang J, Zhan Q, Huang K, Wang H, Zhang G, Xu Y, Yao J, Sun R, Huang Q, Ye F. The safety and efficacy of 2% vitamin C solution spray for relief of mucosal irritation caused by Lugol chromoendoscopy: a multicenter, randomized, double-blind, parallel trial. *Gastrointest Endosc* 2020; **92**: 554-564 [PMID: 31783028 DOI: 10.1016/j.gie.2019.11.028]

30 The Paris endoscopic classification of superficial neoplastic lesions: esophagus, stomach, and colon: November 30 to December 1, 2002. *Gastrointest Endosc* 2003; **58**: S3-43 [PMID: 14652541 DOI: 10.1016/s0016-5107(03)02159-x]

31 **Schlemper RJ**, Riddell RH, Kato Y, Borchard F, Cooper HS, Dawsey SM, Dixon MF, Fenoglio-Preiser CM, Fléjou JF, Geboes K, Hattori T, Hirota T, Itabashi M, Iwafuchi M, Iwashita A, Kim YI, Kirchner T, Klimpfinger M, Koike M, Lauwers GY, Lewin KJ, Oberhuber G, Offner F, Price AB, Rubio CA, Shimizu M, Shimoda T, Sipponen P, Solcia E, Stolte M, Watanabe H, Yamabe H. The Vienna classification of gastrointestinal epithelial neoplasia. *Gut* 2000; **47**: 251-255 [PMID: 10896917 DOI: 10.1136/gut.47.2.251]

32 **Yokoyama A**, Ohmori T, Makuuchi H, Maruyama K, Okuyama K, Takahashi H, Yokoyama T, Yoshino K, Hayashida M, Ishii H. Successful screening for early esophageal cancer in alcoholics using endoscopy and mucosa iodine staining. *Cancer* 1995; **76**: 928-934 [PMID: 8625217 DOI: 10.1002/1097-0142(19950915)76:6<928::aid-cncr2820760604>3.0.co;2-5]

33 **Liu M**, Zhou R, Guo C, Xu R, Liu A, Yang H, Li F, Duan L, Shen L, Wu Q, Liu Z, Liu F, Liu Y, Pan Y, Cai H, Weiss NS, He Z, Ke Y. Size of Lugol-unstained lesions as a predictor for risk of progression in premalignant lesions of the esophagus. *Gastrointest Endosc* 2021; **93**: 1065-1073.e3 [PMID: 32950597 DOI: 10.1016/j.gie.2020.09.020]

34 **Kuehni RG**. Color-tolerance data and the tentative CIE 1976 L a b formula. *J Opt Soc Am* 1976; **66**: 497-500 [PMID: 932844 DOI: 10.1364/josa.66.000497]

35 **Tsunoda M**, Miura Y, Osawa H, Khurelbaatar T, Sakaguchi M, Fukuda H, Lefor AK, Yamamoto H. New Diagnostic Approach for Esophageal Squamous Cell Neoplasms Using Linked Color Imaging and Blue Laser Imaging Combined with Iodine Staining. *Clin Endosc* 2019; **52**: 497-501 [PMID: 31499608 DOI: 10.5946/ce.2018.195]



Published by **Baishideng Publishing Group Inc**
7041 Koll Center Parkway, Suite 160, Pleasanton, CA 94566, USA

Telephone: +1-925-3991568

E-mail: bpgoftice@wjnet.com

Help Desk: <https://www.f6publishing.com/helpdesk>
<https://www.wjnet.com>

